Microstructural, techno-functional, and *in vitro* starch digestion characterization of New Zealand Pea Varieties: a template to design sustainable low glycaemic foods.

A dissertation presented in partial fulfilment

of the requirements for the degree of

Doctor of Philosophy in Food Technology

at Massey University, Palmerston North, Manawatū, New Zealand

Abayomi Ajala

2023

Abstract

The results presented in this dissertation provided a systematic investigation into the microstructural components (starch granules, protein matrix, and encapsulating cell wall) in the different forms of pea seed microstructure from four (4) varieties and how the interaction between these structural components during processing influence its starch gelatinization and hydrolysis properties. Based on the fundamental information provided above, the thesis explored a sustainable processing technique to transform pea seeds into a novel pea ingredient with low glycaemic features.

This first study examined how the microstructure of New Zealand pea varieties: White/yellow (WP), Marrowfat (MFP), Blue (BP), and Maple (MP) respond to pre-and-post starch gelatinization conditions. The microstructural characteristics of raw pea seeds were evaluated via scanning electron microscopy and image analysis before studying their hydration kinetics at 30, 40, 50, or 60 °C (pre-starch gelatinization conditions) while *in-vitro* oral-gastro small intestinal digestion was performed on the cooked pea seeds (post-starch gelatinization condition). For the raw sample, the cell wall thickness for the pea varieties differed significantly from each other and followed a decreasing order of MP > MFP > BP > WP. The shortest time (139 min) for the soaked pea to reach its saturation point was exhibited by BP at 60 °C while the lowest moisture content of soaked peas at saturation point was found in MP at 60 °C. The starch hydrolysis (%) of the cooked pea varieties during oral-gastro-intestinal digestion *in vitro* followed a decreasing order of WP > MP > MFP > BP. The discernible irregular particles (protein bodies, fibre fragments) attached to or between the starch granules observed in both hydrated and cooked pea seed microstructure seemed to modulate the inflow of water and starch-degrading enzymes.

The next study investigated the role of cell wall permeability in the microstructure and rate of starch digestibility in intact cotyledon cells from different varieties of pea seeds. PFG-NMR coupled with light and confocal microscopy were employed to evaluate the cotyledon cells' diffusion coefficients and cell wall permeability. The diffusion coefficients and cell wall permeability of the cotyledon cells followed a decreasing trend; WP>MFP>MP>BP. The varying size of internal cavities in the microstructure in the cotyledon cells as observed by the light and confocal micrographs may be responsible for this trend. The extent of starch hydrolysis

recorded from the cotyledon cells somewhat followed the same trend of the cell wall permeability. Thus, indicating that the more permeable the cotyledon cell to the starch-degrading enzymes, the higher the extent of intracellular starch hydrolysis. The microstructure changes in the cotyledon cells during digestion also confirmed this observation.

Based on the fundamental insights provided by the previous studies, the next study compared the microstructural, nutritional, and starch digestibility properties of a novel cotyledon flour prepared via micronization techniques (colloid milling) with a blended flour from the same botanical sources. The SEM characterization of both flours showed a distinct difference in their microstructural arrangement. The protein and fibre contents of cotyledon flour were higher than those of the blended flour from the same plant sources. The starch hydrolysis and glycaemic response of cotyledon flour were almost 10 % lower than that of the blended flour. This could result in the cell wall of cotyledon cells acting as a primary barrier that regulates the inflow of starch-degrading enzymes to the intracellular starch granules. Also, the high-quality protein/cellular matrix found in the cotyledon flour may reduce the exposure of the extracellular starch granules to degrading enzymes. This study provided fundamental insights into how to sustainably process whole pulse seeds.

Finally, wheat flour for making bread was replaced with 25 and 50 % of cotyledon flour and the effect of this on the microstructure, physical-functional properties, starch digestion *in vitro,* and the glycaemic response were investigated. The micrographs of these three bread samples showed a distinct microstructural organization between the cotyledon flour-formulated bread and the control bread samples. Intact cotyledon cells and high levels of cellular materials were observed in the cotyledon flour-formulated bread samples. The protein, fibre, and resistant starch in the cotyledon flour-formulated bread were significantly higher than the control bread. The bake loss, volume, and specific volume decreased with an increased percentage of cotyledon flour used in the bread formulation. The colour of the crumb and crust of the cotyledon flour-formulated bread was significantly different from the control bread while the textural profile showed that the crumb hardness and cohesiveness of the bread samples increased with an increase in the percentage of the cotyledon flour added to the formulation of the bread. The starch hydrolysis for this study showed bread made with 25 and 50 % cotyledon flour was significantly lower than the control bread sample. The intact cotyledon

cells with high cellular integrity observed in the microstructures of the bread samples confirmed this trend.

In conclusion, this thesis provided fundamental insights into forms of microstructure (cotyledon cells and pulse flour) that can be generated from whole pulse seed via size-reducing techniques structural components (starch granules, protein matrix, and cell wall) in each form and how the interaction between these components influences the starch hydrolysis in each form. One of the significant fundamental knowledge areas provided by this dissertation was that achieving a sort of equilibrium between “applicable particle size” and “intactness of microstructure” in processing a pulse seed could be a suitable template for designing a “wholesome” pulse food ingredient with medium glycaemic features.

Acknowledgments

I would like to give all glory and adoration to God Almighty, the author and the perfecter of my faith. My deepest appreciation to my main supervisor, Professor Jaspreet Singh, and Co-supervisors, Dr Sung Jee Lee and Dr Lovedeep Kaur for their visionary guidance and support during this PhD journey. I am sincerely grateful to my main supervisor for his encouragement, and guidance throughout my PhD journey.

I am immensely grateful to Massey University Doctoral Scholarship for providing a full PhD scholarship (tuition fees plus stipends) for my research.

I would like to thank Dr. Patrickk Edwards (BioNMR facility, Massey University) for his interest in my work and assistance in developing a PFG-NMR method for my samples. Also, I would like to thank Raoul Solomon (Manawatu Microscopy and Imaging Center) for the training on Scanning electron and Confocal microscopy.

I would like to appreciate laboratory managers, Mr. Steve Glasgow, Ms. Michelle Tamehana (School of Food and Advanced Technology), and Mrs. Maggie Zou (Riddet Institute) for providing me with training in the use of laboratory equipment and ordering materials for the PhD. Special thanks to Mr. Garry Rashford and Mr Warwick Johnson (Food pilot and product Development laboratory) for their assistance in the colloid milling, freeze-drying, and baking sessions in their respective laboratory.

Finally, I would like to thank my wife, Mrs Temitope Ajala, my family, and my friends for the emotional support, prayers, and encouragement received throughout this PhD journey.

Table of Contents

Abstract i
Acknowledgement iv
Lists of Tables x
Lists of Figures xi
Lists of Abbreviations xiv
Lists of publications & conference proceedings xvi
Chapter 1: Introduction 1
1.1 Background information 1
1.2 Thesis overview 2
Chapter 2: Review of literature 4
2.2 Introduction 4
2.3 Overview of Pulse seed production and consumption 6
2.4 Environmental benefits of pulse production 7
2.5 Nutritional and health benefits of pulse diet 9
2.6 Application of pulse as a food ingredient 10
2.7 Pulse as a low glycaemic index food 13
2.8 Peas nutritional composition 13
2.9 Pulse seed microstructure 16
2.10 Recent advances in pulse microstructure: three (III) forms of microstructure from pulse seeds 17
2.10.1 Form I: Whole pulse seed 17
2.10.2. Form II: Isolated cotyledon cells from pulses. 19
2.10.2.1.1. Cell wall. 22
2.10.2.1.2. Starch 27
2.10.3. Form III: Flours from pulse seed 28
2.10.3.1. Effects of milling techniques on the microstructural features of pulse flour 30
2.10.3.1.2. Fiber 30
2.11 Influence of different forms of pulse microstructure on starch digestion 31
2.12 Conclusions 36
Chapter 3: Experimental design 37
3.1 Research questions and hypotheses 37

Chapter 4: Influence of seed microstructure on the hydration kinetics and oral-gastro-small intestinal starch digestion *in vitro* of New Zealand pea varieties ... 39
4.1 Abstract ... 39
4.2 Introduction ... 40
4.3 Material and methods ... 42
4.3.1 Materials ... 42
4.3.2 Methods ... 42
4.3.3. Microstructural characteristics of raw pea seeds. ... 42
4.3.3.1. Microstructure of pea seed during hydration kinetics ... 43
4.3.4. Physical properties of raw pea seed. ... 43
4.3.5. Proximate composition and cooking characteristics of raw pea seeds. ... 44
4.3.6 Textural properties of cooked pea seeds ... 45
4.3.7 Hydration Kinetics ... 45
4.3.7.1 Hydration kinetics calculations ... 46
4.3.7.2 Application of Peleg Model to hydration kinetics of pea seeds ... 46
4.3.8 In vitro oral gastro-small intestinal digestion of the pea seeds ... 46
4.3.9 Statistical analysis ... 48
4.4 Result & discussion ... 48
4.4.1 Microstructural characteristics of the raw pea seeds ... 48
4.4.2 Physical properties of pea seeds ... 49
4.4.3 Proximate composition and cooking characteristics of pea seeds ... 50
4.4.4 Textural properties of cooked pea seeds ... 56
4.4.5 Hydration Kinetics ... 57
4.4.5.1 The role of microstructure on the hydration kinetics ... 59
4.4.6 In vitro oral gastro-small intestinal digestion of the pea seed ... 62
4.4.6.1 Influence of microstructure on starch hydrolysis of pea seeds ... 68
4.4.7 Principal component analysis (PCA) ... 68
4.5 Conclusions ... 70
Chapter 5: Cell wall permeability in relation to *in vitro* starch digestion of pulse cotyledon cells ... 71
5.1 Abstract ... 71
5.2 Introduction ... 71
5.3 Materials and methods ... 73

5.3.1 Material....73
5.3.2. Isolation of cotyledon cells from the pea seed varieties.....73
5.3.3 Morphological properties....73
5.3.3.1 Light microscopy....74
5.3.3.2 Microstructural characterization....74
5.3.3.3 Particle size....74
5.3.3.4 Confocal characterization of the cells....74
5.3.4 Cell wall permeability of cotyledon cells....75
5.3.4.1 Sample preparation....75
5.3.4.2 PFG-NMR diffusion measurement....75
5.3.5 Proximate composition of the cotyledon cells....75
5.3.6 Thermal properties....76
5.3.7 X-ray diffraction (crystallinity)....76
5.3.8 *In vitro* gastro-small intestinal digestion of the cotyledon cells....76
5.3.9 Statistical analysis....77
5.4 Results and Discussion....77
5.4.1 Microstructural characterization of isolated intact cotyledon cells from pea varieties....77
5.4.2 Diffusion coefficient of the cotyledon cells using PFG-NMR....78
5.4.3 Nutritional composition of the cotyledon cells....83
5.4.4 Crystallinity and thermal properties....85
5.4.5 *In vitro* gastro-intestinal starch digestion of cotyledon cells....86
5.5 Conclusions....92
Chapter 6: Microstructural, nutritional, and *in vitro* starch digestion properties of a novel cotyledon flour designed via Micronization Techniques. 93
6.1 Abstract....93
6.2 Introduction....93
6.3 Material and Methods....95
6.3.1. Material....95
6.3.2 Preparation of novel cotyledon flours from pea seeds....95
6.3.2.1 Acid and alkali treatment....95
6.3.2.2 Colloid milling....95
6.3.3. Morphological properties....96
6.3.3.1 Microstructural characterization....96

6.3.3.2. Particle size distribution 96
6.3.4. Proximate composition and water-holding capacity 96
6.3.5 Pasting Properties 97
6.3.6 Thermal properties 97
6.3.7 X-ray diffraction (crystallinity) 98
6.3.8. *In vitro* oral gastro-small intestinal digestion 98
6.3.9. Statistical analysis 99
6.4. Result and discussion 99
6.4.1 Description of "Cotyledon Flour" and its Morphological Properties 99
6.4.2 Proximate and Water holding capacity. 103
6.4.3 Pasting Properties. 106
6.4.4. Thermal Properties and Crystallinity 110
6.4.5 Starch digestion and glycaemic response 112
6.5 Conclusions 120
Chapter 7: The effect of cotyledon flour as a new food ingredient on the techno-functional properties of a food system 122
7.1 Abstract 122
7.2 Introduction 122
7.3 Material and Methods 123
7.3.1 Ingredients 123
7.3.2 Bread preparation 124
7.3.3 Proximate composition of bread 125
7.3.4 Physical Characterization of the Bread 126
7.3.4.1 Bake loss 126
7.3.5 Volume and specific volume of the loaf 126
7.3.6 Bread PH 126
7.3.7 Colour analysis of the bread crust and crumbs 126
7.3.8 Textural profile analysis of bread 126
7.3.9 *In vitro* oral gastro-small intestinal digestion of the bread 127
7.3.9.1 Microstructural characterization of the baked bread and the digest 128
7.3.10 Statistical tool 128
7.4 Result and Discussion 128
7.4.1 Nutritional value of bread samples 128

7.4.3 Colour and textural properties of the bread samples 131
7.4.5 Starch Digestion and the glycaemic response of the bread samples 134
7.5 Conclusions 138
Chapter 8: General Discussion, conclusions, and future directions 139
8.1 Summary and Discussion 139
8.1.1 Microstructural components in whole pulse seed and its influence on intracellular starch gelatinization and hydrolysis 139
8.1.2 The cell wall permeability and its influence on entrapped starch digestion *in vitro* 140
8.1.3 Characterisation of cotyledon flour developed via colloid milling. 142
8.1.4 The effect of cotyledon flour as a new food ingredient on the techno-functional properties of a food system. 143
8.2 Conclusions and Recommendations for future works 144
Bibliography 146
Appendix 172

Lists of Tables

Table 2.1: Some applications of pulse flour and their fractions 12

Table 2.2 Nutritional composition of some pulse grain 15

Table 2.3: Isolation methods of pulse cotyledon cells from some pulse seeds. 24

Table 2.4: Summary of starch hydrolysis of different forms of microstructure from pulse seed 32

Table 3.1 Research question and hypotheses 37

Table 4.1 Morphological properties of raw whole peas from different varieties as examined using scanning electron microscopy and ImageJ analysis. 49

Table 4.2 Different physical parameters of the pea seeds varieties. 53

Table 4.3 Proximate composition and cooking time of the four different pea seed varieties .54

Table 4.4 Peleg constants at different temperatures and Degree of Fit Based on Eq. (5) 59

Table 4.5 Properties examined with Principal Component Analysis (PCA) 65

Table 4.6 Pearson correlation coefficient for various pea properties of different varieties. 66

Table 5.1. Particle size of the cotyledon cells from four different pea seed varieties 79

Table 5.2 Nutritional composition of the cotyledon cells 84

Table 6.1. Particle size distribution and yield of cotyledon and blended pea flours. 102

Table 6.2 Proximate composition and water holding capacity of cotyledon and blended pea flours. 104

Table 6.3: Pasting properties and estimated glycaemic index of cotyledon and blended pea flours 107

Table 7.1 Ingredient formulations for making breads. 125

Table 7.2 Nutritional Properties of bread samples 130

Table 7.3 Physical properties of bread samples 131

Table 7.4 Colour analysis of bread samples 132

Table 7.5 Textural Properties of bread samples 132

Table 7.6 Starch hydrolysis and glycaemic index of the bread samples 134

Lists of Figures

Fig 2.1: Global production of pulses (in million tonnes) by region between 1997-2017. 6

Fig 2.2: Consumption of pulses (in Kg/person/year) by region between 1997-2013.....7

Fig 2.3: Application of pea ingredients in food.....11

Fig 2.4: Classification of Glycaemic index of various food products using glucose as the reference. Reproduced from Bornet *et al.* (1997).....13

Fig 2.5: Two forms of pulse microstructure from pulse seed. Form I, II & III are whole pulse seed, intact pulse cotyledon cells, and pulse flour, respectively.....18

Fig 2.6: SEM micrographs of different varieties of raw New Zealand pea seeds. A, B, C, and D represent White/yellow, Marrowfat, Blue, and Maple pea, respectively, at 1000X. Note: E; starch granules and protein bodies encapsulated in the cell Wall, SG: starch granule, PB: protein bodies, and CW: cell wall.....20

Fig 2.7. SEM electrographs of four different varieties of peas at 30 and 60 °C soaking temperatures. A B, C, and D represent WP, MFP, BP, and MP, respectively. Note (1 & 2 indicate 30 and 60 °C). CW; cell wall, and D.CW; distorted cell wall. 22

2.10.2.1. Effects of pre-treatments on microstructural features of isolated cotyledon cells ..22

Fig 2.8: Scanning electron microscope (SEM) images of pea flour milled with the impact (4000 rpm) (left) or the jet (4000 rpm) (right) mill. Starch granules (S) and clusters of cellular material (CM) can be distinguished.....29

Fig 2.9: Scanning electron micrographs of representative White/yellow, Marrowfat, Blue, and Maple peas sampled during *in vitro* oral-gastro and small intestinal digestion. G0, I60, and I120 represent after zero min at the gastric phase, 60 and 120 min at the small intestinal digestion phase.. 34

Figure 4.1: SEM micrographs of different varieties of raw New Zealand pea seeds. A, B, C, and D represent White/yellow, Marrowfat, Blue, and Maple peas, respectively, at 1000X. Note: E; starch granules and protein bodies encapsulated in the cell wall, SG: starch granule, PB: protein bodies, and CW: cell wall.....52

Fig. 4.2: Texture profile analysis (TPA) of cooked pea seed varieties. WP, White/yellow pea; MFP, Marrowfat pea; BP, Blue pea; MP, Maple pea. $^{a, b, c}$ Values in each set of bar charts with the same superscript letters are not significantly different ($p > 0.05$).....55

Fig. 4.3. Hydration kinetics of the pea variety. A. White/yellow pea; B. Marrowfat pea; C. Blue pea; D. Maple pea. 61

Figure 4.4. SEM electrographs of four different varieties of peas at 30 and 60 °C soaking temperatures. A B, C, and D represent WP, MFP, BP, and MP, respectively. Note (1 & 2 indicate 30 and 60 °C). CW; cell wall, and D.CW; distorted cell wall 61

Fig. 4.5. Starch hydrolysis (%) of a cooked pea; White/yellow pea (WP), Marrowfat pea (MFP), Blue pea (BP), and Maple pea (MP) during simulated oral-gastro-small intestinal digestion. .62

Fig. 4.6. Hydrolysis index (HI) and the estimated Glycaemic index (eGI) of the pea varieties. Note: The hydrolysis index (HI) and estimated Glycaemic index (eGI) for white bread. 62

Fig.4.7 Scanning electron micrographs of representative White/yellow, Marrowfat, Blue, and Maple peas sampled during *in vitro* oral-gastro and small intestinal digestion. Where G0, I60 and I120 are gastric digestion at 0 min, small intestinal digestion at 60 and 120 min.....67

Fig. 4.8: Principal component analysis (PCR): score plot of PC1 and PC2 describing the overall variation between pea seed varieties. 69

Fig. 4.9: Principal component analysis (PCR): Loading plot of PC1 and PC2 describing the overall variation between properties of pea seed varieties.....70

Fig 5. 1. Light microscope images of cotyledon cells from four different pea seed varieties (A: White/yellow pea, B: Marrowfat pea, C: Blue pea and D: Maple pea).....80

Fig 5.5. Relative crystallinity of cotyledon cells. Where, WP, MFP, BP, and MP cotyledon cells are White/yellow, Marrowfat, Blue, and Maple cotyledon cells respectively.....85

Figure 5.6 Starch hydrolysis of the cotyledon cells during in vitro gastro-small intestinal digestion. Where, WP, MFP, BP, and MP cotyledon cells are White/yellow, Marrowfat, Blue, and Maple cotyledon cells respectively. 87

Fig 5.7 Scanning electron micrographs of cotyledon cells samples isolated from four pea varieties (White/yellow pea, Marrowfat pea, Blue pea and Maple pea) during *in vitro* gastro and small intestinal digestion. Where G30 is gastric digestion at 30 min while I10 and 1120 are small intestinal digestion at 10 and 120 min respectively.....90

Fig 5.8 Scanning electron micrograph of the waste (retentate) generated during cotyledon cell isolation. Note. The circle indicated large clusters of cotyledon cells.....91

Fig 6.1 Schematic representation of the colloid milling process. 103

Fig 6.2 Particle size distribution of A) cotyledon flour and B) blended flour from the same botanical sources. Where, WP, MFP, BP, and MP are White/yellow, Marrowfat, Blue, and Maple cotyledon/flour respectively. 105

Fig 6.3 Pasting properties of A) cotyledon flour and B) blended flour. Where, WP, MFP, BP, and MP are White/yellow, Marrowfat, Blue, and Maple cotyledon/flour respectively. 108

Fig 6.4 Relative crystallinity of A) cotyledon and B) blended flours. Where, WP, MFP, BP, and MP are White/yellow, Marrowfat, Blue, and Maple cotyledon/flour respectively. Note. “cc” and “b” stands for cotyledon and blended flour. 109

Fig 6.5. Starch hydrolysis of the cooked (A) cotyledon flours, and (B) blended flours. Where, WP, MFP, BP, and MP are White/yellow, Marrowfat, Blue, and Maple cotyledon/flour respectively. G0, G15, and G30 (0, 15, and 30 min of gastric digestion), and I0, I5, I10, I15, I30, I60, I90, and I120 (0, 5, 10, 15, 30, 60,90, and 120 min of the small intestinal digestion).....113

Fig 6.6. Raw microstructure of cotyledon and blended flour. IC, intact cotyledon cells, S, starch granules & CM, and other cellular materials.....114

Where, A, B, C, and D represented White/yellow, marrowfat, blue, and maple cotyledon flours while E, F, G, and H represented White/yellow, marrowfat, blue, and maple blended flour.114

Fig 6.7. Scanning electron micrographs of cotyledon and blended flour digests from the same plant sources (White/yellow pea, Marrowfat pea, Blue pea and Maple pea) sampled during *in vitro* oral-gastro and small intestinal digestion. Where G30 is gastric digestion at 30 min while I10 and 1120 are small intestinal digestion at 10 and 120 min respectively.....119

Fig 7.1 Starch hydrolysis of bread samples. G0, G15, and G30 (0, 15, and 30 min of gastric digestion), and I0, I5, I10, I15, I30, I60, I90, and I120 (0, 5, 10, 15, 30, 60,90, and 120 min of the small intestinal digestion.....133

Fig 7.2 Scanning electron microscopy image of baked and digested bread samples (control, 25 and 50 % cotyledon flour). Where G30 is gastric digestion at 30 min while I10 and 1120 are small intestinal digestion at 10 and 120 min respectively.....137

Lists of Abbreviations

%	Percent
µm	Micro metre
a	cotyledon cell size
AACC	American Association of Cereal Chemists
AOAC	Association of Official Analytical Chemists
CW	Cellular Wall
CLSM	Confocal laser scanning microscope
cP	Centipoise
Da	Arithmetic mean
D.CW	Distorted cell wall
Dg	Geometric mean
DIC	Differential interference contrast
DSC	Differential Scanning Calorimeter
D∞	Diffusion coefficient at 1250ms
D_o	Diffusion coefficient at 30ms.
E	Encapsulating
g	Gram
h	Hour
IC	Intact cotyledon cell
HCl	Hydrochloric acid
J.g-1	Joule per gram
L	Length
LM	Light microscope
M	Molar
Mg	Milli gram
min	Minute
mL	Milli litre

NaOH	Sodium hydroxide
nm	Nanometre
°C	Degree centigrade
P	permeability
PB	protein bodies
PFG	pulsed field gradient
RO	Reverse osmosis
Rpm	Revolutions per minute
RVA	Rapid visco analyser
S	Sphericity
SEM	Scanning electron microscope
SG	Starch granule
SGF	Simulated gastric fluid.
SIF	Simulated small intestinal fluid.
T	Thickness
T*c*	Conclusion temperature of gelatinisation
T*gel*	Gelatinisation temperature
T*o*	Onset temperature of gelatinisation
T*p*	Peak temperature of gelatinisation
U	Unit
USP	Unit of enzyme activity
W	Width
w/v	Weight by volume
w/w	Weight by weight
α	Alpha
β	Beta
ΔH*gel*	Enthalpy of gelatinisation

Lists of publications & conference proceedings

Some of the chapters have been either been published, under review, or were presented at a conference.

Publications

1. Ajala, A., Kaur, L., Lee, S. J., & Singh, J. (2023). Native and processed legume seed microstructure and its influence on starch digestion and glycaemic features: A Review. *Trends in Food Science & Technology, 133*, 65-74. doi:10.1016/j.tifs.2023.01.011
2. Ajala, A., Kaur, L., Lee, S., & Singh, J. (2022). Influence of seed microstructure on the hydration kinetics and oral-gastro-small intestinal starch digestion in vitro of New Zealand pea varieties. *Food Hydrocolloids, 129*, 107631. https://doi.org/10.1016/j.foodhyd.2022.107631
3. Ajala, A., Kaur, L., Lee, S., & Singh, J. (2022). Microstructural, nutritional, and *in vitro* starch digestion properties of a novel cotyledon flour designed via Micronization Techniques. *Food Hydrocolloids* (under review)
4. Ajala, A., Kaur, L., Lee, S., Edwards, P.J & Singh, J. Cell wall permeability in relation to *in vitro* starch digestion of pulse cotyledon cells. *Manuscripts in preparation*

Conference Proceedings

1. Ajala, A., Kaur, L., Lee, S., & Singh, J. (2021, 7-9 April) *The influence of microstructure on the hydration kinetics of whole pea grain*. Poster session presented at the Riddet Institute conference, Wellington, New Zealand.
2. Ajala, A., Kaur, L., Lee, S., & Singh, J. (2021, 17-18 November), *Microstructural characteristics of raw and processed NZ pea varieties and their influence on hydration kinetics and oral-gastro-small intestinal starch digestion in vitro*. Poster session presented at the Cereal and Grain Conference for the American Association of Cereal Chemists (AACC), Virtual Meeting Series.
3. Ajala, A., Kaur, L., Lee, S., & Singh, J. (2023, 3-5 July) *Influence of seed microstructure on the hydration kinetics and oral-gastro-small intestinal starch digestion in vitro of New*

Zealand pea varieties. A presentation to be given at the NZFIST annual conference University of Otago, Dunedin, New Zealand.

Chapter 1: Introduction

1.1 Background information

Recently, two criteria have been established by consumers to define “wholesome food”. Namely, what are the nutritional and health-related benefits of consuming such food? These two criteria have been a major driver of the modern food industry.

Pulse seeds have recently been highlighted to fulfill the two criteria of a wholesome food because of their excellent sources of protein, starch, and micronutrients. Specifically, starch in pulse seed exhibits low glycaemic features and a high level of resistant starch (Robinson et al., 2019, Do & Singh, 2019 & Singh et al., 2017). These unique nutritional and health-related benefits of pulse seeds have been attributed to their microstructure, i.e., the arrangement of starch in cotyledon cells and interactions of starch with other non-starch macromolecules (protein, lipids, fiber) during processing (such as milling and extrusion) (Ma et al., 2011). The microstructural features of native pulse seed entail starch granules embedded within a protein matrix whereas the whole structure is encapsulated under the fibrous cell wall material (Edwards et al., 2021).

It has also been observed that the application of different processing techniques such as wet and dry milling to pulse seed transforms the native pulse seed microstructure into new forms of microstructure; cotyledon cells and pulse flour (Ajala et al., 2023). The different forms of microstructure from pulse seed exhibit distinct structural differences such as particle sizes and intactness of their microstructure which could determine their varying physicochemical, digestibility properties and food application potentials. For example, the pulse seed exhibits the slowest rate of starch hydrolysis compared to the other forms (e.g., cotyledon cells and pulse flour), but its large particle size impairs its broad application in food products. On the other hand, pulse flour has a suitable particle size for numerous food applications, but its microstructure is the least intact due to its starch granules being highly exposed to water and starch-degrading enzymes, thus resulting in a high rate of starch hydrolysis. In the case of cotyledon cells, they tend to have an applicable particle size and a reasonably intact microstructure, however, their extraction from pulse seeds is not efficient and sustainable (Ajala et al., 2023).

Therefore, understanding the underpinning mechanism of the interaction between the microstructural components in the different forms of pulse seed microstructure would provide fundamental insight into how to develop a low glycaemic "wholesome food" ingredient.

The objectives of this research were

1. To investigate the microstructural components of a raw whole pulse seed and how the interactions amongst these components influence the rate of intracellular starch granules gelatinization and digestion in four NZ pea varieties.
2. To objectively measure the cell wall permeability of an isolated cotyledon cell from four NZ pea varieties and its influence on entrapped starch digestion *in vitro.*
3. To explore a sustainable size-reducing technique (colloid milling) to transform the whole pulse seed to a new functional ingredient (cotyledon flour) with low glycaemic features in four NZ pea varieties.
4. To investigate the effect of cotyledon flour as a new food ingredient on the techno-functional properties of a food system.

1.2 Thesis overview

The research presented in this thesis provides a systematic investigation into the microstructural components (starch granules, protein matrix, and encapsulating cell wall) in the different forms of pea seed microstructure from four (4) different varieties and how the interaction between these structural components during processing influences starch gelatinization and hydrolysis properties. The thesis explored a sustainable processing technique (colloid milling coupled with acid/alkali pre-treatment) to transform pea seeds into a novel pea ingredient with moderate glycaemic features.

This thesis is comprised of eight chapters described as follows.

Chapter 1 describes the rationale behind the objectives of this thesis.

Chapter 2 is a literature review of the different forms of microstructures that can be obtained from pulse seed via size-reduction techniques, the different structural components of these

forms of microstructure, and how the interactions between these components influence starch hydrolysis.

Chapter 3 lists an overview of research questions based on the research gaps identified from the literature review provided in Chapter 2. It also outlines the hypotheses and the corresponding experimental chapters to test the hypotheses outlined.

Chapter 4 describes the microstructural components (starch and non-starch components in native microstructure) in whole pea seed and how these microstructure components interact and respond to pre-starch gelatinization (hydration kinetics set at 30, 40, 50, and 60 °C) and post starch gelatinization (*in-vitro* oral-gastro small intestinal digestion of cooked whole pea seed).

Chapter 5 discusses the specific role of cell wall permeability in the hydrolysis of intracellular starch granules in cotyledon cells using pulsed field gradient (PFG)-NMR coupled with light, confocal, and scanning electron microscopy.

In Chapter 6, based on the fundamental information obtained from Chapters 2,4 and 5, the use of a transformative technology (colloid milling coupled with acid/alkali treatments) to transform whole pea seed into a novel food ingredient known as “cotyledon flour” was investigated.

Chapter 7 discusses the effect of cotyledon flour as a novel food ingredient on the techno-functional properties of a standard food system (bread).

Finally, the general summary of the experimental work, conclusions, and future recommendations are presented in Chapter 8.

Chapter 2: Review of literature

2.1 Abstract

Background: Legume seeds are known to possess low glycaemic features and high levels of resistant starch. The seed microstructure, i.e., the arrangement of starch in cotyledon cells and interactions of starch with other non-starch macromolecules (protein, lipids, fiber) during processing, has been suggested to be responsible for these unique properties. The influence of various types of processing on their native microstructures and functional characteristics and the subsequent impact on their glycaemic features have not been examined.

Scope and approach: This review outlined two forms of legume seed microstructure (pulse cotyledon cells and pulse flour) that can be generated from whole seed during processing. The microstructural features of each form of microstructure generated and their subsequent influence on starch digestion properties were discussed.

Key findings and conclusions: The interactions between the above-mentioned microstructural features differ significantly and influence the functionality of the legumes and their processed products. The rate of starch digestion decreased in this order; seed flour > cotyledon cells > whole seed. Cell walls and protein matrices act as primary and secondary physical barriers responsible for modulating the activity of the starch-degrading enzymes for various legumes and pulses. Summarily, the intactness of the seed microstructure is a significant factor that affects the rate of starch digestion in whole pulse-based food ingredients. Whole pulse seed and pulse cotyledon cells have shown the potential for the development of low glycemic foods. However, optimization of the extraction yield of intact cotyledon cells and the sustainable use of the enormous waste generated during the extraction procedure should be further investigated to maximize their food application prospects.

2.2 Introduction

The importance of food microstructure in designing food processes and studying changes induced by various food processing operations cannot be overemphasized (Tiwari & Singh, 2012). Microstructural studies of food, in general, are essential, because most of the elements that are pivotal in transport properties and physical, rheological, textural, and sensorial behaviors are below the 100 µm size range (Aguilera, 2005). Also, food microstructure controls

the nutrient bioavailability, and digestibility of food products (Norton et al., 2007; Parada & Aguilera, 2007).

Specifically, low glycaemic index and high levels of resistant starch exhibited in pulse-based food products had been attributed to their microstructure i.e., the arrangement of starch in cotyledon cells, and interactions of starch with other non-starch macromolecules (protein, lipids, fiber) during processing (Ma et al., 2011). The microstructural features of native pulse seed entail starch granules embedded within a protein matrix whereas the whole structure is encapsulated under fibrous cell wall material (Edwards et al., 2021). The application of different processing techniques (such as cooking, milling, and extrusion) to pulse seed transforms the native pulse seed microstructure into new forms of microstructure. For example, via dry milling, pulse seed over the centuries has been transformed into pulse flours with varying particle sizes (Wood & Malcolmson, 2011). The main purposes of pulse milling include particle size reduction from seed to ground flour, separation of components (starch, protein, and fiber enrichment), and mechanochemical changes to the components (Pelgrom et al., 2013; Scanlon et al., 2018; Thakur et al., 2019). It has been shown that the structural differences observed in the microstructure of pulse seed and pulse flour ultimately determine the varying physicochemical and digestibility properties exhibited between the pulse seed and flour. Recently, different isolation procedures were developed to obtain a new pulse ingredient called “cotyledon cells” from pulse seeds (Junejo et al., 2021, Huang et al., 2021, Palchen ¨ et al., 2021. Edwards et al., 2020, Gwala et al., 2020; Li et al., 2020, 2020a, 2020b, Do et al., 2019; Xiong et al., 2018, 2019, Rovalino-Cordova ´ et al., 2019 & 2018, Pallares et al., 2018, Bhattarai et al., 2017 & Dhital et al., 2016). A detailed overview of the isolation procedures and the effects on the microstructural characteristics of cotyledon cells from pulse seed has been reviewed somewhere else (Pallares et al., 2021). Based on the available literature, pulse flours and cotyledon cells are major microstructural forms of pulse seed. However, detailed information on the microstructural features of these forms from pulse seed and the mechanism of how their microstructure influences starch digestion have not been reviewed. This review aims to conduct a comparative study of three forms of pulse microstructure: Whole pulse seed, Pulse flour, and cotyledon cells, their distinct microstructural features, and their influence on starch digestion.

2.3 Overview of Pulse seed production and consumption

Production of pulse globally experienced a steady growth of ≤ 62 million tonnes between 1997 and 2007 which was followed by a steep growth to reach 96 million tonnes in 2017(Figure 2.1). Asia represents the highest pulse-producing region with 43% of the global pulse production in 2017. Africa and America contributed about 20% of the total global production, while Oceania recorded 4% of the global production. The great increase in global pulse production could be attributed to the contribution of the Asia region (Joshi & Rao, 2016). The pea market seems to take a significant portion of the global pulse production with 10.4 million tonnes in 2011 and expected to increase by 5.49% in 2024 (Mordor Intelligence, 2020 & Miller Magazine, 2020)

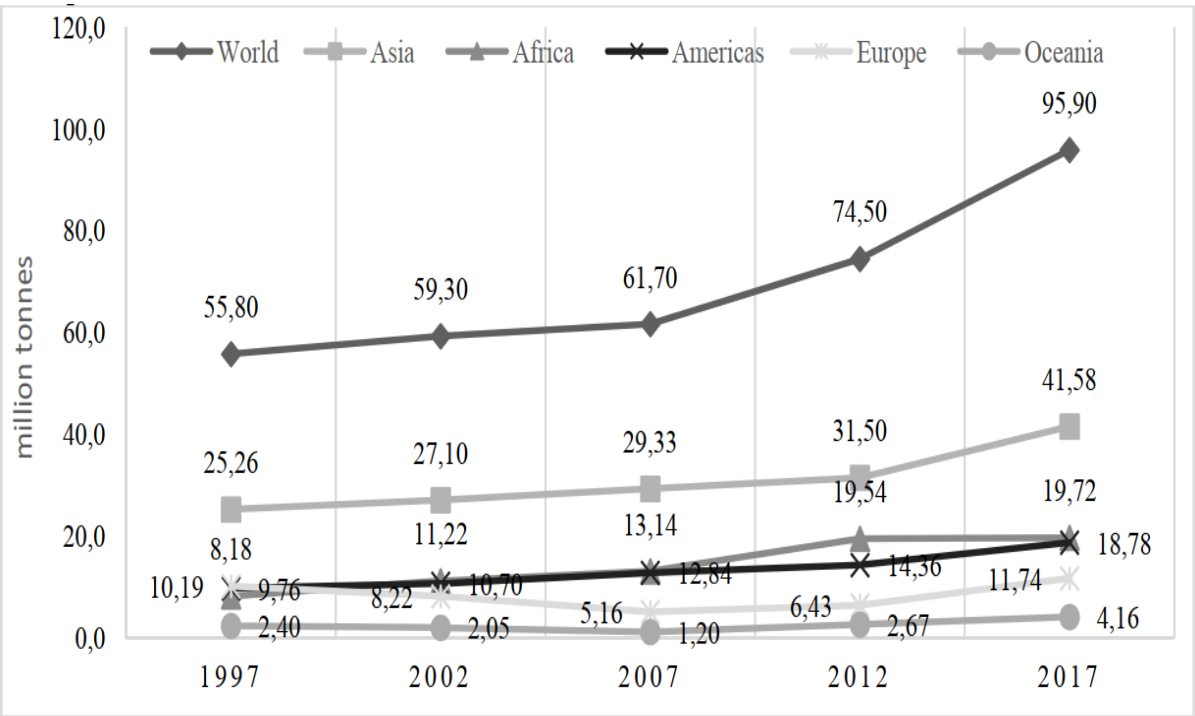

Fig 2.1: Global production of pulses (in million tonnes) by region between 1997-2017 (FAOSTAT, 2017).

America contributed 4.4 million tonnes of global pea production in 2014, followed by Europe (3.3 million tonnes), Asia (2.3 million tonnes), Africa (662,000 tonnes), and Oceania (361 tonnes) (Miller Magazine, 2020). The main pulse crop grown in New Zealand is field peas, field beans, and lentils (Millner et al., 2013). The average annual production of peas and beans is 59,850 and 14,725 tons from 2017 -to 2020 (Curran-Cournane & Rush, 2021). The average

person on the global scale consumed 7.2kg of pulse in 2013, which is 1.2 higher than the amount consumed in 1997 (Figure 2.2).

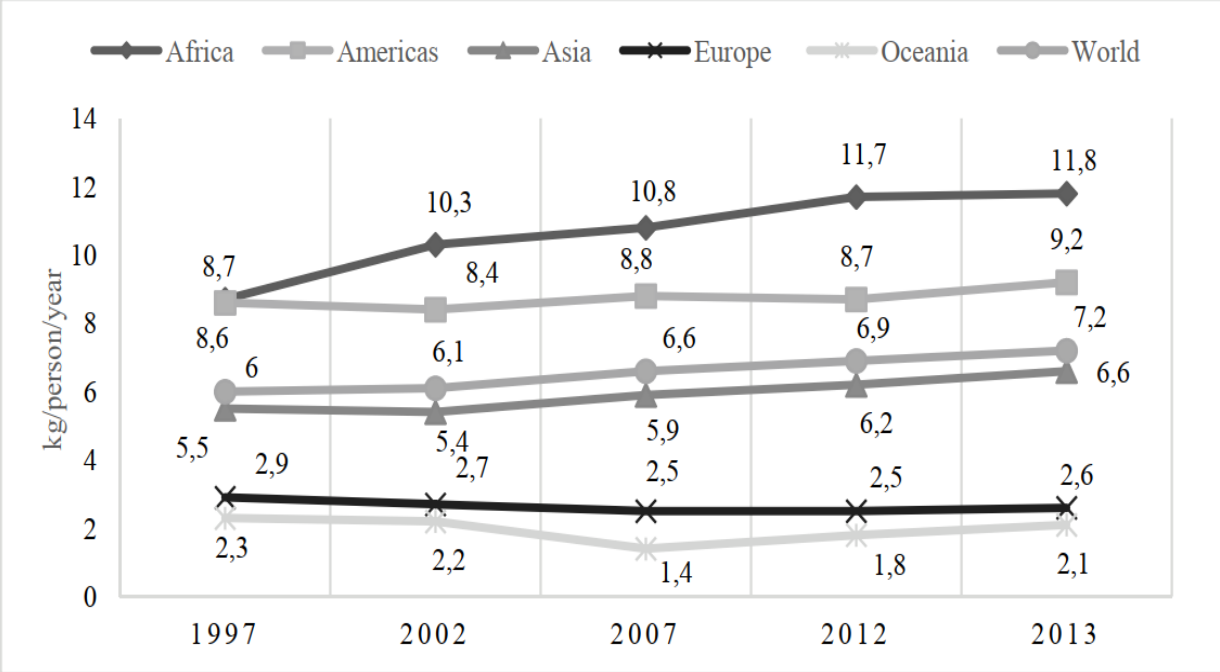

Fig 2.2: Consumption of pulses (in Kg/person/year) by region between 1997-2013 (FAOSTAT, 2017).

The consumption rate in Africa was observed to steadily increase over the years the study was conducted (1997-2013) with the highest at 11.8kg/person in 2013. The reason for the high rate of consumption in Africa is the dynamic population growth in the region. America and Asia also experienced a somewhat increase in consumption of pulse at 0.6 and 1.2 kg/person, respectively in 2013 compared to 1997. The consumption rate for Europe and Oceania seemed to be unchanged over the years.

2.4 Environmental benefits of pulse production

The agricultural processes from farm to stead (Crop production, food processing, and product marketing) generate greenhouse gases (GHG) that absorb infrared radiation in the atmosphere, trapping heat and warming the surface of the Earth, contributing to global climate change (Oliveira et al., 2019). Agricultural practices in 2010, produced approximately 12 gigatonnes of CO_2 equivalent emissions (GtCO2eq), accounting for 24 % of the 49 GtCO2eq total GHG emissions for that year (IPCC, 2014). Carbon dioxide (CO_2), methane (CH_4), and

nitrous oxide (N_2O) are the GHGs associated with agricultural practices, and they tend to trap the atmosphere heat to a different degree (EPA, 2012).

The symbiotic relationship of pea crops with soil microorganisms such as *Rhizobia* enables peas to fixate nitrogen from atmospheric nitrogen into the soil, therefore reducing the need for energy-intensive synthetic nitrogen (Tulbek et al., 2017). For example, based on 12 years of field data (1987-98), Zentner et al. (2004) reported that growing pea crops required half the energy input of spring wheat in western Canada. Pulses due to their relatively high protein content present a low carbon footprint by reducing farmers' dependence on synthetic N fertilizers (N inputs) responsible for generating N_2O emissions (Lemke et al., 2007, Tongwane et al., 2016). Pulse crops can present a carbon footprint due to their ability to fix atmospheric nitrogen(N_2) into the NH_4+ that is largely used to form protein compounds, thus, reducing the N availability for nitrification and subsequent denitrification that is associated with N_2O emission (Snyder et al., 2009).

Furthermore, in a diversified crop rotation study, Gan et al. (2011) observed a lower carbon footprint of durum wheat grown after pulse crop in a diversified cropping system than in a monoculture cereal system. Also, the total energy requirement of the entire system was reduced by 13% when 1 year of pea was included in a 4-year crop rotation cycle (Pulse Canada, 2020).

Compared to other crops such as cereal and oilseeds, pulses require less water for production, for instance, water required to produce one kilogram of beef, mutton, chicken and lentils are approximately 13,000, 5,520, 4,325, and 1,250 L, respectively (FAO, 2016). Hence, pulse crops can be cultivated in regions with erratic or limited rainfall and can with drought stress better compared to wheat (Cutforth et al., 2009).

Food spoilage and wastage from the storage of pulses are quite low due to the long storage capacity of pulse crops at room temperature. The nutritional content of a pulse crop can be retained for a year if stored in dry places (at room temperature), in airtight containers, and protected against rodent, insect, and micro-organism attacks (Tiwari & Singh 2012, FAO, 2016). This attribute makes pulses an essential grain in developing countries where the development of advanced storage technology is still underway (FAO, 2012)

2.5 Nutritional and health benefits of pulse diet

Malnutrition is a global issue that occurs as a result of protein, energy, and/or micronutrient deficiencies (including low bioavailability) in commonly consumed foods, however, pulse contains a relatively high concentration of protein (~30 %) are low in fat, slowly-digestible carbohydrates and essential micronutrients (Fe, Zn, and Se, folates, and carotenoids), hence it is a potential staple crop to tackle malnutrition Table 2.1; (Thavarajah et al.,2019 & Oliveira et al., 2019). The average content of Fe, Zn, Se and Folates and beta-carotene in peas range from 4.15-8.15 mg/100g, 2.95-4.4 mg/100g, 32.5-51.5 mg/100g, 83.5-253 µg/100g, and 152.5-553 µg/100g respectively (Roe et al., 2015, Sen Gupta et al., 2013 & Johnson et al., 2013). This further buttressed the potential of a pulse as superior food.

The soluble fiber content of pulses has been reported to positively affect colon health through the production of short-chain fatty acids (SCFA), control blood glucose levels, and reduce blood LDL-cholesterol levels, which can lower the risk of heart attack and stroke (Curran, 2012, Ha et al., 2014, Tosh & Yada, 2010 & Bazzano et al., 2011). The insoluble pulse fiber, on the other hand, promotes the movement of material through the digestive system, thereby improving laxation, and being associated with fecal bulking through its water-holding capacity (McCrory et al., 2010 & Tosh & Yada, 2010).

Pulses have a low glycaemic index, meaning that they do not cause a fast rise in blood sugar after eating, which is particularly important for preventing or managing diabetes (Hosseinpour-Niazi et al., 2011, Singhal et al., 2013, Foster-Powell et al., 2002). For instance, Marinangeli & Jones (2010) investigated glycaemic response and insulin resistance of whole and split pea flour in hypercholesterolemic overweight patients in a 56-day study. It was discovered that whole pea flour reduced fasting insulin more than split pea flour which was due to the presence of the pea hull fiber. Resistant, slowly digestible starch and the raffinose family of oligosaccharides are the other complex carbohydrates that are present in pulse grain (McCrory et al. 2010). The oligosaccharides and resistant starch function by resisting digestion; and when fermented by the colon's microflora, they produce gases that give flatulence, and SCFA that support the health of the intestinal mucosa (Tosh & Yada, 2010 & Hoover et al., 2010).

Finally, pulses are a low-fat source, containing zero cholesterol, and are free of gluten, hence they are also an ideal food for celiac patients and can also serve as part of healthy vegetarian diets (Leterme, 2002 & Hall et al.,2017).

2.6 Application of pulse as a food ingredient

Most pulses are sold as a food product in whole or split dried seed form, however, the schematic diagram below (Figure 2.3) shows that tremendous food industry-based applications are available for pea flour and factions (Table 2.1).

In general, 10-30 % wheat flour had been replaced by pulse flour in a gluten-free formulation which subsequently had a minimal effect on the on-end quality and processing conditions (Malcolmson et al., 2019). However, the pulse flavor could negatively impact the sensory properties of the end products. Both pea hull and inner cell wall fiber fractions around a 5 % level of inclusion have been added to gluten-free formulations to increase the fiber content of foods and improve the functional properties of food formulations. Also, pea cell wall fiber has been shown to have good fat-retaining and texture-modifying properties in low and high-fat beef patties (Anderson & Berry 2000, 2001).

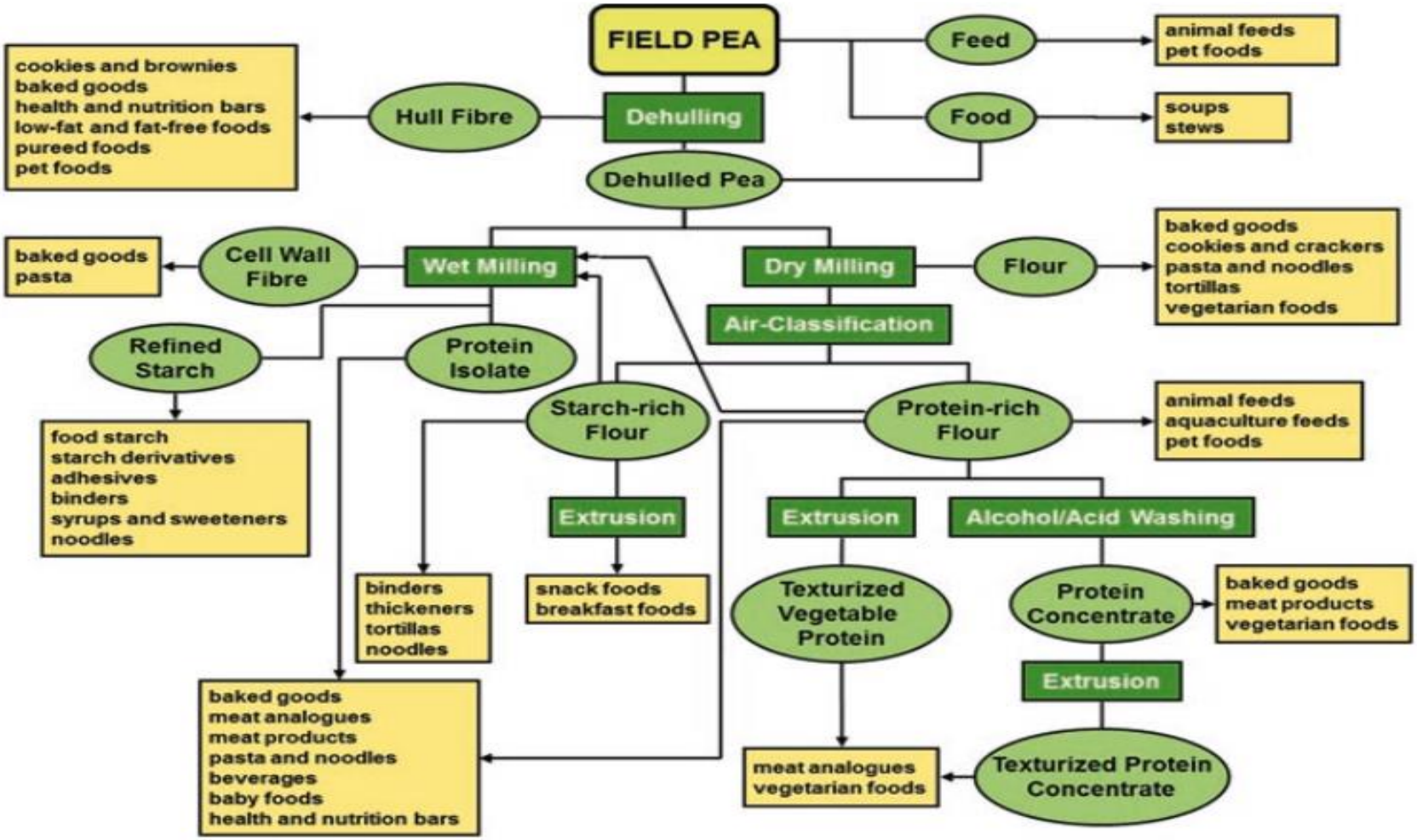

Fig 2.3: Application of pea ingredients in food. Reproduced from Han et al. (2010)

Table 2.1: Some applications of pulse flour and their fractions

Pulse Ingredient	Food products	Objective	Reference
Pea, lentil, chickpea hull fibers and cell wall fibers	Bread, Bagels and tortillas, Pasta, Cookies	Fiber enrichment	Dalgetty & Baik, 2006; Rosell et al., 2005; Wang & Daun, 2004; Gómez *et al*., 2008; Tudorică et al., 2002; Piteira et al.,2006.
Lentil, bean flour	Cookies, Crackers	Nutrient fortification	Malcolmson et al. (2013);Zucco et al. (2011)
Bean, chickpea, pea, lentil Flours	Tortillas, cake		Anton etal., (2008); Malcolmson et al. (2013); Gómez et al., (2008)
Pea, lentil, chickpea flours, pea hull fiber	Extruded products		Frohlich et al. (2014); Anton etal., (2008, 2009),
Bean flour			Simons et al. (2015); Kelkar et al. (2012); Hood-Niefer & Tyler (2010)
Chickpea, lentil flours, pea hull fiber, pea protein	Beverages		Zare et al. (2015)
Chickpea, lentil, pea flour	Salad dressings		Ma et al. (2016a, b)
Lentil flour	Yogurt		Zare et al. (2011)
Chickpea, pea, lentil flours	Pizza crust, Cookies	Gluten-free	Malcolmson et al. (2013),
Bean flour	Crackers		Simons & Hall (2018)
Chickpea, lentil, pea, bean flours, pea protein, starch, fiber	Bread		Han et al. (2010), Miñarro et al. (2012)
Pea protein isolate, pea cell wall fiber	Low-fat fish sausage	Texture modification	Osen et al. (2014), Cardoso et al. (2008)
Chickpea flour	Low-fat bologna		Sanjeewa et al. (2010)
Pea flour, fiber, starch	Low-fat beef patties		Pietrasik & Janz (2010)
Pea cell wall fiber	Low-fat sausages		Anderson & Berry (2000)
Pea flour	Meat analog		Kaack & Pedersen (2005)

2.7 Pulse as a low glycaemic index food

Grain legumes were first identified as Low glycaemic food over 20 years ago (Jenkins et al., 1981, 1983; Thorne et al., 1983 & Bornet et al., 1997). Jenkins introduced the term "Glycaemic index" in 1981 to classify carbohydrates foods based on the potential of a rise in blood sugar post-prandial (Wolever et al., 1991). Bornet et al. (1997) classified the glycaemic index value of various food products including legumes as shown in Figure 2.4. The chart showed that Legumes produced the lowest glycaemic response (20-40 %) in this order Soya beans > Lentils > Split peas while bread and potatoes had the highest glycaemic indices (79-90).

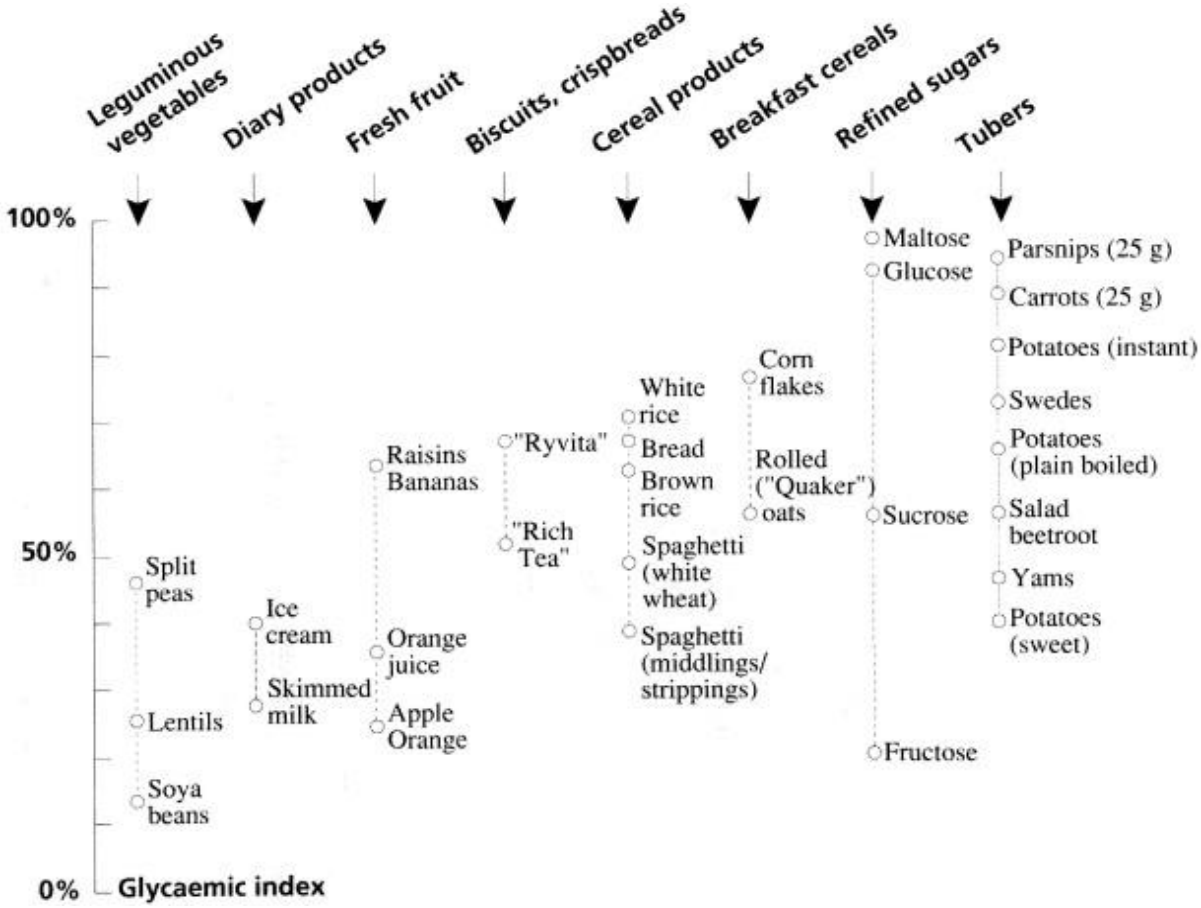

Fig 2.4: Classification of Glycaemic index of various food products using glucose as the reference. Reproduced from Bornet *et al.* (1997)

2.8 Peas' nutritional composition

The nutritional composition of some pulses including peas are reported in Table 2.2 The protein content of these pulses generally falls between the range of 14 % to 31 %. Lupin had the highest protein content on average (38 %), while chickpea and kidney had on average almost half of that of Lupin (22-23 %). Also, the variability in pulse protein contents reported in Table 2.3 may be attributed to the environment and cultivars (Wang & Daun, 2004, 2006). Pulse protein is twice the amount found in cereals, which is characterized by low sulfur-containing amino acids and high lysine (Malcolmson & Han, 2019). A wide variation of results has been observed in the carbohydrate contents for each pulse species (Table 2.2). Besides the variation in cultivars which may be responsible for the range of pulse carbohydrate content, differences in carbohydrate evaluation methods could also be a contributing factor. The carbohydrate value of the reported pulse varies in the decreasing order as follows; Pinto bean > Navy bean > Black gram > Broad bean > Kidney bean > Pea > Lupin > Lentils. In the same vein, the starch content of the selected pulses reportedly varied in increasing order as follows; Lupin (1-9 %)< Navy bean and Pinto bean (27-40 % and 21-40 %) < Kidney bean (31-43 %) < Chickpea (30-56 %) < Lentils (37-59 %) (Frimpong et al., 2009, Karaca et al.,2011, Ghumman et al., 2016, Fouad & Rehab, 2015, Wang et al.,2010, Hoover & Ratnayake, 2002, Calabrò et al., 2015 & Jha et al., 2015).

Lipids content in pulses are generally lower (> 3 %) than in cereals (Hall et al., 2017). Black gram (1.6 %), Lentils (1-3 %), Broad bean (2.3 %), Navy Bean (2 %), and Pinto Bean (1-2 %) represent the typical lipid content of pulse as shown in Table 2.3. However, Lupin and chickpea reported 15 % and 7 % lipids content, respectively. Caprioli et al. (2016) observed the same trend when they compared the lipid content of over 10 pulses using 6 different extraction methods. They found the lipid content ranges from 2.1 %- 14 %, the high lipids in some of the pulses would be attributed to extraction protocol.

Table 2.2 Nutritional composition of some pulse grain

Pulse Type	Crude Protein (%)	Lipids (%)	Crude fiber (%)	Ash(%)	Carbohydrates (%)	References
Black gram	26.9	1.6	1.0	3.6	66.9	Asif et al., (2013).
Chickpeas	19 - 27	2-7	3.0	1.8-3.5	52 -71	Cai et al., (2002), Sreerama et al., (2012), Karaca et al., (2011), Masood et al., (2014), Xu et al., (2013) Ray et al., (2014), Asif et al., (2013).
Kidney bean	17-27	1-5	NA	3.2-5.2	63-74	Wang et al.,(2010), Sutivisedsak et al., (2010), Fan et al.,(2014), Caprioli et al., (2016), Oomah et al., (2008).
Lentil	23-31	1-3	0.8	2.1-3.2	42-72	Ray et al., (2014), Fouad & Rehab, (2015), Ghumman et al., (2016), Zhang et al.,(2014a & 2014b), Asif et al., (2013).
Broad bean	26.7	2.3	7.2	3.6	64.0	Asif et al., (2013).
Pinto bean	18-25	1-2	NA	2.5-4.7	70-76	Wang et al.,(2010), Hoover & Ratnayake, (2002), Audu & Aremu, (2011).
Navy bean	19-27	2	NA	4.0-4.9	67-75	Caprioli et al., (2016), Gujska & Khan, (1991), Hoover & Ratnayake, (2002), Moraghan & Grafton,(2001).
Lupin	32-44	5-15	NA	2.6-3.9	47	Erbaş et al., (2005), Ertaş & Bilgiçli, (2014), Sujak et al., (2006), Calabrò et al., (2015).
Pea	14-31	1-4	1.6	2.3-3.7	55-72	Asif et al., (2013), Alonso et al., (2000), Tzitzikas et al., (2006), Fan et al.,(2014).

2.9 Pulse seed microstructure

The seed coat, germ, and cotyledon are the three main parts that are considered when studying the microstructure of pulse seed (Tiwari & Singh, 2012). The seed coat functions as a protective outer shell encapsulating the embryo, while cotyledon constitutes the largest portion of the mature seed and stores nutrients required for the early growth of the seedling (Yousif et al., 2007). Generally, the cotyledon accounts for an average of 80–90 % of the total pulse seed while seed coat and germ contribute 8–16 % and 1–3 %, respectively (Tiwari & Singh, 2012 & Yousif et al., 2007).

The seed coat develops from the formation of inner and outer integuments surrounding the growing ovule. The several distinct cell layers from the seed coat (testa) structure are later formed from outer integuments during seed development (Souza & Marcos-Filho, 2001).

The seed coat layers of pulses fundamentally consist of cuticle, epidermis, hypodermis, and interior parenchyma, respectively. These seed coat layers change when subjected to different processing techniques. The germ is also known as an embryonic axis which is made up of two main parts: embryonic roots (radicle) and embryonic shoots (plumule) (Tiwari & Singh, 2012). This is part of the seed that functions as a reproductive site (Souza & Marcos-Filho, 2001).

Pulses are classified as dicotyledonous or dicots, which contain highly organized structures with major components distributed within discrete cellular compartments as shown in Fig.2.5. The cotyledon tissue is mainly made up of large parenchyma cells. The cell walls of two adjacent cells of these parenchyma cells are joined to each other by the pectin-rich middle lamella. The surrounding subcellular organelles such as starch granules, protein bodies, and oil bodies are enclosed within the cell membrane of each parenchyma cell by a cytoplasmic network fill (Bhattacharya et al., 2005 & Wood et al., 2011). The cotyledon is an essential functional part of the pulse seed, that is, changes in the microstructural organization of the cellular component of the cotyledon during food processing such as cooking, and storage could ultimately affect the functional properties and starch digestibility of food ingredients derived from the pulse seed.

2.10 Recent advances in pulse microstructure: three (III) forms of microstructure from pulse seeds

Based on the available literature, two groups of particle size reduction techniques (dry and wet-based) can generate two sub-forms of new microstructure from a whole pulse seed (Form I), namely, pulse flour (Form III) and pulse cotyledon cells (Form II) (Fig. 2.5).

2.10.1 Form I: Whole pulse seed

There is a dearth of information on the microstructure of intact whole pulses before processing. Diedericks et al. (2020) employed cryo-SEM (Cryo-scanning Electron Microscopy) and CLSM (Confocal Laser Scanning Microscopy) to investigate the changes in the natural microstructure of Bambara groundnut whole seed subjected to two pre-treatments (soaking and roasting). They illustrated distinct locations and characteristics of starch granules, protein bodies, oil bodies, and cell wall components in the Bambara seed. The size of starch granules, protein, and oil bodies for this study ranged from 7 to 45 µm, 1–5 µm, and > 0.5 µm, respectively, and they agree with the previous report for other pulses (Do & Singh, 2019; Kaptso et al., 2014; Kornet et al., 2020).

On the other hand, Ajala et al. (2022) with the aid of SEM and image analysis observed how the microstructures of four different varieties of New Zealand pea seeds respond to pre-and post-processing conditions. The image of the pea microstructure provided by this study as shown in Fig. 2.6 afforded a more objective distinction of the components of the pea microstructure (starch granules, protein bodies, and cell wall materials) than what was reported by Diedericks et al. (2020). This means that morphological properties of the pulse's microstructure can be better characterized from the image provided by SEM and image analysis compared to cryo-SEM. From their study, Ajala et al. (2022) reported the number of starches per cell, cotyledon cell diameter, the thickness of cotyledon cell wall, and the average size of starch granules as 9.6–12.0/cell, 83.90–99.17 µm, 3.66–8.77 µm, and 20.36–31.96 µm, respectively.

In linking the microstructural changes in the Bambara seed after subjecting to soaking (for 48 h) and roasting (70–179 °C), Diedericks et al. (2020) could only provide an overview of the changes that might occur in the pulse's microstructure without a clearly defined role of each component of the seed microstructure during the pre-treatment conditions. Surprisingly,

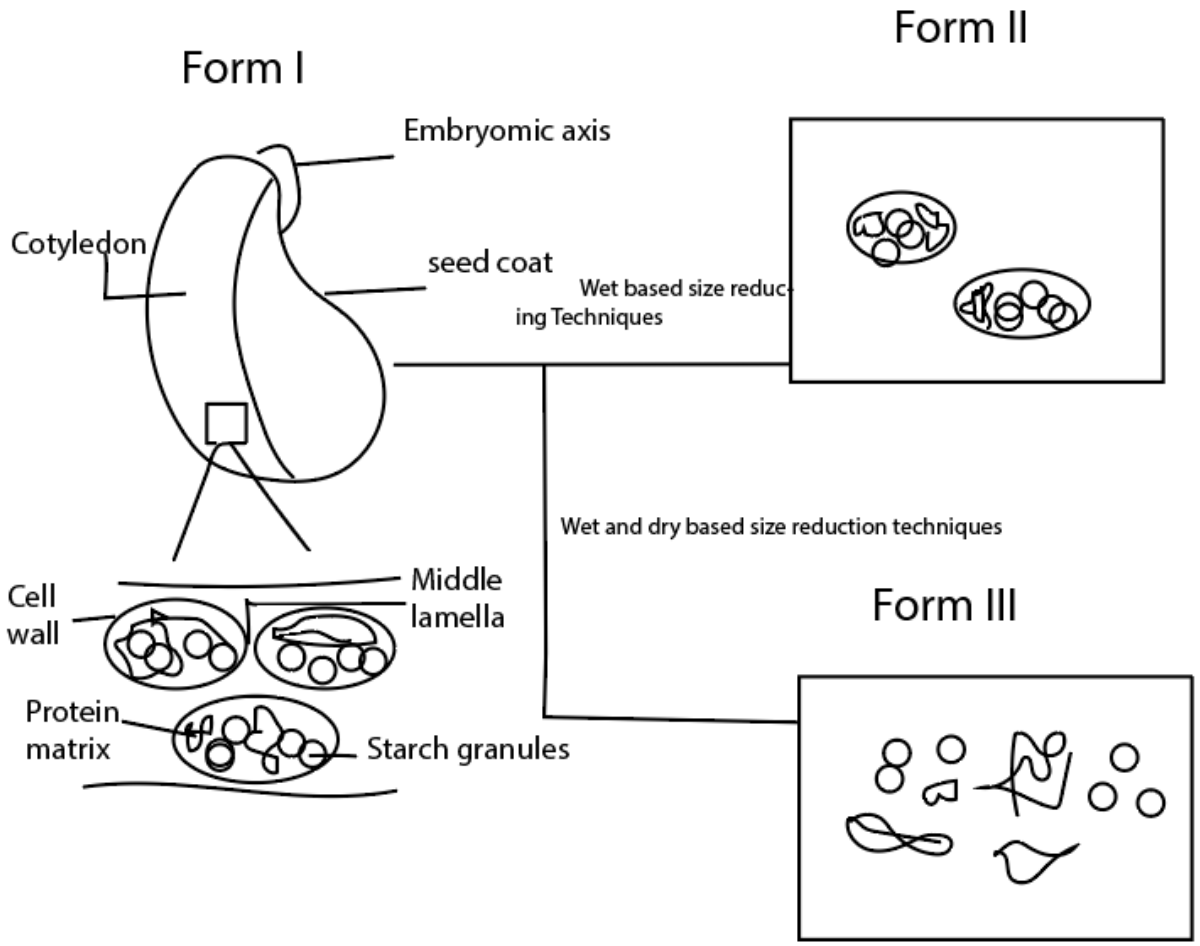

Fig 2.5: Two forms of pulse microstructure from pulse seed. Form I, II & III are whole pulse seed, intact pulse cotyledon cells, and pulse flour, respectively.

however, Ajala et al. (2022) reported a direct relationship between the components of the microstructure of pea seed with pre-processing conditions (Hydration kinetics set at 30, 40, 50, and 60 °C). They observed that there was a decrease in the intactness of the cotyledon structure from raw (room temperature) to 60 °C. The distortion of the cell wall enclosing starch, protein, and other macromolecules was less observed in the Maple pea (Fig. 2.7) variety at 60 °C compared to the other varieties. This probably explained the low rate of water uptake by the MP variety because of the strong interconnecting cell wall network holding the cotyledon structure together across different soaking temperatures. Furthermore, the number of starch granules per cell followed the same decreasing pattern with equilibrium moisture content at 30 and 60 °C (Ajala et al., 2022). During the initial phase of hydration kinetics in

pulses, the quantity of water uptake by the cotyledon of the pulses into the intracellular space is determined by the amount required for starch gelatinization, protein denaturation, and dissolution of the middle lamella (Mikac et al., 2015; Zhang & Mccarthy, 2013). Thus, the number of starch granules per cell will determine the maximum uptake of water required for its gelatinization as shown by Marrowfat pea varieties for this study. Berg et al. (2012) and Edwards et al. (2021) in their separate studies showed that hydrothermally processed navy beans and chickpeas at high temperatures (121 °C) and extended cooking time (1 h 25 min) respectively do not significantly disrupt the microstructure of the pulse seeds.

Under these cooking conditions, the starch granules are gelatinized, and the protein bodies are denatured, however, the interconnecting cotyledon cells that made up the cotyledon structure of the pulse seed are still largely intact. The extremely high cellular integrity exhibited by the pulse seeds after cooking could be attributed to the relatively high level of type I primary cell wall (mainly composed of pectic polysaccharides and xyloglucans) found in cotyledon cell walls that made up the pulse seeds (Berg et al., 2012; Edwards et al., 2021).

2.10.2. Form II: Isolated cotyledon cells from pulses.

The particle size distribution in a potential food ingredient is somewhat inversely proportional to the extent of its application in a food product. That is, a smaller particle size distribution in an intended food ingredient would find its application in a broader food product. A whole pulse seed has limited application in the food industry due to its size; 6.91–9.07 mm (Length) x 6.12–7.71 mm (Width) x 6.46–7.83 mm (Thickness) (Ajala et al., 2022). Based on the available literature on the microstructure of whole pulse seeds, they are largely made up of a network of cotyledon cells joined together by intracellular water-soluble fibrous materials that give the seed its crystalline structure (Singh, 2017).

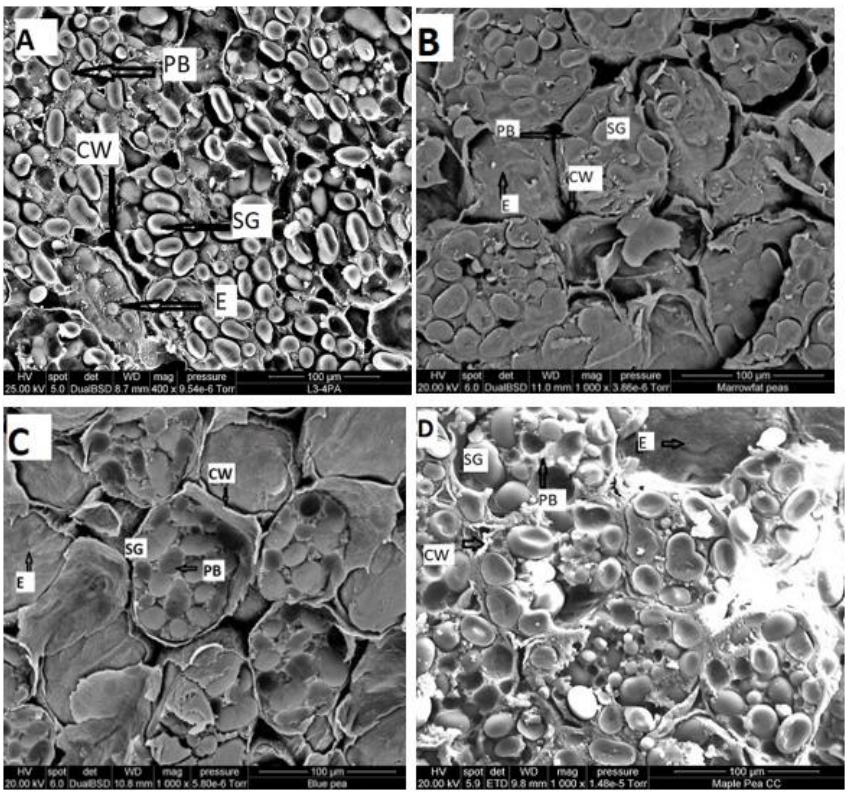

Fig 2.6: SEM micrographs of different varieties of raw New Zealand pea seeds. A, B, C, and D represent White/yellow, Marrowfat, Blue, and Maple pea, respectively, at 1000X. Note: E; starch granules and protein bodies encapsulated in the cell wall, SG: starch granule, PB: protein bodies, and CW: cell wall (Ajala et al., 2022).

In addition, the cotyledon cells seem to be the "functional unit" of the whole seed. Besides, the cells house the macromolecules (starch granules, protein bodies, lipids, and fiber), and the cell wall materials enclosing these nutritional molecules regulate the inflow of water (soaking), enzymes (starch and protein digestion), temperature (starch gelatinization and protein denaturation) and pressure during various processing techniques. Therefore, isolating these cells would be an important step toward establishing a novel food ingredient from pulse seed. An array of isolation methods of cotyledon cells from pulse grains have been explored by different researchers in recent years (Junejo et al., 2021, Huang et al., 2021, Palchen ¨ et al., 2021. Edwards et al., 2020, Gwala et al., 2020, Li et al., 2020, Li et al., 2019a, Li et al., 2019b, Do et al., 2019, Xiong et al., 2019, Rovalino-Cordova ´ et al., 2019 & 2018, Xiong et al., 2018, Pallares et al., 2018, Bhattarai et al., 2017 & Dhital et al., 2016). A detailed overview of the isolation techniques, yield, shape, and particle size distribution of isolated cotyledon cells from different pulse seeds are covered in this review (Table 2.1). The underpinning mechanism in the array of isolation methods of cotyledon cells primarily involves soaking of dry pulse seed

in either water or strong acid/alkali solutions (Do et al., 2019; Edwards et al., 2020; Gwala et al., 2020; Huang et al., 2021; Junejo et al., 2021; Li et al., 2019a, 2019b). The soaking of dry pulse seed in different media is to facilitate the hydration of the seed (Palchen et al., 2021). The adequate hydration of dry pulse seed in excess media is an important step that would help preserve the integrity of the isolated cotyledon cells. The main function of soaking media (water or strong acid/alkali) is to efficiently dissolve the middle lamella that fused the cotyledon cells while minimizing damage to the underlying primary cell wall (Li, Gidley, & Dhital, 2019). The temperature-time and acid/alkali-concentration relationship of the soaking media is primarily engineered to enhance the easy separation of the individual cotyledon cells. From the isolation methods shown in Table 2.3, it could be observed that the thermal-assisted method tends to achieve the pectin solubilization in the middle lamella faster than the acid/alkali-assisted method. After soaking, the pulse seed is manually crushed (gently) with mortar and pestle, then a series of sieves arranged in a stack with the different mesh sizes (53–250 µm) are used to separate the isolated cotyledon cells under running water.

The overall shape and particle size distribution of the isolated cotyledon cells range from spherical to ellipsoidal and 40–200 µm, respectively. Furthermore, the yield of the isolated cotyledon cells is scarcely reported in the available studies. However, few authors recorded a total yield of less than 30% (both wet and dry basis) for the isolated cotyledon cells (Bhattarai et al. 2017 & Palchen ¨ et al., 2021). It is assumed that the low yield of isolated cotyledon cells could be attributed to the nature of the isolation techniques used. More specifically, the soaking and cooking temperatures, pH, type of salts, acid, and alkali used, and concentration. A detailed insight into the relationship between isolation techniques and the total yield of cotyledon cells could only be established if more information on the yield of the isolated cotyledon cells is provided in the literature.

The pre-treatment used in the isolation techniques for cotyledon cells from pulse seeds has been categorized into three types, i) thermal treatment of pulse seed below starch gelatinization temperature, ii) thermal treatment of pulse seed above starch gelatinization temperature, and iii) acid/alkali treatment at room temperature (Pallares et al., 2021). Ideal microstructural features of cotyledon cells in their native nature would entail an encapsulating cell wall housing densely packed starch granules and protein bodies in the intracellular space of the cell. The pre-treatment techniques employed during the isolation procedure on the

pulse seed would invariably affect the structural integrity of the microstructural features of the resulting isolated cotyledon cells. This would in turn affect the physicochemical and functional behavior exhibited by the isolated cotyledon cells.

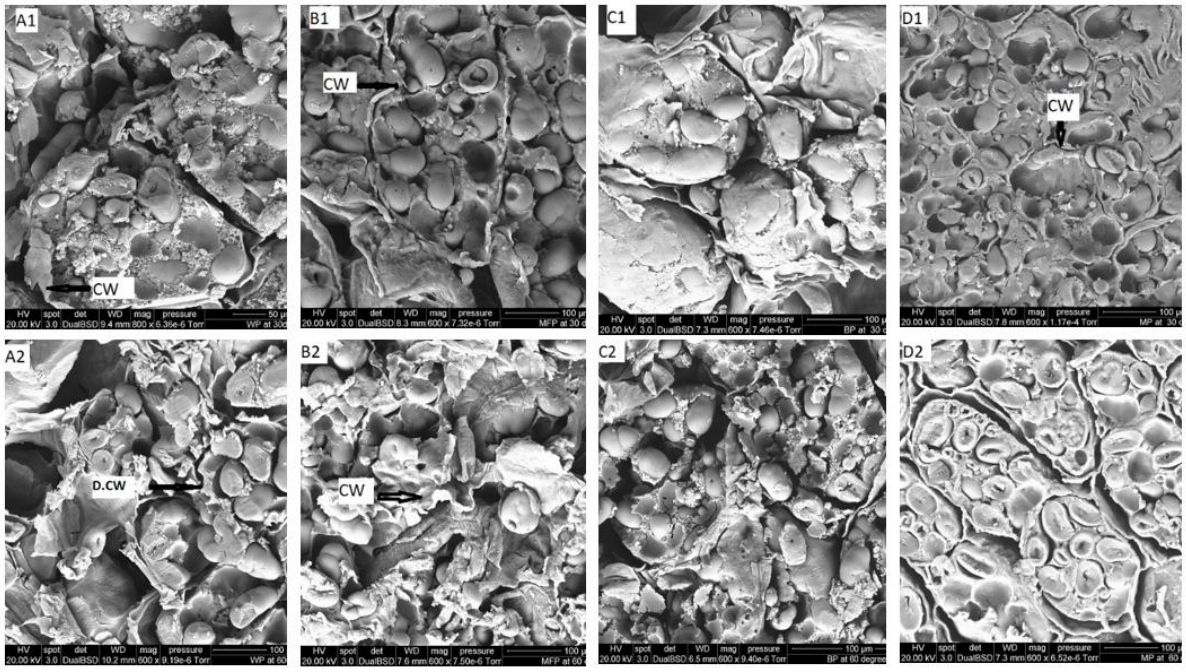

Fig 2.7. SEM electrographs of four different varieties of peas at 30 and 60 °C soaking temperatures. A B, C, and D represent WP, MFP, BP, and MP, respectively. Note (1 & 2 indicate 30 and 60 °C). CW; cell wall, and D.CW; distorted cell wall (Ajala et al., 2022).

2.10.2.1. Effects of pre-treatments on microstructural features of isolated cotyledon cells

2.10.2.1.1. Cell wall.

The cell wall of an isolated cotyledon cell from pulse seed mainly comprises pectin polysaccharides and xyloglucans. It modulates the inflow of water and enzymes from the cell's outer surroundings during processing. The level of cell porosity and/or permeability of these structural features could be indicative of the changes that have occurred during different pre-treatments applied for cotyledon cell isolation. In recent years, authors have preferred employing the fluorescently labeled dextran method to the linear dextran method for evaluating cell porosity and/or permeability properties in plant cells.

This is because the latter method could not provide a full representation of the interaction between the cell wall and digestive enzymes (Pallares Pallares et al., 2021). A fluorescein-

labeled dextran method is used to evaluate the porosity/permeability of plant cells (cell wall) when subjected to different molecular weights of FITC-dextran solutions (Li, Gidley, & Dhital, 2019 &2019b). Li, Gidley, & Dhital (2019) investigated the cell wall porosity/permeability using the fluorescently labeled dextran method for isolated cells from red kidney beans with two different pre-treatment techniques; namely cooked at 90 °C for 1 h and acid/alkali treatment (0.05 M HCl, 0.025 M NaOH) at room temperature. They reported that the cell wall from acid and alkali treatments was more permeable to 20 and 70 kDa dextran than from the cooked cell wall. Also, permeability was exhibited by the cells from acid/alkali treatments to 150 kDa dextran while permeability was not observed in the cell wall from cooked cells. The authors concluded that low cell wall porosity is observed in the cooked cells compared to the cells from acid/alkali treatments. On the other hand, Li, Zhang, & Dhital (2019) showed that cotyledon cells obtained from acid/alkali treatments (0.05 M HCl, 0.05 M NaOH) showed less permeability than the cells obtained thermally at 80 °C for 30 min (above starch gelatinization conditions) when subjected to 70 and 150 kDa fluorescently labeled dextran probes. This differing result may be attributed to the different isolation conditions in each study such as the acid/alkali concentration was not replicable for the two studies. For the permeability behavior of the cell wall obtained thermally from below starch gelatinization temperature, Xiong et al. (2019) observed that the cell walls of the cells obtained from common beans via thermal treatments at 60 °C for 1 h were not permeable to 20 kDa fluorescently labeled dextran probe. Furthermore, Huang et al. (2021) showed pinto beans cell wall permeability increased with an increase in thermal treatment from 60 to 100 °C when subjected to a 70 kDa fluorescently labeled dextran probe.

Table 2.3: Isolation methods of pulse cotyledon cells from some pulse seeds.

References	Pulses	Isolation methods	Shape and particle size distribution (um)	Yield (%)
Junejo et al., 2021	Smooth pea	Soaked in a solution of $NaHCO_3$ (1.5 %, w/v) and Na_2CO_3 (0.5 %, w/v) at 4 °C Thermal treatments (60 °C, 1 h, 500 rpm).	Ellipsoidal or elongated.153 µm ($D_{0.5}$ median particle diameter).	Not reported
Huang et al., 2021	Pinto beans	Soaked in ice-chilled water (12h) Thermal treatments (60,80, & 100 °C, 1 h, 800 rpm).	Ellipsoidal.50-100 µm	Not reported
Pälchen et al., 2021	Chickpeas	Soaked in water (1:5 w/w, 16 h) Thermal treatments (95 °C, 60 min)	Elliptical and elongated 80-125 µm	27 % (Wet-weight basis)
*Edwards et al., 2020	Common beans, butter beans, green lentils, red lentils, green-split pea, yellow-split pea, chickpeas	Soaked in water Thermal treatment (100 °C; 15, 25, 30,50, or 90 min depending on the cooking time of each pulse)	Spherical ~ 200 µm (Average particle size diameter of all the pulses)	44.9 – 62.7 % (Dry Matter)
Gwala et al., 2020	Bambara groundnuts	Soaked in water Thermal treatment (95 °C for 40 and 120 min)	130 µm	Not reported
Li et al., 2020	Garbanzo Pinto bean	Soaked in chilled water overnight Thermal treatments (60 °C, 1 h).	Ellipsoidal or elongated 100-200 µm Spherical or oval	Not available

			100 to 150 µm	
Li et al., 2019 b	Kublai bean (chickpeas)	A. Soaked in chilled water overnight. Dehulled seed cut into cubes. Soaked in 0.05 M HCL (100 rpm, 6 h) and 0.05 NaOH (room temp). B. Soaked in a solution of $NaHCO_3$ (1.5 %, w/v) and Na_2CO_3 (0.5 %, w/v) at 4 °C Thermal treatments (70,80 & 100 °C, 1 h,). C. Soaked in distilled water (1:5 w/v), then autoclaved at 150 kPa (100 °C for 30 min)	Ellipsoidal or elongated 100-200 µm	Not available
Li et al., 2019 a	Red kidney bean	Soaked in 0.05M HCL (100 rpm, 6 h) and 0.025 NaOH (room temp). Soaked in chilled water overnight, thermal treatment (90 °C & 1 h).	Spherical	Not available
Do et al., 2019	Adzuki beans, chickpeas, lentils, lima bean	Soaked in HCl (0.1 M, pH 1.3) at 20 °C for 24 h Soaking in NaOH (0.06 M, pH 12.5) at 20 °C for 24 h.	Elliptical – Spherical 98.9-117.7 µm (mean diameter) 0.056-0.063 m^2/g (Specific surface area).	Not available

Xiong et al., 2019	Pinto beans	Soaked in a solution of $NaHCO_3$ (1.5 %, w/v) and Na_2CO_3 (0.5 %, w/v). Thermal treatments (60 °C, 1 h,).	Round/oval shape	Not available
Rovalino-Córdova et al (2019, 2018)	Red kidney beans	Soaked in water (2:1, overnight) Thermal treatments (95 °C, 60 min)	Round 100 µm	Not available
Xiong et al., 2018	Pinto beans, chickpeas, green-split pea, black-eyed pea	Soaked in water (overnight) Thermal treatments (95 °C, 60 min)	108.5-139.0 µm	Not available
Pallares Pallares et al 2018	Dried Canadian Wonder beans	Soaked in water. High pressure treatments (95 °C, 0.1 & 600 Mpa) and (25°C, 600 Mpa)	Individual cells (40-200 µm) Clusters of cells (200-2000 µm	
Bhattarai et al 2017	Red Kidney bean, chickpea, pea, and mung bean	Soaked in water (overnight) Thermal treatments (95 °C, 60min)	Not available	19.30-22.05 % (Dry Matter)
Dhital et al., 2016	Red Kidney bean, chickpea, pea, and mung bean	Soaked in water (overnight) Thermal treatments (95 °C, 60 min)	Ellipsoidal- Spherical	Not available

In summary, it was suggested that varying permeability of the cell walls from different pre-treatment methods to fluorescently labeled dextran probes may be explained by the degree of the densely packed intracellular environment in each cell, posing as an additional barrier for the diffusion of representative probes (Li et al., 2019a, 2019b & Xiong et al., 2019). Also, the increase in permeability when the thermal treatment is increased from 70 °C and above could be attributed to the pores naturally present in the cell wall, which became large enough for the FITC probe to access induced by the swelling of the entrapped starch granules (Huang et al., 2021).

2.10.2.1.2. Starch. Gelatinization enthalpy and crystallinity are two important tools that have been adopted by researchers to quantify the microstructural changes that occur in starch granules entrapped in the pulse cell during the isolation of cotyledon cells (Dhital et al., 2016; Huang et al., 2021; Pallares et al., 2018; Xiong et al., 2018). The degree of temperature used for the thermal treatment, the amount of water available for soaking, and the rigidity of the cell wall might be extrinsic and intrinsic factors, respectively, that affect the extent of gelatinization and de-crystallization of the embedded starch granule structure in the isolated cotyledon cells. Huang et al. (2021) investigated the extent of loss of birefringence in pinto-isolated cotyledon cells from different thermal treatment temperatures (60, 80, and 100 °C) in excess water (4:1; water: seed). As expected, the authors observed that the intensity of the birefringence of the intracellular starch granules reduced with an increase in thermal temperature. Nonetheless, some birefringence intensities were still found in some cotyledon cells isolated via 100 °C treatment. This observation is in tandem with some other researchers (Dhital et al., 2016; Do et al., 2020; Pallares et al., 2018; Xiong et al., 2018). The authors concluded that the intactness and rigidity of the cell wall of isolated cells are predominantly responsible for this trend by limiting the inflow of water and space required by the intracellular starch granules to swell and subsequently destroy their ordered structure.

Similarly, Junejo et al. (2021) established the role of the cell wall of isolated cells in determining the extent of gelatinization and crystallinity in the intracellular starch granule's structure. The authors investigated the effect of different degrees of the broken cell wall (IC; intact cotyledon cell, SDC; slightly damaged cell, HDC; highly damaged cell and BC; broken cell) of isolated cells

(60 °C, 1 h) from pea seed on the gelatinization and crystallinity of its embedded starch granule's structure. They reported that the total relative crystallinity of the isolated samples increased from BC to IC with an increase in the cell wall integrity. Also, IC showed a higher enthalpy of gelatinization compared to the other forms of isolated cells with low cell wall integrity. This is likely attributed to the cell wall structure of the IC and its intracellular protein components, both limiting water absorption and complete gelatinization of the intracellular starch granules. On the other hand, an increase in an extrinsic factor such as water has been shown to lead to a high degree of disruption of ordered starch structure and gelatinization of the intracellular starch granules in the isolated cells (Palchen et al., 2021; Xiong et al., 2019). In their respective publications, Xiong et al. (2019) & Palchen et al. (2021) isolated cotyledon cells by cooking the pulse seed with increased water availability. The former authors cooked the dehulled pulse seed at 100 °C with varying moisture content (15, 25, and 35%) while the latter cooked the dehulled pulse seed at 95 °C with a seed-to-water ratio (1:5). Xiong et al. (2019) observed the cell processed at 35 % moisture level exhibited more swelling and gelatinization of its intracellular starch granules. Also, Palchen ¨ et al. (2021) showed a polarised microscopic observation that suggested a complete gelatinization of the embedded starch granules in the isolated cell samples.

In terms of cotyledon cells isolated via acid/alkali treatment methods at room temperature, Do et al. (2019) showed no significant difference in the degree of gelatinization enthalpy between the intracellular starch granules and free starch granules from the same pulse seed. Nevertheless, Li et al. (2019) compared the effect of three different isolation techniques (acid/alkali, thermal; 70–100 °C, and pressure-heating treatments) on chickpea-isolated cells. It was reported that isolated cells via acid/alkali treatment had higher gelatinization enthalpy and starch crystallinity than cells isolated using thermal or pressure–heating treatment.

2.10.3. Form III: Flours from pulse seed

Pulse flour has been a major source of value-added ingredients from pulse seed over the years. Pulse flour is generally obtained via milling, which involves the removal of the seed coat; splitting of the cotyledons to produce "splits"; and flour milling, which produces ground flour (Wood & Malcolmson, 2011). The flour milling techniques are generally categorized as "wet" and "dry" milling. The main purposes of pulse milling include particle size reduction from seed to ground flour, separation of components (starch, protein, and fiber enrichment), and

mechanochemical changes to the components (Pelgrom et al., 2013; Scanlon et al., 2018; Thakur et al., 2019). Stone, roller, impact mill, and classifier milling techniques are some of the types of size reduction techniques for obtaining pulse flour from pulse seed that have been explored by various researchers (Maskus et al., 2016; Pelgrom et al.,2013; Ribereau et al., 2017). The particle size distribution of the resulting flour from these various milling techniques quite differs significantly. These differences can be attributed to the difference in the grinding machine, the speed of cutting and shear force, the speed of air classifier, and screen sizes (Bourr´e et al., 2019; Maskus et al., 2016; Pelgrom et al., 2013). The particle size distribution of yellow pea flour obtained via three milling techniques (pin, hammer, and roller milling) increased from pin mill (fine flour) to hammer mill (large particle size) (Maskus et al., 2016). Also, Pelgrom et al. (2013) observed that an increase in the air classifier speed from 2500 to 8000 rpm for impact and jet milling of yellow pea reduced the average particle size diameter from 17.5 to 7.05 µm. Bourr´e et al. (2019) noticed that the average particle size distribution of flours increased with the increment of the screen size from 0.50 mm to 1.27 mm used during the milling of a split yellow pea, whole navy bean, and decorticated red lentil. The main microstructural features of pulse flour are detached starch granules, clusters of cell wall materials, and protein bodies (Fig. 2.8).

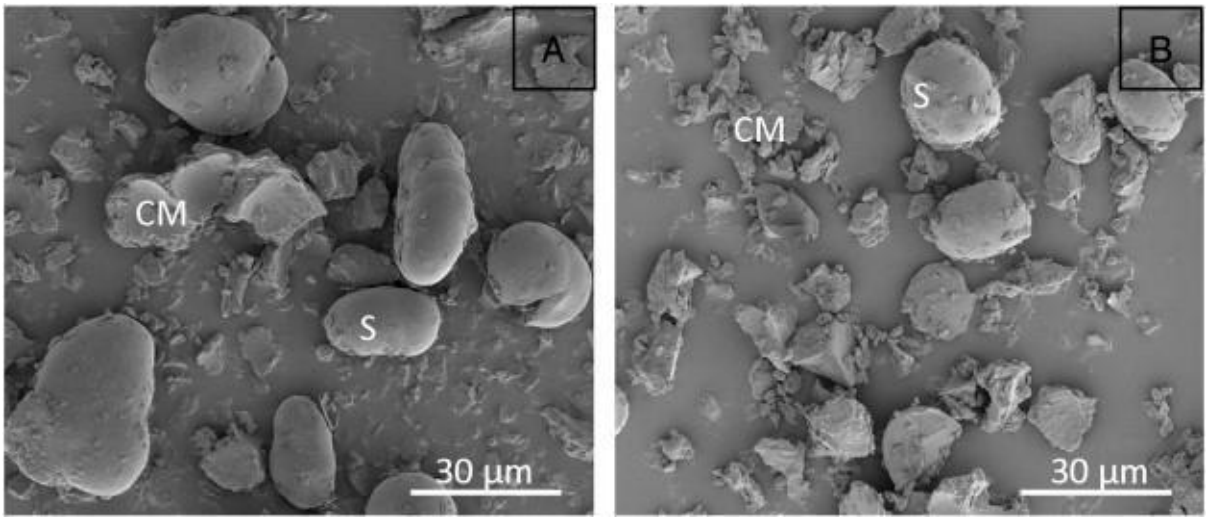

Fig 2.8: Scanning electron microscope (SEM) images of pea flour milled with the impact (4000 rpm) (left) or the jet (4000 rpm) (right) mill. Starch granules (S) and clusters of cellular material (CM) can be distinguished (Pelgrom et al., 2013).

2.10.3.1. Effects of milling techniques on the microstructural features of pulse flour

2.10.3.1.1. Starch.

Various milling techniques and parameters have been designed concerning starch damage in pulse flours (Thakur et al., 2019). Many studies have reported that starch damage in pulse flours is directly influenced by fine milling techniques (Bourr´e et al., 2019; Kathirvel et al., 2019; Price et al., 2021). Bourr´ e et al. (2019) observed that the starch damage in split yellow peas, whole navy beans, and decorticated red lentil flour decreased with an increase in the screen size from 0.50 mm to 1.27 mm using a Ferkar multipurpose knife mill. A similar trend was observed during a pin milling of raw lentil seed into the varying forms of fines from coarse (710–1190 µm) to superfine flour (80 µm) (Kathirvel et al., 2019). The authors reported an increase in starch damage from 0.3 to 2.7% as the particle size distribution moved from coarse to superfine lentil flour. They attributed the low starch damage in the pulse flour to the presence of a hull which would have a dilution effect (Maskus et al., 2016). Furthermore, the differences in the pulse seed hardness would affect the seed's grinding properties, thereby affecting the starch damage levels (Bourr´ e et al., 2019). The starch granules in pulse flours are larger with a non-smooth with fissures on the surfaces and are irregularly shaped (Gujska et al., 1994).

2.10.3.1.2. Fiber. The physicochemical properties of fiber components in pulse flours do change during the milling process (Dogan et al., 2017). There is a dearth of information on the direct method of evaluating these fiber components in pulse flours. However, various researchers have used the evaluation of hull content as an indirect way of determining the insoluble and soluble dietary fiber components of pulses (Thakur et al., 2019). The water retention capacity of navy bean flour was high in a coarsely milled (425–850 µm) fraction as compared to finely milled fractions (<150 µm) (Thakur et al., 2019). The water and oil absorption capacity of pulse flour is affected by many factors such as starch, protein, fiber, starch damage, and particle size distribution. The whole navy bean and coarse lentil flours which contain a high level of hulls (high fiber contents) tend to have a high level of water and oil absorption capacity (Bourr´e et al., 2019; Kathirvel et al., 2019). This would mean that the microstructural changes of the fiber components during milling induced an interaction with the other macronutrient molecules in the flour, thus limiting their absorbing abilities.

2.11 Influence of different forms of pulse microstructure on starch digestion

The starch digestion in the three different forms of microstructure from pulse could be assumed to follow this decreasing pattern: pulse flour < isolated cotyledon cells < whole pulse seed Table 2.4 The starch hydrolysis of whole pulse seed, isolated cotyledon cells, and pulse flour is 18.2–40.1, 60–80.3, and 76–85 %, respectively (Ajala et al., 2022; Berg et al., 2012; Chavez-Murillo ´ et al., 2018; Dhital et al., 2016; Do et al., 2019; Germaine et al., 2008; Romano et al., 2018). This trend can generally be attributed to the reduction in physical barriers (such as cell wall materials and protein matrix) in the intracellular starch granules of the pulse microstructure from whole pulse seed to pulse flours. Ajala et al. (2022) investigated the influence of pulse seed microstructure on the *in vitro* starch digestion in four cooked (100 °C for ~30 min) New Zealand pea varieties. The starch-degrading enzyme was added to the cooked pulse seed before homogenizing for 30 seconds. They reported low starch hydrolysis (18.2–27.6 %) for the cooked pea varieties which were comparable with the results reported by the other authors (Germaine et al., 2008 & Pallares Pallares et al., 2019). Healthy adult participants aged 18–75 years with body mass index (BMI) < 30 kg m- 2 and without diabetes were fed 8 different varieties of freshly cooked lentils (Ramdath et al., 2017). The *in vivo* glycaemic response from the human clinical study showed that all the cooked lentil varieties showed a low glycaemic index (10–23 %) (Ramdath et al., 2017). The low starch hydrolysis reported for the study could be attributed to the presence of seed coat material-rich fraction (>2000 µm) providing a strong physical barrier to the starch-degrading enzymes (Ajala et al., 2022). A further barrier to starch degrading enzymes was likely due to the activity of richly localized phenolic compounds in the seed coat and cotyledon of the cooked pea varieties which form a two-way interaction with the degrading enzymes and starch granules during starch digestion *in vitro* (Sun & Miao, 2019). A strong network of fibrous interaction with partly gelatinized starch and denatured protein bodies illustrated in Fig. 2.9 showed the influence of microstructure on intracellular starch granules in cooked pulse seed.

Table 2.4: Summary of starch hydrolysis of different forms of microstructure from pulse seed

Forms of microstructure	Pulse	Starch hydrolysis (%)	Glycaemic Index	Reference
Whole pulse seed	Peas	18.2-27.6	47.5-50.9	Ajala et al.,2022
	Red kidney beans	~60-70		Pallares Pallares et al., 2019
	Navy bean	~60		Berg et al., 2012
Isolated cotyledon cells	Smooth pea	16.2-37		Junejo et al., 2021
	Chickpeas	65-77		Pälchen et al., 2021
	Green lentils, red lentils, butter beans, red kidney beans, green split peas, and yellow split peas	~ less than 40		Edwards et al., 2020
	Bambara groundnuts	67.94 -84.77		Gwala et al., 2020
	Garbanzo bean	17-84.2		Li et al., 2020
	Pinto bean	8.1-82.1		
	Kubali bean	9.7-74.1		Li et al., 2019b
	adzuki bean, chickpea, lentil, and lima bean	66.1-80.3		Do et al., 2019
	Pinto bean	23.7-79.6		Xiong et al., 2019
Flour	Grass pea flour	79.6		Romano et al., 2018
	Black & broad bean, chickpea, lentils	59.6 -85.26	65.43 – 87.15	Chávez-Murillo et al., 2018
	Navy bean	90		Berg et al., 2012
	Pea	23.7- 24.1	36.9 - 37.7	Chung & Liu, 2012
	Peas, lentils, chickpeas	33.4 -43.1	41.4 -56.1	Chung et al., 2008

For the isolated cotyledon cells, the presence of a strong physical barrier to the intracellular starch granules tends to reduce compared to the whole pulse seed, thus showing a higher rate of starch hydrolysis (Dhital et al., 2016; Do et al., 2019; Gwala et al., 2020; Palchen ¨ et al.,

2021). However, recent research on starch hydrolysis of isolated cotyledon cells has shown that its rate of hydrolysis is comparable to that of whole pulse seed (Junejo et al., 2021; Li et al., 2020; Xiong et al., 2019). The influence of varying degrees of cell wall integrity, such as IC, SDC, HDC, and BC of pea-isolated cotyledon cells (cooked at 60 °C for 1 h), on starch digestion *in vitro* was investigated (Junejo et al., 2021). They reported that the starch hydrolysis of the intact pea cotyledon cell (16.2–34.5%) increased with a decrease in cell wall integrity (from IC to BC). That is because the barrier provided to the intracellular starch granules by the cell wall is reduced with a decrease in cell wall integrity. A similar experimental design was conducted on isolated red kidney bean cells (cooked at 95 °C for 1 h) by modifying the cell wall structure to mechanically damage cells; MDC and enzymatically damaged cells; EDC, respectively (Rovalino-Cordova ´ et al., 2018). The authors observed a significantly high rate of hydrolysis (70–77%) compared to the results reported by Junejo et al. (2021). It can be observed that two different isolation temperatures (60 or 95 °C) have a drastic effect on the microstructural features (cell wall and starch) of the isolated cells. At a temperature above starch gelatinization temperature (95 °C), the cell wall integrity was assumed to be more destroyed and allowed more inflow of the starch degrading enzymes compared to the pulse isolated cells below starch gelatinization temperature. Li et al. (2020) confirmed this hypothesis when they investigated the influence of treating the isolated garbanzo and pinto cells obtained by cooking hydrothermally at different incubation temperatures (60,70, 80, 90, and 100 °C). They reported a significantly low rate of starch hydrolysis for both garbanzo (17.0) and pinto (8.1%) isolated cells, respectively, when they were heat treated at 60 °C. Nevertheless, there was a steady increase in the rate of starch hydrolysis from 17.0 to 41.9 and 8.1–35.5% for both pulse-isolated cells as the hydrothermal treatment temperature increased from 60 to 100 °C. This established the fact that the intactness of the cell wall of an isolated pulse cotyledon cell might be the primary barrier in modulating the inflow of starch-degrading enzymes, other extrinsic factors like cooking temperature could affect the structural integrity (permeability) of the isolated cell wall.

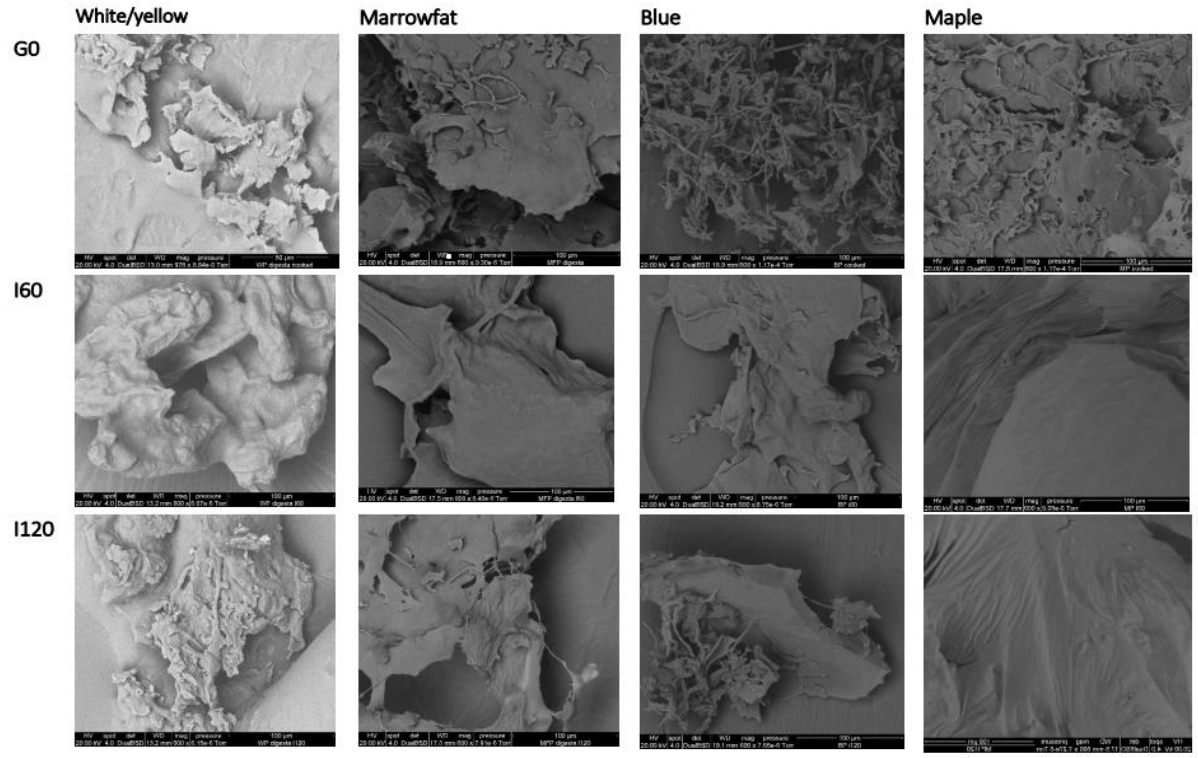

Fig 2.9: Scanning electron micrographs of representative White/yellow, Marrowfat, Blue, and Maple peas sampled during *in vitro* oral-gastro and small intestinal digestion. G0, I60, and I120 represent after zero min at the gastric phase, and 60 and 120 min at the small intestinal digestion phase. (Ajala et al., 2022).

Other extrinsic factors such as an increase in moisture content of intracellular starch granules, changes in gastric pH, and different cooking times and hardness of the pulse seed would affect the ability of primary and secondary barriers (cell wall and protein matrix) of the pulse isolated cell to modulate the activities of starch-degrading enzymes during starch digestion *in vitro* (Gwala et al., 2020; Palchen ¨ et al., 2021; Pallares Pallares et al., 2018; Xiong et al., 2019). Palchen ¨ et al. (2021) conducted a comparative study of the influence of static gastric (pH at 2, 3, and 6) versus gradual decrease in gastric pH (6.3–2.5) on the starch hydrolysis of isolated chickpea cotyledon cells (cooked at 95 °C for 1 hr). The rate of starch hydrolysis at pH 3 was comparable to that of pH 6 (65 %) but was lower than the hydrolysis reported for pH 2 (77 %). This shows that the more acidic the gastric phase, the higher the rate of starch hydrolysis. Also, comparing the hydrolysis at static gastric pH 3 with a gradual decrease in gastric pH (6.3–2.5) reported that a gradual reduction in gastric pH of the digested pulse cells increased its starch hydrolysis to 93.35 %. It can be observed that changes in the digestion condition induced some

structural changes such as changes in the isoelectric points of cell protein in the starch-protein interactions and permeability or binding affinity of amylase to the cell wall (Palchen ¨ et al., 2021). The isolated cells obtained from Bambara seed were pre-cooked at 95 °C for 40 and 120 min before the isolation procedure.

After cooking, other sets of seeds were sorted based on hardness categories (high and low) before the isolation process (Gwala et al., 2020). The first category of isolated cells obtained from seed cooked at 95 °C for 40 min showed that hydrolysis was 27 % lower than the seed cooked for 120 min. The starch hydrolysis for the cells that were sorted based on hardness categories (high and low) was significantly high (62.58–95.53 %). This result suggests that the primary barrier which is the cell wall of the isolated cells is not significantly affected by processing intensity or hardness category (Gwala et al., 2020). Xiong et al. (2019) studied the effect of increasing the starch moisture content of pinto isolated cells (cooked at 60 °C for 1 h) via heat-moisture treatment to 15, 25, and 35 %, respectively. They observed that the rate of starch hydrolysis of the treated cells followed a decreasing pattern; 35 %-treated cells <25 %-treated cells <15 %-treated cells < non-treated cells. This observation indicates that the permeability of the cell wall to starch-degrading enzymes increased with an increase in starch moisture content.

For the cell isolated at room temperature, Do et al. (2019) reported the starch hydrolysis of adzuki, chickpea, lentil, and lima bean cells isolated via acid/alkali methods falls in the range of 66.1–80.3 %. These results correspond to those reported by Rovalino-Cordova ´ et al. (2018) & Dhital et al. (2016). This result was significantly higher than what was reported for Kublai bean cells (6.6 %) isolated at room temperature via acid/alkali methods (Li, Zhang, & Dhital, 2019). The variation in the hydrolysis results was largely due to the cooking process (95 °C for 20 min) and mixing process (at 300 rpm) that Do et al. (2019) subjected their cells to a prior *in vitro* protocol. It is a fact that cooking the cells at high temperatures drastically reduces the structural integrity of the primary barrier (cell wall) to the intracellular starch granules in the cells. From a nutritional standpoint, the potential application of isolated cotyledon cells as a food ingredient would invariably involve cooking or heating at high temperatures, so the extremely low starch hydrolysis of pinto cells reported by Li et al. (2019) via an *in vitro* protocol that excludes cooking of the isolated cells underestimates the exact value of the starch hydrolysis of the cells.

The microstructural features of pulse flour illustrated in Fig. 2.4 showed that exposed starch

granules have little or no physical barrier such as the clusters of cell wall materials and protein. This phenomenon is assumed to be the reason for the high starch hydrolysis of 79.6 % and over 90 % for grass pea raw flour and navy bean flour, respectively (Berg et al., 2012; Romano et al., 2018). Other authors have reported that hydrothermal treatments can be used to reduce the rate of starch digestion (Chavez-Murillo ´ et al., 2018). They observed that annealed (incubated at 65 °C) and heat moisture (incubated at 120 °C) treated flours (black bean, broad bean, lentils, and chickpea) reduced the rapidly digestible starch (RDS) by an average of 8 and 22 % for annealed and heat moisture treated flour, respectively. Furthermore, the hydrothermal treatments increased the slowly digestible starch (SDS) of the flour by an average of 15 %. On the other hand, a low rate of starch digestibility has been reported for peas, lentils, chickpeas, and common bean cultivars (Chung et al., 2008; Chung & Liu, 2012). The average starch hydrolysis reported for these studies ranges from 33.1 to 41.7 % for pulse flour. The high content of protein reported for the studies could have enhanced the starch–protein interaction leading to the formation of a cytoplasmic matrix strong enough to regulate the effects of starch-degrading enzymes.

2.12 Conclusions

This review provided a detailed comparative study on the three forms of pulse microstructure and the role of type of microstructure on starch digestibility *in vitro*. Similar microstructural features namely, cell wall materials, protein bodies, and starch granules were observed in the three forms of pulse microstructure. The intactness and compactness of the pulse microstructure increased from *Form* III (pulse flour) < *Form* II (pulse cotyledon cells) < *Form* I (whole pulse seed). Conversely, the rate of starch digestion in the pulse microstructure decreased from pulse flour > pulse cotyledon cells > whole pulse seed. It was observed that the cell wall and protein matrix act as primary and secondary physical barriers responsible for modulating the activity of the starch-degrading enzymes in the form of pulse microstructure.

Overall, pulse microstructure forms I and II (whole pulse seed and pulse cotyledon cells) have shown the potential of developing a new low glycaemic index food product. However, the following recommendations and suggestions should be further investigated to maximize their food application prospects.

- There is a dearth of information on the microstructure of the whole pulse seed and the underpinning mechanism on how its microstructure influences its rate of starch digestion.
- From a food ingredient application standpoint, pulse cotyledon cells (Form II) have the potential for new functional food ingredients because of their applicable particle size and low glycaemic nature features. However, its extraction yield is less than 30 %, therefore, more research should be devoted to optimizing the yield of pulse cotyledon cells from pulse seed.
- From a sustainability perspective, the waste generated during the isolation of cotyledon cells falls between 70 and 85 %. This waste is a composite of starch granules, fiber fractions, protein matrix, and clusters of cotyledon cells. New food ingredient applications should be developed to put this enormous waste to use.
- An objective-based method such as pulsed field gradient (PFG)-NMR and gas adsorption methods needs to be developed to evaluate the roles of pores and cell wall structures in modulating starch degrading enzymes in whole pulse seed and isolated cotyledon cells

Chapter 3: Research questions and hypotheses

3.1 Research questions and hypotheses

Based on the research gaps highlighted in Chapter 2 (review of literature), the research questions and the corresponding hypotheses addressed in this thesis are presented systematically in Table 3.1.

Table 3.1 Research question and hypotheses

Research questions	Hypotheses	Chapters to test the hypotheses
What are the microstructural components of a raw whole pulse seed?	Intracellular starch granules embedded in a protein matrix encapsulated by fibrous cell walls are the main components of the native microstructure of a whole pulse seed.	Chapter 4

How do these components interact during processing conditions?	The cell wall acts as a primary barrier in regulating the extent of intracellular starch gelatinization during processing.	Chapter 4
How does the interaction among the components influence the rate of starch hydrolysis in the whole pulse seed?	The cell wall modulates the extent of intracellular starch hydrolysis during digestion	Chapter 4
How does the cell wall of isolated cotyledon cells modulate the ingress of water and starch-degrading enzymes?	The diffusion of water and starch-degrading enzymes into the cotyledon cells is directly proportional to the cell wall permeability	Chapter 5
Is the isolation procedure of the cotyledon cells efficient?	The yield percentage of cotyledon cells from whole pulse seed is < ~30 % with a waste of ~75-80 %	Chapters 5 & 6
Is the isolation of cotyledon cells from the whole pulse seed sustainable?	A Micronization technique (colloid milling) can be used to sustainably process whole pulse seed to “cotyledon flour”.	Chapter 6
How does the novel “cotyledon flour” affect the techno-functional properties of a standard food system?	It improves the food system's protein, fiber, and resistant starch content.	Chapter 7

Chapter 4: Influence of Seed Microstructure on the Hydration Kinetics and oral-gastro-small Intestinal Starch Digestion *in Vitro* of New Zealand pea varieties

4.1 Abstract

This study shows how the microstructure of New Zealand pea varieties: White/yellow (WP), Marrowfat (MFP), Blue (BP), and Maple (MP) respond to pre-and-post starch gelatinization conditions. The microstructural characteristics of raw pea seeds were evaluated via scanning electron microscopy and image analysis before studying their hydration kinetics at 30, 40, 50, or 60 °C (pre-starch gelatinization conditions) while *in-vitro* oral-gastro small intestinal digestion was performed on the cooked pea seeds (post-starch gelatinization condition). For the raw sample, the thickness of the cell wall for the pea varieties differed significantly from each other and followed a decreasing order of MP > MFP > BP > WP. The highest average number of starch granules per cell was found in MFP (12.0/cell). The shortest time (139 min) for the soaked pea to reach its saturation point was exhibited by BP at 60 °C while the lowest moisture content of soaked peas at saturation point was found in MP at 60 °C (89.92 % d.b). The starch hydrolysis (%) of the cooked pea varieties during oral-gastro-intestinal digestion *in vitro* fall between the range of 18.2–27.6 % and followed a decreasing order of WP > MP > MFP > BP. The estimated glycaemic index (*e*GI) was thus lowest for BP (47.5 %). The number

of starch granules per cell and fibre content was correlated positively ($p \leq 0.01$) with the starch hydrolysis of the pea varieties. The discernible irregular particles (protein bodies, fibre fragments) attached to or between the starch granules observed in both hydrated and cooked pea seed microstructure seemed to modulate the inflow of water and starch-degrading enzymes.

4.2 Introduction

The term "pulses or grain legumes" as defined by FAO are annual leguminous crops solely harvested for their dry seeds which are consumed directly (Thavarajah et al., 2019). Pulses are classified by the FAO into 11 primary groups (dry beans, dry broad beans, dry peas, chickpeas, cowpeas, pigeon peas, lentils, Bambara beans, vetches, lupins, and pulse-derived products). Beans, lentils, peas, and chickpeas are recognized as the group important to human nutrition and worldwide trade (Szczebyło et al., 2019). The global pulse market is expected to increase by 3.2% by 2025 (Rawal & Navarro (2019). The main pulse crop grown in New Zealand is field peas, field beans, and lentils (Millner et al., 2013). The average annual production of peas and beans is 59,850 and 14,725 tons from 2017 -to 2020 (Curran-Cournane & Rush, 2021). The increased market demand for pulse crops is usually attributed to their sustainable nature, nutritional (protein, 17–29, carbohydrate 60–63 & total starch, 36–75% respectively), and health-related benefits (EPA, 2012; Thavarajah et al., 2019; Hall et al., 2017; Roe et al., 2015; Johnson et al., 2013).

Starch in pulse seeds such as peas provides some additional health benefits, such as low glycaemic index and high levels of resistant starch (Do & Singh, 2019 & Singh et al., 2017). It is imperative to note that some of these unique attributes are related to their microstructure, i.e., the arrangement of starch in cotyledon cells and interactions of starch with other non-starch macromolecules (protein, lipids, fiber) during processing (Ma et al., 2011). The main features of pulse microstructure entail a starch granule embedded within a protein matrix and the whole structure is encapsulated with fibrous cell wall material (Edwards et al., 2021). Ma et al. (2011) reported a reduction in the length and width of starch granules (raw) for lentils, chickpeas, and pea flours after roasting.

Moreover, the starch granules observed in the microstructure of the raw and roasted flours were quite distinct from the boiled legume flours (Benmeziane-Derradji et al., 2020; Shevkani et al., 2021). The starch granules in the raw and roasted flour were joined by a discernible

irregular particle believed to be protein bodies or fibre fragments. On the other hand, there are no distinct starch granules in the boiled flour except for a homogenous network of amorphous flakes formed due to cross-linking between starch granules and protein bodies during the pre-gelatinization stage.

Other researchers investigated the impact of various processing techniques on nutritional composition and starch digestion in pulse flour (Rehman & Shah, 2005 & Alonso et al., 2000a &b). Rehman & Shah (2005) reported that starch digestibility in four-pulse flours increased as the processing techniques moved from conventional cooking (boiling) to pressure cooking. A similar trend was observed by Alonso et al. (2000), who reported the starch digestibility of faba and kidney bean flours increased with the degree of processing (raw < germinated < extrusion).

This increment in starch digestibility after processing could be attributed to the higher extent of starch gelatinization in pulse flours. Nonetheless, the mechanism of how the microstructural characteristics of pulse flour regulate starch digestibility was not explored. The low glycaemic index nature of pulse could potentially lead to the developing of a new food product that might help maintain and regulate the postprandial release of glucose in the bloodstream of people with type II diabetes (Singhal et al., 2013 & McCrory et al., 2010). The low glycaemic nature is essentially observed in whole pulse seed than in pulse flour (Alonso et al., 2000; Ma et al., 2011; Raigar et al., 2016; Rehman & Shah, 2005; García-Alonso et al*.,* 1998 & Germaine et al., 2008). That is, the glycaemic index of pulse food products increases with processing. The nature of microstructure in whole pulse seed and pulse flour might explain the differences in their glycaemic index. However, the application of whole pulse seed in food products is limited compared to pulse flour due to its larger particle size. Therefore, a novel new food ingredient from pulse seed with a moderately low glycaemic index with applicable particle size is required to be developed. The development of this new food ingredient would not be achieved without understanding the basic mechanism of how the microstructure (arrangement of starch, protein lipids, and fibre) in a pulse seed modulates starch digestibility *in vitro*.

In light of the above, this study aimed to understand the relationships between starch and non-starch components in their natural pea microstructure and how they respond to pre- and post-starch gelatinization conditions. Scanning electron microscopy (SEM) and ImageJ software were used to characterize raw pea seed microstructure, such as the number of starch granules per cell and cotyledon cell wall thickness. The experimental design for this study was in two

steps; 1) hydration kinetics set at 30, 40, 50, or 60 °C were employed as a pre-starch gelatinization condition for the raw pea seed, and 2) *in-vitro* oral-gastro small intestinal digestion was used as the post-starch gelatinization condition for the cooked whole pea seed. Four New Zealand pea varieties, such as White/yellow (WP), Marrowfat (MFP), Blue (BP), and Maple (MP) peas, were selected for this study because pea seed is a staple pulse seed usually consumed both as a whole seed and food ingredients (pea flour).

4.3 Material and Methods

4.3.1 Materials

Four locally grown whole dry pea seed varieties, White/yellow pea (WP), Marrowfat pea (MFP), Blue Pea (BP), and Maple pea (MP), were supplied by Cates Grain and Seed (Ashburton, New Zealand). Each pea variety was vacuum sealed and stored at 4 °C until further studies. Pepsin (porcine gastric mucosa, 800–2500 U/mg protein), pancreatin (hog pancreas, 4 × USP), and invertase (Invertase, grade VII from baker's yeast, 401 U/mg solid), were all purchased from Sigma–Aldrich Ltd. (St Louis, USA) and alpha-amylase (3000 U/mL) and amyloglucosidase (3260 U/mL) were from Megazyme International Ireland Ltd. (Wicklow, Ireland). All other chemicals were of analytical grade.

4.3.2 Methods

4.3.3. Microstructural characteristics of raw pea seeds

The morphological properties of the whole pea seeds were evaluated according to the method described by Shapter et al. (2008) with minor modifications. Three dry pea seeds were carefully selected as representatives of each variety and fixed for 48 h in a primary Electron Microscopy (EM) fixative (3 % glutaraldehyde and 2 % formaldehyde in 0.1 M phosphate buffer) to ensure acceptable structure preservation of the pea seed. The combination of two fixatives was employed to ensure complete penetration of the fixative into the thick tissue of the pea seed. This was followed by washing of seeds with distilled water for 15 min to remove excess fixative from the surface of the seed then a standard graded series of ethanol (25, 50, 75, and 95 %) was used to dehydrate the seed for 20 min each. The series of ethanol was employed to ensure the complete dehydration of water from the seed due to its large particle size. The samples

were then washed three times in 100 % ethanol for 30 min and immediately dried using a Polaron E3000 series II critical point dryer (Quorum Technologies, England). The resulting dried pea seed was cut along one side with a scalpel blade and snapped in half transversely between two pairs of forceps. The resulting pea specimen was then gold coated (Baltec SCD 050 sputter coater, New York, USA) and viewed using the FEI Quanta 200 Environmental Scanning Electron Microscope (Oregon, USA) at an accelerating voltage of 20 kV. Several electron micrographs were captured for each pea variety. A suitable electron micrograph was selected for each variety and analyzed by ImageJ software (National Institutes of Health, Bethesda, MD, USA) (Abramoff et al., 2004; Scafaro et al., 2011). The software was used to evaluate the number of starch granules per cell, cotyledon cell diameter, the thickness of the cotyledon wall, and the average diameter of starch granules. Each parameter was measured 20 times from a different angle for each pea variety.

4.3.3.1. Microstructure of pea seed during hydration kinetics.

Samples of whole pea seed were collected after they reached saturation points at 30 and 60 °C, then the samples were prepared for SEM, and the micrographs were captured as described above.

4.3.3.2. Microstructural characteristics of cooked pea digesta.

Digested samples were collected at G0, G30, I60, and I120 into an Eppendorf tube and submerged in liquid nitrogen, then kept in the freezer for freeze drying. The freeze-dried samples were mounted on a stub and gold coated (Baltec SCD 050 sputter coater, New York, USA), then viewed on the FEI Quanta 200 Environmental Scanning Electron Microscope (Oregon, USA) at an accelerating voltage of 20 kV.

4.3.4. Physical properties of raw pea seed

Each pea seed was randomly selected, and physical parameters were evaluated before and after soaking for 24 hours at room temperature. Three principal dimensions, length (L), width (W), and thickness (T), of randomly selected pea samples, were measured using a Vernier caliper (Blu-Mol Vertex) reading to 0.01 mm. An average of ten measurements was calculated and evaluated per variety. Other physical parameters: Geometric mean diameter, Arithmetic mean diameter, Sphericity, and Surface area of the pea seeds were also determined based on the following relationship (Eqs. (1)– (4)) (Mohsenin, 1970).

$$Dg = (LWT)^{1/3} \quad (1)$$

$$Da = {(L + W + T)}/{3} \quad (2)$$

$$\emptyset = {Dg}/{L} \quad (3)$$

$$S = \pi L^2 \quad (4)$$

where Dg is the Geometric mean diameter of the pea, Da is the Arithmetic mean diameter of the pea, Ø is the Sphericity of the pea and S is the Surface area of the pea.

4.3.5. Proximate composition and cooking characteristics of raw pea seeds.

The pea seeds were milled to flour via an impact milling machine (Universal Impact mill B series, Grain Tech Ltd, New Zealand) and passed through a 0.5 mm screen. The moisture content of the resulting pea samples was determined by an air oven drying method at 108°C (AOAC 2011). Subsequently, the contents of crude protein and crude fat in pea varieties were analyzed by the Kjeldahl method using a conversion factor of 6.25 from nitrogen to protein and the Mojonnier method respectively (AACC 2000 & AOAC 2011). The acid/alkali hot extraction method (AOAC 2011) was used to quantify the fiber content of peas while the gravimetric method which involved heating the pea sample at 600°C for 3hr was used to determine the ash content (AACC 2000). The carbohydrate contents of the pea samples were estimated via calculation by subtracting the summation of all other components from 100%. All experiments were conducted in triplicate.

The total starch content of the pea varieties was analyzed using a total starch assay kit (KTSTA, Megazyme International Ireland Ltd., Ireland) following the manufacturer's instructions. Results were reported on a dry weight basis (%).

The cooking time for the pea varieties was studied according to a method described by Parmar et al. (2016) with some modifications. Distilled water (125 mL) was brought to boiling point in a 250 ml conical flask fitted with a condenser to avoid evaporation losses during boiling and then 13 g seed was added. Boiling at 100°C was continued and boiled seeds were drawn at different time intervals to test the softness of the seed at the core. This was determined by pressing the cooked pea sample between two glass slides. The time taken to achieve the desired softness at the core of the pea seed was recorded as the cooking time of the sample.

The time taken was done in triplicate for each pea variety. The cooking time was analyzed both for soaked (soaking duration was 24 h at room temperature) and un-soaked pea seeds.

4.3.6 Textural properties of cooked pea seeds

The texture of the cooked pea seeds was analyzed by using a texture analyzer (Model XT2i; Stable Micro Systems Ltd., England). Pea seed was placed at its natural rest position on the heavy-duty platform of the texture analyzer and a texture profile analysis (TPA) test was performed with a disk probe of 61 mm diameter for 75% compression at a test speed of 2.0 mm/s (Hutchings et al., 2009). Hardness, fracturability, gumminess, chewiness, and resilience were calculated from the TPA curve. An average of ten measurements was reported per variety.

4.3.7 Hydration Kinetics

The hydration experiment for the pea varieties was set up according to the method described by Balkrishna & Visvanathan (2019) with some adjustments. A thermostat-controlled water bath (JN5 Grant Instruments, UK) fitted with a heater was filled with water up to one-fourth of its volume. About 20 g peas of each pea variety were weighed (to an accuracy of 0.01 g) into a muslin bag (20 x 10 cm) and soaked into the water bath pre-set at the desired temperature. The temperature of the heated water was measured at intervals to ensure an accuracy of ± 0.5°C.

After 10 mins of soaking, the soaked muslin bag was taken out and surface-dried by centrifuging at 2800 rpm (878 g-forces) (Multifuge 1S-R, Thermofisher Scientific, USA) for 2 mins at room temperature. The resulting dried muslin bag containing the pea sample was weighed to an accuracy of 0.01 g. After recording the weight, the bag was again kept in the water bath until the recording of the next weight. This procedure was repeated after 20, 30, 60, 120, 240, and 480 mins. The sample was soaked in water until it attained saturation as indicated by the constant mass of the pea sample between the consecutive weighings. The hydration experiment was repeated for peas for the four varieties at four different temperatures (30,40, 50, and 60°C).

4.3.7.1 Hydration kinetics calculations

The relationships and equations according to Balkrishna & Visvanathan (2019) were used to estimate the intermediate moisture content at various intervals of soaking and equilibrium moisture content.

4.3.7.2 Application of Peleg Model to hydration kinetics of pea seeds

To understand the hydration characteristics of the pea varieties, the Peleg model was applied to the data generated from the studies. Peleg (1988) proposed that moisture sorption curves for food products could be described using a simplified two-parameter empirical model. The linearized version of the Peleg model (Peleg 1988) was fitted into the data generated from the hydration analysis of the pea varieties to describe the hydration characteristics at each soaking temperature. Linear regression was used to determine k_1 and k_2 which are Peleg's rate constant (mins/%) and Peleg's capacity constant (per %) respectively.

$$\frac{t}{M-M_0} = k_1 + k_2 t \qquad (5)$$

Where t; Time required for the seed to reach equilibrium moisture content (mins), M; equilibrium moisture content at a soaking temperature (%), M_0; initial moisture content at a soaking temperature (%). k_1 and k_2 which are Peleg's rate constant (mins/%) and Peleg's capacity constant (per %) respectively.

4.3.8 In vitro oral gastro-small intestinal digestion of the pea seeds

Pea seeds were mixed with water in a ratio of 1:4(w/v) in a beaker to obtain a heterogeneous mixture containing approximately 4% starch concentration. The resulting mixture was covered with aluminum foil to avoid evaporation and cooked on a hot plate according to the cooking time obtained for each variety (section 4.2.3) and immediately cooled down in a pre-set water bath at 37°C. A simulated saliva fluid (SSF) prepared according to Schwanz et al. (2019), with α- amylase concentration of 0.3U/mL, was added to the cooked pea at a ratio of 1:1. The resulting solution was stirred with the aid of a magnetic stirrer bar, then incubated at 37±1°C for 2 mins. To mimic the chewing procedure, the cooked pea seeds were homogenized in a grinder (Breville, BCG200BSS) for 30 sec to achieve a particle size distribution like real human chewing (Eckelkamp, 2021).

For the gastro-small intestinal digestion, simulated gastric fluid (SGF) and simulated intestinal fluid (SIF) were prepared (Pharmacopeia, 1995 & 2000). A two-stage gastro-small intestinal *in vitro* digestion model was used for this study as described by Dartois et al. (2010) with some modification.

Approximately 170 g of chewed pea samples from the oral phase were introduced into a nylon mesh placed in the jacketed glass reactor to prevent contact with the stirrer bar in the reactor. The reactor temperature was maintained at 37 ± 1°C by circulating water in the reactor jacket. The reactor contents were mechanically stirred by a magnetic stirrer bar at 300 rpm throughout digestion. The pH was initially adjusted to 2.0 (using 3 M HCl solution), then 25 mL of SGF (pepsin: starch ratio of 1.765:100, w/w) was added to start the hydrolysis; and the final pH was adjusted to 1.2 (using 0.5 HCl solution). After 30 mins, the pH was adjusted to 6.8 to inactivate the pepsin enzyme. Subsequently, 22 mL of SIF (pancreatin /starch ratio, 1.3:100, w/w, amyloglucosidase /starch ratio, 0.26:1, v/w, and invertase /starch ratio, 1:1,000, w/w) was added to start the small intestinal digestion, and pH was maintained at 6.8 using 0.5 and 3 M NaOH solution. The total time to complete the gastric and small-intestinal digestion was 30 and 120 mins, respectively.

A 0.5 mL of aliquot was withdrawn from the reactor after 0, 15, and 30 min of gastric digestion (G0, G15, and G30), and 0, 5, 10, 15, 30, 60, 90, and 120 min of the small intestinal digestion (I0, I5, I10, I15, I30, I60, I90 and I120). The glucose concentration of the incubated mixture was measured using the D-glucose assay kit (GOPOD Format K-GLUK 07/11, Megazyme International Ireland Ltd, Ireland). Starch hydrolysis results were expressed in percentages as described by Dartois et al. (2010).

The estimated glycaemic index (*eGI*) of the digested pea varieties was calculated with the following equation described by García-Alonso et al. (1998).

$$eGI = 0.549(\mathrm{HI}) + 39.71 \qquad (6)$$

Where HI is the hydrolysis Index which was calculated by evaluating the area under the curve during small intestinal digestion using white bread as the reference.

4.3.9 Statistical analysis

The average mean and standard deviation were evaluated for all reported values. All reported values were subjected to statistical analysis using Minitab 19.1.1.0 statistical software (Minitab LLC, Chicago, USA) at $p \leq 0.05$. Pearson correlation coefficient (r) was calculated to establish the relationships between various reported pea properties. The similarities and differences in terms of pea properties among the four pea varieties were visualized using principal component analysis (PCA).

4.4 Result & Discussion

4.4.1 Microstructural characteristics of the raw pea seeds

The number of starch granules per cotyledon cell (Table 4.1) for all pea varieties was in the range of around 9-12 which did not differ significantly, except for MFP which had a higher number of starch granules per cell. The cotyledon cell diameter (96.89 µm) for MP was significantly higher than the average value of other pea varieties.

The thickness of the cell wall for the pea varieties differed significantly from each other which was in a range of 3.66 - 8.77 µm with the decreasing order of MP~MFP~BP>WP. On the other hand, the average diameter of starch granules ranged from 22.78 to 31.96 µm which followed the decreasing order of MFP>MP>WP~BP. The SEM micrographs for the pea varieties are illustrated in Fig.4.1. These micrographs further support the raw seed morphological properties detailed in Table 4.1. The cell/granule packing observed in Fig. 4.1 showed distinct differences among pea varieties. The pea seed from the MP variety exhibited higher cell/granule packing compared to the other varieties. The shapes of starch granules from all the SEM micrographs of the pea varieties have been previously characterized as oval, round, and irregular shapes (Hoover et al., 2010). However, the predominant shapes of the starch granules observed in this study were oval and round shapes. Also, the surface of the starch granules was observed to be largely smooth without any rough areas and pinholes.

Table 4.1 Morphological properties of raw whole peas from different varieties as examined using scanning electron microscopy and ImageJ analysis.

Pea variety	Number of starch granules/cell	Cotyledon cell diameter (µm)	Thickness of the cotyledon cell wall (µm)	Average diameter of starch granules (µm)
White/Yellow (WP)	10.6 ± 2.12[a]	86.46± 6.83[a]	3.66 ± 1.30[a]	22.78 ± 4.77[ab]
Marrowfat (MFP)	12.0 ± 1.94[b]	88.80 ± 4.80[ab]	7.10 ± 2.82[bc]	31.96 ± 5.34[c]
Blue (BP)	10.4 ± 1.58[a]	92.35± 5.26[b]	5.78 ± 1.64[b]	20.36 ± 3.46[a]
Maple (MP)	9.6 ± 1.50[a]	96.89 ± 5.55[c]	8.77 ± 2.09[c]	24.17 ± 3.23[b]

[a, b, c] Values in each column with the same superscript letters do not differ significantly ($p > 0.05$).

4.4.2 Physical properties of pea seeds

The three principal dimensions (Length, Width, and Thickness) of the pea seed varieties differed significantly before and after soaking in water at room temperature for 24 hrs as shown in Table 4.2. As expected, all pea varieties had a significant increase in all three dimensions after soaking. Before soaking, the length of the pea seeds for all varieties was in the range of 6.91-9.07 mm being different significantly from each other, except for MFP and WP. The same trend was observed after soaking for 24 hours. In terms of width, the WP seed had the highest width (7.71 mm) compared to the other pea varieties (6.12-7.24 mm) before soaking but no significant difference in width between MFP and MP. On the other hand, after soaking for 24 hrs, the pea seed varieties followed a decreasing order of WP~MFP>BP~MP. The same trend was exhibited for the thickness of the pea seed varieties before soaking, whereas MFP seed showed the highest thickness (10.7 mm) after soaking compared to the other pea varieties (7.97-9.25 mm). The range of results for the three principal dimensions (Length, Width, and Thickness) of pea seeds observed in this study (Table 4.2) was comparable to the results reported by Paksoy & Aydin (2005). However, Yalçın et al. (2007) reported the average length, width, and thickness for Bolero pea cultivar were 7.80, 6.41, and 5.55 mm, respectively, which was lower than the reported range from this study. The three principal dimensions of the pea seeds correlated positively with the cooking time for soaked and unsoaked peas. The

length of the pea seeds tended to have a stronger positive correlation with the cooking time for soaked (r= 0.851, p ≤ 0.01) and unsoaked pea seeds (r= 0.671, p ≤ 0.01) than the width and thickness of the pea seed. Besides, the three-principal dimension of pea seed correlated positively with equilibrium moisture content at 50 and 60°C. Nonetheless, length and thickness correlated with the equilibrium moisture content at 30 (r= 0.438 & r= 0.578, $p \leq 0.01$) and 40°C (r = 0.552 & r = 0.565, $p \leq 0.01$), respectively. Similarly, the number of starch granules in a cotyledon cell correlated positively with the length and thickness of the pea seed. However, the number of starch granules had a very poor correlation with both the cotyledon cell thickness (r= 0.292, p ≤ 0.01) and length (r =0.275, $p \leq 0.05$). Size and shape are important physical attributes of seeds used to design screens for separating foreign materials and for heat and mass transfer calculations (Sahin & Sumnu, 2011).

The arithmetic and geometric mean diameters (D_a & D_g) for the pea seed varieties in this study (Table 4.2) differed significantly from each other ($p < 0.05$). Before soaking, the arithmetic and geometric mean diameter followed the increasing order: BP<MP< WP~MFP. While, after soaking, both parameters exhibited the same increasing order: BP<MP~WP<MFP. The mean diameters reported for this study were within the range of values described by Wani et al. (2017) & Paksoy & Aydin (2005).

The sphericity (Ø) of pea varieties for this study varied significantly before soaking except for MP and WP. The sphericity value for pea varieties followed the increasing order: MFP<MP~WP<BP. However, the sphericity values for pea varieties after soaking did not differ significantly from each other. Also, the surface area of the pea varieties followed the decreasing trend: MFP~WP>MP>BP and MFP>WP>MP~BP before and after soaking, respectively. Summarily, the distinct physical properties evaluated for the pea varieties in this study would provide the information required by food plant designers for developing equipment such as pea shelling, dehulling, and cleaning machines (Wani et al., 2017).

4.4.3 Proximate composition and cooking characteristics of pea seeds

The composition of the pea seeds from four varieties is shown in Table 4.3. The protein content of the pea samples was in the range of 18.58-20.70% being higher in MFP than the other samples. The protein content for the pea samples was within the range reported by Asif et al. (2013) & Fan et al. (2014). The fibre contents of 5.56-7.16% in this study were quite higher than those reported by Asif et al. (2013). The differences in varieties, expression of genes,

enzymes, and environmental factors could be responsible for the higher values reported in this study (Hall et al. 2017). Among the four varieties, the fiber content was significantly (P>0.05) higher for MP than the other varieties. The fibre content of the pea seeds correlated with the thickness of the cotyledon cell wall ($r= 0.516$, $p \leq 0.01$). On the other hand, the thickness of the seed ($r= -0.263$, $p \leq 0.05$) was shown to be correlated negatively with the fibre content of the pea seed varieties but it was not highly significant. This means the thickness of the cotyledon cell wall may have contributed more to the amount and functionality of the fibrous materials present in the pea seed varieties.

The moisture and carbohydrate contents followed the pattern of WP>MP>BP>MFP and WP~BP>MFP>MP pattern, respectively. The fat content of all the pea varieties was very low lower than 2% similar to those reported in the literature (Tzitzikas et al., 2006; Fan et al., 2014).

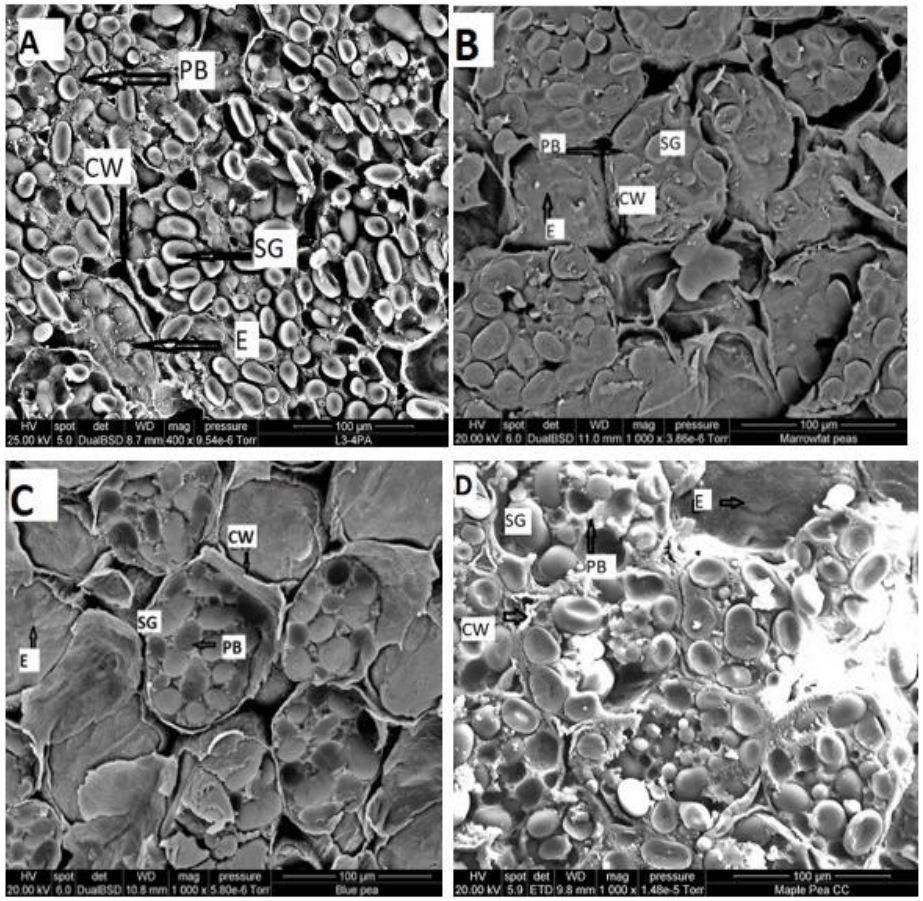

Fig 4.1: SEM micrographs of different varieties of raw New Zealand pea seeds. **A, B, C,** and **D** represent White/yellow, Marrowfat, Blue, and Maple peas, respectively, at 1000X. Note: E; starch granules and protein bodies encapsulated in the cell wall, SG: starch granule, PB: protein bodies, and CW: cell wall.

Table 4.2 Different physical parameters of the pea seed varieties.

Parameter	Pea variety							
	White/yellow	Marrowfat	Blue	Maple	White/yellow	Marrowfat	Blue	Maple
	Before soaking				After soaking			
Length (mm)	8.63 ± 0.47^{c}	9.07 ± 0.53^{c}	6.91 ±0.25^{a}	7.79 ± 0.52^{b}	10.7 ± 0.62^{b}	12 ± 0.55^{c}	9.33 ± 0.30^{a}	10.5 ± 0.81^{b}
Width (mm)	7.71 ± 0.51^{c}	7.24 ± 0.21^{b}	6.12 ± 0.21^{a}	6.92 ± 0.57^{b}	9.48 ± 0.38^{b}	9.43 ± 0.49^{b}	8.44 ± 0.48^{a}	8.75 ± 0.72^{a}
Thickness (mm)	7.48 ± 0.47^{b}	7.83 ± 0.68^{b}	6.56 ± 0.33^{a}	6.46 ± 0.35^{a}	9.25 ± 0.49^{b}	10.7 ± 0.72^{c}	7.97 ± 0.79^{a}	9.08 ± 1.08^{b}
Arithmetic mean diameter (mm)	7.92 ± 0.31^{c}	8 ± 0.27^{c}	6.52 ± 0.16^{a}	7.03 ± 0.32^{b}	9.76 ± 0.26^{b}	10.6 ± 0.38^{c}	8.55 ± 0.32^{a}	9.39 ± 0.67^{b}
Geometric mean diameter (mm)	7.94 ±0.32^{c}	8.04 ± 0.29^{c}	6.53 ± 0.16^{a}	7.06 ± 0.32^{b}	9.8 ± 0.26^{b}	10.7 ± 0.39^{c}	8.58 ± 0.30^{a}	9.44 ± 0.68^{b}
Sphericity Ø	0.92 ± 0.04^{ab}	0.89 ± 0.03^{a}	0.94 ± 0.02^{b}	0.9 ± 0.04^{a}	0.92 ± 0.04^{a}	0.89 ± 0.02^{a}	0.92 ± 0.05^{a}	0.89 ± 0.04^{a}
Surface area S (mm^2)	197.3 ± 15.97^{c}	201.4 ± 13.95^{c}	133.4 ± 0.02^{a}	155.5 ± 14.03^{b}	300.4 ± 16.35^{b}	356.3 ± 25.7^{c}	229.9 ± 17.6^{a}	278.6 ±40.4^{b}

$^{a, b, c}$ Values in each row with the same superscripts do not differ significantly ($p > 0.05$).

Table 4.3 Proximate composition and cooking time of the four different pea seed varieties

Pea variety	Moisture %	Protein %	Fat (%)	Fibre (%)	Ash (%)	Carbohydrate (%)	Total starch (%)	Cooking time (min)	
								unsoaked	soaked
White/Yellow	10.32 ± 0.03^{c}	18.62 ± 0.09^{a}	1.56 ± 0.05^{b}	5.80 ± 0.20^{a}	2.45 ± 0.29^{a}	61.23 ± 0.32^{c}	41.87 ± 2.20^{ab}	68.0 ± 2.64^{a}	29.2 ± 1.02^{b}
Marrowfat	9.67 ± 0.09^{a}	20.70 ± 0.08^{c}	1.00 ± 0.00^{a}	6.10 ± 0.20^{a}	2.64 ± 0.18^{a}	59.90 ± 0.17^{b}	40.54 ± 6.61^{ab}	85.3 ± 5.85^{b}	33.6 ± 1.58^{c}
Blue	9.85 ± 0.02^{ab}	18.58 ± 0.23^{a}	2.00 ± 0.00^{c}	5.56 ± 0.15^{a}	2.51 ± 0.05^{a}	61.50 ± 0.20^{c}	49.23 ± 0.77^{b}	62.2 ± 3.11^{a}	24.4 ± 0.78^{a}
Maple	10.01 ± 0.09^{b}	20.31 ± 0.03^{b}	1.00 ± 0.00^{a}	7.16 ± 0.25^{b}	2.76 ± 0.20^{a}	58.76 ± 0.28^{a}	37.14 ± 0.59^{a}	66.2 ± 2.75^{a}	26.7 ± 0.32^{a}

$^{a, b, c}$ Values in each row with the same superscripts do not differ significantly ($p > 0.05$).

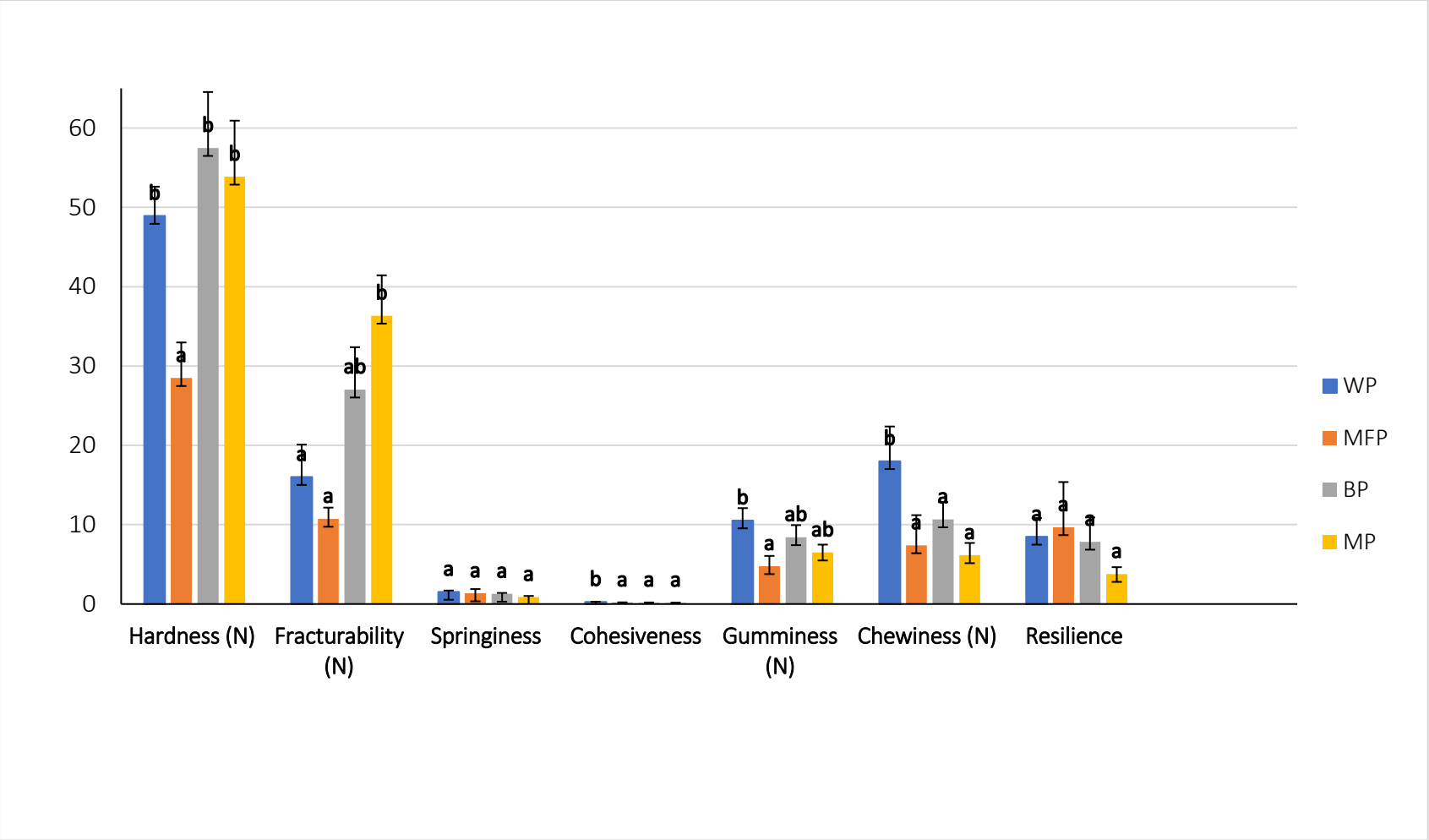

Fig. 4.2: Texture profile analysis (TPA) of cooked pea seed varieties. WP, White/yellow pea; MFP, Marrowfat pea; BP, Blue pea; MP, Maple pea. [a, b, c] Values in each set of bar charts with the same superscript letters are not significantly different ($p > 0.05$)

The total starch content of BP was 49.23% which was 12.09 % higher than MP (37.14%), which had the lowest starch, while the starch content value observed for MFP was comparable to that of WP. The overall total starch contents from this study were similar to the ranges reported by Chung et al. (2008) & Huang et al. (2007). The total starch content of the pea seed had a negative correlation with an average diameter of starch granules ($r = -0.382$, $p \leq 0.01$) and a mild correlation with the thickness of the cotyledon cell wall ($r = -0.241$, $p \leq 0.05$). Furthermore, the total starch had a negative correlation with protein ($r= -0.560$, $p \leq 0.01$).

The average cooking time was observed to follow the decreasing order of MFP>WP>MP>BP, irrespective of the soaking treatment (Table 4.3). The cooking time for MFP was observed to be significantly higher compared to the other varieties. Similar trends have been reported for field peas and pigeon peas, respectively (Parmar et al., 2016 &Tiwari et al., 2008). Cooking time for soaked and unsoaked pea seeds correlated negatively with the hardness ($r = -0.524$, $r = -0.594$, $p \leq 0.01$) and fracturability ($r = -0.437$, $r = -0.494$, $p \leq 0.01$) of the pea seeds, respectively. The negative correlation was expected because the cooking time of the pea seeds is inversely proportional to the hardness or firmness. That is, as the cooking time increases, the hardness of the soaked or unsoaked pea declines. The average diameter of the starch granules correlated strongly with the cooking time ($r= 0.711$, $r= 0.624$, $p \leq 0.01$).

4.4.4 Textural properties of cooked pea seeds

The textural properties of the cooked pea varieties are described in Fig. 4.2. BP, MP, and WP varieties exhibited significant resistance to the compression force (Hardness). They required 57.48, 53.86, and 48.92N, respectively, to overcome this resistance. These results were within the range reported for cooked bean (121°C for 30 min) cultivars (Saha et al., 2009). The amount of compressing force required to penetrate through the outer layer (Fracturability) of the pea varieties followed the decreasing order of MP>BP>WP>MFP. Both textural parameters (Hardness and Fracturability) are usually used as the quality index to measure the firmness of whole-grain cereals and pulses in the food industry. The hardness and fracturability of pea seeds did not correlate with the thickness of the cotyledon cell wall. However, they both had a strong correlation with the number of starch granules in the cotyledon cell, the average diameter of the starch granules, and the thickness of the pea seed. The hardness had a negative correlation with the protein content ($r= -0.355$, $p \leq 0.01$) while fracturability had a positive correlation with fibre ($r= 0.347$, $p \leq 0.01$).

Springiness measures the extent of the effect of initial compression on the grain structure. This means that after the first texture profile analysis compression, the grain structure could be broken down into a few large pieces (high springiness) or many small pieces (low springiness) (Singh et al., 2010 & Wani et al., 2010). In other words, a pea variety with low springiness will tend to break down easily to smaller pieces during mastication than the pea seed variety with high springiness. In this study, the range of springiness was measured to be 0.89-1.54 but no significant difference was observed between the four pea seed varieties. The results of cohesiveness for the pea varieties were in the range of 0.17-0.26 with no significant difference between the pea varieties except for WP. Cohesiveness directly measures the response of food material to the second deformation, relative to its behavior under the first deformation.

Chewiness is an index that quantifies the energy required to transform semisolid food via mastication into a fluidized state before swallowing. The range of chewiness for the pea varieties was 6.15(MP) - 18.01 N(WP) for their proper mastication. The chewiness for the WP seed variety was significantly higher because of the large few pieces resulting from the initial deformation (high springiness) compared to the other pea varieties. Gumminess was measured to be in the range of 4.77-10.54 N and decreased in the following order: WP>BP>MFP>MP while the resilience of the cooked pea varieties tended to increase from MP (3.79) to MFP (9.68) seed varieties. Gumminess ($r = -0.296$, $p \leq 0.01$). and chewiness ($r= -0.256$, $p \leq 0.05$) were negatively correlated with the thickness of the cotyledon cell wall.

4.4.5 Hydration Kinetics

Fig. 4.3 illustrates the hydration kinetics of pea seeds from WP, MFP, BP, and MP, respectively. Generally, the equilibrium moisture content for all pea varieties somewhat decreased as the soaking temperature moved from 30 to 60 °C. The MFP variety absorbed more water at each soaking temperature (30, 40,50, and 60 °C) than the other pea varieties. The absorption rate of MP was found to be lowest at 30, 40, and 60°C while the BP pea variety exhibited the lowest absorption rate at 50 °C The soaking time required for each pea variety to attain saturation point generally decreased as the soaking temperature increased from 30 to 60 °C. At room temperature (30 °C), the soaking time required for WP to get to the saturation point was comparable to that of MFP. The same trend was observed for BP and MP, however, the soaking time required by WP~MFP is greater than the time for BP~MP. The soaking duration required by MP is 120 mins, more than the requirement for BP variety to reach a saturation point at a

soaking temperature of 40 °C, while an approximately similar amount of time was needed by WP and MFP at the same soaking temperature to attain equilibrium moisture content. The soaking duration to attain the equilibrium moisture content for WP, BP, and MP were comparable at a soaking temperature of 50 °C. On the other hand, the soaking time required by MFP was greater than WP~BP~MP. Lastly, at 60 °C of soaking temperature, the soaking time required for each pea variety followed this trend, MFP>WP~MP>BP. The overall trend for the hydration kinetics of the pea varieties showed that as the soaking duration increased, the amount of water absorbed by the pea varieties increased with an increase in soaking temperature (Balkrishna & Visvanathan, 2019). This invariably increased the saturation point of the pea varieties.

The application of the Peleg model to hydration studies was presented in Table 4.4 $k_{1,}$ which shows the Peleg model rate constant decreased for all the pea varieties as the temperature increased from 30 to 60°C. This pattern was similar to the study reported by Turhan et al. (2002); Resio et al. (2006) & Hung et al., (1993). According to Peleg's (1988) hydration model, the reciprocal of k_1 represents the water absorption rate at the initial stages of the hydration process. Therefore, the decrease in k_1 with an increase in temperature indicates an increased water absorption rate at a higher temperature.

Furthermore, k_2 is related to the equilibrium moisture content or maximum water absorption capacity, hence, the lower the value of $k_{2,}$ the higher the water absorption capacity and vice versa. From the results presented in Table 4.4, WP followed the abovementioned pattern, while the other pea varieties showed an erratic trend as the temperature increased.

Generally, the hydration experiment data fitted well at all temperatures and adequately characterized the hydration behavior of seed (R^2 = 0.97 -0.99) for all pea varieties. However, taking a closer look into the degree of fit (R^2) reported in Table 4.4, the R^2 value for MFP and MP increased as the soaking temperature rose.

Table 4.4 Peleg constants at different temperatures and Degree of Fit Based on Eq. (5)

Pea variety	Temperature°C	K_1 (min/%)	K_2 (per %)	R^2
White/yellow (WP)	30	0.263	0.0096	0.9902
	40	0.165	0.0099	0.9952
	50	0.144	0.0112	0.9987
	60	0.1	0.0115	0.9983
Marrowfat (MFP)	30	0.3676	0.0088	0.9936
	40	0.2053	0.0084	0.9980
	50	0.1992	0.0105	0.9988
	60	0.1562	0.0102	0.9992
Blue (BP)	30	0.3422	0.0097	0.9957
	40	0.270	0.0096	0.9887
	50	0.1603	0.0116	0.9961
	60	0.1603	0.0111	0.9930
Maple (MP)	30	0.5721	0.0108	0.9704
	40	0.4048	0.0095	0.9892
	50	0.2766	0.0101	0.9971
	60	0.1908	0.0116	0.9951

K1 represents the water absorption rate at the initial stages of the hydration process.

K2 is related to the equilibrium moisture content or maximum water absorption capacity.

The degree of fit value for WP also increased with the temperature increase up to 50°C and BP exhibited an erratic trend. The distinct microstructural arrangement of the (starch granules and protein bodies) in each pea variety and the changes that occur in the arrangement at each soaking temperature may have been responsible for the above-mentioned trend exhibited during the hydration studies.

4.4.5.1 The role of microstructure on the hydration kinetics

The microstructure of raw and soaked (at 30 and 60 °C) pea seeds are illustrated in Fig. 4.1 and 4.4 respectively. It was observed that there was a decrease in the intactness of the cotyledon structure from raw (room temperature) to those cooked at 60 °C. However, the distortion of the cell wall enclosing starch, protein, and other macromolecules was less observed in the MP variety at 60 °C, compared to the other varieties. This explains the low rate of water uptake by the MP variety because of the strong interconnecting cell wall network holding the cotyledon

structure together across different soaking temperatures. The underlying mechanism for this observation is that the cell wall encapsulating the starch and protein matrix act as a physical barrier to the inflow of water into the matrix at different soaking temperature (Chigwedere et al., 2019).

The number of starch granules per cell (Table 4.1) followed the same decreasing pattern with equilibrium moisture content at 30 and 60°C (MFP>WP>BP>MP). Furthermore, the equilibrium moisture content of 40°C somewhat followed the same pattern MFP>WP>BP~MP. There is a significant positive correlation between the number of starch granules per cell with equilibrium moisture content 30, 40, and 60 °C respectively ($r= 0.349$, $p \leq 0.01$; $r= 0.382$, $p \leq 0.01$; $r= 0.386$, $p \leq 0.01$). During the initial phase of hydration kinetics in pulses, the quantity of water uptake by the cotyledon of the pulses into the intracellular space is determined by the amount required for starch gelatinization, protein denaturation, and dissolution of the middle lamella (Mikac et al.,2015 & Zhang & McCarthy, 2013). Thus, the number of starch granules per cell will determine the maximum uptake of water required for their gelatinization as shown by MFP pea varieties for this study. Furthermore, the average diameter of the starch granules in pea seed varieties correlated significantly with the equilibrium moisture content 30, 40, 50, and 60 °C respectively ($r= 0.370$, $p \leq 0.01$; $r= 0.600$, $p \leq 0.01$, $r= 0.451$, $p \leq 0.01$ and $r= 0.349$, $p \leq 0.01$). This further supports the fact that MFP seed, which has the highest number of starches per cell, will also have the highest average diameter of starch granules.

For this study, the overall trend observed during the hydration kinetics showed that the amount of water uptake to reach an equilibrium moisture content at 30,40, and 60 °C for the pea samples are highest in MFP and lowest in MP pea seed. The thickness of the cotyledon cell wall and the fibre content of the pea seed may also be responsible for this trend. Cotyledon of pulses are observed to hydrate from the (permeable) outer surface, So the thickness or the thinness of this outer surface would determine the rate of hydration in pulses (Mikac et al.,2015; Zhang& McCarthy, 2013 & Chigwedere et al., 2019). Therefore, the MP seed which has the thickest cotyledon cell wall, and the highest content of fibrous material exhibited the lowest hydration rate. The correlation between the thickness of the cotyledon wall ($r= -0.223$, $p \leq 0.05$ & $r= 0.252$, $p \leq 0.05$) and the fibre content ($r= -0.625$, $p \leq 0.01$ & $r= 0.427$, $p \leq 0.01$) with the equilibrium moisture content 30 and 50 °C further established this relationship. The same trend was observed with BP and WP seed except for MFP which do not conform to the

postulated trend, and this may be explained by the structural differences in the thickness of the MFP such as different diameter pores in the MFP cotyledon cell wall.

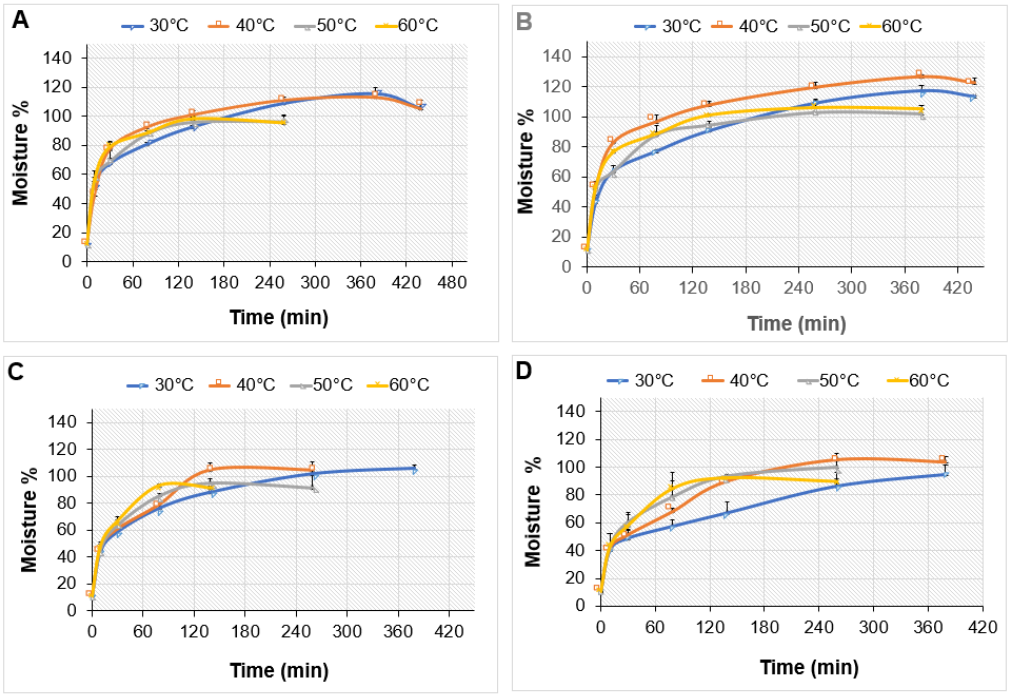

Fig. 4.3. Hydration kinetics of the pea variety. A. White/yellow pea; B. Marrowfat pea; C. Blue pea; D. Maple pea. This is an Excel line to data generated from the relationships and equations according to Balkrishna & Visvanathan (2019). These were used to estimate the intermediate moisture content at various intervals of soaking and equilibrium moisture content.

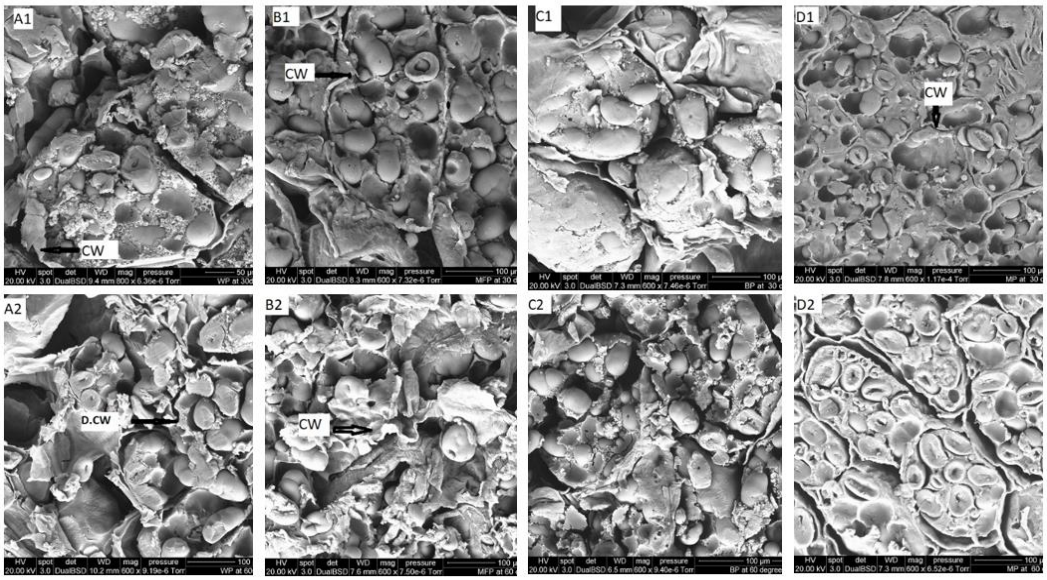

Fig 4.4. SEM electrographs of four different varieties of peas at 30 and 60 °C soaking temperatures. A B, C, and D represent WP, MFP, BP, and MP, respectively. Note (1 & 2 indicate 30 and 60 °C). CW; cell wall, and D.CW; distorted cell wall

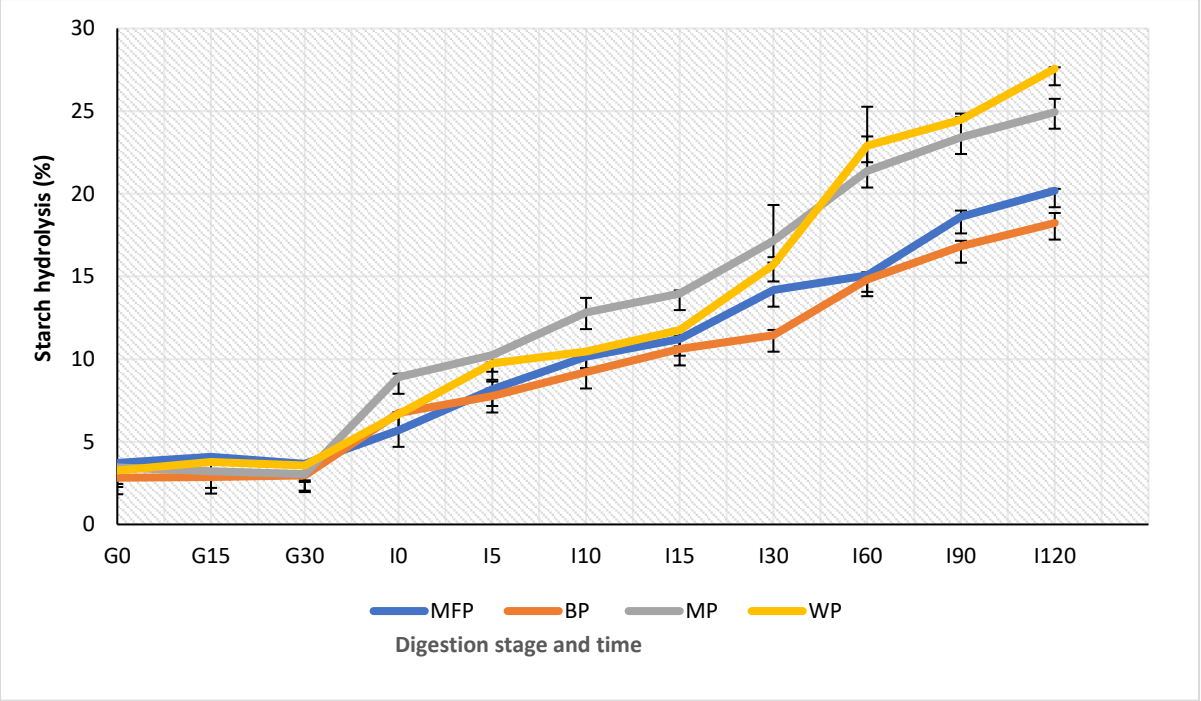

Fig. 4.5. Starch hydrolysis (%) of a cooked pea; White/yellow pea (WP), Marrowfat pea (MFP), Blue pea (BP), and Maple pea (MP) during simulated oral-gastro-small intestinal digestion.

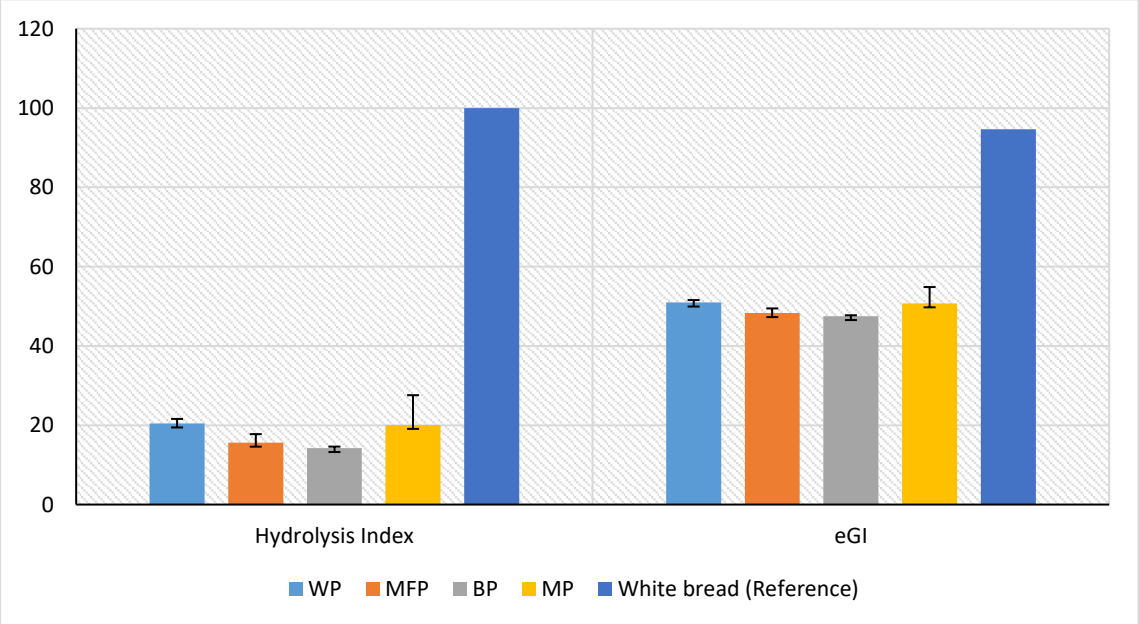

Fig. 4.6. Hydrolysis index (HI) and the estimated Glycaemic index (eGI) of the pea varieties. Note: The hydrolysis index (HI) and estimated Glycaemic index (eGI) for white bread were reproduced from García-Alonso et al. (1998).

4.4.6 In vitro oral gastro-small intestinal digestion of the pea seed

The oral gastro-small intestinal digestion profiles of the four pea varieties (WP, MFP, BP, and MP) are illustrated in Fig. 4.5. The starch hydrolysis observed at the gastric stage is due to the

combined effect of starch-degrading enzymes (α- amylase) introduced to the cooked pea at the oral phase and the mimicked chewing effect of the homogenizer blade. The range of starch hydrolysis at G0 and G30 is (2.8 – 3.5) and (2.9 – 3.6 %) respectively. Also, throughout the gastric digestion phase, BP exhibited the lowest starch hydrolysis compared to other varieties.

For small intestinal digestion, the rate of starch hydrolysis in all the cooked pea varieties steadily increased from I0 to I30. At I30, the MP variety exhibited the highest amount of degraded starch (17.2 %), while BP was observed to have the lowest amount of hydrolyzed starch (11.4 %). Nonetheless, the rate of starch hydrolysis in WP and MP increased sharply from I30 to I60, then followed a steady increase till I120. Summarily, the final starch hydrolysis for these four New Zealand pea varieties falls between the range of (18.2-27.6 %) with WP exhibiting the highest while BP showed the lowest rate of starch hydrolysis.

The starch hydrolysis of pea varieties for this study falls somewhat within the range (16.2 - 40.1 %) as reported for red kidney beans and peas (Germaine et al., 2008 & Junejo et al., 2021). This range of starch hydrolysis could be explained by the difference in particle size and the presence of a non-starch component in the mimicked boluses for this study**.** Pallares et al., (2019) characterized the particle distribution in boluses of common beans and its effect on *in vitro* starch digestion. They reported two distinct fractions, starch-rich (40-125µm) and seed coat material-rich fraction (>2000 µm). Unlike Pallares et al., (2019), both fractions were included in this study, thus the activity of starch-degrading enzymes would be greatly regulated. The cell-wall-rich fraction of dried milled chickpea (1850 µm) also reported a similar low starch digestibility (33.0 %) to this study (Edwards et al., 2021). Furthermore, starch hydrolysis correlated strongly with the fibre content of the pea ($r = 0.325$, $p \leq 0.01$), thereby this correlation supported the above-mentioned explanation.

Some antioxidants such as phenolic compounds are richly localized in seed coats and cotyledons of grain legumes (Singh et al., 2017 & Giusti et al., 2019). The deep coloration of the medium containing the pea varieties observed in this study during cooking and *in vitro* digestion suggests the presence of these phenolic compounds. These compounds have been reported in research to form a two-way interaction with the degrading enzymes and starch granules during starch digestion *in vitro* (Sun & Miao, 2019). This would result in the inhibition of the activity of the starch-degrading enzymes, thereby reducing the extent of starch hydrolysis.

The starch hydrolysis of peas also correlated strongly with their total starch content ($r= -0.276$, $p \leq 0.01$) and the number of starch granules /cells ($r= -0.273$, $p \leq 0.01$) respectively. The starch hydrolysis for the whole peas correlated negatively with the cooking time ($r=-0.253$, $p \leq 0.01$) but did not correlate with the hardness of the seed. This is in agreement with the phenomena postulated by Pallares et al., (2019) that thermally induced hardness (such as cooking of legumes) demonstrates a greater effect on *in vitro* starch digestibility kinetics than mechanical degradation in the mouth.

Table 4.5 Properties examined with Principal Component Analysis (PCA)

Pea seed properties	Notation
Number of Starch granules/ cell	Ns/c
Cotyledon cell diameter	C_d
Thickness of cotyledon cell wall	T_{cw}
Average diameter of starch granules/ cell	$A_{d/s}$
Cooking time for unsoaked peas	$C_{t.us}$
Cooking time for soaked peas	$C_{t.s}$
Equilibrium moisture content 30^oC	E.30
Equilibrium moisture content 40^oC	E.40
Equilibrium moisture content 50^oC	E.50
Equilibrium moisture content 60^oC	E.60
Protein	P
Fibre	F
Carbohydrate	C_r
Total Starch	T_s
Length	L
Width	W
Thickness	T
Arithmetic mean diameter	A_r
Geometric mean diameter	G
Sphericity	S
Surface area	S_A
Hardness	H
Fracturability	F_r
Springiness	S_p
Cohesiveness	C_o
Gumminess	G_u
Chewiness.	C_h
Resilience	R
Starch Hydrolysis	SH

Table 4.6 Pearson correlation coefficient for various pea properties of different varieties.

	Ns/c	Cd	Tcw	Ad/s	Ct.us	Ct.s	E.MC 30°C	EMC.40°C	EMC 50°C	EMC.60°C	P	F	Ts	L	W	T	Ar	S	Sa	H	Fr	Gu	Ch
Cd	-0.069																						
Tcw	0.006	0.331**																					
Ad/s	0.328**	-0.001	0.236*																				
Ct.us	0.496**	-0.132	0.084	0.711**																			
Ct.s	0.388**	-0.149	-0.074	0.624**	0.883**																		
E.MC30°C	0.349**	-0.356**	-0.223*	0.370**	0.559**	0.507**																	
E.MC40°C	0.382**	-0.108	0.116	0.600**	0.852**	0.766**	0.584**																
E.MC50°C	0.195	0.145	0.252*	0.451**	0.559**	0.617**	-0.026	0.503**															
E.MC60°C	0.386**	-0.203	-0.082	0.538**	0.825**	0.816**	0.520**	0.837**	0.293**														
P	0.140	0.195	0.546**	0.601**	0.660**	0.517**	0.014	0.611**	0.646**	0.429**													
F	-0.181	0.364**	0.516**	0.155	0.017	-0.008	-0.625**	-0.092	0.427**	-0.210	0.637**												
Ts	-0.181	-0.180	-0.241*	-0.382**	-0.442**	-0.423**	0.218	-0.097	-0.622**	0.009	-0.560**	-0.641**											
L	0.275*	-0.177	-0.022	0.522**	0.671**	0.851**	0.438**	0.552**	0.483**	0.597**	0.427**	0.056	-0.403**										
W	0.125	-0.036	-0.121	0.168	0.330**	0.623**	0.156	0.202	0.309**	0.322**	0.158	0.099	-0.380**	0.721**									
T	0.292**	-0.156	-0.212	0.467**	0.636**	0.746**	0.578**	0.565**	0.324**	0.628**	0.193	-0.263*	-0.155	0.676**	0.411**								
Ar	0.271*	-0.146	-0.139	0.455**	0.642**	0.867**	0.461**	0.518**	0.436**	0.606**	0.307**	-0.043	-0.364**	0.937**	0.823**	0.811**							
S	-0.169	0.141	-0.238*	-0.437**	-0.444**	-0.472**	-0.168	-0.387**	-0.395**	-0.330**	-0.510**	-0.272*	0.336**	-0.702**	-0.230	-0.100	-0.415**						
Sa	0.280*	-0.152	-0.144	0.455**	0.642**	0.863**	0.472**	0.523**	0.426**	0.609**	0.297**	-0.060	-0.351**	0.936**	0.817**	0.818**	0.999**	-0.410**					
H	-0.421**	0.139	-0.126	-0.442**	-0.594**	-0.524**	-0.354**	-0.396**	-0.268*	-0.496**	-0.355**	0.042	0.260*	-0.456**	-0.150	-0.464**	-0.420**	0.344**	-0.419**				
Fr	-0.318**	0.327**	0.151	-0.389**	-0.437**	-0.494**	-0.487**	-0.332**	0.005	-0.560**	-0.037	0.347**	-0.087	-0.385**	-0.132	-0.460**	-0.384**	0.230*	-0.387**	0.565**			
Gu	-0.180	-0.000	-0.296**	-0.324**	-0.392**	-0.190	-0.066	-0.202	-0.186	-0.235*	-0.432**	-0.204	0.276*	-0.105	0.102	-0.166	-0.066	0.130	-0.066	0.773**	0.231*		
Ch	-0.113	-0.039	-0.256*	-0.179	-0.219	-0.007	0.059	-0.052	-0.145	-0.033	-0.340**	-0.249*	0.258*	0.064	0.126	-0.006	0.073	-0.035	0.072	0.474**	-0.054	0.863**	
SH	-0.273*	0.115	-0.141	0.147	-0.253*	0.183	-0.411**	-0.291**	0.197	-0.144	-0.086	0.325**	-0.276*	0.339**	0.620**	0.079	0.399**	-0.109	0.385**	0.155	0.034	0.308**	0.307**

*$p \leq 0.05$; **$p \leq 0.01$. Ns/c, Number of Starch granules/cell; Cd, Cotyledon cell diameter; Tcw, Thickness of cotyledon cell wall; Ad/s, Average diameter of starch granules; Ct.us, Cooking time for unsoaked pea; Ct.s, Cooking time for soaked pea; EMC(30°C,40°C,50°C, and 60°C), Equilibrium moisture content at 30°C,40°C,50°C, and 60°C; P, Protein; F, Fibre; Ts, Total Starch; L, Length; W, Width; T, Thickness; Ar, Arithmetic mean diameter; S, Sphericity; Sa, Surface area; H, Hardness; Fr, Fracturability; Gu, Gumminess; Ch, Chewiness and SH, Starch Hydrolysis.

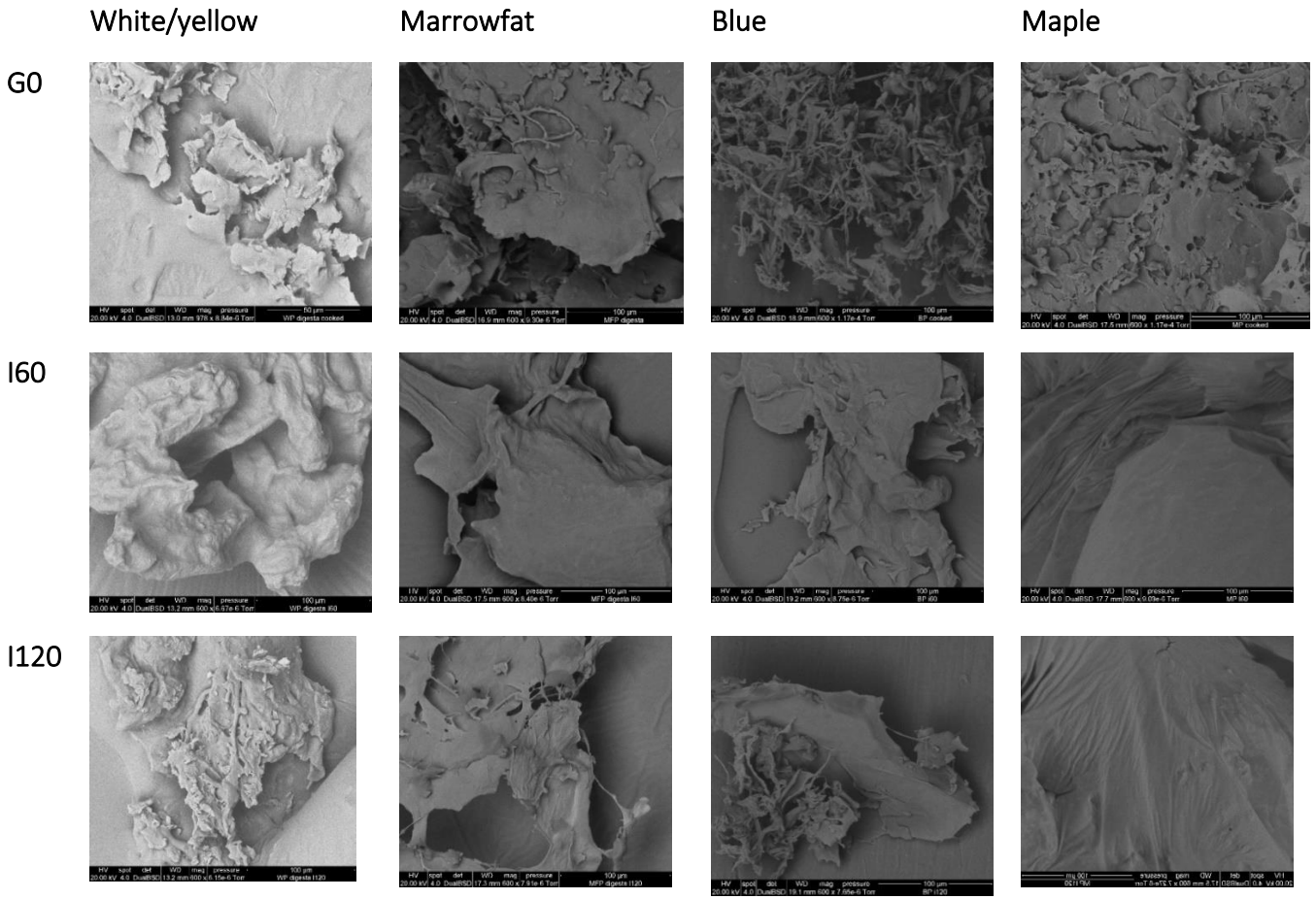

Fig.4.7 Scanning electron micrographs of representative White/yellow, Marrowfat, Blue, and Maple peas sampled during *in vitro* oral-gastro and small intestinal digestion. Where G0, I60, and I120 are gastric digestion at 0 min, and small intestinal digestion at 60 and 120 min.

4.4.6.1 Influence of microstructure on starch hydrolysis of pea seeds

To further explain the effect of pea microstructure during oral gastro-intestinal starch digestion, the SEM micrographs of G0, I60, and I120 were reported in Fig. 4.7. The inclusion of the oral phase (amylase and mimicked chewing) can be seen from the SEM micrograph reported at G0, as there was some evidence of hydrolyzed starch at this stage. Overall, the Blue pea (BP) SEM micrograph tends to exhibit a strong network of fibrous interaction with partly gelatinized and denatured protein bodies at G0 compared to the other cooked pea. This could explain why fewer starch granules of cooked BP were accessible to the starch-degrading enzymes (Fig 4. 5).

The SEM micrograph of the pea digesta at I60 and 120 respectively (Fig 4.7) demonstrated no significant difference in the structural properties except for the digesta of Maple Pea at I60 and I120. A broad sponge-like (amorphous flakes) network was observed in the digesta of MP at I60 and I120, possibly indicating a greater extent of hydrolysis in this variety compared to others.

The estimated glycaemic index (eGI) reported for the digested cooked pea varieties in Fig 4.6 are in the range of 47.5 -50.9, with MP exhibiting the highest eGI. Summarily, the eGI of the digested cooked pea varieties is classified as low compared to the reference (Chen *et al*., 2018). This further supported the role of fibrous and protein interaction (cytoplasmic matrix) with starch granules acting as both primary and secondary physical barriers to enzymatic activity in small intestinal digestion *in vitro*.

4.4.7 Principal Component Analysis (PCA*)*

The PCA analysis provided an overview of the similarities and differences between the seeds of the different varieties, and the interrelationships between the measured properties. Table 4.5 lists all the pea seed properties subjected to PCA analysis and the results of the analysis are shown in Fig. 4.8 and 4.9. The first and the second principal components (PC1 and PC2) explained 33 and 18 %, respectively, of the overall variation. The score plot (Fig.4.8) visualized the difference/similarity between four (4) pea varieties. The distance between the locations of any two pea varieties is directly proportional to the degree to which they differ/close to each other. The farthest difference exhibited on the score plot is shown between BP and MFP seed

varieties. BP seeds are located at the far end of the negative score on the PC1 axis while the MFP seed is on the middle positive score on PC1. On the PC2 axis, MFP and BP border on the zero lines on both positive and negative scores (Fig. 4.8). Similarly, WP and MP seeds border on the zero line on PC1. However, WP and MP seeds are located on the negative and positive scores respectively on the PC2 axis. Also, the degree of variation in each pea seed variety on the score plot (Fig. 4.8) as indicated by the degree of close packing of each cluster showed that BP seeds exhibited the least variation compared to others. Summarily, in terms of the difference in the score plot, BP and MFP exhibited the farthest difference. In terms of similarity, WP and MFP seeds showed a close relationship. The loading plot of the two PCs provided information about correlations between measured morphological, physicochemical, cooking characteristics, and hydration kinetics parameters (Fig.4.9). The general perspective from the loading plots of the two components revealed that the measured properties of pea seed are more positively correlated. Taking a closer look, the average diameter of starch granules, cooking time, hydration kinetics, and physical properties exhibited a positive correlation on PC1. While cotyledon cell diameter, equilibrium moisture content at 50°C, and Fracturability showed a positive correlation on PC 2.

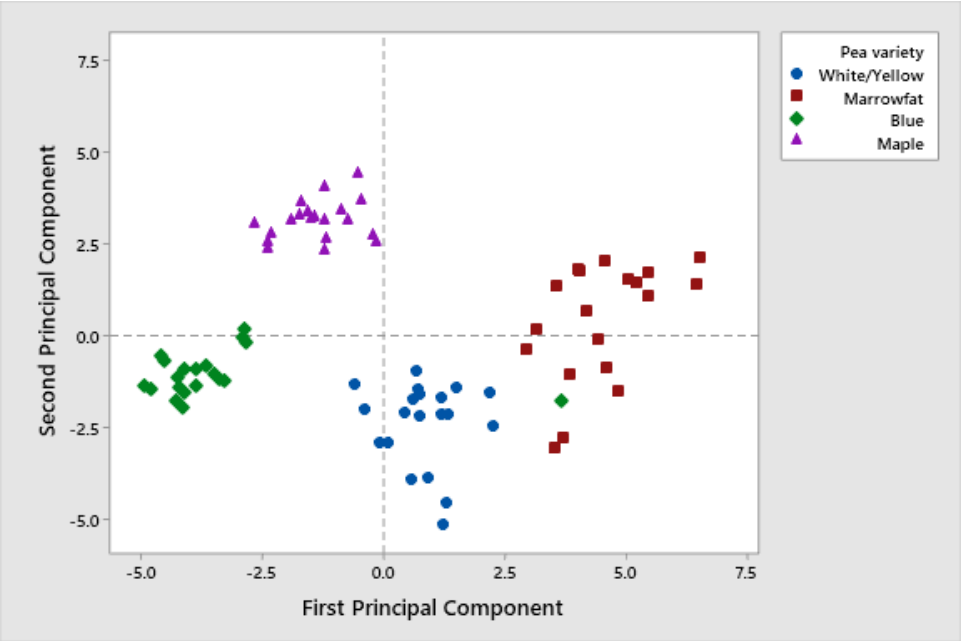

Fig. 4.8: Principal component analysis (PCR): score plot of PC1 and PC2 describing the overall variation between pea seed varieties.

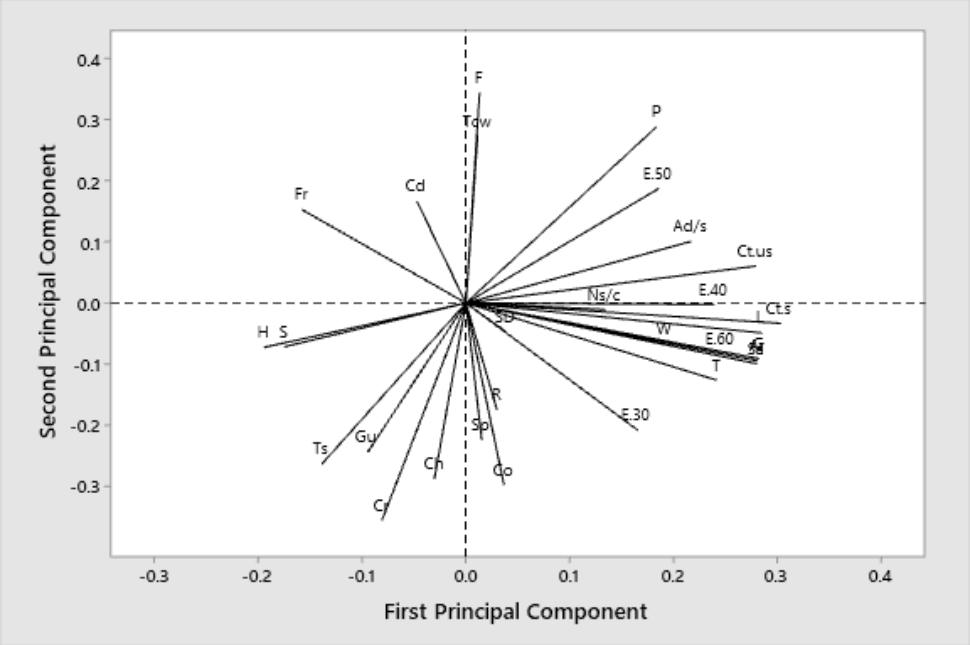

Fig. 4.9: Principal component analysis (PCR): Loading plot of PC1 and PC2 describing the overall variation between properties of pea seed varieties.

4.5 Conclusions

The influence of seed microstructure on the hydration kinetics, cooking properties, and oral gastro-small intestinal digestion *in vitro* of four (4) New Zealand pea varieties was adequately illustrated in this study. The hydration experiment data for the four (4) New Zealand pea varieties fitted well at all temperatures and adequately characterized the hydration behavior of seed (R2 = 0.97–0.99) of all pea varieties. Thus, suggesting the Peleg model is an appropriate tool to predict the hydration behavior of pea seeds. A significant correlation between the number of starches per cell, the thickness of the cotyledon cell wall, fiber content, the hydration rate at different soaking temperatures, cooking time, and *in vitro* starch digestion of pea seed varieties were reported in this study. This implies that the microstructure of a whole pea seed has a role to play in the pre and post-gelatinization conditions. Therefore, it can be inferred that the microstructural characteristics of pea seeds can predict their soaking behavior and cooking characteristics. Furthermore, fundamental information on how pulse seed microstructure plays a significant role in regulating starch digestibility was provided in this study. This is an essential starting point for researchers and product developers in the food industry to explore the potential natural seed microstructure in creating low glycemic foods.

Chapter 5: Cell wall permeability in relation to *in vitro* starch digestion of pulse cotyledon cells

5.1 Abstract

This study investigated the role of cell wall permeability in the microstructure and the rate of starch digestibility in intact cotyledon cells isolated from four different varieties of pea seeds, such as white/yellow pea (WP), marrowfat pea (MFP), blue pea (BP) and maple pea (MP). PFG-NMR coupled with light and confocal microscopes were employed to evaluate the diffusion coefficients and cell wall permeability of cotyledon cells. The diffusion coefficients and cell wall permeability of the cotyledon cells followed a decreasing trend; WP>MFP>MP>BP. The varying size of internal cavities in the microstructure in the cotyledon cells which was observed by the light and confocal micrographs may be responsible for this trend. The extent of starch hydrolysis measured from the cotyledon cells somewhat also followed the same trend of the cell wall permeability. This indicates that the more permeable the cotyledon cell to the starch-degrading enzymes, the higher the extent of intracellular starch hydrolysis. The microstructure changes in the cotyledon cells during digestion also confirmed this observation.

5.2 Introduction

Consumption of whole pulse food had been associated with a reduction in the risk of obesity, type II diabetes, and cardiovascular disease (Fardet & Boirie, 2014, Marsh et al., 2011 & Wang et al., 2019). This is partly due to its low postprandial glycaemic response. The mechanism of how pulse food exhibits the low postprandial glycaemic response has been attributed to the ability of its cell structure and protein matrix to act as a physical barrier to the diffusion of enzymes into the intracellular starch granules in cotyledon cell (Dhital et al., 2016, Bhattarai et al., 2017 & Junejo et al., 2021). Also, the densely packed crystalline structure retained in the cotyledon cells after cooking limits the swelling and gelatinization of entrapped starch granules (Xiong et al., 2019). The effect of cell wall components and protein matrix on the degree of starch digestibility in pulse cotyledon cells has been studied (Junejo et al., 2021, Edwards et al.,2021, Li et al., 2019, Huang et al., 2021, Rovalino-Córdova et al., 2018 & 2019). It was observed from various studies that the cotyledon cell wall is the primary barrier that modulates the extent of intracellular starch digestibility in cells by regulating the ingress of water and

starch-degrading enzymes. Therefore, an intensive study on the cell wall of the cotyledon cell is imperative to help food processors design functional food ingredients/products from pulses.

Cotyledon cell walls mainly consist of cellulose (30 %), xyloglucan (30 %), and pectin (35 %) (Burton et al., 2010 & Voragen et al., 2009). The extent of diffusion of starch degrading enzymes through the cotyledon cell wall is likely to be influenced by numerous factors including cell wall composition and density, cell wall thickness, cellular integrity, the number and size of cell wall pores and processing conditions (Rovalino-Córdova et al., 2018, Grundy et al., 2016, Junejo et al., 2021 & Pallares Pallares et al., 2019). Rovalino-Córdova et al. (2018) & Junejo et al. (2021) observed the effect of damaged cellular integrity of the cotyledon cell wall on the starch hydrolysis in the pulse. They reported that an increase in the damage to the cellular integrity is proportional to the starch hydrolysis in the cell. That is, a reduction in the cellular integrity of the cell will increase the exposure of the intracellular starch to digestive enzymes thus, increasing starch digestibility. On the other hand, Xiong et al. (2019) reported that the permeability of pinto bean cotyledon cells increased after high-moisture treatment (HMT), thus increasing the extent and rate of intracellular starch digestibility. The porosity /permeability of cotyledon cell walls has also been studied by other authors by using fluorescein-labeled dextran to evaluate the porosity/permeability of cotyledon cell walls by subjecting to the different molecular weights of fluorescein isothiocyanate (FITC)-dextran solutions (Huang et al., 2021, Li et al., 2019a & Li et al., 2019b). Fluorescence recovery after photobleaching (FRAP) has also been reported to have been used as a verifying microscopy tool with FITC-dextran to observe the wall porosity in red kidney cotyledon cells (Li et al., 2019a). However, FRAP/FITC-dextran as all microscopy techniques are only meant to corroborate objective measurement of the cell wall porosity/permeability in plant cells (Moud, 2022). Thus, an objective method of measuring the cell wall porosity/permeability of cotyledon cells is needed.

Pulse gradient field-NMR (PFG-NMR) has been highlighted as an accurate and objective technique for directly measuring the characteristics of transfer in plant systems, such as the coefficients of diffusion, permeability, and water flow rate (Anisimov, 2021 & Watanabe & Fukuoka, 1992). It has been used to provide a non-invasive localized diffusion measurement in soybean seed, carrot, and onion tissues and chlorella sp. (Watanabe et al., 1994, Cho et al., 2003, Ando et al., 2009 & Voda et al., 2012).

Considering this, it is hypothesized that the application of PFG-NMR to isolated intact cotyledon cells would provide objective measurements of cell wall properties such as diffusion coefficient and cell wall permeability. Therefore, in this study, the diffusion coefficient and cell wall permeability of isolated cotyledon cells from four pea seed varieties were investigated using PFG-NMR as well as the role of cell permeability on the intracellular starch granule gelatinization and digestion.

5.3 Materials and Methods

5.3.1 Material

Four locally grown whole dry pea seed varieties, White/yellow pea (WP), Marrowfat pea (MFP), Blue pea (BP), and Maple pea (MP), were supplied by Cates Grain and Seed (Ashburton, New Zealand). Each pea variety was vacuum sealed and stored at 4 °C until further studies. Pepsin (porcine gastric mucosa, 800–2500 U/mg protein), pancreatin (hog pancreas, 4 × USP), invertase (Invertase, grade VII from baker's yeast, 401 U/mg solid), fluorescein isothiocyanate isomer I and calcofluor-white stain were all purchased from Sigma–Aldrich Ltd. (St Louis, USA). Alpha-amylase (3000 U/mL) and amyloglucosidase (3260 U/mL) were purchased from Megazyme International Ireland Ltd. (Wicklow, Ireland). All other chemicals were of analytical grade.

5.3.2. Isolation of cotyledon cells from the pea seed varieties.

Raw pea seed varieties were treated with acid and alkali solutions according to the method described by Kugimiya (1990) with slight modifications. Briefly, raw pea seeds were soaked in a 0.1 M hydrochloric acid (HCl) solution (pH ~ 1.3) at room temperature for 24 h. The seed coats were removed manually, and the seed was split into two cotyledons., the resulting cotyledons were rinsed with RO water repeatedly to remove the excess acid, and then soaked in a 0.06 M sodium hydroxide (NaOH) solution (pH ~ 12.5) in Schott bottles. These bottles were shaken in an orbital shaker at 150 rpm and room temperature for 24 h. The resulting softened cotyledons were gently minced (set at the min speed) using a fine mincer screen (Kenwood MG700 series). The resulting paste was passed through a stack of 150 and 53 µm sieves under running RO water repeatedly. The cotyledon cells were collected on the 53 µm sieve then freeze-dried and stored at room temperature until further use.

5.3.3 Morphological properties

5.3.3.1 Light microscopy

The freeze-dried cotyledon cells of each variety were mounted onto a glass slide, and a drop of water was added and sealed with coverslips. The images were viewed under a Zeiss Axiophot light microscope (LM) with Differential Interference Contrast (DIC) optics and a color CCD camera (ZEISS microscopy, Germany) using 20x magnification, respectively.

5.3.3.2 Microstructural characterization

The freeze-dried cotyledon cells and digested cotyledon cells were spread on a scanning electron microscope stub and then gold coated (Baltec SCD 050 sputter coater, New York, USA). The resulting gold-coated stub was viewed using the FEI Quanta 200 Environmental Scanning Electron Microscope (SEM) (Oregon, USA) at an accelerating voltage of 20 kV.

5.3.3.3 Particle size

Cotyledon cells were mixed with water to obtain homogeneous suspensions that were then added into a small volume sample dispersion unit (Hydro 2000S) until an obscuration level of ~15 ± 5 % was obtained. Refractive indices of 1.530 and 1.330 were used for cotyledon cells and water phases, respectively (Do et al.,2019). Particle size was measured with a laser diffraction particle size analyzer (Malvern Mastersizer 2000; Malvern Instruments Ltd., UK) and expressed as volume mean diameter.

5.3.3.4 Confocal characterization of the cells

The confocal characterization of cotyledon cells was carried out according to the method described by Li et al. (2020). Briefly, 5 mg cells were dispersed in 300 µL of FITC solution (1 mg/mL) in a microcentrifuge tube at 4 °C overnight under dark conditions. The suspension was centrifuged at 2000g and then rinsed several times with Milli-Q water to remove the excess dye. The FITC-stained cotyledon cells were transferred into a glass slide, and a drop (~2 µL) of calcofluor-white stain solution was added. The glass slide was covered with a coverslip. The fluorescence emitted by the samples was collected at 405 nm excitation wavelength for calcofluor white and 488 nm for FITC, respectively. Leica SP5 DM6000B scanning confocal microscope (Leica, Germany) was used to observe the morphological features of cotyledon cells.

5.3.4 Cell wall permeability of cotyledon cells

5.3.4.1 Sample preparation

A representative sample of freeze-dried cotyledon cells from section 5.3.2 was rehydrated as follows. The cotyledon cells were soaked in RO water for 2 hours at room temperature, then centrifuged at 4200 rpm for 30 min after which the supernatant water was removed. The centrifugation process was repeated for another 30 min. This resulted in a thick paste of soaked cells with negligible free water

5.3.4.2 PFG-NMR diffusion measurement

The PFG-NMR method described by Ando et al. (2009) was used for the measurement of cell wall permeability with minor modifications. Each variety of centrifuged cotyledon cells was packed into a 5 mm NMR tube. PFG-NMR experiments were made at 298 K using a Bruker Avance 500 MHz spectrometer with a 5 mm QXI probe equipped with a 50 G cm-1 gradient coil. The standard Bruker pulse program *stebpgp1s* was used with the gradient strength, g, ranging from 5 to 40 G cm-1 with 16 steps. The little delta was constant at 1.5 ms and the big delta varied between 30 ms and 1250 ms. Measurements were made over varying diffusion times (30 -1250 ms). Spectra were processed and diffusion constants (D) were extracted by fitting spectra using the Stejskal-Tanner Equation (Stejskal & Tanner, 1965) with Bruker's Topspin 2.1.8 software using standard parameters.

The permeability of the cotyledon cell wall was estimated by the structural model below.

$$1/D_{\infty}=1/D_0 +1/(P \times a)$$

Where D_{∞}= Diffusion coefficient at diffusion time 1250 ms

D_0 = Diffusion coefficient at diffusion time 30 ms

P = Permeability of the cell wall

a = cotyledon cell size

5.3.5 Proximate composition of the cotyledon cells

The moisture content of the freeze-dried cotyledon cells samples was determined by an air oven drying method at 108 °C (AOAC, 2012). Subsequently, the contents of crude protein and crude fat in pea varieties were analyzed by the Kjeldahl method using a conversion factor of 6.25 from nitrogen to protein and the Mojonnier method respectively (AACC, 2000 & AOAC, 2012). The acid/alkali hot extraction method (AOAC, 2012) was used to quantify the fiber content of cells while the gravimetric method which involved heating the cells sample at 600

°C for 3hr was used to determine the ash content (AACC, 2000). The carbohydrate contents of the cell samples were estimated via calculation by subtracting the summation of all other components from 100 %. All experiments were conducted in triplicate.

The total starch content of the cell samples was analyzed using a total starch assay kit (KTSTA, Megazyme International Ireland Ltd., Ireland) following the manufacturer's instructions. Results were reported on a dry weight basis (%).

5.3.6 Thermal properties

Thermal properties were evaluated using a Differential Scanning Calorimeter (DSC) (TA Q100, TA Instruments, Newcastle, DE) according to the method described by Edwards et al. (2020) with slight adjustments. Approximately 4 mg of cotyledon cells were weighed into stainless steel pans and water was added at a ratio of water to flours of 3:1. The pans were sealed, and an empty steel pan was used as a reference sample. The samples were heated from 20 °C to 110 °C at 10 °C/min. Onset temperature (T_o), peak temperature (T_p), conclusion temperature (T_c), and enthalpy of gelatinization (ΔH_{gel}) were calculated using Universal Analysis Software (version 4.5A, TA Instruments).

5.3.7 X-ray diffraction (crystallinity)

X-ray diffraction analysis was conducted using an X-ray diffractometer (D8 Advance, Bruker, Germany), which was operated at 40 kV and 40 mA with Cu Kα radiation (λ = 0.154 nm) (Shi et al.,2017). The cotyledon cells were scanned from 4° to 40° (2θ) at a speed of 2°/min and a step size of 0.02°. The relative crystallinity was calculated as the ratio of the crystalline peak area to the total diffraction using EVA 4.2 software (Bruker, Germany*).*

5.3.8 *In vitro* gastro-small intestinal digestion of the cotyledon cells

Cotyledon cells were mixed with water in a ratio of 1:5(w/v) in a Schott bottle to obtain a heterogeneous mixture containing approximately 4% starch concentration. The resulting mixture was cooked in a boiling water bath at 95°C for 20 min and immediately cooled down in a pre-set water bath at 37 °C.

For the gastro-small intestinal digestion, simulated gastric fluid (SGF) and simulated intestinal fluid (SIF) were prepared (Pharmacopeia, 1995, 2000). A two-stage gastro-small intestinal in vitro digestion model was used for this study as described by Dartois et al. (2010) with some modifications.

Approximately 170 g of the cooked cotyledon cell solution was introduced into the jacketed glass reactor. The reactor temperature was maintained at 37 ± 1 °C by circulating water in the reactor jacket. The reactor contents were mechanically stirred by a magnetic stirrer bar at 300 rpm throughout digestion. The pH was initially adjusted to 2.0 (using 3 M HCl solution), then 25 mL of SGF (pepsin: starch ratio of 1.765:100, w/w) was added to start the hydrolysis; and the final pH was adjusted to 1.2 (using 0.5 HCl solution). After 30 minutes, the pH was adjusted to 6.8 to inactivate the pepsin enzyme. Subsequently, 22 mL of SIF (pancreatin/starch ratio, 1.3:100, w/w, amyloglucosidase/starch ratio, 0.26:1, v/w, and invertase/starch ratio, 1:1,000, w/w) was added to start the small intestinal digestion, and pH was maintained at 6.8 using 0.5 and 3 M NaOH solution. The total time to complete the gastric and small-intestinal digestion was 30 and 120 min, respectively.

A 0.5 mL of aliquot was withdrawn from the reactor after 0, 15, and 30 min of gastric digestion (G0, G15, and G30), and 0, 5, 10, 15, 30, 60, 90, and 120 min of the small intestinal digestion (I0, I5, I10, I15, I30, I60, I90, and I120). The glucose concentration of the incubated mixture was measured using the D-glucose assay kit (GOPOD Format K-GLUK 07/ 11, Megazyme International Ireland Ltd, Ireland). Starch hydrolysis was expressed in percentage as described by Dartois et al. (2010).

5.3.9 Statistical analysis

The mean and standard deviation were calculated and evaluated for all reported values except those stated otherwise. All values were subjected to statistical analysis using Minitab 19.1.1.0 statistical software (Minitab LLC, Chicago, USA) at $p \leq 0.05$.

5.4 Results and Discussion

5.4.1 Microstructural characterization of isolated intact cotyledon cells from pea varieties.

The cotyledon cells isolated for this study showed high cellular integrity and minimal starch gelatinization as shown in Fig 5.1. This result agrees with the other authors that the acid/alkali pre-treatment method for isolating cotyledon cells produces intact cells with negligible free starch granules or broken cell walls (Dhital et al., 2016 & Kim & Kim, 2015). During successive acid-alkali solution treatment isolation methods, the polyvalent metal ions connecting the cells

are separated by the acid, while the solubilization of pectin with β-elimination reaction is promoted by the alkali (Aguilera et al., 2001; Kugimiya, 1990). The total yield (Table 5.1) of the isolated cotyledon cells for this study is less than 20 % (dry matter) which is within the range reported in the literature (Bhattarai et al., 2017 and Pälchen et al., 2021). It was observed that the large amount of retentate generated during the sieving procedure contained large clusters of cotyledon cells as shown in Fig 5.8.

In general, all cotyledon cell samples (Fig 5.1) appear to be elongated, ellipsoidal, or spherical with sizes ranging from 130 to 150 µm (Table 5.1). The particle size of the cotyledon cells from white/yellow pea varieties was significantly different ($P < 0.05$) from the other varieties and it seems the specific surface area decreases with an increased mean diameter (Table 5.1).

The starch granules for all the isolated cotyledon cells are shown to be densely backed within the boundaries of the cell walls (Fig 5.1 & 5.2). There are distinct internal cavities that are obvious with the starch granules as shown in Fig 5.2. Such cavities have been reported by other authors (Li et al., 2018 & 2019). These distinct cavities indicate the negligible effect of the acid/alkali pre-treatment isolation techniques on the intracellular starch granules (limited starch gelatinization) due to the high level of cellular integrity as exhibited by the intact cell wall (Fig 5.2).

5.4.2 Diffusion coefficient of the cotyledon cells using PFG-NMR

The diffusion coefficient of water in all the cotyledon cells decreased with increased diffusion time (Fig 5.3). At the beginning of the diffusion experiment, WP cotyledon cells exhibited a higher diffusion coefficient than cells from the other varieties. Similarly, when the diffusion time was about 80s, the diffusion coefficient shown by the WP cotyledon cells was higher than that of the other cotyledon cells.

Table 5.1. Particle size of the cotyledon cells from four different pea seed varieties

Cotyledon cells	D (0.1) µm	D (0.5) µm	D (0.9) µm	Mean Diameter (µm)	Specific surface area (m^2/g)	Yields (%)
White/yellow	78.91 ± 0.14[a]	128.8 ± 0.24[a]	205.0 ± 0.46[a]	135.3 ± 0.27[a]	0.06± 0.12[a]	19.8
Marrowfat	79.14 ± 1.85[a]	145.5 ± 0.44[c]	264.3 ± 1.32[c]	146.1 ± 2.41[b]	0.06± 0.01[a]	12.7
Blue	91.61 ± 1.69[b]	140.8 ± 0.41[b]	217.0 ± 3.89[a]	146.7 ± 0.27[b]	0.05 ± 0.03[b]	16.8
Maple	90.34 ± 0.11[b]	148.6 ± 0.10[d]	245.6 ± 0.37[b]	146.5 ± 0.13[b]	0.04± 0.02[c]	18.2

[a, b, c] Values in each column with the same superscript letters are not significantly different ($p > 0.05$).

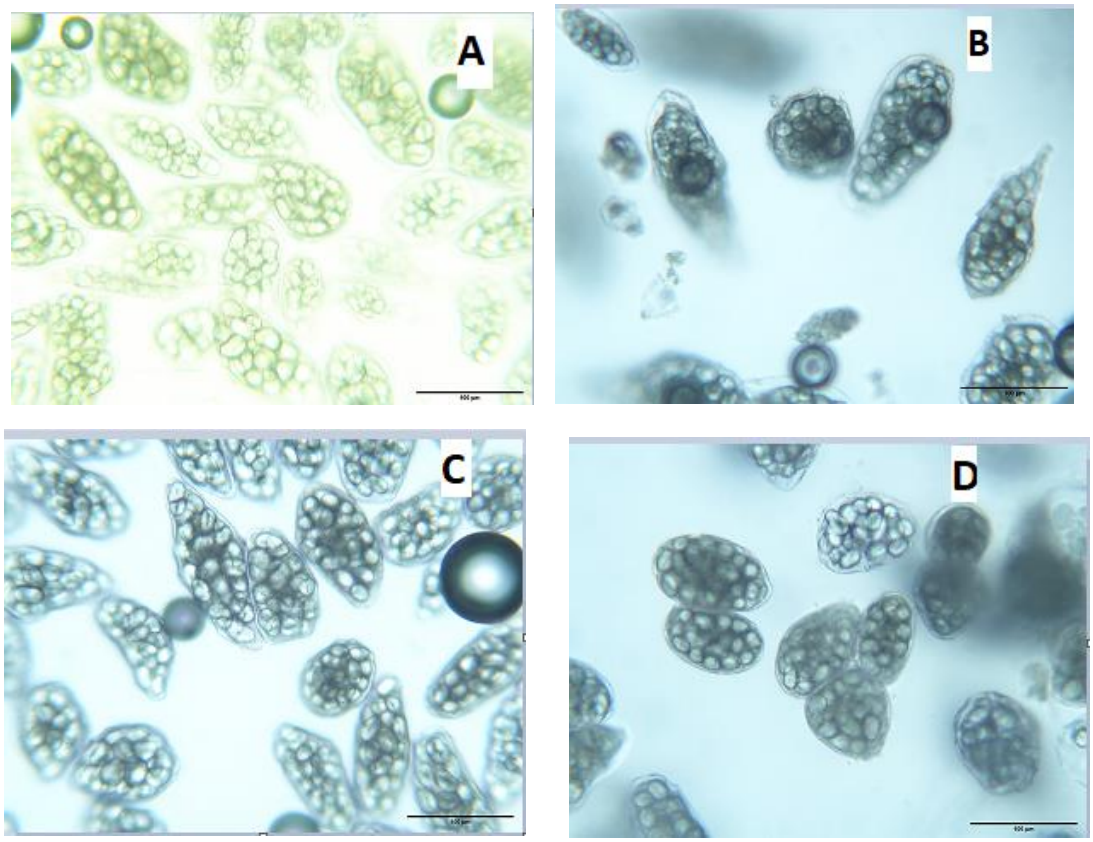

Fig 5. 1. Light microscope images of cotyledon cells from four different pea seed varieties (A: White/yellow pea, B: Marrowfat pea, C: Blue pea, and D: Maple pea).

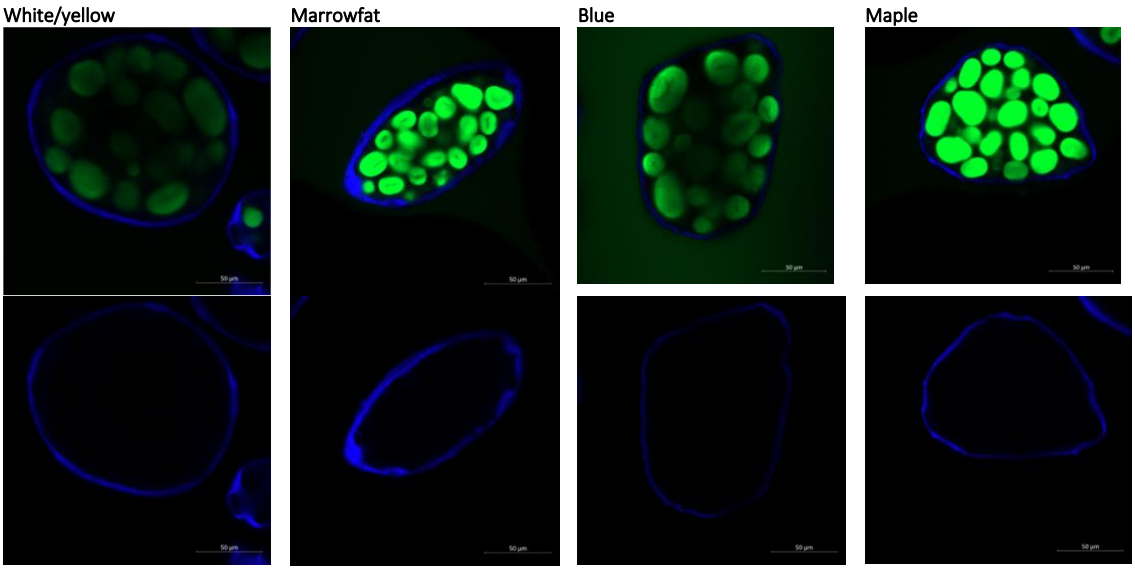

Fig 5.2: Confocal laser scanning microscope images from four different pea seed varieties (White/yellow pea, Marrowfat pea, Blue pea, and Maple pea).

At the end of the diffusion experiment (diffusion time = 1250 ms), the diffusion coefficient of all the cotyledon cells followed a trend; WP > MFP>MP>BP. Overall, between the diffusion time of 30 to 1250 ms, BP cotyledon cells exhibited the highest decrease in diffusion coefficient compared to the other cotyledon cells. The trend of the diffusion coefficient decreasing with increased diffusion time for this study was consistent with the studies reported by some other researchers (Cho et al., 2003 & Ando et al., 2009).

The diffusion coefficient of water in a cell is a quantitative measure of the molecular movement of water in and out of the cell (Kitamura & Kinjo, 2018). There are three main mechanisms for water transportation in plant systems: namely (a). Intracellular water self-diffusion in a cell; (b) molecular diffusion of water between adjacent cells and groups of cells; and (c) long-distance transport associated with the mass flow of water between the organs of the plant (Anisimov, 2021). The diffusion behavior for this study exhibited restricted diffusion, that is, water molecules cannot freely move in the cotyledon cells due to a barrier such as a cell wall or cell membrane (Ando et al., 2009). Therefore, BP-isolated cotyledon cells exhibited more restricted diffusion compared to the other cells.

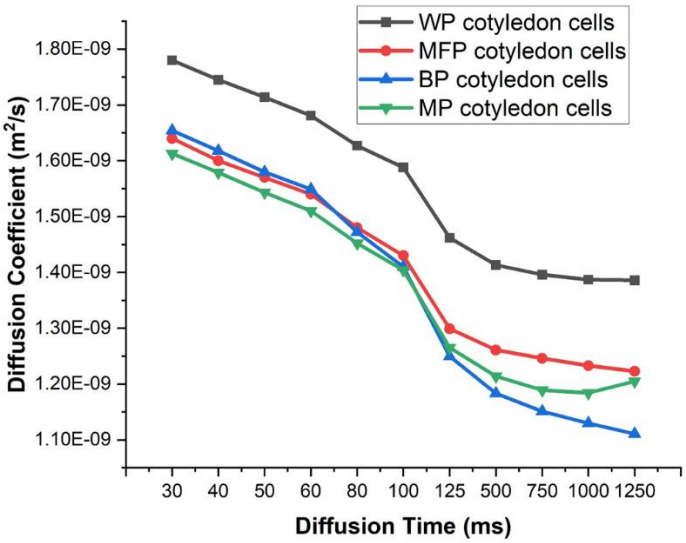

Fig 5.3. The measured diffusion coefficient of water in intact cotyledon cells as a function of diffusion time. Where, WP, MFP, BP, and MP cotyledon cells are White/yellow, Marrowfat, Blue, and Maple cotyledon cells respectively.

The water permeability of the intercellular barrier (cotyledon cell wall) is estimated by the equation shown in section 5.3.4.2. The results showed that the isolated cotyledon cells

followed a decreasing trend; WP > MFP >MP > BP (Fig 5.4). That is, the water permeability tends to be highest and lowest in WP and BP cotyledon cells respectively. It is assumed that the cell wall in BP cotyledon cells is less porous than in WP cotyledon cells. The permeability reported for this study is larger than fresh onion tissue but consistent with freeze-thawed onion tissue reported by other authors (Ando et al., 2009). The larger permeability exhibited by the cotyledon cells for this study can be attributed to the irreversible distorted functionality of the native microstructure of the cell wall caused during the freeze-drying process (Voda et al., 2012). The ice crystals are formed from the intracellular water in the cell during the rapid freeze stage and they sublime via the pores of the cell wall, thus leaving behind a more porous cell. Even after rehydration of the cells in water as described in this study, the native functionality of the cell wall cannot be recovered (Aravindakshan et al., 2021 & Voda et al., 2012).

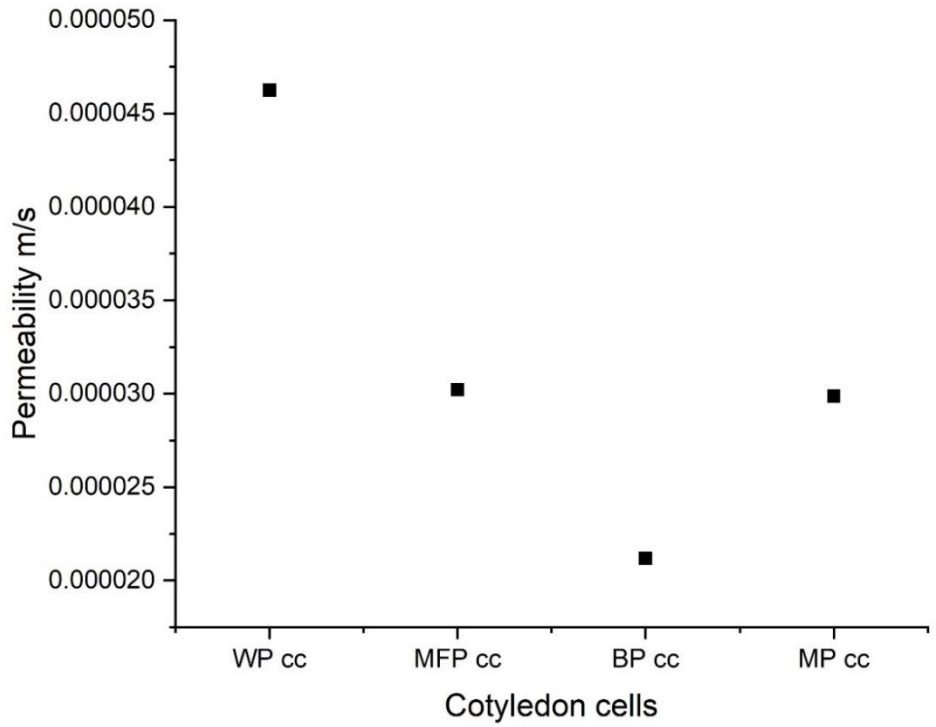

Fig 5.4 Permeability of the intact cotyledon cells. Where, WP, MFP, BP, and MP cotyledon cells are White/yellow, Marrowfat, Blue, and Maple cotyledon cells respectively.

Furthermore, pulse seed cell walls are made up of type I primary cell walls that are rich in xyloglucans and pectic polysaccharides. The interactions between these polymers form an

assembly of complex macromolecular structures that regulate the apoplastic cellular exchange of macromolecules such as enzymes, protein water, and gas (Rondeau-Mouro et al.,2008 & Edwards et al., 2021).

5.4.3 Nutritional composition of the cotyledon cells

The proximate composition of the cotyledon cells for this study tends to be significantly different among the pea varieties ($p < 0.05$) (Table 5.2). The protein content of the cotyledon cells tends to increase from WP <BP<MP<MFP. The fat content on the other hand among the cotyledon cells from the pea varieties was less than 1%. This low-fat content from the cotyledon cells is expected and consistent with other reports (Bhattarai et al., 2017). The fibre content of the cells differs significantly among the pea varieties ($p < 0.05$) and follows the same trend with the protein content. The total starch value available in cells (Table 5.1) seems to be the most abundant component (total starch content for all cells > 50%). The cotyledon cells from blue pea varieties showed a starch content significantly more than the cells from the other varieties. This total starch content agrees with the other authors (Pälchen et al., 2021).

The nutritional composition of the cotyledon cells for this study identified the significant presence of starch, protein, and fibre components. These components are validated with the distinct starch granules, protein bodies, and cellular materials (cell wall) as observed from the light microscope (Fig 5.1), Confocal image (Fig 5.2), and SEM micrograph (Fig 5.7), thus indicating functionality of the cell such as cell wall porosity, starch gelatinization, and digestibility would depend on these components.

Table 5.2 Nutritional composition of the cotyledon cells

Cotyledon cells	Moisture (%)	Protein (%)	Fat (%)	Fibre (%)	Ash (%)	Carbohydrate (%)	Total starch (%)
White/Yellow	10.03 ± 0.12^{b}	14.61 ±0.37^{a}	0.53 ± 0.16^{a}	2.65 ± 0.12^{a}	0.49 ± 0.13^{a}	71.69 ±0.66^{c}	55.23± 0.58^{b}
Marrowfat	9.27 ± 0.31^{a}	21.93 ±0.14^{d}	0.56 ± 0.19^{a}	3.61± 0.33^{d}	0.85 ± 0.06^{c}	63.78 ±0.38^{a}	51.63± 1.34^{a}
Blue	9.63 ± 0.29^{ab}	16.46 ±0.24^{b}	0.48 ± 0.21^{a}	2.94 ± 0.19^{b}	0.73 ± 0.02^{b}	69.75 ± 0.59^{b}	63.44± 0.59^{c}
Maple	11.23 ±0.06^{c}	20.25 ± 0.05^{c}	0.25 ± 0.13^{b}	3.37± 0.47^{c}	0.82 ± 0.09^{c}	64.08 ±0.49^{a}	54.67 ± 0.38^{b}

$^{a, b, c}$ Values in each column with the same superscript letters are not significantly different ($p > 0.05$).

5.4.4 Crystallinity and Thermal Properties

The relative crystallinity of the intracellular starch granules in the cotyledon cells from different pea varieties was analyzed using the X-ray diffraction (XRD) technique. The results are illustrated in Fig 5.5. The XRD pattern of the intracellular starch granules in the cotyledon cell samples presented the characteristics of a C-type polymorphic pattern (mixture of A- and B-type X-ray pattern) with major peaks at 5.6°, 11.5°, 15.4°, 17.6°, and 23.6° 2 theta. The X-ray diffractograms for this study are consistent with the report by other researchers (Junejo et al., 2021). The total relative crystallinity of the entrapped starch granules of the cotyledon cells was less than 30% and increased from MP<BP<MFP< WP. These results fall within the range reported by other researchers (Junejo et al., 2021 & Li et al., 2020). The disruption of the crystalline structure of starch granules in the cotyledon cells and the permeability of the cotyledon cell wall tend to follow a similar trend (Li et al., 2023).

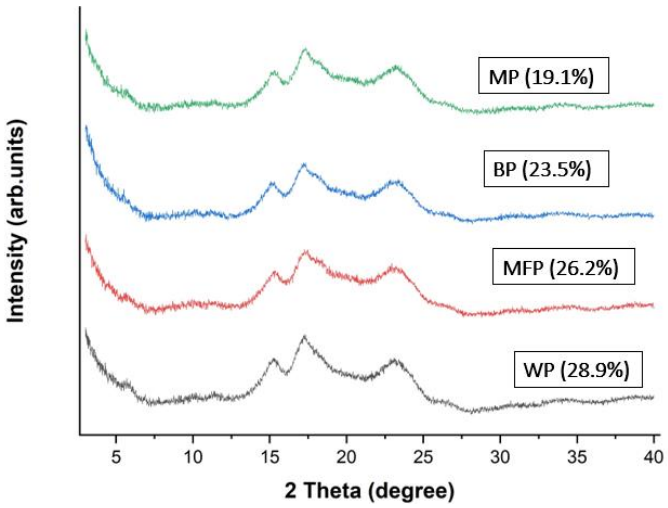

Fig 5.5. Relative crystallinity of cotyledon cells. Where, WP, MFP, BP, and MP cotyledon cells are White/yellow, Marrowfat, Blue, and Maple cotyledon cells respectively.

The thermal properties of the cotyledon cells reported for this study (Table 5.3) showed that all cotyledon cells exhibited a single endothermic transition with broad peaks from 54 to 98 °C, which reflected delayed gelatinization. The onset temperature (T_o), peak temperature (T_p), conclusion temperature (T_c), and enthalpy of gelatinization (ΔH_{gel}) for this study were consistent with those reported in the literature (Li et al., 2019, Do et al., 2019 and Li et al., 2023). The onset temperature (T_o) of the starch granules in the cotyledon cells for the study differed significantly among the varieties ($p < 0.05$). The onset temperature (T_o) of the

entrapped starch granules in the cells increases in the following trend: MPF<MP<WP<BP. The peak temperature (T_p) and conclusion temperature (T_c) values of the intracellular starch granules in MFP and BP cotyledon cells do not differ significantly. The delayed entrapped starch gelatinization in the cells reported for this study reflected the degree of permeability of the cell wall earlier reported in section 5.4.2. That is cotyledon cell walls do regulate the inflow of water into the cell, thereby limiting the degree of starch gelatinization.

Table 5.3 Thermal properties of the cotyledon cells

Cotyledon cells	T_o (°C)	T_p (°C)	T_c (°C)	ΔH_{gel} (J.g-1)
White/yellow	56.45 ± 1.05[b]	63.64 ± 2.09[b]	97.26 ± 1.78[b]	8.83 ± 1.58[a]
Marrowfat	54.17 ± 0.89[a]	64.71 ± 1.41[a]	95.70 ± 3.96[c]	18.13± 3.46[c]
Blue	58.52 ± 0.10[c]	64.65± 0.69[a]	95.46 ± 2.99[c]	8.06 ±1.51[a]
Maple	55.96± 0.58[ab]	62.80 ± 0.02[c]	98.84± 0.76[a]	10.64 ± 0.70[b]

[a, b, c] Values in each column with the same superscript letters are not significantly different ($p > 0.05$.

The enthalpy of gelatinization (ΔH_{gel}) for this study (Table 5.3) showed a significant difference in value between the MFP and MP cotyledon cells while the starch granules in WP and BP cells do not differ significantly in their enthalpy of gelatinization value. ΔH_{gel} can predict the energy required to break down the intermolecular hydrogen bonds of the amylopectin crystallites in legume starch granules (Hoover et al., 2010 & Ahmed et al., 2021). This implies that the energy required to provide the order-disorder transition of starch granules in both WP and BP cotyledon cells respectively is similar. On the other hand, the starch granules in MFP required more energy than MP.

5.4.5 *In vitro* gastro-intestinal starch digestion of cotyledon cells

In vitro gastro-small, intestinal digestion of the cooked cotyledon cells is illustrated in Fig 5.6. As expected, no starch hydrolysis occurred at the gastric stage because of the absence of starch-degrading enzymes (α-amylase) in the simulated gastric fluid (SGF). For the small

intestinal digestion, after 10 min, the starch hydrolysis of all the cotyledon cells was between the range of 27.25-54.46 %. The starch hydrolysis of the cooked cotyledon cells then moved sharply to the range of 44.52-73.71% after 30 min. After 90 minutes, the starch hydrolysis in MP cotyledon cells was less than the other cotyledon varieties. The starch hydrolysis then rose steadily until the end of 120 min of the small intestinal starch digestion. Overall, the final starch hydrolysis of the cooked cotyledon cells ranges between 71.1-83.8 %. The MP and BP cotyledon cells recorded the lowest and highest starch hydrolysis respectively (Fig 5.6).

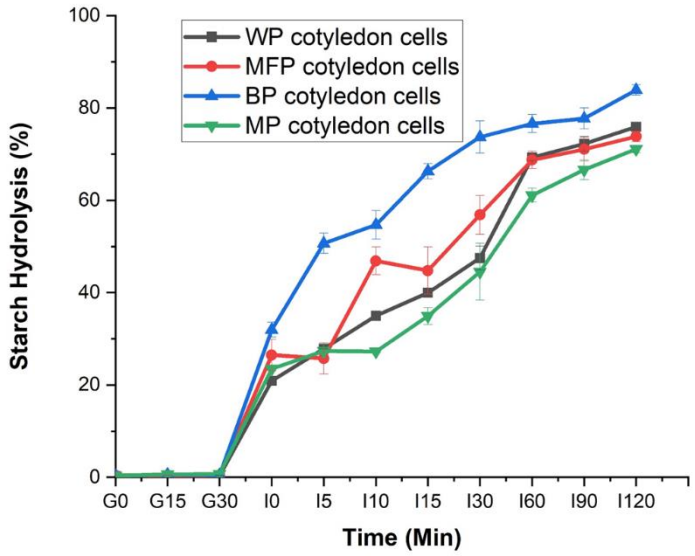

Fig 5.6 Starch hydrolysis of the cotyledon cells during in vitro gastro-small intestinal digestion. Where, WP, MFP, BP, and MP cotyledon cells are White/yellow, Marrowfat, Blue, and Maple cotyledon cells respectively.

The starch hydrolysis of the cotyledon cells for this study was lower than the reported value from other authors (Junejo et al., 2021, Li et al., 2020) but was consistent with some other researchers (Do et al., 2019 & Rovalino-Córdova et al., 2019). The discrepancy between the starch digestibility in the cotyledon cells for this study and other authors could be attributed to the effect of processing treatment (such as different isolation methods and using of uncooked cotyledon cells for digestion) on the structural modification in the cotyledon cell wall (Rondeau-Mouro et al.,2008).

It is imperative to note that, the cotyledon cells that tend to show lower starch digestibility from other reports were subjected to more heating(cooking) at the isolation stage and before the starch digestion procedure than the cotyledon cells for this study. This is important because literature has reported that the structure type I primary cell wall (Xyloglucan and pectic polysaccharides) of pulse cotyledon cells exhibit high cellular integrity after cooking (Berg et al., 2012, & Edwards et al., 2021). Thus, hypothesizing that the reinforcement of pectin-rich polysaccharide polymers in the cell wall from several heating procedures would limit the ingress of starch degrading enzymes in the cell far better.

Nonetheless, the moderately low starch hydrolysis reported amongst the cotyledon cells for this study corroborates the permeability study conducted on the cells. WPF and MFP cotyledon cells that showed large permeability to water tend to show high starch hydrolysis (Fig 5.6). This implies that, though the molecular weight of water used for the permeability experiment is lower than the digestive enzymes, the porosity of WPF and MFP cotyledon cell walls allowed more ingress of the starch degrading enzymes than MP cotyledon cell during digestion. The BP cotyledon cells, on the other hand, exhibited the highest starch hydrolysis despite having shown to have a cell wall that is less permeable to water (Fig 5.6). One of the probable reasons for this could be attributed to the distinct internal cavities observed in the confocal images of the cells (Fig 5.2). The internal cavities in the BP cotyledon cells seem to be largely due to the less densely packed starch granules in the cells compared to other cells. What this means is that complete gelatinization (complete swelling and disruption of the crystalline starch granules) is observed more in BP cotyledon cells compared to the cotyledon cells variety.

	White/Yellow	Marrowfat	Blue	Maple
Raw		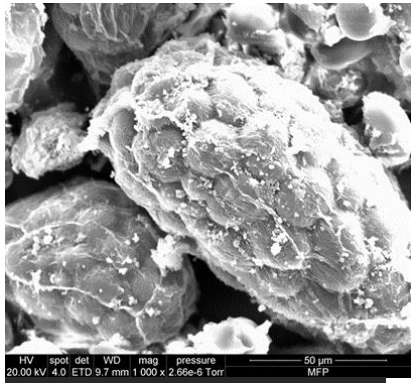		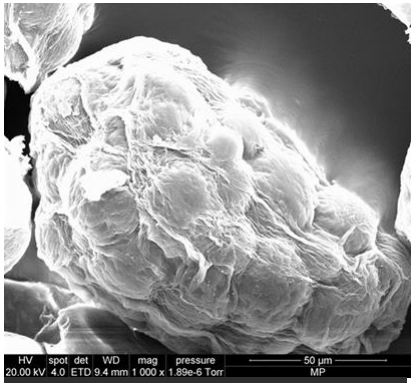
Cooked	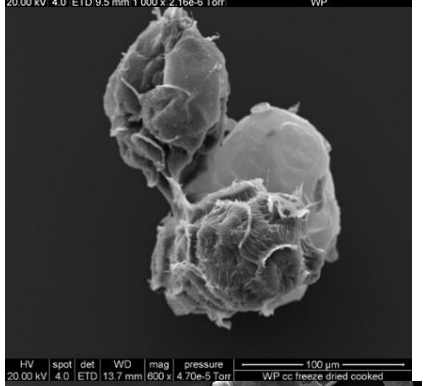	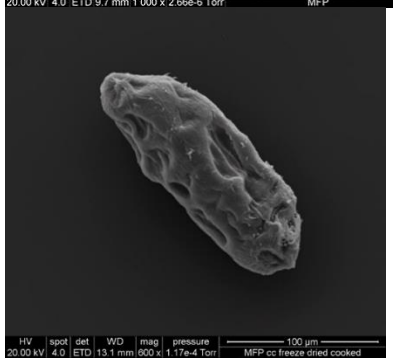	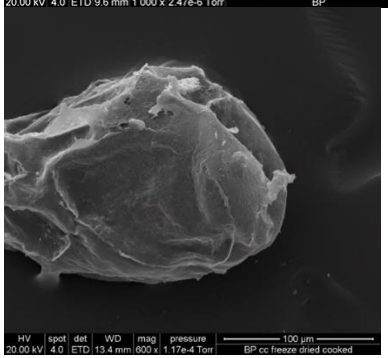	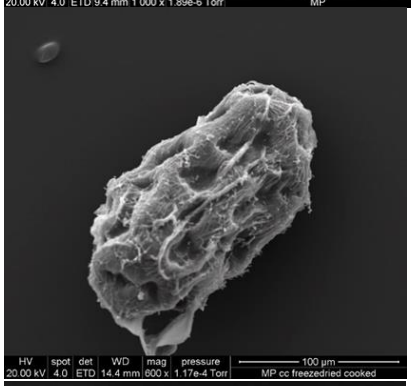
G30	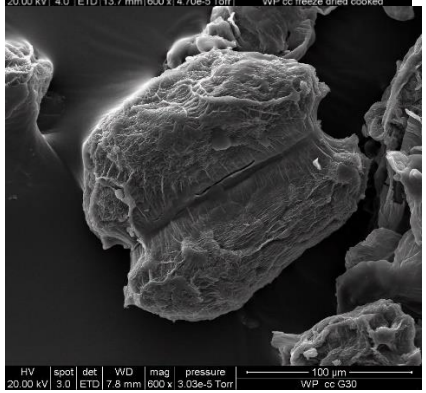	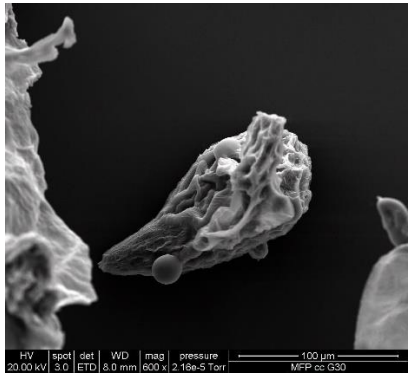	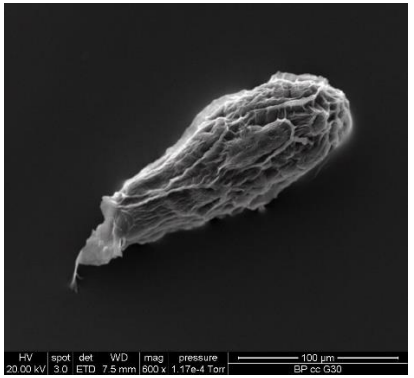	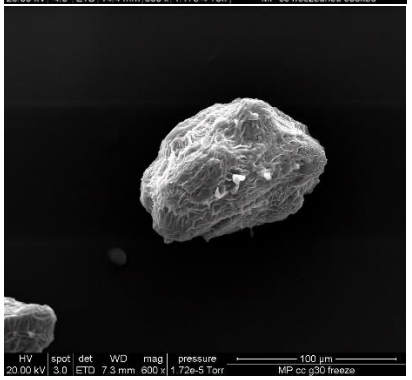

I10

I120

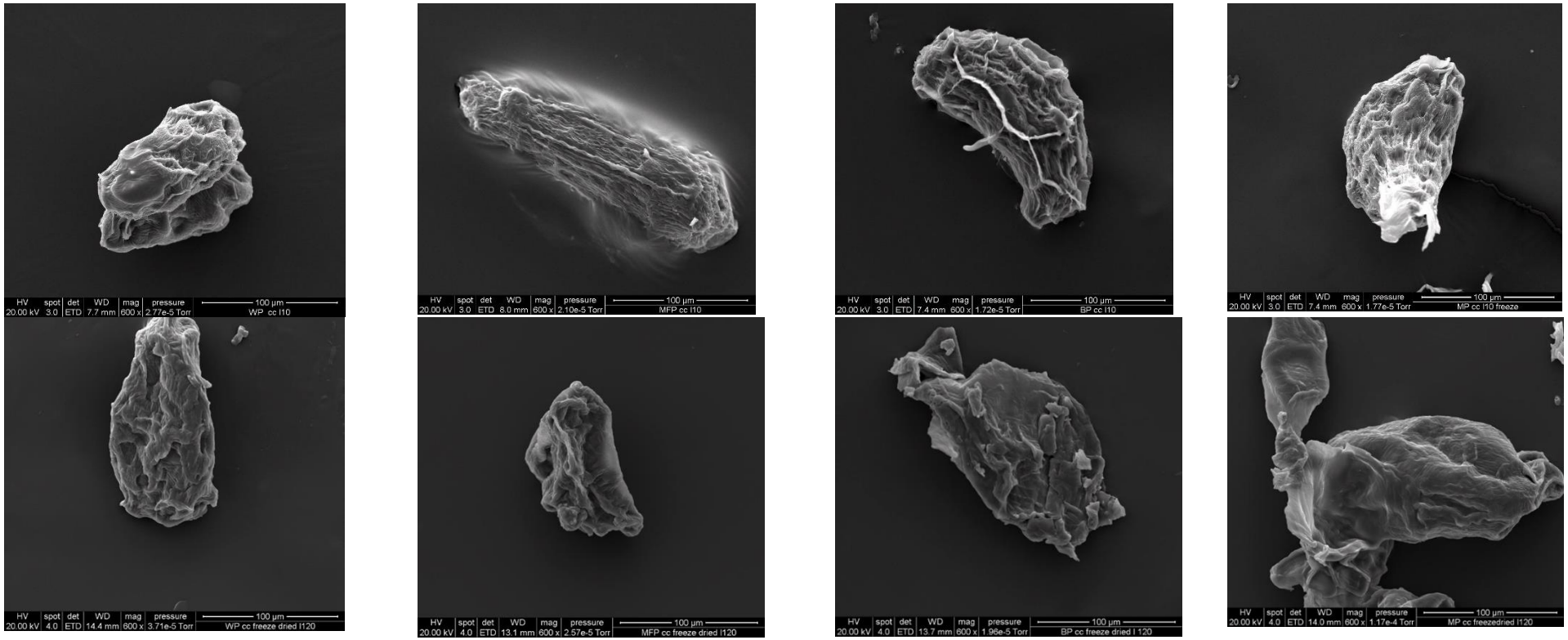

Fig 5.7 Scanning electron micrographs of cotyledon cell samples isolated from four pea varieties (White/yellow pea, Marrowfat pea, Blue pea, and Maple pea) during *in vitro* gastro and small intestinal digestion. Where G30 is gastric digestion at 30 min while I10 and 1120 are small intestinal digestion at 10 and 120 min respectively

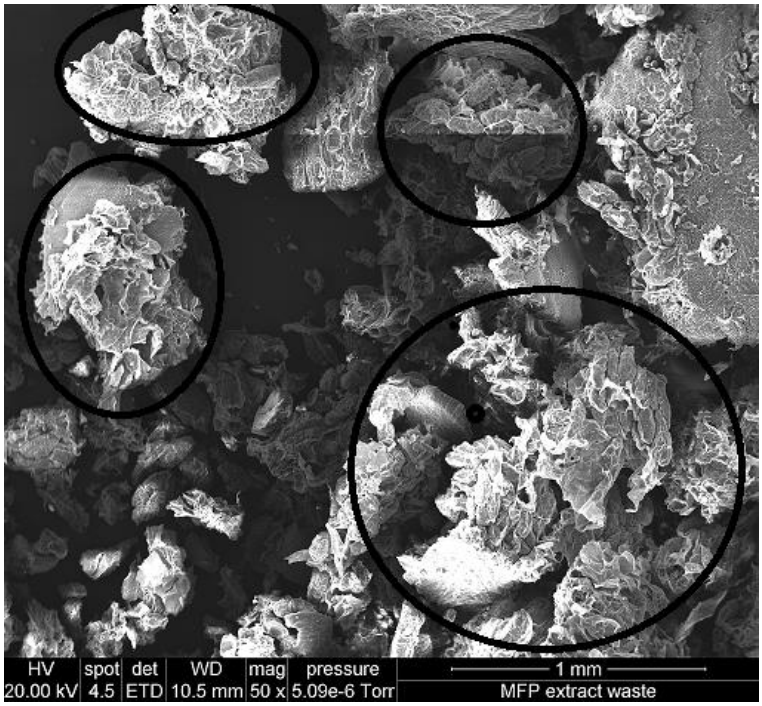

Fig 5.8 Scanning electron micrograph of the waste (retentate) generated during cotyledon cell isolation. Note. The circle indicated large clusters of cotyledon cells.

The overview of the microstructure of the cotyledon cells in their raw state, after cooking, at the end of the gastric phase (G30), and in the small-intestinal digestion stage (I10 &I120) are summarised in Fig 5.7. The SEM micrograph of the raw cotyledon cells varied in different shapes and sizes with distinct identifiable densely packed starch granules encapsulated by a cell wall. At the cooking stage, major structural changes such as indentations and wrinkles were observed on the surface of largely intact cotyledon cells. The internal components (intracellular starch and protein bodies) of the cell undergo physicochemical changes (partially gelatinized starch, leached amylose, and denatured protein in the presence of heat and water introduced during cooking. At this point, it is important to assume that a drastic structural change had happened to the cotyledon cell wall. A similar observation has been reported by other authors (Do et al., 2019 & Berg et al., 2012). At the end of the gastric stage, there were no distinct changes observed in the cotyledon cell. As the digestion proceeded in the small intestine from I10 to I120, numerous indentations and pits were observed on the surface of the cotyledon cells. This could have resulted from the leaching of some digested intracellular molecules during the digestion process. Overall, the cell walls of the cotyledon cells at the end of the digestion process are larger and intact (Fig 5.7) with some cotyledon cells exhibiting more

collapse structure (multiple layers of folding and shrinking) than others. The degree of drastic microstructural changes that occur in the cotyledon cells from raw to cooked (introduction of water and heat), gastric, and small intestinal stages (introduction of starch degrading enzymes) depends on the extent of porosity or permeability of the cell wall.

5.5 Conclusions

The role of cell wall permeability in the microstructure and the extent of *in vitro* starch hydrolysis of intracellular starch in cotyledon cells were investigated for this study. The light and confocal micrographs observed a high level of cellular integrity of the cotyledon cells before diffusion experiments. The PFG-NMR provided an objective measurement of the diffusion coefficients and the cell and how its cell wall is permeable to water during the diffusion experiment. The light and confocal micrograph confirmed the trend observed in the cell permeability behavior of the cotyledon cells. The degree of starch hydrolysis somewhat buttressed the cell wall permeability trend observed by the PFG-NMR. The study provided a fundamental objective measurement in understanding the role of cell wall permeability in cotyledon cells, however, for a holistic investigation on the cell wall of pulse cotyledon cells, other specific characteristics such as the number and size of cell wall pores should be investigated.

Chapter 6: Microstructural, nutritional, and *in vitro* starch digestion properties of a novel cotyledon flour designed via Micronization Techniques.

6.1 Abstract

This study compared the microstructural, nutritional, and starch digestibility properties of a novel cotyledon flour prepared via micronization techniques (colloid milling) with blended flour (traditional grinding) from the same botanical sources. The SEM characterization of both flours showed a distinct difference in their microstructural arrangement. The protein and fibre contents of cotyledon flour were 10 and 3 % higher than those of the blended flour from the same plant sources. The starch hydrolysis and glycaemic response of cotyledon flour were almost 10 % lower than that of the blended flour. This could result in the cell wall of cotyledon cells acting as a primary barrier that regulates the inflow of starch-degrading enzymes to the intracellular starch granules. Also, the high-quality protein/cellular matrix found in the cotyledon flour may reduce the exposure of the extracellular starch granules to degrading enzymes. This study provided fundamental insights into how to sustainably process whole pulse seeds.

6.2 Introduction

There has been a recent highlight on pulses/legumes as a sustainable nutrient-dense plant-based food /food ingredient due to changing trends in consumer food patterns over the years (Ahmed et al., 2021). One of the reasons for this shift towards pulses/legumes can be attributed to their nutritional (high amount of protein) and health benefits (low glycaemic features and high levels of resistant starch (Ajala et al., 2022 & Ahmed et al., 2021). The microstructure of pulse /legumes, i.e., the configuration and interaction of intracellular (starch in cotyledon cells) and extracellular starch with non-starch macromolecules (protein, lipids, and fiber/cell wall materials) during processing conditions may be responsible for these unique properties (Edwards et al., 2021).

The effects of various processing conditions on the microstructure of pulse seed and the subsequent impact on the functional properties have been reviewed recently (Ajala et al., 2023). It was discovered that three forms/types of microstructures, namely whole pulse seed,

pulse isolated cotyledon cells, and pulse flour, can be generated via different size-reducing techniques (wet and dry-based milling). In recent years, the whole pulse seed and isolated cotyledon cells have been highlighted as a potential source of new functional ingredients with low glycaemic features (Berg et al, 2012, Bhattarai et al., 2017, Do et al.,2019, Pälchen et al., 2021, Edwards et al., 2020 & Ajala et al., 2023).

Nonetheless, there are a few limitations in applying whole pulse seed and isolated cotyledon cells in developing new food products with low glycaemic features. The large particle size of the whole pulse seed limits the extent to which it can be applied to food products. That is, one of the important prerequisites that define functional ingredients is an applicable particle size that can be used in a broad range of food products. Although the development of isolated cotyledon cells tends to solve these limitations (particle size 40 - 250 µm), however, the total extraction yield available in the literature is less than 30 % of the weight of the pulse/legume seeds (Bhattarai et al 2017, Pälchen et al., 2021). From a sustainability perspective, approximately 70-85 % of waste (unevenly distributed mixture of starch granules, protein/cell wall matrix materials, and many clusters of cotyledon cells) is generated during the extraction procedure of cotyledon cells (Ajala et al., 2023). Therefore, new processing techniques or methods need to be developed to overcome these numerous challenges to optimally produce pulse/legume food ingredients in an application for food products.

Micronization techniques such as colloid milling have been used in the food industry for quite some time to enhance food quality and functionalities (Chen et al., 2017). These are wet-based size reduction techniques that confer many advantages compared to the traditional grinder. The advantages include mixing, emulsifying, and homogenizing effects, smaller damage to starch granules, improved soluble dietary fiber, and increased adsorption and surface area properties of food materials (Sharma et al.,2008, Vishwanathan et al., 2011, Shakerardekani et al., 2012, Chau et al., 2007, Zhao et al.,2009 & Zhao et al.,2010).

In this regard, this study then hypothesized that the application of micronization technologies (colloid milling) to whole pulse seed would generate flour with unique microstructural, nutritional, and starch digestion properties. Therefore, this study compared the microstructural, nutritional, pasting, thermal, crystallinity, and starch digestion properties of flours prepared via colloid milling and traditional grinder from the pulse of the same botanical sources.

6.3 Material and Methods

6.3.1. Material

White/yellow pea (WP), Blue Pea (BP), Maple pea (MP), and Marrowfat pea (MFP) dry pea varieties were used for this study (Cates Grain and Seed Ashburton, New Zealand). Amyloglucosidase (3260 U/mL) and alpha-amylase (3000 U/mL) were supplied from Megazyme International Ireland Ltd. (Wicklow, Ireland). invertase (Invertase, grade VII from baker's yeast, 401 U/mg solid), Pepsin (porcine gastric mucosa, 800–2500 U/mg protein) and pancreatin (hog pancreas, 4 × USP) were all from Sigma–Aldrich Ltd. (St Louis, USA). All other chemicals were of analytical grade.

6.3.2 Preparation of novel cotyledon flours from pea seeds

6.3.2.1 Acid and Alkali Treatment

Before milling, raw pea seed varieties were treated with acid and alkali solutions according to the method described by Kugimiya (1990) with slight modifications. Briefly, raw pea seeds were soaked in a 0.1 M hydrochloric acid (HCl) solution (pH ∼ 1.3) at room temperature for 24 h. This is done to enhance the separation of the polyvalent metal ions connecting the cells (Kugimiya (1990). The swollen pea seeds were rinsed with RO water repeatedly to remove the excess acid, and then the swollen pea seeds were soaked in a 0.06 M sodium hydroxide (NaOH) solution (pH ∼ 12.5) in bottles. The bottles were shaken in an orbital shaker at 120 rpm and room temperature for 24 h. The NaOH solution was discarded, and the resulting softened pea seeds were rinsed with RO water and then gently minced using a fine mincer screen (Kenwood MG700 series) into a thick paste.

6.3.2.2 Colloid milling

The minced pea seed paste was subjected to colloid milling as described in Fig 6.1. This method was optimized as described in the Appendix (Table 1). A premix of the minced pea paste was prepared by adding excess RO water to the pea paste and ensuring no lump was in the suspension. The colloid mill rotor speed (Bematek CZ-60-PB, Salem, Massachusetts) was set at 30 Hz, and the gap between the stator and rotor was set at approximately 300 µm. This was the initial setting for the milling process. The premix pea suspension was passed through the colloid mill via the milling head. This process was repeated for the resulting suspension from the first milling process at a fixed rotor speed, but the gap between the stator and the rotor

was adjusted in decreasing order (from 300 – 50 µm). The resulting suspension at the end of the milling process was freeze-dried and stored at room temperature for further analysis. The freeze-dried pea powder was passed through 212 µm and the cotyledon flour was collected on the 53 µm sieves. The yield was calculated as the % of flour recovered after sieving over the original dry matter recovered after freeze-drying.

For comparison, blended flour was prepared from the same batch of pea variety according to the method described by Edwards et al. (2020) with slight modifications. The pea seeds were blended in a grinder (Breville, BCG200BSS) for 2 min with an interval of 25 s. The blended flour was then passed through 212 and 150 µm, and the blended flour was harvested after passing through the 150 µm sieve. The flour particle retained on the 150 µm sieve is re-blended. This is done to ensure all large flour particles are broken down. The blended flours were stored at room temperature until further analysis.

6.3.3. Morphological properties

6.3.3.1 Microstructural characterization

Cotyledon flour and blended flour were spread on a scanning electron microscope stub and then gold coated (Baltec SCD 050 sputter coater, New York, USA). The resulting gold-coated stub was viewed using the FEI Quanta 200 Environmental Scanning Electron Microscope (Oregon, USA) at an accelerating voltage of 20 kV.

6.3.3.2. Particle size distribution

Cotyledon/blended flour was mixed with water to obtain homogeneous suspensions that were then added into a small volume sample dispersion unit (Hydro 2000S) until an obscuration level of ∼15 ± 5 % was obtained. Refractive indices of 1.530 and 1.330 were used for cotyledon/blended flour and water phases, respectively (Do et al., 2019). Particle size distribution was measured with a laser diffraction particle size analyzer (Malvern Mastersizer 2000; Malvern Instruments Ltd., UK).

6.3.4. Proximate composition and water-holding capacity

The moisture content of all flour samples was determined by an air oven drying method at 108 °C (AOAC, 2012). The total starch content of the cotyledon and blended flour was evaluated and reported on a dry weight basis (%) using a total starch assay kit (KTSTA, Megazyme International Ireland Ltd., Ireland) according to the manufacturer's instructions. The fiber content of all the flour samples was evaluated using the acid/alkali hot extraction methods (AOAC, 2012). The ash content of all the flour samples was estimated using the gravimetric method which involved heating the flour samples at 600 °C for 3 hr (AACC, 2000). The crude fat and protein in all the flour samples were analyzed by Mojonnier (AACC,2000) and Kjeldahl method respectively (AOAC,2012). The carbohydrate contents of the flour samples were estimated via calculation by subtracting the summation of all other components from 100%. All experiments were conducted in triplicate.

The water holding capacity of cotyledon and blended flours was determined with a modified version of the AACC method no. 51-61 (AACC, 2000). A suspension of flour in water (1:5 ratio, w/v) was prepared and centrifuged for 15 min at 1000 g at 20 °C. The resulting supernatant was removed, and the remaining wet paste was weighed. The water holding capacity was calculated from the mass of water absorbed divided by the mass of dry flour (g water/g solids).

6.3.5 Pasting Properties

The pasting profile of cotyledon and blended flours was analyzed using a Rapid Visco Analyser (RVA-4, Newport Scientific Pty Ltd, Warriewood, Australia) following the Standard Method (STD 2) (AACC method 76-21; AACC, 2000). Cotyledon/blended flour and water suspensions were prepared by mixing 3.5 g flour (14 % moisture basis) and 25 g distilled water. The suspensions were equilibrated at 50 °C for 1 min, heated at 6 °C/min to 95 °C, held at 95 °C for 5 min, cooled at 6 °C/min to 50 °C, and held at 50 °C for 2 min. Peak, trough, and final viscosities were determined from the viscogram.

6.3.6 Thermal properties

Thermal properties of cotyledon and blended flours were evaluated using a Differential Scanning Calorimeter (DSC) (TA Q100, TA Instruments, Newcastle, DE) according to the method described by Edwards et al. (2020) with slight adjustments. Approximately 4 mg of cotyledon/blended flour were weighed into stainless steel pans and water was added at a ratio of water to flours of 3:1. The pans were sealed, and an empty steel pan was used as a reference sample. The samples were heated from 20 °C to 110 °C at 10 °C/min. Onset temperature (T_o),

peak temperature (T_p), conclusion temperature (T_c), and enthalpy of gelatinization (ΔH_{gel}) were calculated using Universal Analysis Software (version 4.5A, TA Instruments).

6.3.7 X-ray diffraction (crystallinity)

X-ray diffraction analysis was conducted using an X-ray diffractometer (D8 Advance, Bruker, Germany), which was operated at 40 kV and 40 mA with Cu Kα radiation (λ = 0.154 nm) (Shi et al.,2017). The cotyledon/blended flour was scanned from 4° to 40° (2θ) at a speed of 2°/min and a step size of 0.02°. The relative crystallinity was calculated as the ratio of the crystalline peak area to the total diffraction using EVA 4.2 software (Bruker, Germany*).*

6.3.8. *In vitro* oral gastro-small intestinal digestion

Cotyledon/blended flour was mixed with water in a ratio of 1:5 (w/v) in a Schott bottle to obtain a heterogeneous mixture containing approximately 4% starch concentration. The resulting mixture was cooked in a boiling water bath at 95 °C for 20 min and immediately cooled down in a pre-set water bath at 37 °C. A simulated saliva fluid (SSF) prepared according to Schwanz et al. (2019), with an α-amylase concentration of 0.3 U/mL, was added at a ratio of 1:1 to the cooked flour samples suspension. The resulting solution was stirred with the aid of a magnetic stirrer bar and then incubated at 37 ± 1 °C for 2 min. To mimic the chewing procedure, the cooked flour sample solution was homogenized in a grinder (Breville, BCG200BSS).

A two-stage gastro-small intestinal *in vitro* digestion model was used for this study as described by Dartois et al. (2010) with some modifications. The simulated gastric fluid (SGF)(Pharmacopeia, 1995) and simulated intestinal fluid (SIF)(Pharmacopeia, 2000) for gastro-small intestinal digestion were prepared.

The gastro-digestion phase began by adding approximately 170 g of flour samples from the oral phase into the jacketed glass reactor. The reactor temperature was maintained at 37 ± 1 °C by circulating water in the reactor jacket. The reactor contents were mechanically stirred by a magnetic stirrer bar at 300 rpm throughout digestion. The pH was initially adjusted to 2.0 (using 3 M HCl solution), then 25 mL of SGF (pepsin/starch ratio of 1.765:100, w/w) was added to start the hydrolysis; and the final pH was adjusted to 1.2 (using 0.5 M HCl solution). After 30 minutes, the pH was adjusted to 6.8 to inactivate the pepsin enzyme. For the small intestinal digestion, 22 mL of SIF (pancreatin/starch ratio of 1.3:100, w/w, amyloglucosidase/starch ratio of 0.26:1, v/w, and invertase/starch ratio, 1:1,000, w/w) was added to the reactor jacket, and

pH was maintained at 6.8 using 0.5 and 3 M NaOH solution. The total time to complete the gastric and small-intestinal digestion was 30 and 120 min, respectively.

A 0.5 mL of aliquot was withdrawn from the reactor after 0, 15, and 30 min of gastric digestion (G0, G15, and G30), and 0, 5, 10, 15, 30, 60, 90, and 120 min of the small intestinal digestion (I0, I5, I10, I15, I30, I60, I90, and I120). The aliquots were immediately transferred to 15 mL centrifuge tubes containing 2 mL of absolute ethanol to stop enzymatic activities. The glucose concentration of the incubated mixture was measured using the D-glucose assay kit (GOPOD Format K-GLUK 07/ 11, Megazyme International Ireland Ltd, Ireland). Starch hydrolysis was expressed in percentage as described by Dartois et al. (2010).

$$\%SH = 0.9\ x\ \frac{Gp}{Si}$$

Where %SH is the percentage of starch hydrolysis, Gp is the glucose produced, and Si is the initial amount of starch. The estimated glycaemic index (eGI) of the digested flour samples was calculated with the following equation described by García-Alonso et al. (1998).

$$eGI = 0.549(HI) + 39.71$$

where HI is the hydrolysis Index which was calculated by evaluating the area under the curve during small intestinal digestion using white bread as the reference.

6.3.9. Statistical analysis

All values were estimated in triplicate and the mean, and standard deviation were evaluated. All reported values were subjected to statistical analysis using Minitab 19.1.1.0 statistical software (Minitab LLC, Chicago, USA) at $p \leq 0.05$.

6.4. Result and discussion

6.4.1 Description of “Cotyledon Flour” and its Morphological Properties

The term “flour” has been defined based on the particle size criterion as a powder where not less than 98% passes through a cloth or sieve not larger than 212 µm (FDA, 2018). This term accurately defines “wheat flour”, however, it cannot be adopted to define “pulse flour” due to the absence of a valid comparison of milling studies of pulse flour from different laboratories. A somewhat loose definition has been adopted to describe “pulse flour” as the powder produced from pulse seeds that are grounded either coarsely, with medium coarseness or fineness, or finely (Thakur et al., 2019). This study tends to slightly apply the above-mentioned

definition of flour in the preparation of “cotyledon flour”. On a significant note, a more objective description of pulse flour was suggested by this study from the microstructural constituents of the pulse flour. That is, a typical flour would constitute mainly discernible starch granules, protein bodies, and cell wall materials. Specifically, the “cotyledon flour” would comprise discernible cotyledon cells (intact, some broken), starch granules, protein bodies, and cell wall materials as shown in Fig 6.6.

The acid/alkali pretreatment and the micronization techniques (colloid milling) were used in this study to create the above-defined cotyledon flour. The acid/alkali sequential pre-treatment used in this study was shown to effectively separate cotyledon cells with high cellular integrity and minimal starch gelatinization (Do et al., 2019 & Kugimiya 1990). It achieved this by breaking down the pectic polymers in the middle lamella that are responsible for cell-cell adhesion. During successive acid-alkali solution treatment isolation methods, the polyvalent metal ions connecting the cells are separated by the acid, while the solubilization of pectin with β-elimination reaction is promoted by the alkali (Kugimiya, 1990). It is important to note that the softened acid/alkali-treated pea seeds were minced with a fine screen (reduced to ∼ 347 μm) before colloid milling. This was done to address a disadvantage in using the colloid mill, i.e., the maximum gap between the stator and the rotor (Fig 6.1) is less than 1000 μm which is 10 times lesser than the average size of swollen pea seed (Ajala et al., 2022). The resulting thick paste after mincing was a heterogeneous mixture of single intact cotyledon cells, starch granules, protein/cellular material matrix, and large clusters of cotyledon cells. The heterogeneous mixture was then passed through the colloid mill to mix, emulsify, and homogenize the mixture to a more uniform and refined mixture (Chen et al., 2017). That is, large clusters of cotyledon cells were reduced to isolated intact/broken cotyledon cells and other components were evenly distributed as shown in Fig 6.1. Not only that but the colloid mill has also been reported to impart smaller damage to starch granules compared to the stone grinder which uses a large compressive force (Sharma et al., 2008). This specific attribute was quite essential for this study in largely persevering cotyledon cells released from the colloid milling process.

The yield of cotyledon flour from each of the pea varieties varied from 68.8 % (white/yellow) to 80.12 % (Blue) as shown in Table 6.1. The yield for this study was significantly higher than those reported for cotyledon cells by other authors (Bhattarai et al., 2017 & Palchen et al.,

2021) although the difference in composition of cotyledon flour and cotyledon cells might be a major reason. From a food ingredient application standpoint, the yield for the cotyledon flour (> 50 %) obtained in this study indicates its potential use as a new functional food ingredient compared to isolated cotyledon cells.

The particle size distribution for both cotyledon flour and blended flour from the same botanical sources is reported in Table 6.1 and Fig 6.2. Cotyledon flour showed a unimodal distribution with a single peak at approximately less than 300 µm while blended flour exhibited a bimodal distribution with the first peak around 78-89 µm and the second peak close to 200 µm (Fig 6.2). The mean diameter of cotyledon flour was significantly different from that of the blended flours (Table 6.1). The significant difference between the two flours could be attributed to the presence of more cellular materials (cotyledon cells/cellular materials) in the cotyledon flours. Because of their larger mean particle size, the specific surface area for the cotyledon cells was significantly lower than that of the blended flours from the same botanical source.

Table 6.1. Particle size distribution and yield of cotyledon and blended pea flours.

Pea Variety	Flour type	D (0.1) µm	D (0.5) µm	D (0.9) µm	Mean Diameter (µm)	Specific surface area (m^2/g)	Yields (%)
White/yellow	*Cotyledon flour*	50.37 ± 2.19^{cd}	147.9 ± 1.23^{de}	305.5 ± 4.62^{c}	166.5 ± 2.39^{c}	0.09 ± 0.00^{a}	68.80
	Blended flour	8.14 ± 0.44^{a}	33.49 ± 0.54^{a}	240.0 ± 25.7^{a}	80.98 ± 5.79^{a}	0.38 ± 0.01^{d}	
Marrowfat	*Cotyledon flour*	53.76 ± 2.28^{d}	157.2 ± 0.29^{f}	309.2 ± 0.84^{c}	171.5 ± 0.43^{c}	0.08 ± 0.00^{a}	79.24
	Blended flour	10.73 ± 0.69^{a}	41.83 ± 2.02^{b}	189.8 ± 10.2^{a}	74.36 ± 1.76^{a}	0.31 ± 0.01^{bc}	
Blue	*Cotyledon flour*	44.23 ± 2.63^{b}	143.5 ± 1.15^{d}	286.5 ± 2.86^{bc}	157.1 ± 1.67^{c}	0.09 ± 0.00^{a}	80.12
	Blended flour	12.59 ± 0.37^{a}	49.92 ± 1.91^{c}	215.9 ± 5.84^{a}	86.56 ± 2.66^{a}	0.29 ± 0.01^{b}	
Maple	*Cotyledon flour*	46.48 ± 1.69^{b}	148.1 ± 2.93^{d}	306.4 ± 3.36^{c}	159.8 ± 4.29^{c}	0.09 ± 0.02^{a}	76.65
	Blended flour	9.17 ± 0.05^{a}	39.13 ± 1.33^{b}	314.1 ± 79.5^{c}	108.2 ± 17.6^{b}	0.34 ± 0.00^{c}	

[a, b, c] Values (means ± SEM) in each column with the same superscript letters are not significantly different ($p > 0.05$).

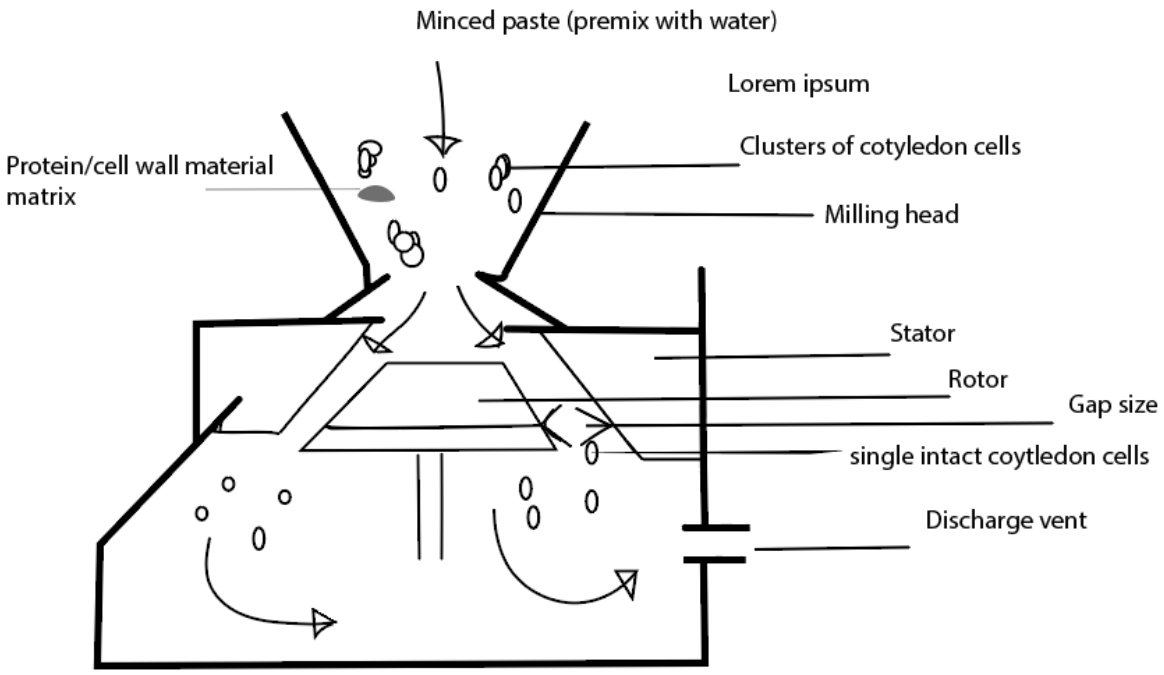

Fig 6.1 Schematic representation of the colloid milling process.

6.4.2 Proximate and Water holding capacity.

The proximate composition of the cotyledon flour was compared with that of the blended flour from the same plant sources (Table 6.2). The cotyledon flour contained about 10 % more protein than the blended flour except for the maple pea variety where there is no significant difference between the cotyledon and blended flour. The significant increase in protein content after colloid milling is in tandem with other reports (Vishwanathan et al., 2011 & Shakerardekani et al., 2012).

Similarly, the dietary fibre for the cotyledon flour is twice as much as that of the blended flour from the same botanical source. The fibre content varied from 2.74 to 4.47 % for the cotyledon flour, while the fibre content for the blended flour was less than 2 %. The presence of a higher proportion of resistant starch in cotyledon flour might be responsible for the difference in fibre content (Edwards et al., 2020). The total starch content of both cotyledon and blended flours showed no significant difference (Table 6.2) except for the flours for white/yellow variety which was almost 20 % higher in cotyledon flour than the blended flour.

Table 6.2 Proximate composition and water holding capacity of cotyledon and blended pea flours.

Pea Variety	Flour type	Moisture (%)	Protein (%)	Fat (%)	Fibre (%)	Ash (%)	Carbohydrate (%)	Total starch (%)	Water Holding Capacity (g water/g solids)
White/yellow	*Cotyledon flour*	6.13 ± 0.21^{bc}	31.94 ± 0.31^{d}	1.61 ± 0.146^{a}	4.47 ± 0.15^{d}	1.97 ± 0.09^{ab}	53.86 ± 0.28^{b}	43.32 ± 5.54^{a}	2.71 ± 0.01^{e}
	Blended flour	10.73 ± 0.21^{de}	20.63 ± 0.29^{a}	1.34 ± 0.25^{a}	1.46 ± 0.17^{a}	2.43 ± 0.02^{c}	63.41± 0.33^{d}	60.02 ± 2.85^{b}	1.27 ± 0.00^{c}
Marrowfat	*Cotyledon flour*	5.23 ± 0.39^{a}	37.07 ± 0.09^{e}	2.11 ± 0.09^{cd}	3.32 ± 0.22^{c}	1.87 ± 0.09^{a}	50.38 ±0.50 ^{a}	51.32 ± 0.18^{ab}	3.47 ± 0.01^{g}
	Blended flour	12.23 ± 0.32^{f}	22.13 ± 0.33^{b}	1.45 ± 0.10^{a}	1.38 ± 0.05^{a}	2.51 ± 0.09^{c}	60.29 ± 0.41^{c}	51.48 ± 1.11^{ab}	1.12 ± 0.01^{a}
Blue	*Cotyledon flour*	5.88 ± 0.17^{ab}	31.66 ± 0.22^{d}	2.46 ± 0.05^{d}	3.44 ± 0.14^{c}	2.16 ± 0.03^{b}	54.39 ± 0.52^{b}	54.78 ± 6.05^{b}	2.87 ± 0.01^{f}
	Blended flour	11.23 ± 0.25^{e}	20.55 ± 0.35^{a}	1.95 ± 0.09^{bc}	1.67 ± 0.26^{a}	2.46 ±0.14^{c}	62.77 ± 0.29^{d}	56.86 ± 1.33^{b}	1.17 ± 0.00^{b}
Maple	*Cotyledon flour*	6.70 ± 0.10^{c}	25.01 ± 0.16^{c}	1.38 ± 0.16^{a}	2.74 ± 0.14^{b}	2.05 ± 0.08^{ab}	62.11 ± 0.51^{d}	53.28 ± 1.95^{b}	2.32 ± 0.01^{d}
	Blended flour	10.50 ± 0.26^{d}	24.85 ± 0.45^{c}	1.54 ± 0.04^{a}	1.38 ± 0.21^{a}	2.39 ±0.04^{c}	59.32 ± 0.81^{c}	57.51 ± 0.78^{b}	1.28 ± 0.01^{c}

$^{a, b, c}$ Values (means ± SEM) in each column with the same superscript letters are not significantly different ($p > 0.05$).

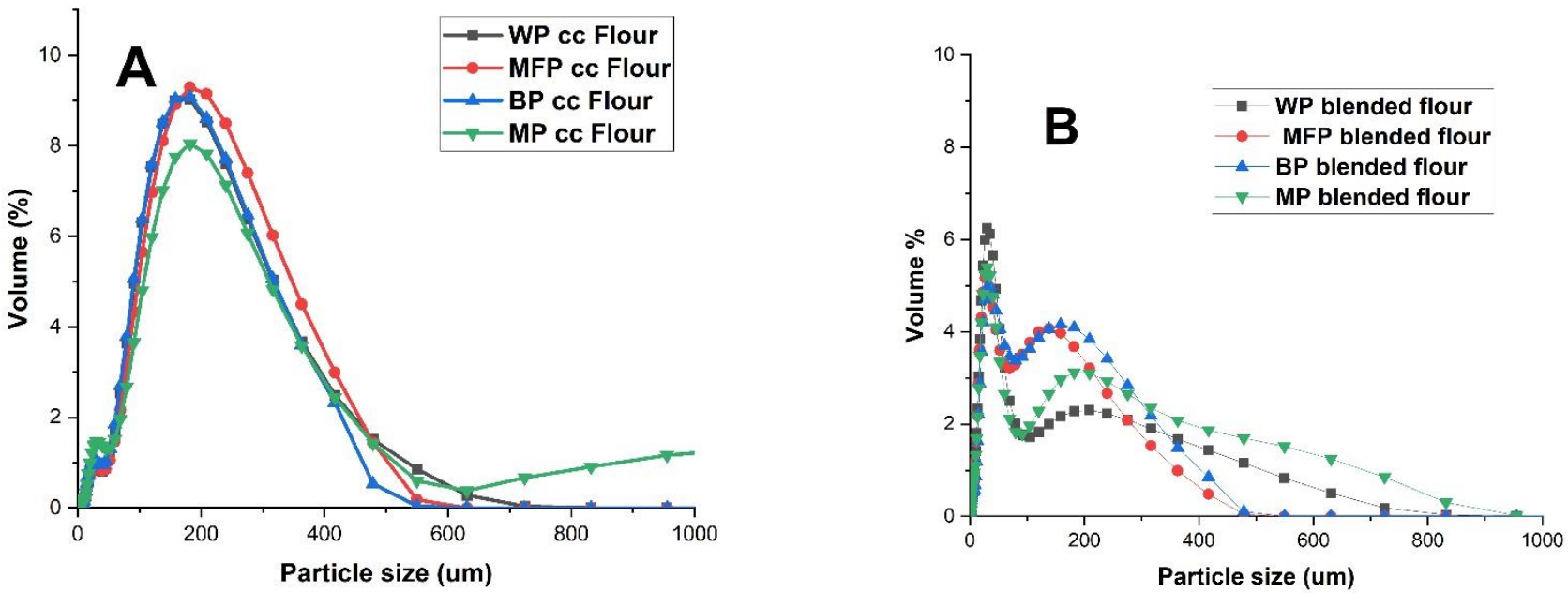

Fig 6.2 Particle size distribution of A) cotyledon flour and B) blended flour from the same botanical sources. Where, WP, MFP, BP, and MP are White/yellow, Marrowfat, Blue, and Maple cotyledon/flour respectively.

The water-holding capacity of cotyledon flour was higher (almost 2.5 times) than the blended flours from the same source (Table 6.2). The water-holding capacity of plant-based powder has been shown to increase after Micronization (Zhao et al., 2009 & Zhao et al., 2010). The colloid milling tends to redistribute the fibre components of the cotyledon flour from insoluble to soluble dietary fibre through the degradation of hemicellulose, cellulose, and lignin into small molecules with improved functionality (Chau et al., 2007). A new surface hydrophilic group created in the degraded cellulose and hemicellulose of the powder after micronization is exposed, thus resulting in easy integration with water that finally led to an increase in water holding capacity (Zhao et al., 2010)

6.4.3 Pasting Properties.

The pasting properties of cotyledon flour/blended flour are reported in Table 6.3 and Fig 6.3, respectively. The pasting profile of cotyledon flour and blended flour (Fig 6.3) were identical to that of a typical pulse flour reported by other authors (Kumar et al., 2021, Maninder et al., 2007 & Acevedo et al., 2013). The peak viscosity for both cotyledon and blended flours was significantly different ($p < 0.05$). The peak viscosity of all the blended flours was higher than the corresponding cotyledon flours except for white/yellow and maple cotyledon flours. The peak viscosity is a point during the heating stage when the highest number of swollen starch granules results in pasting. Pasting occurs through the combined effect of swelling and the rate of starch granule disruption (Leon et al., 2010). Since swelling of starch granules (uptake of water) is an important prerequisite for pasting to occur, the water-holding capacity of starch granules would play a major role in the swelling and rate of disruption of starch granules. That is, the lower degree of swelling of starch granules would result in lower peak viscosity. The microstructural configuration in Fig 6.3 tends to show that starch granules in cotyledon flour were less exposed (starch in cotyledon cells and protein/cellular matrix) compared to the blended flour of the same plant sources. Thus, the swelling and subsequent leaching of amylose from starch granules in cotyledon flour would be lower compared to blended flour. The water holding capacity reported for cotyledon and blended flour in Table 6.2 also confirmed this hypothesis. However, superfine grinding such as colloid milling tends to generally increase the surface area and porosity of materials (Chen et al., 2017). This could probably explain the higher peak viscosity exhibited by white/yellow and maple cotyledon flour.

Table 6.3: Pasting properties and estimated glycaemic index of cotyledon and blended pea flours

Pea Variety	Flour type	Peak Viscosity (cP)	Trough Viscosity(cP)	Final Viscosity(cP)	Hydrolysis Index	Estimated Glycaemic index
White/yellow	*Cotyledon flour*	959.0 ± 3.00^{h}	765.0 ± 2.65^{e}	1040.0 ± 7.55^{c}	70.62 ± 2.08^{abc}	78.47 ± 1.14^{abc}
	Blended flour	949.3 ± 2.52^{g}	934.3 ± 3.21^{h}	1477.7 ± 7.09^{g}	75.05 ± 1.26^{d}	80.91 ± 0.69^{d}
Marrowfat	*Cotyledon flour*	723.7 ± 3.79^{b}	609.0 ± 2.00^{a}	935.0 ± 3.61^{b}	69.19 ± 1.43^{ab}	77.69 ± 0.79^{ab}
	Blended flour	796.3 ± 3.79^{c}	752.3 ± 2.52^{d}	1033.7 ± 3.51^{c}	73.74 ± 1.95^{cd}	80.19 ± 1.07^{cd}
Blue	*Cotyledon flour*	854.3 ± 3.06^{e}	816.7 ± 2.52^{f}	1233.7 ± 3.51^{e}	71.92 ± 1.54^{bcd}	79.19 ± 0.85^{bcd}
	Blended flour	865.3 ± 4.04^{f}	859.0 ± 2.00^{g}	1339.7 ± 2.08^{f}	81.64 ± 1.74^{e}	84.53 ± 0.96^{e}
Maple	*Cotyledon flour*	824.3 ± 3.05^{d}	731.3 ± 2.52^{c}	871.0 ± 2.00^{a}	66.82 ± 1.10^{a}	76.39 ± 0.60^{a}
	Blended flour	674.3 ± 3.21^{a}	653.3 ± 2.08^{b}	1032.7 ± 3.79^{c}	70.06 ± 0.51^{abc}	78.17 ± 0.28^{abc}

$^{a, b, c}$ Values (means ± SEM) in each column with the same superscript letters are not significantly different ($p > 0.05$).

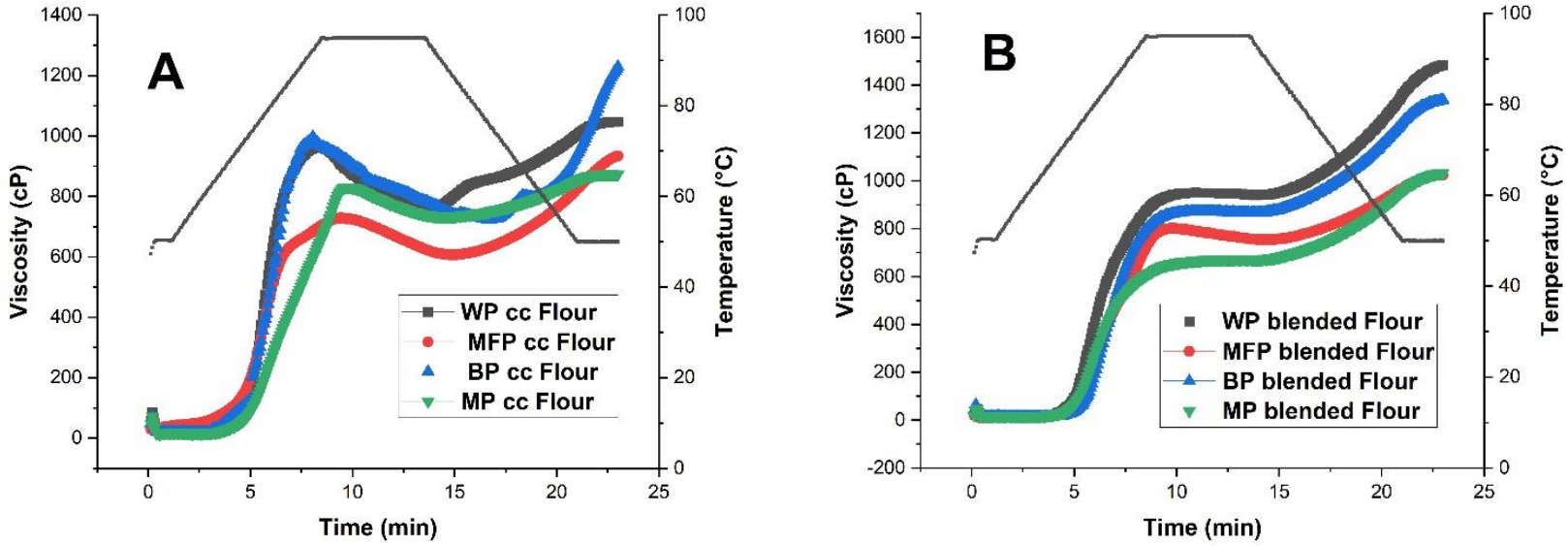

Fig 6.3 Pasting properties of A) cotyledon flour and B) blended flour. Where, WP, MFP, BP, and MP are White/yellow, Marrowfat, Blue, and Maple cotyledon/flour respectively.

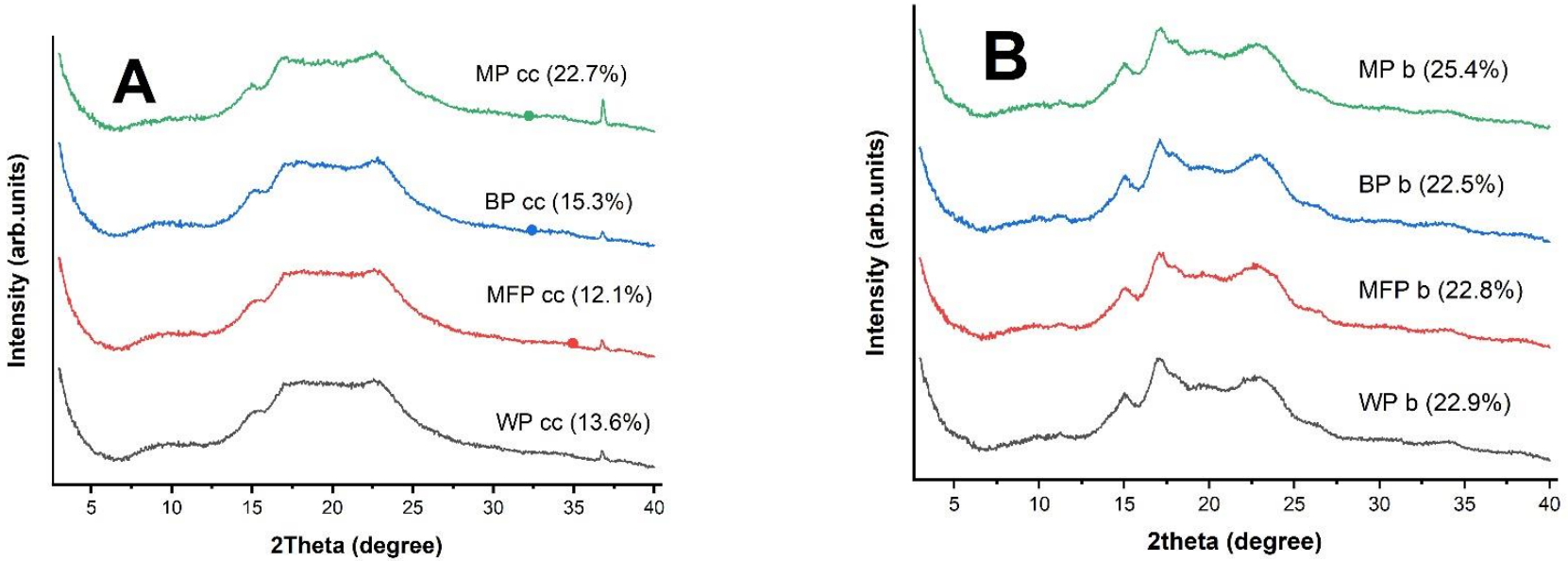

Fig 6.4 Relative crystallinity of A) cotyledon and B) blended flours. Where, WP, MFP, BP, and MP are White/yellow, Marrowfat, Blue, and Maple cotyledon/flour respectively. Note. “cc” and “b” stands for cotyledon and blended flour.

Trough viscosity for cotyledon/blended flour (Table 6.3) differed significantly from each other. All the blended flours had higher trough viscosity compared to the cotyledon flours from the same botanical sources. The final viscosity also followed the same trend. This is the viscosity that continues to climb until a plateau is reached while the heating temperature remains constant. The blue cotyledon flour and blended flour showed the highest final viscosity in (cp) (Table 6.3) while maple cotyledon flour and blended flour had the lowest. The final viscosity indicates the ability of flour to form a viscous paste after cooking and cooling in breadmaking (Leon et al., 2010).

Table 6.4. Thermal properties of cotyledon and blended pea flours.

Pea Variety	Flour type	T_o (°C)	T_p (°C)	T_c (°C)	ΔH_{gel} (J.g-1)
White/yellow	*Cotyledon flour*	62.47 ±5.19^{a}	64.64 ± 1.82^{a}	78.25 ± 0.97^{de}	4.09 ± 0.90^{c}
	Blended flour	60.37 ± 0.60^{a}	64.06 ± 0.18^{a}	69.43 ± 0.14^{a}	1.98 ± 0.20^{ab}
Marrowfat	*Cotyledon flour*	62.60±1.04^{a}	71.44 ± 0.79^{d}	81.94 ± 1.02^{ef}	1.15 ± 0.23^{a}
	Blended flour	61.03 ± 0.04^{a}	66.17 ± 0.97^{a}	77.41 ± 1.34^{cd}	2.49 ± 0.58^{ab}
Blue	*Cotyledon flour*	62.59±1.06^{a}	72.06 ± 1.37^{d}	84.60 ± 2.17^{f}	2.53 ± 0.61^{ab}
	Blended flour	61.13 ± 1.03^{a}	68.49 ± 0.75^{bc}	74.05 ± 0.96^{ab}	2.72 ± 0.04^{bc}
Maple	*Cotyledon flour*	62.61±1.08^{a}	69.58 ± 0.61^{cd}	83.42 ± 0.50^{f}	2.30 ± 0.64^{ab}
	Blended flour	60.14± 0.18^{a}	64.54 ± 0.22^{a}	72.87 ± 2.30^{ab}	2.49 ± 0.59^{ab}

$^{a, b, c}$ Values (means ± SD) in each column with the same superscript letters are not significantly different ($p > 0.05$).

6.4.4. Thermal Properties and Crystallinity

The thermal properties of cotyledon/blended flours reported in Table 6.4 showed that all tested flours exhibited a single endothermic transition from 60 to 85 °C, which reflects gelatinization. The onset temperature (T_o), peak temperature (T_p), conclusion temperature (T_c), and enthalpy of gelatinization (ΔH_{gel}) for this study were consistent with those reported in the literature (Chávez-Murillo et al., 2018, Xu et al., 2019 & Guo et al., 2018). There was no significant difference in the onset gelatinization temperature (T_o) for cotyledon & blended

flours from the same botanical sources. The peak temperature (T_p) on the other hand for the cotyledon flour differed significantly ($p < 0.05$) from the blended flour except for white/yellow cotyledon/blended flour. Both blue cotyledon (72.06 °C) and blended flour (68.49 °C) showed the highest peak temperature, respectively (Table 6.4). Following the same trend, the conclusion temperature (T_c) for the cotyledon/blended flour differed significantly with T_c for the cotyledon flour almost 5-10 °C higher than that of the blended flour from the same plant sources. These results suggest that starch gelatinization in the cotyledon flour extended/occurred at a higher gelatinization temperature than blended flour from the same botanical source. Since the phase transition stages in starch gelatinization occur in the presence of excess water, the microstructural organization of cotyledon flour (starch granules housed by the cotyledon cell wall and embedded in protein/cell materials matrix) would limit the inflow of water for adequate swelling and crystalline disruption of the amorphous region (Fujimura & Kugimiya, 1994).

The enthalpy of gelatinization (ΔH_{gel}) measures the loss of molecular (double-helical) order and loss of crystallinity within the starch granules (Cooke & Gidley, 1992). That is, it can predict the energy required to break down the intermolecular hydrogen bonds of the amylopectin crystallites in legume starch granules (Hoover et al., 2010 & Ahmed et al., 2021). In this study, the enthalpy of gelatinization (ΔH_{gel}) (Table 6.4) for the cotyledon flour was not different significantly from the blended flour of the same plant sources except for white/yellow and marrow fat cotyledon flours which were almost 2 times higher than that of their blended flours. This result may imply that the enthalpy required to provide the order-disorder transition of starch granules in both cotyledon and blended flour was somewhat similar except for white/yellow cotyledon flour which required higher energy. The type of crystals, their architecture, and processing conditions may be responsible for this difference in the enthalpy of gelatinization (ΔH_{gel}) (Ahmed et al., 2021).

The X-ray diffractograms and relative crystallinity of the cotyledon/blended flours are shown in Figure 2. The XRD pattern for this study (Figure 6.4) exhibited a C-type polymorphic pattern with major peaks at ~5.6°, 15.2°, 17.2°, 18.0° and 23.2° 2theta, which is the mixture of A-type and B-type crystalline types. The XRD pattern followed the sampling trend reported by other authors (Kaptso et al., 2016 & Ancona et al., 2011). The relative crystallinity of cotyledon flour (13-22.7 %) differed from the blended flour (22- 25.4 %) of the same botanical sources. This

lower crystallinity exhibited by the cotyledon flour may be attributed to the alterations of the molecular packing caused by the freeze-drying process (Zhang et al., 2014). Also, the loss of crystallinity in the cotyledon flour may be because of the micronization techniques used for this study (Raza et al., 2019).

6.4.5 Starch digestion and glycaemic response

In vitro, oral gastro-small intestinal digestion of the cooked cotyledon/blended flours is illustrated in Fig 6.5. The starch hydrolysis observed at the gastric stage for the blended flours (3.5 – 14.35 %) was significantly higher than the cotyledon flour (0.1-1.3 %). As expected, the starch hydrolysis of the cooked flours at the gastric stage was because of starch-degrading enzymes (α-amylase) introduced during the first 2 min of the oral phase. For the small intestinal digestion, after 10 min, the starch hydrolysis of both the cooked cotyledon and blended flours rose sharply to 51.2-54.9 % and 58.6 – 61.8 %, respectively. The starch hydrolysis of the cooked cotyledon/blended flours then moved steadily until the end of 120 min of the small intestinal starch digestion. Overall, the final starch hydrolysis of the cooked cotyledon flour (71-81 %) was approximately 10 % lower than that of the blended flour (79-91%) from the same plant sources.

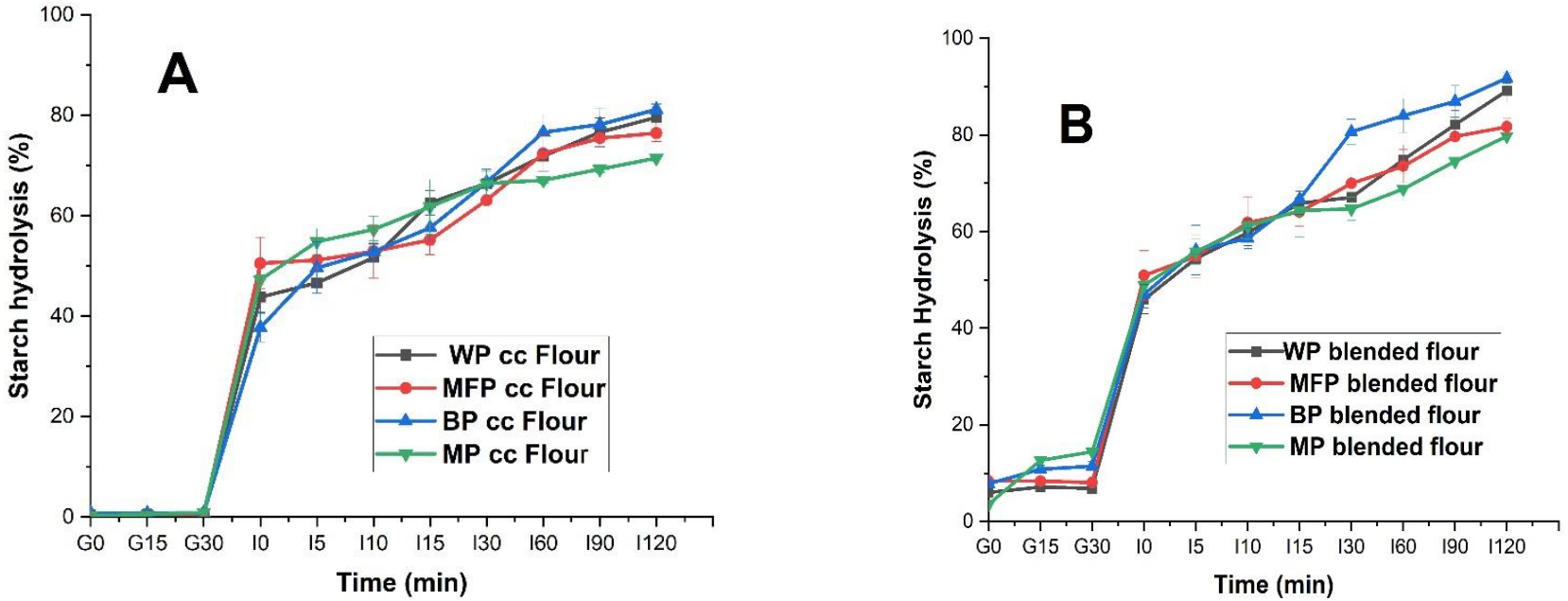

Fig 6.5. Starch hydrolysis of the cooked (A) cotyledon flours, and (B) blended flours. Where, WP, MFP, BP, and MP are White/yellow, Marrowfat, Blue, and Maple cotyledon/flour respectively. G0, G15, and G30 (0, 15, and 30 min of gastric digestion), and I0, I5, I10, I15, I30, I60, I90, and I120 (0, 5, 10, 15, 30, 60,90, and 120 min of the small intestinal digestion)

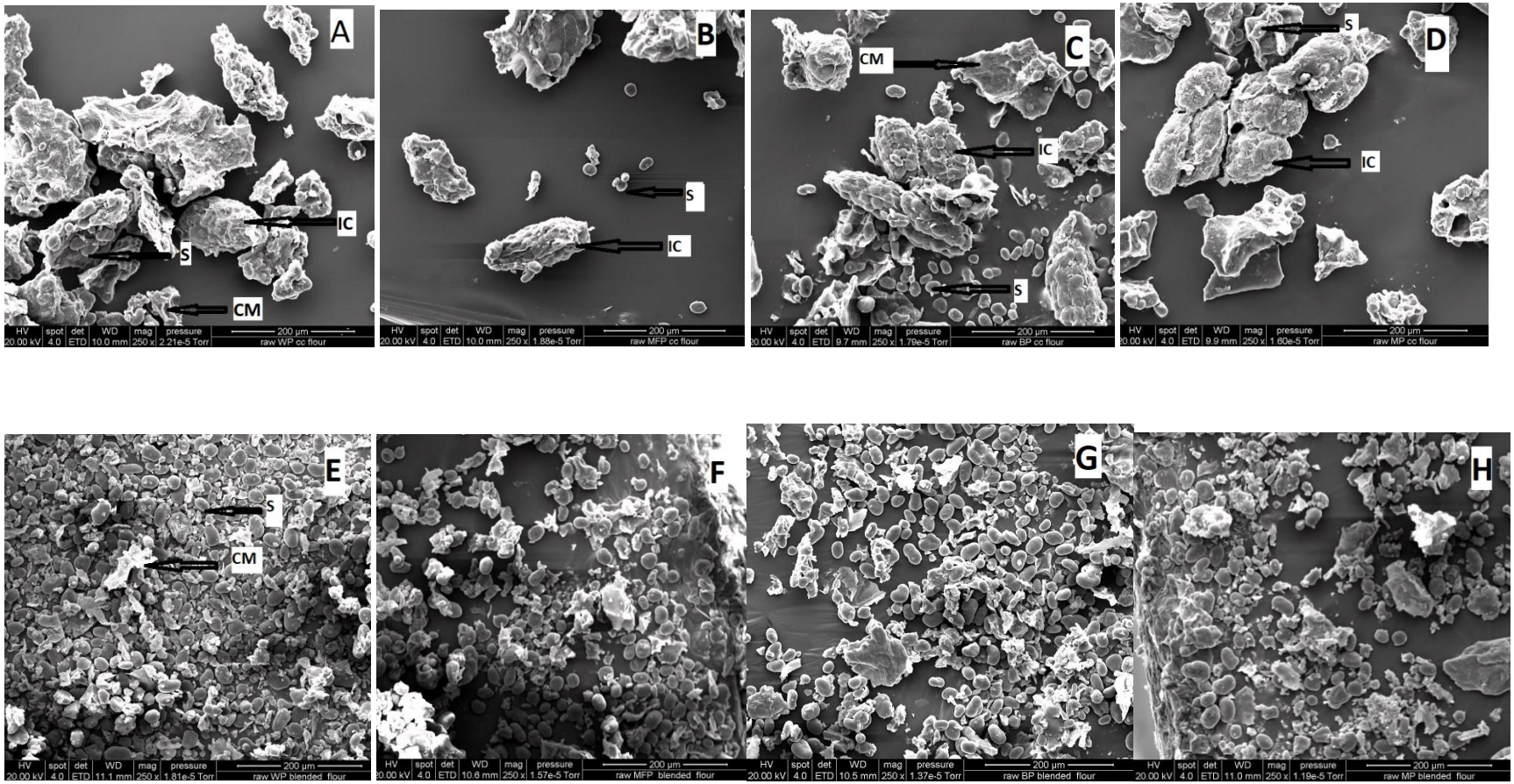

Fig 6.6. Raw microstructure of cotyledon and blended flour. IC, intact cotyledon cells, S, starch granules & CM, and other cellular materials. Where, A, B, C, and D represented White/yellow, marrowfat, blue, and maple cotyledon flours while E, F, G, and H represented White/yellow, marrowfat, blue, and maple blended flour.

The starch hydrolysis of the cotyledon flour for this study was within the range for intact cotyledon cells (Do et al., 2019 & Rovalino-Córdova et al., 2019) and lower than the pulse flour reported by other authors (Berg et al., 2012 & Romano et al., 2018). The lower rate of starch digestion exhibited by the cotyledon flour may be due to the cell wall of the cotyledon cells present in the cotyledon flour. The relatively high level of type 1 primary cell wall (xyloglucan and pectic polysaccharides) of pulse cotyledon cells has been reported to exhibit high cellular integrity after cooking and *in vitro* starch digestion (Berg et al., 2012, Do et al., 2019 & Edwards et al., 2021). That is, the cell wall of the cotyledon cell limits the extent of starch gelatinization and subsequently starch digestion by acting as a barrier to the inflow of water and starch-degrading enzymes during cooking and *in vitro* digestion, respectively. This may be the mechanism behind the lower rate of starch digestion observed for the cotyledon flour in this study.

Another underpinning mechanism that might be responsible for the slow rate of starch digestion of the cotyledon flour might be the protein/cell wall matrix (cytoplasmic matrix) around the starch granules in the microstructural configuration of the cotyledon flour. The micronization techniques (colloid milling) used for the preparation of the cotyledon flour for this study significantly affected the protein/cell wall matrix by increasing the content of protein and soluble dietary fibre of the cotyledon flour (Chau et al., 2007, Vishwanathan et al., 2011 & Shakerardekani et al., 2012). The colloid milling tends to redistribute the fibre components of the cotyledon flour from insoluble to soluble dietary fibre through the degradation of hemicellulose, cellulose, and lignin into small molecules with improved functionality (Chau et al., 2007). The resulting increase in the protein and fibre content after colloid milling is reflected in Table 6.4 for this study. This subsequent results in a high-quality protein/cell wall matrix might have exhibited as a secondary physical barrier to enzymatic activity in small intestinal digestion in vitro.

The SEM micrographs of cotyledon/ blended flour digesta (cooked, G30, I10, and I 120) are shown in Fig 6.7 This is an overview of microstructural components of cotyledon/blended flour responses to cooking, gastric, and small intestinal digestion conditions. At the cooking stage, the microstructure of cooked cotyledon flour and blended flour exhibited a distinct microstructural configuration in the presence of heat and water during cooking.

	White/yellow	Marrowfat	Blue	Maple
Cooked	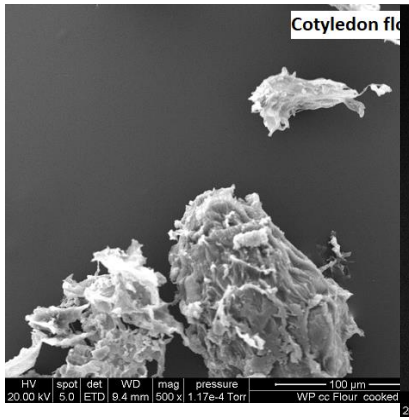	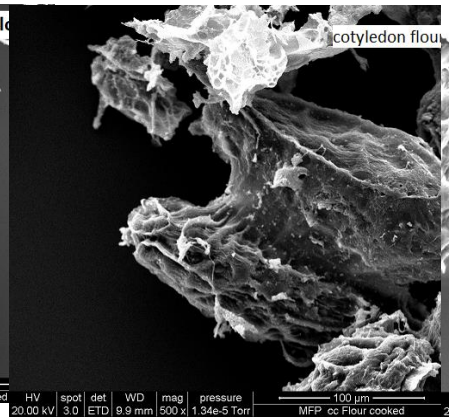	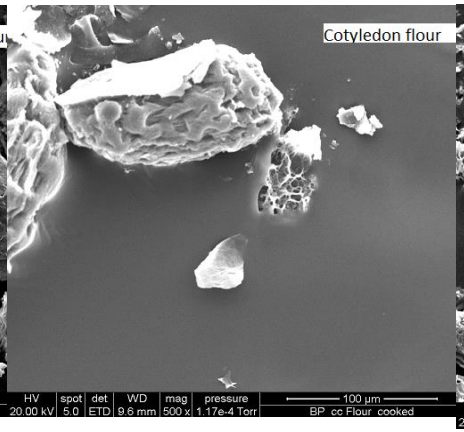	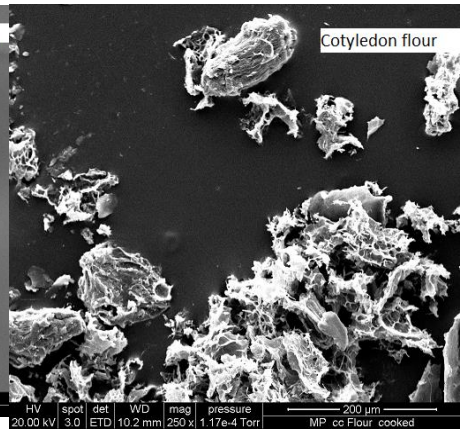
	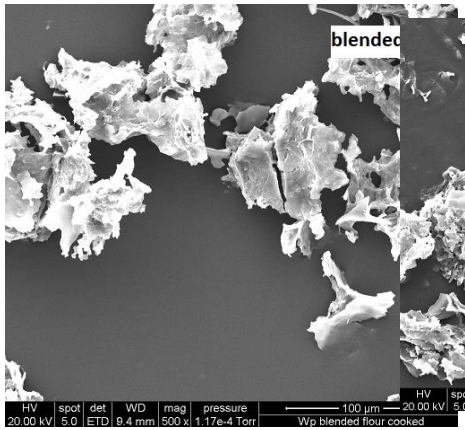	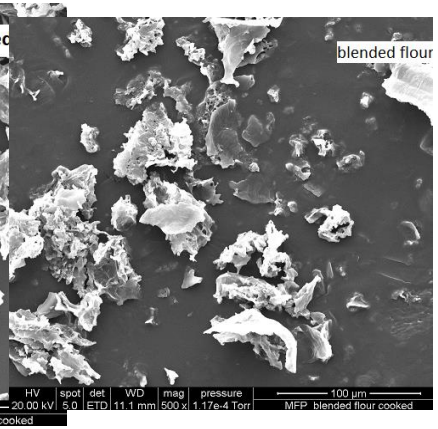	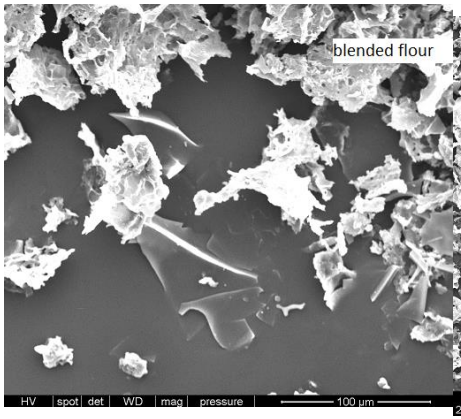	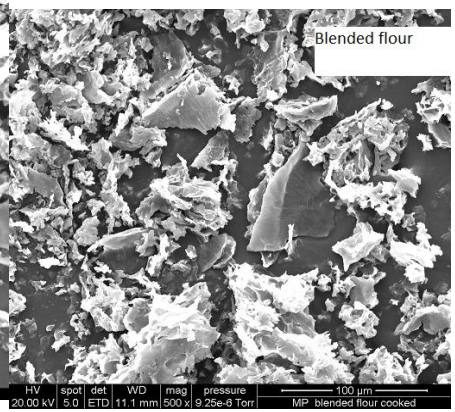

G30

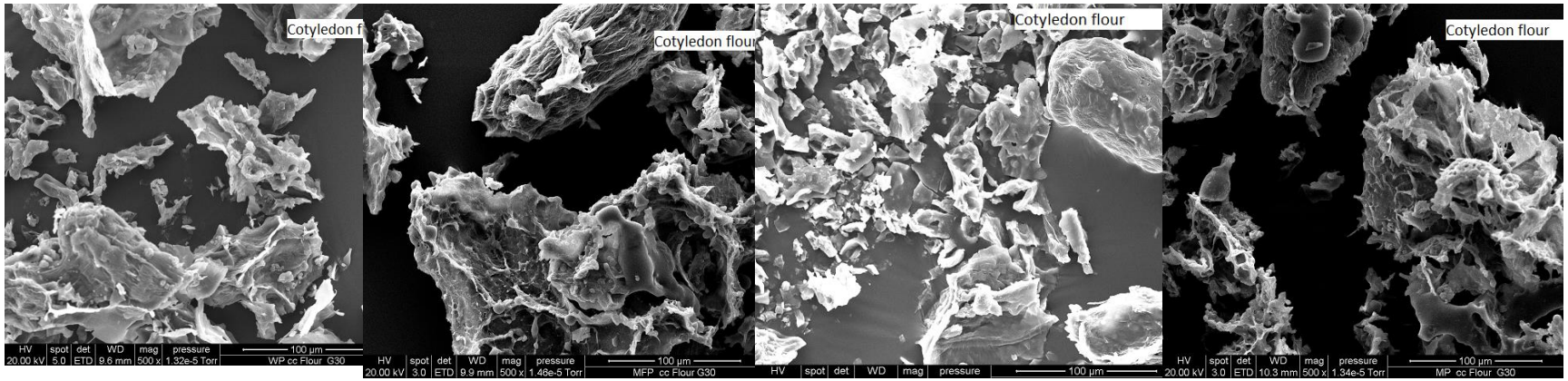
Cotyledon f
Cotyledon flour
Cotyledon flour
Cotyledon flour

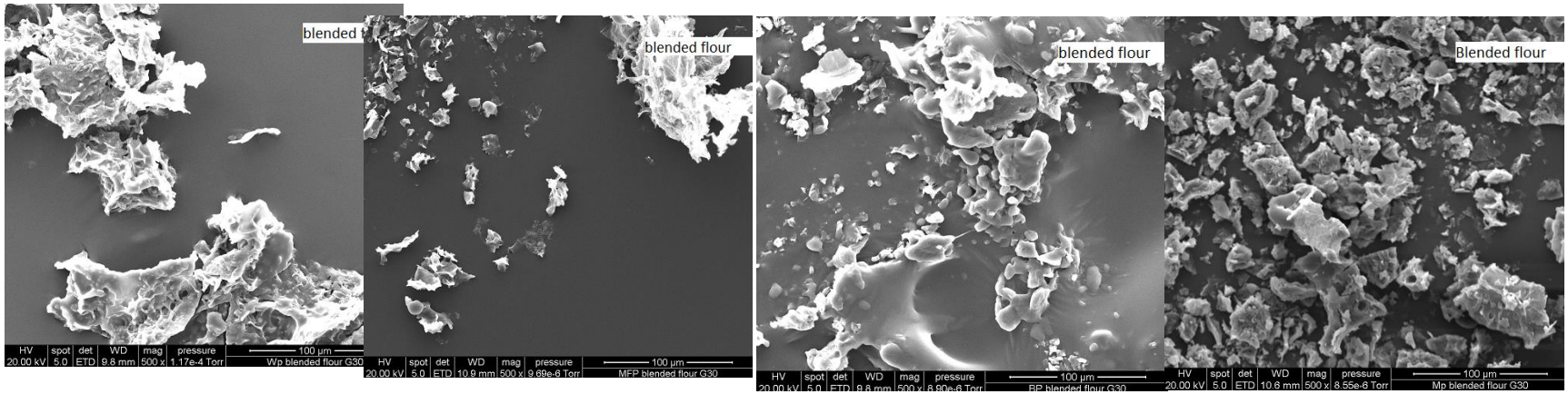
blended f
blended flour
blended flour
Blended flour

I10

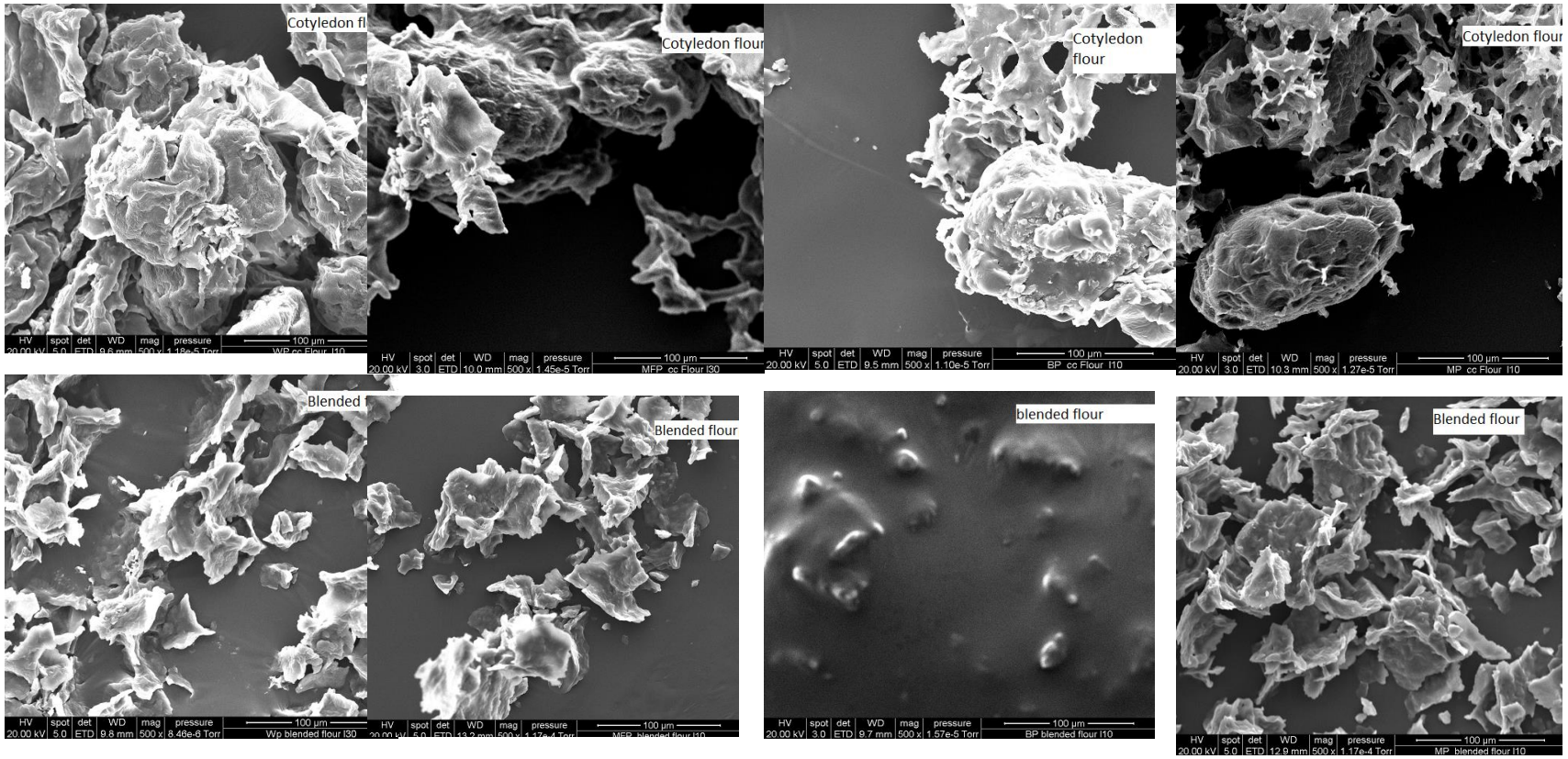
Cotyledon fl
Cotyledon flour
Cotyledon flour
Cotyledon flour
Blended
Blended flour
blended flour
Blended flour

I120

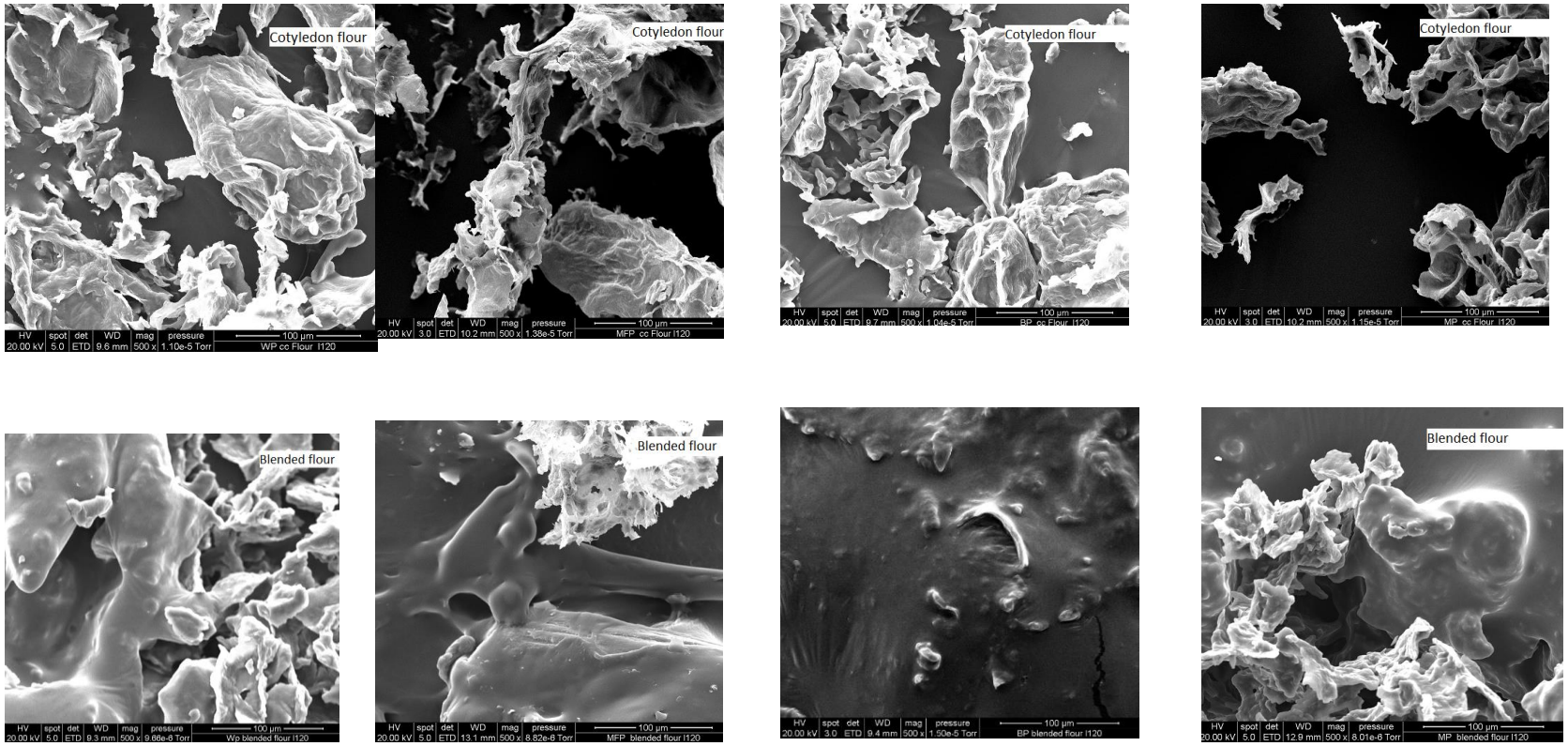

Fig 6.7. Scanning electron micrographs of cotyledon and blended flour digests from the same plant sources (White/yellow pea, Marrowfat pea, Blue pea, and Maple pea) sampled during *in vitro* oral-gastro and small intestinal digestion. Where G30 is gastric digestion at 30 min while I10 and 1120 are small intestinal digestion at 10 and 120 min respectively

The cotyledon flour (Fig 5) exhibited some changes on the cellular surface of the cotyledon cells while the blended flour showed some partially gelatinized starch granules. After 30 min of the gastric stage, a few partially gelatinized extracellular starch granules and denatured protein matrix were exhibited by the cotyledon flour while more starch gelatinized, and denatured protein occurred in the blended flour. At the small intestinal digestion stage (I10 and I120), the presence of swollen honey-comb-like cotyledon cells and dented protein/cellular matrix in the cotyledon flour digesta suggested a great number of starch granules were either undigested or partially digested after the end of the digestion process. A sponge-like (amorphous flakes) network was observed for the blended flour which showed a greater extent of starch hydrolysis compared to the cotyledon flour.

The estimated glycaemic index (eGI) for the cooked cotyledon/ blended flours shown in Table 6.3 was significantly different from each other ($p < 0.05$) from the same plant sources. The eGI for maple cotyledon and blended flours was the lowest while blue cotyledon and blended flours were the highest.

6.5 Conclusions

The microstructural, nutritional, and starch digestion properties of a novel cotyledon flour prepared via micronization techniques (colloid milling) were compared with the blended flour from the same botanical sources in this study. The SEM images of the cotyledon flour showed distinct microstructural components from the blended flour from the same plant source. The protein and fibre contents of the cotyledon flour were substantially higher than those of the blended flour from the same plant sources. The extent of starch gelatinization and subsequent starch digestion was lower in the cotyledon flour compared to the blended flour of the same botanical sources due to some differences in their microstructural configuration. That is, the presence of the primary cotyledon cell wall and a strong protein/cell wall matrix in the cotyledon flour were responsible for the lower extent of starch digestion exhibited by the cotyledon flour.

From both food ingredient application and sustainability standpoint, the higher average yield (>50 %) and its improved nutritional and functional properties (applicable particle size, higher protein, and fiber content, better pasting profile, and medium glycaemic response) of cotyledon flour make it a better potential food ingredient in developing a wider range of

low/medium glycaemic food products compared to whole pulse seed, cotyledon cells, and pulse flour.

Chapter 7: The effect of cotyledon flour as a new food ingredient on the techno-functional properties of a food system

7.1 Abstract

In this study, wheat flour for making bread was replaced with 25 and 50 % cotyledon flour and its effect on the microstructure, physical-functional properties, starch digestion *in vitro,* and glycaemic response was investigated. The micrographs of these three bread samples showed a distinct microstructural organization between the cotyledon flour-formulated bread and the control bread samples. Intact cotyledon cells and high levels of cellular materials were observed in the cotyledon flour-formulated bread samples. The protein, fibre, and resistant starch in the cotyledon flour-formulated loaves of bread were significantly ($p < 0.05$) higher than the control bread. The bake loss, volume, and specific volume decreased with an increased percentage of cotyledon flour used in the bread formulation. The colors of the crumb and crust of the cotyledon flour-formulated bread were significantly different from the control bread ($p < 0.05$) while the textural profile showed that the crumb hardness and cohesiveness of the bread samples increased with an increase in the percentage of the cotyledon flour added to the formulation of the bread. The starch hydrolysis for this study showed bread made with 25 and 50 % cotyledon flour was significantly lower than the control bread sample. The intact cotyledon cells with high cellular integrity observed in the microstructures of the bread samples confirmed this trend.

7.2 Introduction

In the previous study (Chapter 6), a novel cotyledon flour created through micronization techniques (colloid milling) was compared to its corresponding blended flour from the same botanical sources. A distinct microstructural organization was observed in the two flour types. That is, the cotyledon flour contained more cellular materials (cotyledon cells and other cellular materials) than the blended flour. Furthermore, the protein/cellular matrix with the extracellular starch granules was stronger in cotyledon flour than in blended flour from the same plant sources. Other characterizations recorded for the cotyledon flour include particle size (< 200 µm), water holding capacity, and pasting properties somewhat comparable to the

blended flour. The important highlight from the research was that the starch hydrolysis and the estimated glycaemic index of the cotyledon flour were somewhat significantly lower than the blended flour from the same sources. This means when consumed as part of a food product, it theoretically has the potential of regulating the rate at which glucose would be released into the bloodstream, thus could help prevent diseases like type 2 diabetics and cardiovascular diseases (Berrios et al., 2010 & Wang et al., 2019). However, this hypothesis needs to be tested using a suitable and viable food system.

Bread is considered an important staple food and an integral part of modern diets globally (Rosell et al., 2015 & Dong & Karboune, 2021). The consumption of bread is recommended in all dietary guidelines mainly because it is an important source of protein, dietary fiber, complex carbohydrates (starch), vitamins, and minerals (Cauvain & Young, 2007 & Rosell, 2011). The main ingredients for making bread are water, flour, salt, yeast, sugar, and fat, which are mixed and fermented to form a viscoelastic dough before being baked (Goesaert et al., 2009). This creates a suitable heterogeneous food system where numerous macromolecular interactions (e.g. starch-protein, protein-fibre, starch-protein-fibre, etc) confer desirable functional, nutritional, and textural properties on the finished product (baked bread). Researchers have used this food system template to test out the effects of new formulations such as the replacement of wheat flour with legume on the techno-functional properties of bread (Miñarro et al., 2012, Millar et al., 2019, Sadowska et al., 2003, Boukid et al., 2019 & Paladugula et al., 2021).

In this regard, bread would be a suitable food system to test out the quality and techno-functional properties of the novel cotyledon flour. Therefore, wheat flour for making bread was replaced with 25 and 50 % cotyledon flour, and the effect of this on the microstructure, physical-functional properties, starch digestion *in vitro,* and glycaemic response was evaluated.

7.3 Material and Methods

7.3.1 Ingredients

A locally grown whole dry pea seed variety, Maple pea (MP), was supplied by Cates Grain and Seed (Ashburton, New Zealand). The novel MP cotyledon flour was created via colloid milling as described in Chapter 4, freeze-dried, and stored at 4 °C until further use. The MP cotyledon flour was selected because it exhibited the lowest starch hydrolysis compared to other cotyledon flours as reported in the previous chapter. All-purpose wheat flour, gluten, and yeast

were purchased from Davis Food Ingredients Ltd. (Palmerston North, New Zealand). Other ingredients, such as sugar, salt, milk powder, butter, and eggs, were purchased from Pak 'Save (Palmerston North, New Zealand). Pepsin (porcine gastric mucosa, 800–2500 U/mg protein), pancreatin (hog pancreas, 4 × USP), and invertase (Invertase, grade VII from baker's yeast, 401 U/mg solid) were all purchased from Sigma–Aldrich Ltd. (St Louis, USA) and alpha-amylase (3000 U/mL) and amyloglucosidase (3260 U/mL) were from Megazyme International Ireland Ltd. (Wicklow, Ireland). All other chemicals were of analytical grade.

7.3.2 Bread preparation

The ingredient formulations for making breads are presented in Table 7.1 and the bread-making process was conducted based on AACC method 10.09. Briefly, dry yeast was reconstituted in warm water, and other dry ingredients (Table 7.1) were mixed well with a wire whip in a bowl using a stand mixer (KSM195) at low speed for 1 min. The reconstituted yeast solution was added to the flour mixture and then mixed with a dough hook blade attached to the stand mixer at speed 2 for 15 min until a translucent membrane was formed in the dough. The butter was added and mixed for another 5 min until the dough formed a ball-like shape that was cleanly separated from the side of the bowl. The dough was weighed and covered with a plastic film to allow proof at 31 °C for 1 hour until it doubled its size. The proofed dough was divided into three parts and then rolled evenly into a rectangular form in a jelly-roll manner, and the dough was sealed properly by pinching its end. Then, the rolled doughs were proofed for another 10 min and the rolling process was repeated. The shaped dough was placed in lightly greased medium rectangular baking pans and allowed to rise for around 30-40 min. The loaf was then baked at 176 °C for 25 min. the baked loaf was removed immediately after removal from the oven (Combi oven, NZ) cooled for 1 hour on a wire rack, and then weighed.

Table 7.1 Ingredient formulations for making bread.

	Flour /g	Cotyledon flour/g	Gluten /g	Yeast /g	Sugar /g	Salt /g	Milk powder/g	Butter /g	Egg white /g	Water /g
Control	250	/	/	3	15	4	25	25	28	~130
25% of cotyledon flour	187.5	62.5	9.42	3	15	4	25	25	28	~165
50% of cotyledon flour	125	125	18.83	3	15	4	25	25	28	~230

7.3.3 Proximate composition of bread

The moisture content of the resulting bread samples was determined by an air oven drying method at 108 °C (AOAC, 2012). Subsequently, the contents of crude protein and crude fat in bread samples were analyzed by the Kjeldahl method using a conversion factor of 6.25 from nitrogen to protein and the Mojonnier method, respectively (AACC, 2000 & AOAC, 2012). The acid/alkali hot extraction method (AOAC, 2012) was used to quantify the fiber content of bread. The gravimetric method which involved heating the bread samples at 600 °C for 3hr was used to determine the ash content (AACC, 2000). The carbohydrate contents of the bread samples were estimated via calculation by subtracting the summation of all other components from 100 %. All experiments were conducted in triplicate.

The total starch and resistant starch contents of the bread samples were analyzed using a total starch and resistant starch assay kit (KTSTA and K-RSTAR, Megazyme International Ireland Ltd., Ireland) following the manufacturer's instructions. Results were reported on a dry weight basis (%).

7.3.4 Physical Characterization of the Bread

7.3.4.1 Bake loss

The bake loss for this study was calculated according to the formula described by Miñarro et al. (2012)

$$Bake\ loss\ (\%) = \frac{(Inital\ weight\ of\ batter - weight\ of\ \ bread\ after\ cooling) \times 100}{Inital\ weight\ of\ batter}$$

7.3.5 Volume and specific volume of the loaf

The bread volume was determined by the rapeseed displacement method according to AACC method 10-05.01. The specific loaf volumes were obtained by dividing the volume of the bread loaf by the loaf weight (expressed as mL/g).

7.3.6 Bread PH

The bread pH was determined using a method described by Yu et al. (2018). A 10 g of bread crumbs were homogenized with 90 mL of distilled water in a blender. The pH value was measured and recorded using a pH electrode (Hanna, HI1131B).

7.3.7 Colour analysis of the bread crust and crumbs

The color parameters, L*, a*, and b* values for the crust and crumb were determined by Minolta chroma CR-400 colorimeter (Konica Minolta Sensing Americas, Inc., USA). The brown index was calculated as a 100 - L* value (Giannone et al., 2018). The colorimeter was calibrated using a standard white plate before its use. Samples were measured in triplicate.

7.3.8 Textural profile analysis of bread

The texture profile analysis (TPA) was performed according to the method described by Tóth et al. (2022) with some adjustments. The middle slices of the bread were used as a representative of the samples. The TPA was performed on two middle slices at room temperature using a texture analyzer (Stable Micro Systems TA.XT2) with a 36-mm diametric acryl cylindrical probe. The applied settings were 50kg load cell, 40 % compression at 2 mm/s, and 5 s of waiting time between compressions.

7.3.9 *In vitro* oral gastro-small intestinal digestion of the bread

A bread sample containing approximately 4% starch concentration was mixed with simulated saliva fluid (SSF) prepared with an α-amylase concentration of 0.3U/mL, at a ratio of 1:1. The mixture was stirred with the aid of a magnetic stirrer bar, and then incubated at 37 ± 1 °C for 2 min. To mimic the chewing procedure, the resulting mixture was homogenized in a grinder. For the gastro-small intestinal digestion, simulated gastric fluid (SGF) and simulated intestinal fluid (SIF) were prepared (Pharmacopeia, 1995, 2000). A two-stage gastro-small intestinal *in vitro* digestion model was used as described by Dartois et al. (2010) with some modifications.

Approximately 170 g of chewed bread samples from the oral phase were introduced into nylon mesh and placed in the jacketed glass reactor to prevent contact with the stirrer bar in the reactor. The reactor temperature was maintained at 37 ± 1 °C by circulating water in the reactor jacket. The reactor contents were mechanically stirred by a magnetic stirrer bar at 300 rpm throughout digestion. The pH was initially adjusted to 2.0 (using 3 M HCl solution), then 25 mL of SGF (pepsin: starch ratio of 1.765:100, w/w) was added to start the hydrolysis; and the final pH was adjusted to 1.2 (using 0.5 HCl solution). After 30 minutes, the pH was adjusted to 6.8 to inactivate the pepsin enzyme. Subsequently, 22 mL of SIF (pancreatin/starch ratio, 1.3:100, w/w, amyloglucosidase/starch ratio, 0.26:1, v/w, and invertase/starch ratio, 1:1,000, w/w) was added to start the small intestinal digestion, and pH was maintained at 6.8 using 0.5 and 3 M NaOH solutions. The total time to complete the gastric and small-intestinal digestion was 30 and 120 min, respectively.

A 0.5 mL of aliquot was withdrawn from the reactor after 0, 15, and 30 min of gastric digestion (G0, G15, and G30), and 0, 5, 10, 15, 30, 60, 90, and 120 min of the small intestinal digestion (I0, I5, I10, I15, I30, I60, I90, and I120). The glucose concentration of the incubated mixture was measured using the D-glucose assay kit (GOPOD Format K-GLUK 07/ 11, Megazyme International Ireland Ltd, Ireland). Starch hydrolysis was expressed in percentage as described by Dartois et al. (2010).

The estimated glycaemic index (eGI) of the digested bread samples was calculated with the following equation described by García-Alonso et al. (1998).

$$eGI = 0.549(HI) + 39.71$$

where HI is the hydrolysis index which was calculated by evaluating the area under the curve during small intestinal digestion.

7.3.9.1 Microstructural characterization of the baked bread and the digest

The middle parts of breadcrumbs were cut into small rectangular shapes and were attached to a scanning electron microscope stub and then gold coated (Baltec SCD 050 sputter coater, New York, USA). The resulting gold-coated stub was viewed using the FEI Quanta 200 Environmental Scanning Electron Microscope (SEM) (Oregon, USA) at an accelerating voltage of 20 kV. The digesta bread samples from G30, I10, and I120 were freeze-dried and viewed under the SEM as described above.

7.3.10 Statistical tool

The mean and standard deviation were evaluated for all reported values. All reported values were subjected to statistical analysis using Minitab 19.1.1.0 statistical software (Minitab LLC, Chicago, USA) at $p \leq 0.05$.

7.4 Result and Discussion

7.4.1 Nutritional value of bread samples

The proximate composition of three different bread samples is shown in Table 7.2. There was a significant difference in protein content between the bread samples. The bread sample made from 50 % cotyledon flour had a protein content of 17 % which was higher than the control bread. The fibre content of the bread made from 25 and 50 % cotyledon flours was almost two times higher than the control bread samples. The carbohydrate and total starch contents of the bread samples were reduced as the amount of cotyledon flour used to replace wheat flour was increased (Table 7.2). On the other hand, the resistant starch of the bread sample increased with an increase in the amount of cotyledon flour in the formulations. The resistant starch content of 50% cotyledon flour bread was approximately six times as much as that of 100 % wheat bread (control). The increase in protein content in the bread samples incorporated with cotyledon flour was in agreement with a study reported by Millar et al. (2019). The improved nutritional value (i.e., an increase in protein and fiber contents but a decrease in total starch content) of the bread products observed in this study simply typified

the usual trend of incorporating legumes/or pulse ingredients in bakery products (Dovi et al., 2017 & Johnson et al., 2004).

7.4.2 Physical Properties of the bread samples

The bake loss during baking recorded for this study decreased with an increased percentage of cotyledon flour used in the bread formulation (Table 7.3). Although there was no significant difference in bake loss (%) between the control and 25 % cotyledon flour-formulated bread, the 50 % cotyledon flour-formulated bread had a lower bake loss than the control and 25 % cotyledon bread samples. The trend exhibited by this study is consistent with the study reported by Miñarro et al. (2012).

The volume and the specific volume of bread samples decreased with an increase in the percentage of cotyledon flour used. The results for the volume and specific volume for this study are in tandem with other authors (Paladugula et al., 2021 & Millar et al., 2019). Specific volume is a quality indicator in bread, which implies freshness (high crumb porosity) (Cauvain, 2015). Dough composition, processing conditions, and dough rheology are factors that affect specific volumes of bread during proofing and baking (Clark & Aramouni, 2018). During proofing, carbon dioxide produced via fermentation is trapped as tiny pockets of air within the dough, this causes the dough to rise (Cauvain, 2015). The abovementioned factors impart gas retention capabilities to sustain the volume during proofing and baking.

Table 7.2 Nutritional Properties of bread samples

Bread composition	Moisture (%)	Protein (%)	Fat (%)	Fibre (%)	Ash (%)	Carbohydrate (%)	Total starch (%)	Resistant starch (%)
Control	5.23 ± 0.15[a]	13.21 ± 0.10[a]	8.17 ± 0.08[a]	0.78 ± 0.07[a]	2.24 ± 0.08[a] .	70.35 ± 0.08[c]	50.33 ±0.08[c]	0.36 ± 0.05 [a]
25% cotyledon flour	5.86 ± 0.05[b]	17.07 ± 0.04[b]	9.38 ± 0.11[c]	1.59. ± 0. 39[b]	2.49 ± 0.04[b]	63.59 ± 0.13[b]	48.96 ±0.48[b]	1.28 ± 0.28[b]
50% cotyledon flour	5.00 ±0.30[a]	20.20 ± 0.07[c]	8.65 ± 0.11[b]	1.59 ± 0.32[b]	2.61 ± 0.01[b]	61.94 ± 0.18[a]	42.30 ±0.15[a]	2.17 ± 0.28[c]

[a, b, c] Values in each column with the same superscript letters are not significantly different ($p > 0.05$).

The results from this study indicate that the formation and stabilization of this gas network during proofing and baking were affected as the percentage of the cotyledon flour increased in the formation.

The pH of bread products is characterized by sourness or bread flavor (Clark & Aramouni, 2018). The pH of the bread samples was reduced with increased incorporation of cotyledon flour. The abovementioned trend is consistent with other authors (Liu et al., 2018).

Table 7.3 Physical properties of bread samples

Bread composition	Bake loss (%)	Volume(ml)	Specific volume(ml/g)	pH
Control	9.45 ± 0.01[b]	1386.6 ± 32.14[c]	3.21 ± 0.07[c]	6.32 ±0.03[c]
25% cotyledon flour	9.05 ± 0.13[b]	1236.6 ± 32.15[b]	2.66 ± 0.06[b]	6.02 ± 0.01[b]
50% cotyledon flour	7.99 ± 0.26[a]	1126.6 ± 55.07[a]	2.30 ± 0.11[a]	5.85 ±0.04[a]

[a, b, c] Values in each column with the same superscript letters are not significantly different ($p > 0.05$).

7.4.3 Colour and textural properties of the bread samples

The colour and textural properties of the bread samples are reported in Tables 7.4 and 7.5. The incorporation of cotyledon flour in bread considerably imparted the colour dynamics of the bread samples in this study. As expected, the crust and crumb of the control bread were significantly lighter (L^*) than the bread formulated with cotyledon flour ($P < 0.05$). The reduction in L^* for the pulse-formulated bread samples can be attributed to an increase in protein content which leads to an increase in the Maillard-browning reaction (Millar et al., 2017). The brown indexes of the crust and crumb in the cotyledon flour-formulated bread were higher than in the control bread sample.

Table 7.4 Colour analysis of bread samples

Bread composition	Crust Colour L	a*	b*	Brown index	Crumb Colour L	a*	b*	Brown index
Control	37.82 ±0.01[b]	16.65 ±0.45[c]	1.75 ± 1.01[c]	62.18 ± 1.01[a]	73.47 ± 0.77[c]	-1.95 ± 0.10[a]	18.90 ± 1.19[a]	26.52 ± 0.77[a]
25% cotyledon flour	28.40 ± 3.26[a]	13.05 ±0.64[a]	2.45 ±1.41[b]	71.59 ± 3.26[b]	58.66 ± 0.97[b]	3.66 ± 0.30[b]	18.04 ± 0.48[a]	41.33 ±0.97[b]
50% cotyledon flour	28.86 ±2.35[a]	13.59 ± 2.43[a]	1.88 ± 1.08[a]	71.14 ± 2.35[b]	53.63 ±0.20[a]	5.26 ± 0.08[c]	18.22 ± 0.28[a]	46.36 ± 0.20[c]

[a, b, c] Values in each column with the same superscript letters are not significantly different (p > 0.05).

Table 7.5 Textural Properties of bread samples

Bread composition	Hardness (N)	Springness	Cohesiveness	Gumminess (N)	Chewiness (N)	Resilience
Control	2174.0± 208.2[a]	0.86 ±0.05[a]	0.71 ± 0.06[a]	1539.5 ± 23.7[a]	1344.6 ± 46.76[a]	0.1992 ± 0.03[a]
25% cotyledon flour	6786.4±732.5 [b]	0.96±0.04 [b]	0.78 ± 0.07[ab]	5903.4 ± 890.9[b]	5846.15 ± 916.4[b]	0.2387 ± 0.03[a]
50% cotyledon flour	8602.5 ± 743.4[c]	0.82 ±0.20[a]	0.87 ± 0.06[b]	5398.9 ± 510.1[b]	5333.2 ± 261.0[b]	0.3307 ± 0.00[b]

[a, b, c] Values in each column with the same superscript letters are not significantly different (p > 0.05).

The textural profile analysis (Table 7.5) showed that the crumb hardness and cohesiveness of bread samples increased with an increase in the percentage of cotyledon flour added to the formulation of bread. The springiness of the bread formulated with 25 % cotyledon flour was significantly different ($P < 0.05$) from the control and 50 % cotyledon flour bread. The gumminess and chewiness of the bread formulated with cotyledon flour were almost 4 times higher than the control bread. The resilience of the bread samples increased with an increased percentage of the cotyledon flour added to the formulation. The trend recorded for crumb hardness for this study agreed with the study reported by Bourré et al. (2019). The significant difference in crumb hardness between the control and the cotyledon flour-formulated bread samples could be related to the specific volume of bread samples which was much lower in the pulse-formulated bread. The gas cells in the dough of the pulse-formulated bread sample have a thicker cell wall than the control bread, so when they collapse during baking, they tend to form coalescence which leads to more tightly packed breadcrumbs (Smith et al., 2012).

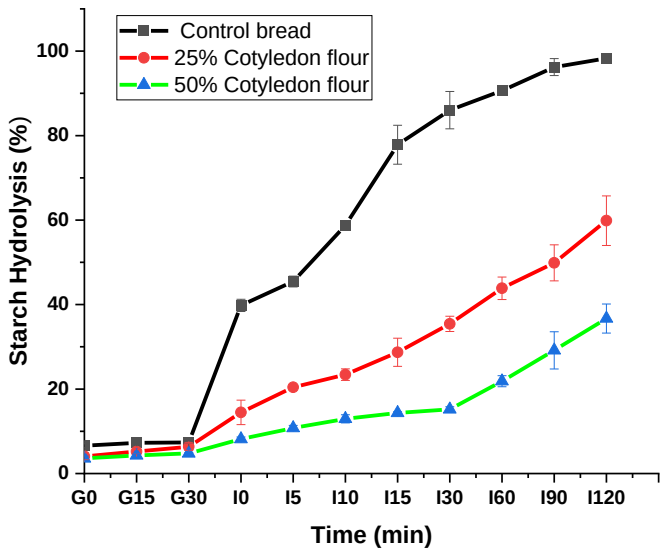

Fig 7.1 Starch hydrolysis of bread samples. G0, G15, and G30 (0, 15, and 30 min of gastric digestion), and I0, I5, I10, I15, I30, I60, I90, and I120 (0, 5, 10, 15, 30, 60,90, and 120 min of the small intestinal digestion.

Table 7.6 Starch hydrolysis and glycaemic index of the bread samples

Bread composition	Final Starch hydrolysis (%)	Hydrolysis Index	Estimated Glycaemic index
Control	98.29 ± 0.64[c]	87.85 ±0.89[c]	87.94 ±0.49[c]
25% cotyledon flour	59.86 ±5.86[b]	42.57 ±2.09[b]	63.08 ±1.15[b]
50% cotyledon flour	36.69 ±3.43[a]	22.82 ±1.77[a]	52.24 ±0.97[a]

[a, b, c] Values in each column with the same superscript letters are not significantly different ($p > 0.05$).

7.4.5 Starch Digestion and the glycaemic response of the bread samples

The results of starch hydrolysis measured for the In vitro oral gastro-small intestinal digestion of the control, 25 % and 50 % cotyledon flour bread samples are illustrated in Figure 7.1. The starch hydrolysis observed at the gastric stage for the control bread sample (6.59 -7.38 %) was higher than 25 % (4.07 -6.35 %) and 50 % (3.5 -4.7 %) cotyledon flour-formulated bread samples. The starch hydrolysis of the bread samples at the gastric stage was because of starch-degrading enzymes (α-amylase) introduced during the first 2 min of the oral phase. For the small intestinal digestion, after 10 min, the starch hydrolysis for the control, 25 %, and 50 % cotyledon flour-formulated bread samples rose to 58.75, 23.41, and 12.95 %, respectively. After 60 min, the starch hydrolysis exhibited in the control bread samples was two and four times higher than in the 25 % and 50 % cotyledon flour-formulated bread samples. The starch hydrolysis of the bread samples then moved steadily until the end of 120 min of the small intestinal starch digestion. Overall, the final starch hydrolysis (Table 7.6) of 25 % (36.69 %) and 50 % (59.86) cotyledon flour-formulated bread samples was significantly ($P < 0.05$) lower than that of the control bread sample (98.29 %).

The starch hydrolysis results of the bread samples (control, 25 and 50 % cotyledon flour-formulated) for this study were within the range reported by other researchers (Boukid et al., 2019, Collar & Angioloni, 2017). The lower starch hydrolysis exhibited by the 25 and 50 %

cotyledon flour-formulated bread may be due to the modulating effect of the intact cotyledon cells present in the baked bread (Figure 7.2). That is, the cotyledon cell wall limited the inflow of water and starch-degrading enzymes to intracellular starch granules during baking and *in vitro* oral gastro-small intestinal digestion, respectively. This led to a level of partial gelatinization of intracellular starch granules during baking and subsequently starch digestion. The starch digestibility of pulse-formulated bread samples tends to decrease with an increase in the percentage of the cotyledon flour used. The protein/cellular material matrix presence in the pulse-formulated bread samples may also be responsible for the lower starch hydrolysis exhibited by the samples. Due to the slightly higher protein and fibre contents (Table 7.2) reported for the pulse-formulated bread samples, a stronger cytoplasmic matrix may be formed around the extracellular starch granules (Figure 7.2) compared to the control bread samples, thus, providing a sort of barrier to starch-degrading enzymes during the digestion procedure.

An overview of the microstructural images of bread samples after baking and at gastric (G30) and small intestinal digestion conditions (I10 & I120) is illustrated in Figure 7.2. After baking, the microstructure of the cotyledon flour-formulated bread was characterized by the presence of intact cotyledon cells (Figure 7.2) embedded in the bread structure. The integrity of the cotyledon cells tends to be preserved during the progression of the starch digestion stage from gastric (G0) to small intestinal digestion (I10 & I120) as shown in Figure 7.2. This further explained the lower starch hydrolysis exhibited by pulse-formulated bread samples. This was reflected in the estimated glycaemic index (eGI) of the cotyledon flour-formulated bread (Table 7.6) which was significantly lower than the control bread sample ($P < 0.05$). The resistant starch content of the bread samples for this study (Table 2) may also play a pivotal role in this trend, as it has been proven to influence the glycaemic and insulinemic postprandial responses by slowing the release of glucose (Berrios et al., 2010).

	Control	25% cotyledon flour	50% cotyledon flour
Baked	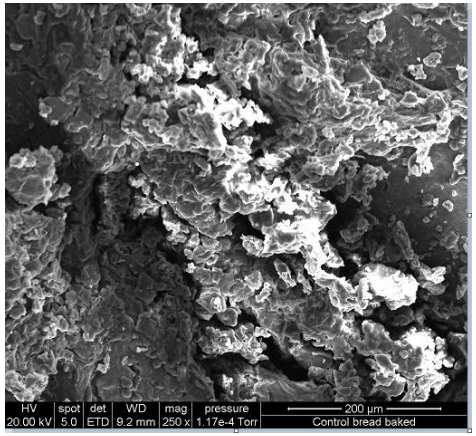	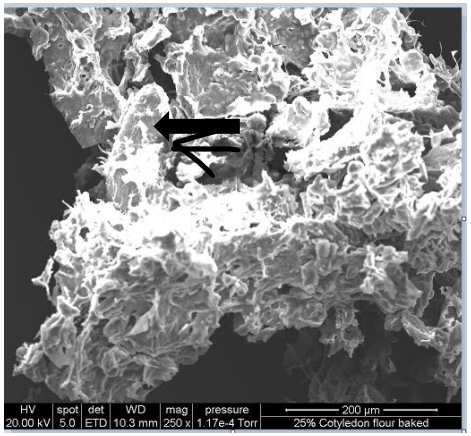	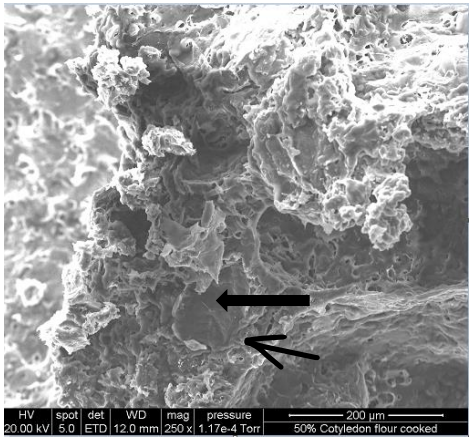
G30	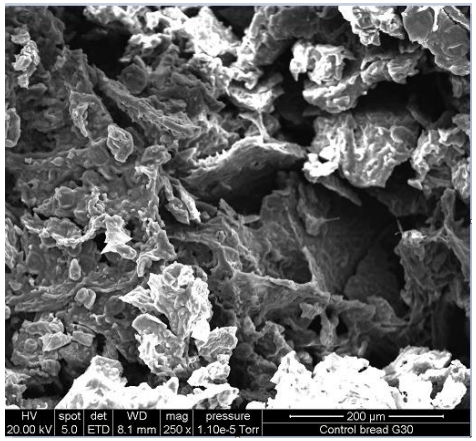	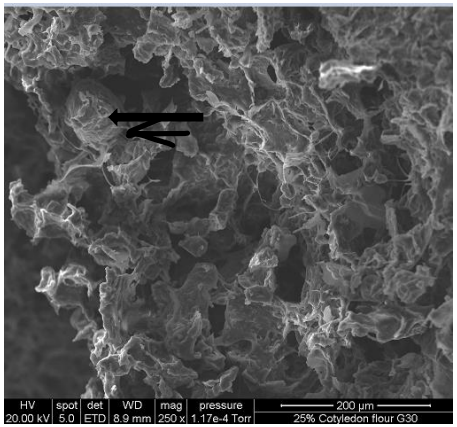	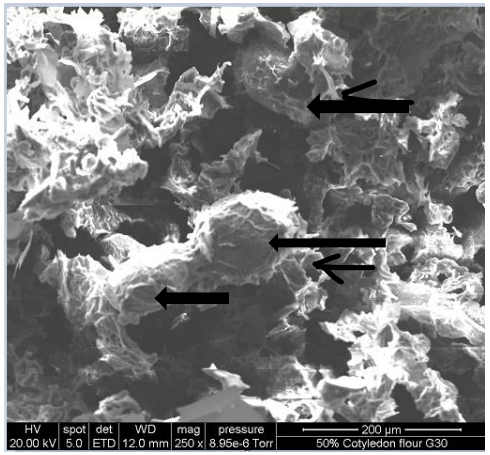

I10

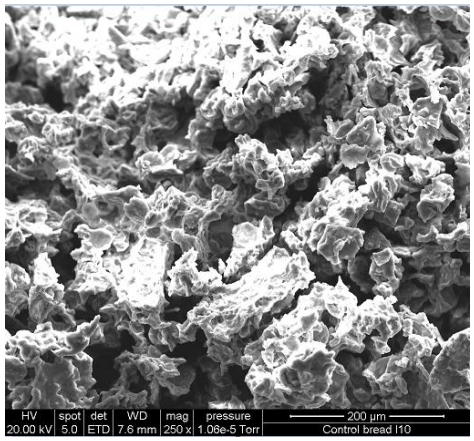

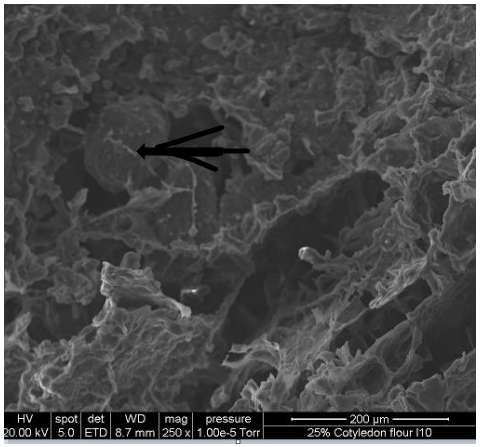

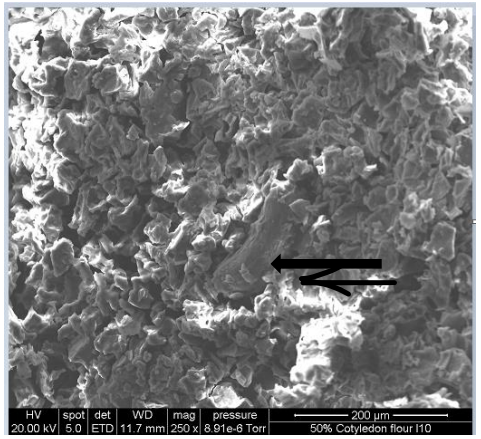

I120

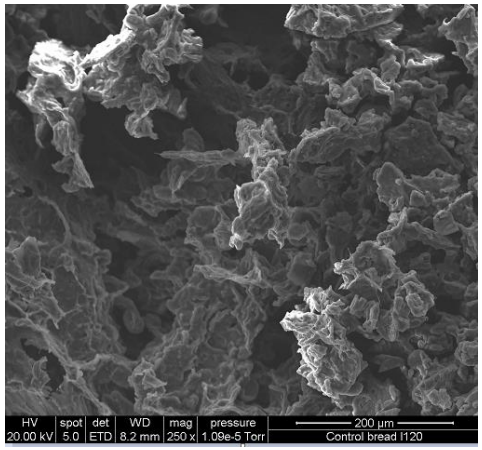

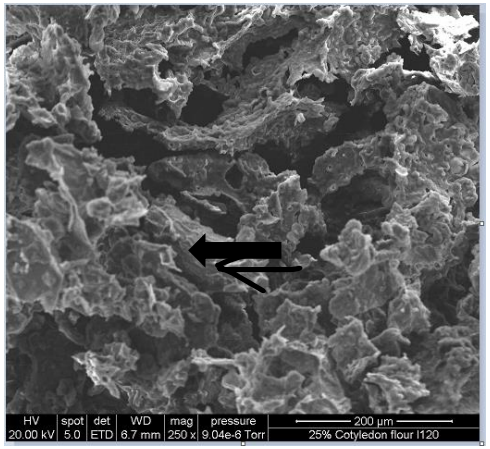

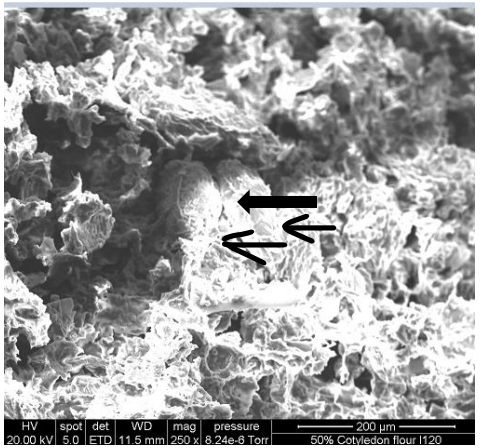

Fig 7.2 Scanning electron microscopy image of baked and digested bread samples (control, 25 and 50 % cotyledon flour). Where G30 is gastric digestion at 30 min while I10 and 1120 are small intestinal digestion at 10 and 120 min respectively

7.5 Conclusions

The microstructure and techno-functional properties of bread made with 25 and 50 % cotyledon flour were compared with the bread made with 100 % wheat flour. It was observed that the protein, fibre, and resistant starch contents in the cotyledon flour-formulated bread were significantly higher than the control bread. Also, the bake loss during baking, volume, and specific volume of bread loaf decreased with an increased percentage of cotyledon flour used in the bread formulation. On the other hand, the textural profile showed that the crumb hardness and cohesiveness of the bread samples increased with an increase in the percentage of the cotyledon flour added to the formulation of the bread. The starch hydrolysis showed the bread made with 25 and 50 % cotyledon flour was significantly lower than the control bread sample. The intact cotyledon cells with high cellular integrity observed in the microstructures of the bread samples confirmed this trend. Besides the presence of intact cotyledon cells in the bread microstructure after digestion, the high protein content in bread samples could lead to a strong protein matrix with extracellular starch granules, thus providing a barrier to the rate of ingress of starch-degrading enzymes during digestion. This could explain the low rate of starch hydrolysis exhibited by cotyledon flour-formulated bread samples.

Summarily, cotyledon flour tends to improve the nutritional and glycaemic features of bread based on the results from this study, however, the sensory characteristics of the bread were poor. Although the sensory characteristics of the bread were not formerly measured, the instrumental measurements and observations indicate a reduction of sensory properties compared with the control". Therefore, further study would be needed to explore how the novel cotyledon flour can optimally enhance the sensory quality of food products.

Chapter 8: General Discussion, conclusions, and future directions

8.1 Summary and Discussion

This thesis aimed to conduct a systematic investigation of the microstructural components (protein matrix and cellular wall) that influence the rate of starch hydrolysis *in vitro* in the three forms of pulse microstructures (whole pulse seed, cotyledon cell, and pulse flour) highlighted in the review of the literature (Chapter 2) from the sample botanical sources.

8.1.1 Microstructural components in whole pulse seed and its influence on intracellular starch gelatinization and hydrolysis

This study provided distinct microstructural components (starch granules, protein bodies, and cell wall materials) of a whole pulse seed with the aid of scanning electron microscopy (SEM) and Image analysis (Chapter 4). The native pulse seed microstructure revealed several pockets of cells containing starch granules embedded in the protein matrix and encapsulated by a fibrous intact cotyledon cell wall (Chapter 4, Fig 4.1). Furthermore, other important characteristics of the native microstructure of whole pulse seed such as the number of starch granules per cotyledon cell, cotyledon cell diameter, thickness of the cell wall, and average diameter of the starch granules per cell were highlighted. It was observed that these characteristics varied significantly ($p < 0.05$) amongst the different varieties of pulse seed (peas) that were used for this study. The abovementioned features of native pulse seed microstructure provide some new fundamental insights into the study of legumes/pulse microstructure.

This Ph.D. study highlighted that microstructure components in whole pulse seed influenced their response to processing conditions (Hydration kinetics set at 30, 40, 50, and 60 °C). There was a decrease in the intactness of the cotyledon structure from raw (room temperature) to 60 °C. This distortion of the cell wall enclosing starch, protein, and other macromolecules varied amongst the pea varieties used for this study but was less obvious with the variety that had the thickest cotyledon cell wall (Chapter 4, Table 4.1 & Figure 4.4). Furthermore, the pea seed variety that exhibited the highest distortion in its microstructural components (Figure 4.4)

also had the highest number of starch granules per cell (Table 4.4). The quantity of water uptake by the cotyledon of the pulses into the intracellular space is determined by the amount required for starch gelatinization, protein denaturation, and dissolution of the middle lamella (Mikac et al., 2015 & Zhang & Mccarthy, 2013). Thus, the variety with the number of starch granules per cell would require the maximum uptake of water for their gelatinization.

The low starch hydrolysis (18.2-27.6%) of the whole pulse seed reported from this study has been attributed to the microstructural reorganization of its intracellular components (starch granules, protein matrix, and cellular material) that occurred during cooking and oral phase of the simulated oral gastro-intestinal digestion experiments applied in this study. The electrographs of the cooked and "simulated chewed" pea seeds (Figure 4.7) before the gastrointestinal digestion showed some varying levels of a strong network of fibrous interaction with partly gelatinized and denatured protein bodies amongst the pea varieties. These images suggested that the network of fibrous interaction observed regulated the rate of hydrolysis in the starch granules by acting as a barrier to the starch-degrading enzymes. However, broad sponge-like (amorphous flakes) networks become apparent amongst the pea seeds digest as the digestion process proceeds. This trend assumes more starch granules are getting completely digested. The conclusion from this study tends to suggest that microstructural components (specifically cellular wall) in whole pulse seeds do regulate the inflow of water and starch-degrading enzymes, thus modulating the degree of intracellular starch gelatinization and digestion respectively. However, how the cotyledon cell wall objectively exhibits these regulatory activities is still not clear. Therefore, this Ph.D. study then investigated an objective way to understand the modulating capacity of the cotyledon cell wall (Chapter 5)

8.1.2 The cell wall permeability and its influence on entrapped starch digestion *in vitro*

The isolated intact cotyledon cells were used as the study sample for this experiment. This was done because intact cotyledon cells from legumes/pulses have been established as a suitable model for studying the microstructure of whole legumes/pulse seeds (Dhital et al., 2016, Bhattarai et al., 2017 & Junejo et al., 2021). Intact cotyledon cells were isolated from four varieties of pea seeds using the acid/alkaline treatment extraction techniques. This technique was selected for this study due to its capacity to produce intact cells with negligible free starch granules or broken cell walls (Dhital et al., 2016 & Kim & Kim, 2015). The pulsed field gradient

-NMR (PFG-NMR) coupled with light and confocal microscopy were used to objectively access the intact cotyledon cell wall diffusion and permeability to water and starch degrading enzymes (Chapter 5).

Before the diffusion and permeability experiments, the light and confocal microscopy revealed distinct microstructural components (starch granules embedded in protein matrix and encapsulated by intact cell wall) like what was observed in the whole pulse seed microstructures (Chapter 5, Figure 5.1 & 5.2). Furthermore, a varying degree of densely packed starch granules and internal cavities were observed amongst the cotyledon cells of different varieties. After, the diffusion and permeability experiments on the isolated cotyledon cells, the diffusion coefficient which is a quantitative measure of the molecular movement of water in and out of the cell varied amongst the isolated cotyledon cells (Chapter 5, Figure 5.4). In the same vein, the cell wall permeability of the cotyledon cell wall followed the same trend and was consistent with other authors (Ando et al., 2009) (Chapter 5, Figure 5.5. It was concluded the cell walls of the cotyledon cells for this study were more porous. The larger permeability exhibited by the cotyledon cells for this study can be attributed to the irreversible distorted functionality of the native microstructure of the cell wall caused during the freeze-drying process and acid/alkali extraction conditions (Voda et al., 2012 & Rondeau-Mouro et al.,2008).

The starch hydrolysis of the intact cotyledon cells and the microstructural changes that occur during the digestion process *in vitro* (Chapter 5, Figure 5.6 & 5.7) somewhat followed the trend observed in the diffusion coefficient and permeability results for the cells. That is, the large porosity/permeability observed in the cotyledon cells leads to more exposure of intracellular starch granules in the cell to starch-degrading enzymes, thus resulting in the medium-high rate of starch hydrolysis (71.10-83.87 %). The study provided fundamental and objective insights into how the cotyledon cell wall affects its modulating capacity to water and starch-degrading enzymes. In addition, an isolated intact cotyledon cell does not only suffice as an appropriate model to explore the possibilities in the whole pulse seed microstructure, but it also solves the limitation of applying whole pulse seed to a broad number of food products without compromising its native microstructure (large particle size) (Chapter 2 & 4). Intact Cotyledon cells have the potential to be used as low-medium glycaemic index food ingredients for a myriad of food products due to their applicable particle sizes (53-250 µm and high cellular integrity after isolation (Chapters 2 & 5). Nonetheless, its application as a new food ingredient

had been hampered due to the ineffective isolation procedures as shown by less than 30% of the cotyledon cells being recovered during the extraction process (Chapter 2). It suffices, to note that detailed insight into the relationship between isolation techniques and the total yield of cotyledon cells needs to be urgently explored.

During the cotyledon cell isolation procedure in this study, the total cotyledon yield was less than 20 % (dry matter) and the enormous residue recovered was examined under light and scanning electron microscopy. It was observed that the waste was an unevenly distributed mixture of starch granules, protein/cell wall materials matrix, and many clusters of cotyledon cells (Chapter 5, Figure 5.7). This suggested that the cotyledon cell isolation procedure is ineffective and unsustainable. This raised the question of whether there is a more effective and sustainable particle size-reducing technique to transform this enormous waste into applicable food ingredients without compromising the unique microstructures of the cotyledon cells. This thesis tends to address that question by adopting a known size-reducing technology (colloid milling) sustainably to create a novel food ingredient known as "cotyledon flour" (Chapter 6).

8.1.3 Characterisation of cotyledon flour developed via colloid milling.

After several preliminary experiments, the novel cotyledon flour was created via the combination of acid/alkali treatment and colloid milling (settings; the speed of the colloid rotor 30 Hz, starting gap between the stator and rotor, 300 µm, then gradually reduced until 50 µm) (Chapter 6, Figure 6.1). The underpinning mechanism observed using colloid milling to generate this cotyledon flour is the ability of the mill to mix, emulsify, and homogenize the heterogeneous mixture to a more uniform and refined mixture (Chen et al., 2017). That is, large clusters of cotyledon cells are reduced to isolated intact/broken cotyledon cells and other components are evenly distributed.

The microstructure, nutritional, and starch digestion properties *in vitro* of the cotyledon flour were compared with pulse flour (made from traditional grinding) from the same botanical sources. The electrographs reported for this study (Chapter 6, Figure 6.6) showed a distinct difference between the microstructural composition of cotyledon flour and blended flour. This study proposed that besides the particle size criterion used to define flour, the microstructure components of flour provide a more objective definition of flour. That is, a typical flour would constitute mainly discernible starch granules, protein bodies, and other cell wall materials.

Therefore, the “cotyledon flour” would comprise discernible cotyledon cells (intact, some broken), starch granules, protein bodies, and other cell wall materials (Chapter 6, Figure 6.3). It is also important to note that, the yield of cotyledon flour from each of the pea varieties varied from 68.8 % - 80.12 % (chapter 6, Table 6.1). From a food ingredient application standpoint, the yield reported for the cotyledon flour (> 50 %) better placed it as a potential new functional food ingredient than isolated cotyledon cells. The proximate composition of the cotyledon flour showed that protein and fibre content was 10 times and 2 times more than what was reported in the blended flour from the same botanical sources (chapter 6, Table 6.2). The water-holding capacity of the cotyledon flour was almost 3 times higher than the blended flour from the same plant source. The increase in water-holding capacity in the cotyledon flour is attributed to the increase in surface area and energy of the cotyledon flour after colloid milling (Zhao et al.,2009 & Zhao et al.,2010).

The starch hydrolysis of cotyledon flour was reported to be 10 times lower than that of the blended flour from the same botanical source (Chapter 6, Figure 6.5). The electrographs of the cotyledon flour and blended flour at the cooking, gastric, and small intestinal digestion stages (Chapter 6, Figure 6.6) also followed this trend. It was observed that two underpinning mechanisms were responsible for the lower starch hydrolysis rate exhibited by cotyledon cells, firstly, the cell wall of the cotyledon cell limits the extent of starch gelatinization and subsequently starch digestion by acting as a barrier to the inflow of water and starch-degrading enzymes during cooking and *in vitro* digestion respectively. Secondly, the limiting effect of the strong protein/cell wall matrix (cytoplasmic matrix) around the extracellular starch granules in the microstructural configuration of the cotyledon flour. This acts as a secondary physical barrier to enzymatic activity in small intestinal digestion *in vitro*. It can be concluded that the adoption and application of transformative technologies (colloid milling) can be used to develop a novel flour from whole pulse seed with high recovery and minimal effect on its microstructure that is responsible for low glycaemic features. Thus, the question then arises, how does the novel cotyledon flour affect the techno-functional properties of a standard food system (Chapter 7)

8.1.4 The effect of cotyledon flour as a new food ingredient on the techno-functional properties of a food system.

Bread was selected as the standard food system for this study because it is a globally established staple food and its consumption is recommended in all dietary guidelines (Cauvain & Young, 2007 & Dong & Karboune, 2021). Besides, the making of bread involves mixing flour, yeast, water, salt, etc, kneading, fermenting to form a viscoelastic dough, and then baking (heating at ~180 °C). These important unit operations create a suitable heterogeneous food system where the cotyledon flour can be tested as a viable new functional ingredient. So, for this study, the wheat flour for making bread was replaced with 25 and 50 % cotyledon flour, and the effect of this on the microstructure, physical-functional properties, starch digestion *in vitro,* and the glycaemic response was evaluated (Chapter 7).

The protein, fibre, and resistant starch in the cotyledon flour-formulated bread were significantly ($p < 0.05$) higher than the control bread (100 % wheat flour). The bake loss during baking recorded for this study decreased with an increased percentage of cotyledon flour used in the bread formulation. The volume and the specific volume of bread samples also decreased with an increase in the percentage of cotyledon flour used. The colour of the crumb and crust of the cotyledon flour-formulated bread was significantly different from the control bread ($p < 0.05$) while the textural profile showed that the crumb hardness and cohesiveness of the bread samples increased with an increase in the percentage of the cotyledon flour added to the formulation of the bread. The starch hydrolysis for this study showed bread made with 25 and 50% cotyledon flour was significantly lower than the control bread sample. The intact cotyledon cells with high cellular integrity observed in the microstructures of the bread samples confirmed this trend (Chapter 7, Figure 7.2). Besides the presence of intact cotyledon cells in the bread microstructure after digestion, the high protein content in bread samples could lead to a strong protein matrix with extracellular starch granules, thus providing a barrier to the rate of ingress of starch-degrading enzymes during digestion. This could explain the low rate of starch hydrolysis exhibited by cotyledon flour-formulated bread samples.

8.2 Conclusions and Recommendations for Future Works

This thesis provided fundamental insights into the forms of microstructure (cotyledon cells and pulse flour) that can be generated from whole pulse seed via size-reducing techniques, structural components (starch granules, protein matrix, and cell wall) in each form and how the interaction between these components influence the starch hydrolysis in each form. One of the significant fundamental knowledge areas provided by this dissertation was that

achieving a sort of equilibrium between “applicable particle size” and “intactness of microstructure” in processing a pulse seed could be a suitable template for designing a “wholesome” pulse food ingredient with medium glycaemic features (Chapter 6).

The findings from this thesis lay a solid foundation for further studies explained below briefly.

(i) The PFG-NMR method coupled with light, confocal, and scanning electron microscopy used in this study provided an objective measurement of the diffusion coefficients and cell wall permeability of the intact cotyledon cells and how these correlated to the rate of intracellular starch hydrolysis (Chapter 5). This provided a framework for which another objective measurement of the intact cotyledon cell wall such as specific pore size and surface area can be further explored.

(ii) The novel cotyledon flour designed by colloid milling coupled with prior acid/alkali treatments reported in this study provided a fundamental insight into how “transformative technologies” can be used to achieve a sort of equilibrium between “applicable particle size” and “intactness of microstructure” in processing pulse seed into pulse ingredients with medium glycaemic features. These need to be further investigated.

(iii) The application of the novel cotyledon flour in a food system (bread) showed the nutritional and glycaemic features of the bread can be greatly enhanced (Chapter 7). However, the sensory characteristics (such as volume and hardness/firmness) which an important quality indicators to consumers were not enhanced. Therefore, further investigation on improving the sensory potentials in cotyledon flour must be conducted. A whole meal bread rather than white bread may reduce the difference in sensory properties between the control bread and bread with cotyledon flour.

Bibliography

AACC. (2000). *Approved methods of the American Association of Cereal Chemists*. St. Paul, Minn.: American Assoc. of Cereal Chemists. 10-09.01, 10.01, 30-10 & 08-01.01.

Abramoff, M., Magalhaes, P., & Ram, S. (2004). Image processing with ImageJ. Biophotonics International, 11(7), 36–42. https://doi.org/10.1017/S1431927607079652

Abu-Ghannam, N., & McKenna, B. (1997). The application of Peleg's equation to model water absorption during the soaking of red kidney beans (Phaseolus vulgaris L.). *Journal of Food Engineering, 32*(4), 391-401. doi:10.1016/s0260-8774(97)00034-4

Acevedo, B., Avanza, M., Cháves, M., & Ronda, F. (2013). Gelation, thermal and pasting properties of pigeon pea (Cajanus cajan L.), dolichos bean (Dolichos lablab L.), and jack bean (Canavalia ensiformis) flours. *Journal of Food Engineering, 119*(1), 65-71. doi: 10.1016/j.jfoodeng.2013.05.014

Adjei-Fremah, S., Worku, M., De Erive, M., He, F., Wang, T., & Chen, G. (2019). Effect of microfluidization on microstructure, protein profile and physicochemical properties of whole cowpea flours. *Innovative Food Science & Emerging Technologies, 57*, 102207. doi:10.1016/j.ifset.2019.102207

Aguilera, J. (2005). Why food microstructure? *Journal of Food Engineering, 67*(1–2), 3–11. https://doi.org/10.1016/j.jfoodeng.2004.05.050.

Aguilera, J. M., Cadoche, L., López, C., & Gutierrez, G. (2001). Microstructural changes of potato cells and starch granules heated in oil. *Food Research International, 34*(10), 939-947. doi:10.1016/s0963-9969(01)00118-1

Ahmed, J., Mulla, M. Z., Siddiq, M., & Dolan, K. D. (2021). Micromeritic, thermal, dielectric, and microstructural properties of legume ingredients: A review. *Legume Science, 4*(1). doi:10.1002/leg3.123

Ajala, A., Kaur, L., Lee, S. J., & Singh, J. (2023). Native and processed legume seed microstructure and its influence on starch digestion and glycaemic features: A Review. *Trends in Food Science & Technology, 133*, 65-74. doi:10.1016/j.tifs.2023.01.011

Ajala, A., Kaur, L., Lee, S., & Singh, J. (2022). Influence of seed microstructure on the hydration kinetics and oral-gastro-small intestinal starch digestion in vitro of New Zealand pea varieties. *Food Hydrocolloids, 129*, 107631. doi:10.1016/j.foodhyd.2022.107631

Ai, Y., Cichy, K., Harte, J., Kelly, J., & Ng, P. (2016). Effects of extrusion cooking on the chemical composition and functional properties of dry common bean powders. *Food Chemistry, 211*, 538-545. doi:10.1016/j.foodchem.2016.05.095

Akibode, C. (2019). Trends in the Production, Trade, and Consumption of Food-Legume Crops in Sub-Saharan Africa. 10, 2019, http://dx.doi.org/10.22004/ag.econ.114247

Alajaji, S., & El-Adawy, T. (2006). Nutritional composition of chickpea (Cicer arietinum L.) as affected by microwave cooking and other traditional cooking methods. *Journal of Food Composition and Analysis, 19*(8), 806-812. doi:10.1016/j.jfca.2006.03.015

Alonso, R., Aguirre, A., & Marzo, F. (2000). Effects of extrusion and traditional processing methods on antinutrients and in vitro digestibility of protein and starch in faba and kidney beans. Food Chemistry, 68(2), 159–165. https://doi.org/10.1016/S0308-8146(99)00169-7

AOAC. (2012). Official Methods. Official methods of analysis of AOAC international (19th ed., Vol. 925). Gaithersburg, Md, USA: AOAC International, 10 & 962.09/978.10.

Ancona, D., Campos, M., Guerrero, L., & Ortíz, G. (2011). Structural and some nutritional characteristics of Velvet bean (Mucuna pruriens) and Lima bean (Phaseolus lunatus) starches. *Starch - Stärke, 63*(8), 475-484. doi:10.1002/star.201000119

Anderson, E., and Berry, B. (2000). Sensory, Shear, and Cooking Properties of Lower-Fat Beef Patties Made with Inner Pea Fiber. *Journal Of Food Science*, *65*(5), 805-810. doi: 10.1111/j.1365-2621.2000.tb13591.x

Anderson, E., and Berry, B. (2001). Identification of Non-meat Ingredients For Increasing Fat Holding Capacity During Heating of Ground Beef. *Journal Of Food Quality*, *24*(4), 291-299. doi: 10.1111/j.1745-4557.2001.tb00610.x

Ando, H., Fukuoka, M., Miyawaki, O., Watanabe, M., & Suzuki, T. (2009). PFG-NMR study for evaluating freezing damage to onion tissue. *Bioscience, Biotechnology, and Biochemistry, 73*(6), 1257-1261. doi:10.1271/bbb.80681

Anisimov, A. (2021). Gradient NMR method for studies of water translational diffusion in plants. *Membranes, 11*(7), 487. doi:10.3390/membranes11070487

Anton, A., Gary Fulcher, R., and Arntfield, S. (2009). Physical and nutritional impact of fortification of corn starch-based extruded snacks with common bean (Phaseolus vulgaris L.) flour: Effects of bean addition and extrusion cooking. *Food Chemistry*, *113*(4), 989-996. doi: 10.1016/j.foodchem.2008.08.050

Anton, A., Ross, K., Lukow, O., Fulcher, R., and Arntfield, S. (2008). Influence of added bean flour (Phaseolus vulgaris L.) on some physical and nutritional properties of wheat flour tortillas. *Food Chemistry*, *109*(1), 33-41. doi: 10.1016/j.foodchem.2007.12.005.

Aravindakshan, S., Nguyen, T. H., Kyomugasho, C., Buvé, C., Dewettinck, K., Van Loey, A., & Hendrickx, M. E. (2021). The impact of drying and rehydration on the structural properties and quality attributes of pre-cooked dried beans. *Foods, 10*(7), 1665. doi:10.3390/foods10071665

Asif, M., Rooney, L., Ali, R., & Riaz, M. (2013). Application and opportunities of pulses in the food system: A review. *Critical Reviews in Food Science and Nutrition*, 53(11), 1168–1179. https://doi.org/10.1080/10408398.2011.574804

Audu, S., & Aremu, M. (2011). Effect of Processing on Chemical Composition of Red Kidney Bean (Phaseolus vulgaris L.) Flour. *Pakistan Journal of Nutrition, 10*(11), 1069-1075. doi:10.3923/pjn.2011.1069.1075

Augustin, L., Chiavaroli, L., Campbell, J., Ezatagha, A., Jenkins, A., Esfahani, A., & Kendall, C. (2015). Post-prandial glucose and insulin responses of hummus alone or combined with a carbohydrate food: A dose–response study. *Nutrition Journal, 15*(1). doi:10.1186/s12937-016-0129-1

Bai, Y., Wu, P., Wang, K., Li, C., Li, E., & Gilbert, R. (2017). Effects of pectin on molecular structural changes in starch during digestion. *Food Hydrocolloids, 69*, 10-18. doi:10.1016/j.foodhyd.2017.01.021

Baik, B., & Han, I. (2012). Cooking, Roasting, and Fermentation of Chickpeas, Lentils, Peas, and Soybeans for Fortification of Leavened Bread. *Cereal Chemistry Journal, 89*(6), 269-275. doi:10.1094/cchem-04-12-0047-r

Balkrishna, S., & Visvanathan, R. (2019). Hydration kinetics of little millet and proso millet grains: Effect of soaking temperature. *Journal of Food Science & Technology*, 56 (7), 3534.

Bazzano, L., Thompson, A., Tees, M., Nguyen, C., and Winham, D. (2011). Non-soy legume consumption lowers cholesterol levels: A meta-analysis of randomized controlled trials.

Nutrition, Metabolism And Cardiovascular Diseases, *21*(2), 94-103. doi: 10.1016/j.numecd.2009.08.012.

Benmeziane-Derradji, F., Djermoune-Arkoub, L., Ayat, N., & Aoufi, D. (2020). Impact of roasting on the physicochemical, functional properties, antioxidant content and microstructure changes of Algerian lentil (lens culinaris) Flour. *Journal Of Food Measurement and Characterization,* 14(5), 2840–2853. https://doi.org/10.1007/ S11694-020-00529-7

Berg, T., Singh, J., Hardacre, A., & Boland, M. (2012). The role of cotyledon cell structure during in vitro digestion of starch in navy beans. *Carbohydrate Polymers, 87*(2), 1678-1688. doi:10.1016/j.carbpol.2011.09.075

Berrios, J. D., Morales, P., Cámara, M., & Sánchez-Mata, M. (2010). Carbohydrate composition of raw and extruded pulse flours. *Food Research International, 43*(2), 531-536. doi:10.1016/j.foodres.2009.09.035

Bhattacharya, S., Narasimha, H., & Bhattacharya, S. (2005). The moisture-dependent physical and mechanical properties of whole lentil pulse and split cotyledon. *International Journal of Food Science and Technology, 40*(2), 213–221. https://doi.org/10.1111/j.1365-2621.2004.00933.x

Bhattarai, R. R., Dhital, S., Wu, P., Chen, X. D., & Gidley, M. J. (2017). Digestion of isolated legume cells in a stomach-duodenum model: Three mechanisms limit starch and protein hydrolysis. *Food & Function, 8*(7), 2573-2582. doi:10.1039/c7fo00086c

Bornet, F., Billaux, M., and Messing, B. (1997). Glycaemic index concept and metabolic diseases. *International Journal Of Biological Macromolecules*, *21*(1-2), 207-219. doi: 10.1016/s0141-8130(97)00066-4.

Boukid, F., Vittadini, E., Lusuardi, F., Ganino, T., Carini, E., Morreale, F., & Pellegrini, N. (2019). Does cell wall integrity in legumes flours modulate physiochemical quality and in vitro starch hydrolysis of gluten-free bread? *Journal of Functional Foods, 59*, 110-118. doi:10.1016/j.jff.2019.05.034

Bourré, L., Frohlich, P., Young, G., Borsuk, Y., Sopiwnyk, E., Sarkar, A., . . . Malcolmson, L. (2019). Influence of particle size on flour and baking properties of yellow pea, navy bean, and red lentil flours. *Cereal Chemistry, 96*(4), 655-667. doi:10.1002/cche.10161

Brand-Miller, J. (2003). Glycemic Load and Chronic Disease. *Nutrition Reviews, 61*(Suppl_5), S49-S55. doi:10.1301/nr.2003.may.s49-s55

Bravo, L., Siddhuraju, P., & Saura-Calixto, F. (1998). Effect of Various Processing Methods on the in Vitro Starch Digestibility and Resistant Starch Content of Indian Pulses. *Journal of Agricultural and Food Chemistry, 46*(11), 4667-4674. doi:10.1021/jf980251f

Bruno, G., Runzo, C., Cavallo-Perin, P., Merletti, F., Rivetti, M., Pinach, S., . . . Pagano, G. (2005). Incidence of Type 1 and Type 2 Diabetes in Adults Aged 30-49 Years: The population-based registry in the province of Turin, Italy. *Diabetes Care, 28*(11), 2613-2619. doi:10.2337/diacare.28.11.2613

Business wire. (2020). Global Pulse Ingredients Market Forecast to 2023: A $21.6 Billion Opportunity - ResearchAndMarkets.com. Retrieved 3, 2020, from https://www.businesswire.com/news/home/20190311005312/en/Global-Pulse-Ingredients-Market-Forecast-2023-21.6

Burton, R. A., Gidley, M. J., & Fincher, G. B. (2010). Heterogeneity in the chemistry, structure and function of Plant Cell Walls. *Nature Chemical Biology, 6*(10), 724-732. doi:10.1038/nchembio.439

Cai, R., Klamczynska, B., and Baik, B. (2001). Preparation of Bean Curds from Protein Fractions of Six Legumes. *Journal Of Agricultural And Food Chemistry*, *49*(6), 3068-3073. doi: 10.1021/jf0013398

Cai, R., McCurdy, A., and Baik, B. (2002). Textural Property of 6 Legume Curds in Relation to their Protein Constituents. *Journal Of Food Science*, *67*(5), 1725-1730. doi: 10.1111/j.1365-2621.2002.tb08713.x

Calabrò, S., Cutrignelli, M., Lo Presti, V., Tudisco, R., Chiofalo, V., and Grossi, M. et al. (2015). Characterization and effect of year of harvest on the nutritional properties of three varieties of white lupine (Lupinus albusL.). *Journal Of The Science Of Food And Agriculture*, *95*(15), 3127-3136. doi: 10.1002/jsfa.7049

Caprioli, G., Giusti, F., Ballini, R., Sagratini, G., Vila-Donat, P., Vittori, S., and Fiorini, D. (2016). Lipid nutritional value of legumes: Evaluation of different extraction methods and determination of fatty acid composition. *Food Chemistry*, *192*, 965-971. doi: 10.1016/j.foodchem.2015.07.102

Cauvain, S. P. (2015). Bread – the Product. In *Technology of Breadmaking* (pp. 1-19). Boston,, MA: Springer. doi:10.1007/0-387-38565-7_1

Cauvain, S., & Young, L. (2007). *Technology of Breadmaking*. Cham, NY: Springer International Publishing.

Chau, C., Wang, Y., & Wen, Y. (2007). Different micronization methods significantly improve the functionality of carrot insoluble fibre. *Food Chemistry, 100*(4), 1402-1408. doi:10.1016/j.foodchem.2005.11.034

Chen, T., Zhang, M., Bhandari, B., & Yang, Z. (2017). Micronization and nanosizing of particles for an enhanced quality of food: A review. *Critical Reviews in Food Science and Nutrition, 58*(6), 993-1001. doi:10.1080/10408398.2016.1236238

Chen, Y., Singh, J., & Archer, R. (2018). Potato starch retrogradation in tuber: Structural changes and gastro-small intestinal digestion in vitro. *Food Hydrocolloids*, 84,552–560. https://doi.org/10.1016/J.Foodhyd.2018.05.044

Chigwedere, C., Njoroge, D., Loey, A., & Hendrickx, M. (2019). Understanding the relations among the storage, soaking, and cooking behaviour of pulses: A scientific basis for innovations in sustainable foods for the future. *Comprehensive Reviews in Food Science and Food Safety*, 18(4), 1135–1165. https://doi.org/10.1111/1541-4337.12461

Cho, C., Hong, Y., Kang, K., Volkov, V. I., Skirda, V., Lee, C. J., & Lee, C. (2003). Water self-diffusion in chlorella sp. studied by pulse field gradient NMR. *Magnetic Resonance Imaging, 21*(9), 1009-1017. doi:10.1016/s0730-725x(03)00206-6

Chung, H., & Liu, Q. (2012). Physicochemical properties and in vitro digestibility of flour and starch from pea (Pisum sativum L.) cultivars. *International Journal of Biological Macromolecules, 50*(1), 131–137. https://doi.org/10.1016/j.ijbiomac.2011.10.004

Chung, H., Liu, Q., Peter Pauls, K., Fan, M., & Yada, R. (2008). In vitro starch digestibility expected glycemic index and some physicochemical properties of starch and flour from common bean (Phaseolus vulgaris l.) varieties grown in Canada. Food Research International, 41(9), 869–875. https://doi.org/10.1016/J.Foodres.2008.03.013

Chung, H., Liu, Q., Hoover, R., Warkentin, T., & Vandenberg, B. (2008). In vitro starch digestibility, expected glycemic index, and thermal and pasting properties of flours from pea, lentil, and chickpea cultivars. *Food Chemistry, 111*(2), 316–321. https://doi.org/10.1016/j.foodchem.2008.03.062

Curran-Cournane, F., & Rush, E. (2021). Feeding the New Zealand family of five million,5+ a day of vegetables? Earth, 2(4), 797–808. https://doi.org/10.3390/earth2040047

Chávez-Murillo, C., Veyna-Torres, J., Cavazos-Tamez, L., De la Rosa-Millán, J., & Serna-Saldívar, S. (2018). Physicochemical characteristics, ATR-FTIR molecular interactions and in vitro

starch and protein digestion of thermally treated whole pulse flours. *Food Research International, 105*, 371-383. doi:10.1016/j.foodres.2017.11.029

Clark, E. A., & Aramouni, F. M. (2018). Evaluation of quality parameters in gluten-free bread formulated with breadfruit (*artocarpus altilis*) flour. *Journal of Food Quality, 2018*, 1-12. doi:10.1155/2018/1063502

Collar, C., & Angioloni, A. (2017). High-legume wheat-based matrices: Impact of high pressure on starch hydrolysis and firming kinetics of composite breads. *Food and Bioprocess Technology, 10*(6), 1103-1112. doi:10.1007/s11947-017-1883-6

Cooke, D., & Gidley, M. (1992). Loss of crystalline and molecular order during starch gelatinisation: Origin of the enthalpic transition. *Carbohydrate Research, 227*, 103-112. doi:10.1016/0008-6215(92)85063-6

Curran, J. (2012). The nutritional value and health benefits of pulses in relation to obesity, diabetes, heart disease and cancer. *British Journal Of Nutrition*, *108*(S1), S1-S2. doi: 10.1017/s0007114512003534

Cutforth, H., Angadi, S., McConkey, B., Entz, M., Ulrich, D., and Volkmar, K. et al. (2009). Comparing plant water relations for wheat with alternative pulse and oilseed crops grown in the semiarid Canadian prairie. *Canadian Journal Of Plant Science*, *89*(5), 823-835. doi: 10.4141/cjps08138

Dalgetty, D., and Baik, B. (2006). Fortification of Bread with Hulls and Cotyledon Fibers Isolated from Peas, Lentils, and Chickpeas. *Cereal Chemistry Journal*, *83*(3), 269-274. doi: 10.1094/cc-83-0269

Dartois, A., Singh, J., Kaur, L., & Singh, H. (2010). Influence of Guar Gum on the In Vitro Starch Digestibility—Rheological and Microstructural Characteristics. *Food Biophysics, 5*(3), 149-160. doi:10.1007/s11483-010-9155-2

Dhital, S., Bhattarai, R. R., Gorham, J., & Gidley, M. J. (2016). Intactness of cell wall structure controls the in vitro digestion of starch in legumes. *Food & Function, 7*(3), 1367-1379. doi:10.1039/c5fo01104c

Diedericks, C., Venema, P., Mubaiwa, J., Jideani, V., & van der Linden, E. (2020). Effect of processing on the microstructure and composition of Bambara groundnut (Vigna subterranea (L.) Verdc.) seeds, flour, and protein isolates. *Food Hydrocolloids, 108*, Article 106031. https://doi.org/10.1016/j.foodhyd.2020.106031

Dogan, M., Aslan, D., & Gurmeric, V. (2017). The rheological behaviors and morphological characteristics of different food hydrocolloids ground to sub-micro particles: In terms of temperature and particle size. *Journal of Food Measurement and Characterization, 12*(2), 770–780. https://doi.org/10.1007/s11694-017-9691-2

Do, D. T., Singh, J., Oey, I., & Singh, H. (2019). Modulating effect of Cotyledon cell microstructure on in vitro digestion of starch in legumes. *Food Hydrocolloids, 96*, 112-122. doi:10.1016/j.foodhyd.2019.04.063

Dong, Y., & Karboune, S. (2021). A review of bread qualities and current strategies for bread bioprotection: Flavor, sensory, rheological, and textural attributes. *Comprehensive Reviews in Food Science and Food Safety, 20*(2), 1937-1981. doi:10.1111/1541-4337.12717

Dovi, K. A., Chiremba, C., Taylor, J. R., & De Kock, H. L. (2017). Rapid sensory profiling and hedonic rating of whole grain sorghum-cowpea composite biscuits by low income consumers. *Journal of the Science of Food and Agriculture, 98*(3), 905-913. doi:10.1002/jsfa.8536

Eckelkamp, S. (2021). I chewed each bite of food 30 times. here's how it changed my digestion. Retrieved 26 May 2021, From https://Www.Mindbodygreen.Com/Articles /Heres-What-Happens-To-Digestion-When-You-Actually-Chew-Your-Food.

Edwards, C. H., Ryden, P., Mandalari, G., Butterworth, P. J., & Ellis, P. R. (2021). Structure–function studies of Chickpea and durum wheat uncover mechanisms by which cell wall properties influence starch bioaccessibility. *Nature Food, 2*(2), 118-126. doi:10.1038/s43016-021-00230-y

Edwards, C., Ryden, P., Pinto, A., Van der Schoot, A., Stocchi, C., Perez-Moral, N., . . . Ellis, P. (2020). Chemical, physical and glycaemic characterisation of PulseON®: A novel legume cell-powder ingredient for use in the design of functional foods. *Journal of Functional Foods, 68*, 103918. doi:10.1016/j.jff.2020.103918

EPA. (2012). Global anthropogenic non-Co2 greenhouse gas emissions: 1990–2030. Washington Dc: The United States Environmental Protection Agency. EPA.

Fan, P., Zang, M., & Xing, J. (2014). Oligosaccharide's composition in eight food legumes species as detected by high-resolution mass spectrometry. Journal of the Science of Food and Agriculture, 95(11), 2228–2236. https://doi.org/10.1002/Jsfa.6940

Fardet, A., & Boirie, Y. (2014). Associations between food and beverage groups and major diet-related chronic diseases: An exhaustive review of pooled/meta-analyses and systematic reviews. *Nutrition Reviews, 72*(12), 741-762. doi:10.1111/nure.12153

FAO. (2016). Pulses—nutritious seeds for a sustainable future. *FAO., Rome*.

FAO. (2019). SOFI 2019 - The State of Food Security and Nutrition in the World. Retrieved 14 September 2019, from http://www.fao.org/state-of-food-security-nutrition/en/

FAOSTAT. (2017). FAOSTAT. Retrieved 4 March 2020, from http://www.fao.org/faostat/en/

Food and Drug Administration (FDA). (2018). *Code of Federal Regulations Title 21, Volume 2.* (p. Sec103.105 Flour. Revised).

Figuerola, F., Hurtado, M., Estévez, A., Chiffelle, I., & Asenjo, F. (2005). Fibre concentrates from apple pomace and citrus peel as potential fibre sources for food enrichment. *Food Chemistry*, *91*(3), 395-401. doi: 10.1016/j.foodchem.2004.04.036

Foster-Powell, K., Holt, S., and Brand-Miller, J. (2002). International table of glycemic index and glycemic load values: 2002. *The American Journal Of Clinical Nutrition*, *76*(1), 5-56. doi: 10.1093/ajcn/76.1.5

Fouad, A., and Rehab, F. (2015). Effect of germination time on proximate analysis, bioactive compounds and antioxidant activity of lentil (Lens culinaris Medik.) sprouts. *Acta Scientiarum Polonorum Technologia Alimentaria*, *14*(3), 233-246. doi: 10.17306/j.afs.2015.3.25

Frimpong, A., Sinha, A., Tar'an, B., Warkentin, T., Gossen, B., and Chibbar, R. (2009). Genotype and growing environment influence chickpea (Cicer arietinumL.) seed composition. *Journal Of The Science Of Food And Agriculture*, *89*(12), 2052-2063. doi: 10.1002/jsfa.3690

Frohlich, P., Boux, G., and Malcolmson, L. (2014). Pulse Ingredients as Healthier Options in Extruded Products. *Cereal Foods World*, *59*(3), 120-125. doi: 10.1094/cfw-59-3-0120

Fujimura, T., & Kugimiya, M. (1994). Gelatinization of Starches inside Cotyledon Cells of Kidney Beans. *Starch - Stärke, 46*(10), 374-378. doi:10.1002/star.19940461003

Gan, Y., Liang, C., Wang, X., and McConkey, B. (2011). Lowering carbon footprint of durum wheat by diversifying cropping systems. *Field Crops Research*, *122*(3), 199-206. doi: 10.1016/j.fcr.2011.03.020

García-Alonso, A., Goñi, I., & Saura-Calixto, F. (1998). Resistant starch and potential glycaemic index of raw and cooked legumes (lentils, chickpeas and beans). *Zeitschrift Fur*

Lebensmitteluntersuchung Und -Forschung A, 206(4), 284-287. doi:10.1007/s002170050258

Germaine, K., Samman, S., Fryirs, C., Griffiths, P., Johnson, S., & Quail, K. (2008). Comparison of in vitro starch digestibility methods for predicting the glycaemic index of grain foods. *Journal of the Science of Food and Agriculture*, 88(4), 652–658. https://doi.org/10.1002/Jsfa.3130

Ghumman, A., Kaur, A., and Singh, N. (2016). Impact of germination on flour, protein and starch characteristics of lentil (Lens culinari) and horsegram (Macrotyloma uniflorum L.) lines. *LWT - Food Science And Technology*, *65*, 137-144. doi: 10.1016/j.lwt.2015.07.075

Giusti, F., Capuano, E., Sagratini, G., & Pellegrini, N. (2019). A comprehensive investigation of the behaviour of phenolic compounds in legumes during domestic cooking and in vitro digestion. *Food Chemistry*, 285, 458–467. https://doi.org/ 10.1016/J.Foodchem.2019.01.148

Giannone, V., Giarnetti, M., Spina, A., Todaro, A., Pecorino, B., Summo, C., . . . Pasqualone, A. (2018). Physico-chemical properties and sensory profile of Durum Wheat Dittaino PDO (protected designation of origin) bread and quality of re-milled semolina used for its production. *Food Chemistry, 241*, 242-249. doi:10.1016/j.foodchem.2017.08.096

Giger-Reverdin, S., Maaroufi, C., Chapoutot, P., Peyronnet, C., & Sauvant, D. (2014). Influence of grinding on the nutritive value of peas for ruminants: Comparison between in vitro and in situ approaches. *Food Science & Nutrition, 2*(4), 308-320. doi:10.1002/fsn3.90

Goesaert, H., Leman, P., Bijttebier, A., & Delcour, J. A. (2009). Antifirming effects of starch degrading enzymes in bread crumb. *Journal of Agricultural and Food Chemistry, 57*(6), 2346-2355. doi:10.1021/jf803058v

Gómez, M., Oliete, B., Rosell, C., Pando, V., and Fernández, E. (2008). Studies on cake quality made of wheat–chickpea flour blends. *LWT - Food Science And Technology*, *41*(9), 1701-1709. doi: 10.1016/j.lwt.2007.11.024

Grundy, M. M., Edwards, C. H., Mackie, A. R., Gidley, M. J., Butterworth, P. J., & Ellis, P. R. (2016). Re-evaluation of the mechanisms of dietary fibre and implications for macronutrient bioaccessibility, digestion and postprandial metabolism. *British Journal of Nutrition, 116*(5), 816-833. doi:10.1017/s0007114516002610

Guo, C., Wang, X., & Wang, Y. (2018). Dielectric properties of soy protein isolate dispersion and its temperature profile during radio frequency heating. *Journal of Food Processing and Preservation, 42*(7), E13659. doi:10.1111/jfpp.13659

Gujska, E., reinhard, W. D.-, & Khan, K. (1994). Physicochemical properties of field pea, pinto, and navy bean starches. *Journal of Food Science, 59*(3), 634–636. https://doi.org/10.1111/j.1365-2621.1994.tb05580.x

Gwala, S., Pallares Pallares, A., Palchen, ¨ K., Hendrickx, M., & Grauwet, T. (2020). In vitro starch and protein digestion kinetics of cooked Bambara groundnuts depend on processing intensity and hardness sorting. *Food Research International, 137*, Article 109512. https://doi.org/10.1016/j.foodres.2020.109512

Ha, V., Sievenpiper, J., de Souza, R., Jayalath, V., Mirrahimi, A., and Agarwal, A. et al. (2014). Effect of dietary pulse intake on established therapeutic lipid targets for cardiovascular risk reduction: a systematic review and meta-analysis of randomized controlled trials. *Canadian Medical Association Journal*, *186*(8), E252-E262. doi: 10.1503/cmaj.131727

Hall, C., Hillen, C., & Garden Robinson, J. (2017). Composition, nutritional value, and health benefits of pulses. Cereal Chemistry Journal, 94(1), 11–31. https://doi.org/10.1094/Cchem-03-16-0069-Fi

Han, J., Janz, J., and Gerlat, M. (2010). Development of gluten-free cracker snacks using pulse flours and fractions. *Food Research International*, *43*(2), 627-633. doi: 10.1016/j.foodres.2009.07.015

Hood-Niefer, S., and Tyler, R. (2010). Effect of protein, moisture content and barrel temperature on the physico-chemical characteristics of pea flour extrudates. *Food Research International*, *43*(2), 659-663. doi: 10.1016/j.foodres.2009.09.033

Hoover, R., and Ratnayake, W. (2002). Starch characteristics of black bean, chick pea, lentil, navy bean and pinto bean cultivars grown in Canada. *Food Chemistry*, *78*(4), 489-498. doi: 10.1016/s0308-8146(02)00163-2

Hoover, R., Hughes, T., Chung, H., & Liu, Q. (2010). Composition, molecular structure, properties, and modification of pulse starches: A Review. *Food Research International, 43*(2), 399-413. doi:10.1016/j.foodres.2009.09.001

Hosseinpour-Niazi, S., Mirmiran, P., Sohrab, G., Hosseini-Esfahani, F., and Azizi, F. (2011). Inverse association between fruit, legume, and cereal fiber and the risk of metabolic

syndrome: Tehran Lipid and Glucose Study. *Diabetes Research And Clinical Practice*, *94*(2), 276-283. doi: 10.1016/j.diabres.2011.07.020.

Huang, Y., Dhital, S., Liu, F., Fu, X., Huang, Q., & Zhang, B. (2021). Cell wall permeability of Pinto Bean Cotyledon cells regulate *in vitro* fecal fermentation and gut microbiota. *Food & Function, 12*(13), 6070-6082. doi:10.1039/d1fo00488c

Hung, T., Liu, L., Black, R., & Trewhella, M. (1993). Water absorption in chickpea (c.arietinum) and field pea (P. sativum) cultivars using the Peleg model. *Journal of Food Science*, 58(4), 848–852. https://doi.org/10.1111/J.1365-2621.1993.Tb09374

Hutchings, S., Bronlund, J., Lentle, R., Foster, K., Jones, J., & Morgenstern, M. (2009). Variation of bite size with different types of food bars and implications for serving methods in mastication studies. *Food Quality and Preference*, 20(6), 456–460. https://doi.org/10.1016/j.foodqual.2009.04.007

IPCC. (2014). *Climate change 2014: mitigation of climate change. Summary for policymakers, technical summary.*. United Kingdom,New York, USA: Cambridge University Press, Cambridge.

Jenkins, D., Wolever, T., Jenkins, A., Thorne, M., Lee, R., and Kalmusky, J. et al. (1983). The glycaemic index of foods tested in diabetic patients: A new basis for carbohydrate exchange favouring the use of legumes. *Diabetologia*, *24*(4). doi: 10.1007/bf00282710

Jenkins, D., Wolever, T., Taylor, R., Barker, H., Fielden, H., and Jenkins, A. (1980). Effect of guar crispbread with cereal products and leguminous seeds on blood glucose concentrations of diabetics. *BMJ*, *281*(6250), 1248-1250. doi: 10.1136/bmj.281.6250.1248

Jeong, D., Han, J., Liu, Q., and Chung, H. (2019). Effect of processing, storage, and modification on in vitro starch digestion characteristics of food legumes: A review. *Food Hydrocolloids*, *90*, 367-376. doi: 10.1016/j.foodhyd.2018.12.039

Jha, A., Tar'an, B., Diapari, M., and Warkentin, T. (2015). SNP variation within genes associated with amylose, total starch and crude protein concentration in field pea. *Euphytica*, *206*(2), 459-471. doi: 10.1007/s10681-015-1510-4.

Johnson, S. K., Thomas, S. J., & Hall, R. S. (2004). Palatability and glucose, insulin and satiety responses of chickpea flour and extruded chickpea flour bread eaten as part of a breakfast. *European Journal of Clinical Nutrition, 59*(2), 169-176. doi:10.1038/sj.ejcn.1602054

Joshi, P., and Rao, P. (2016). Global pulses scenario: status and outlook. *Annals Of The New York Academy Of Sciences*, *1392*(1), 6-17. doi: 10.1111/nyas.13298

Junejo, S. A., Ding, L., Fu, X., Xiong, W., Zhang, B., & Huang, Q. (2021). Pea cell wall integrity controls the starch and protein digestion properties in the INFOGEST in vitro simulation. *International Journal of Biological Macromolecules, 182*, 1200-1207. doi:10.1016/j.ijbiomac.2021.05.014

Kaptso, G., Njintang, N., Nguemtchouin, M., Amungwa, A., Scher, J., Hounhouigan, J., & Mbofung, C. (2016). Characterization of Morphology and Structural and Thermal Properties of Legume Flours: Cowpea (Vigna unguiculata L. Walp) and Bambara Groundnut (Vigna subterranea L. Verdc.) Varieties. *International Journal of Food Engineering, 12*(2), 139-152. doi:10.1515/ijfe-2014-0146

Karaca, A., Low, N., and Nickerson, M. (2011). Emulsifying properties of chickpea, faba bean, lentil and pea proteins produced by isoelectric precipitation and salt extraction. *Food Research International*, *44*(9), 2742-2750. doi: 10.1016/j.foodres.2011.06.012

Kathirvel, P., Yamazaki, Y., Zhu, W., & Luhovyy, B. (2019). Glucose release from lentil flours digested in vitro: The role of particle size. *Cereal Chemistry, 96*(6), 1126–1136. https://doi.org/10.1002/cche.10223

Kelkar, S., Siddiq, M., Harte, J., Dolan, K., Nyombaire, G., and Suniaga, H. (2012). Erratum to "Use of low-temperature extrusion for reducing phytohemagglutinin activity (PHA) and oligosaccharides in beans (Phaseolus vulgaris) cv. Navy and Pinto" [Food Chemistry 133 (2012) 1636–1639]. *Food Chemistry*, *134*(4), 2261. doi: 10.1016/j.foodchem.2012.04.107

Kornet, C., Venema, P., Nijsse, J., van der Linden, E., van der Goot, A., & Meinders, M. (2020). Yellow pea aqueous fractionation increases the specific volume fraction and viscosity of its dispersions. *Food Hydrocolloids, 99*, Article 105332. https://doi.org/10.1016/j.foodhyd.2019.105332

Kim, E., & Kim, H. (2015). Physicochemical properties of dehydrated potato parenchyma cells with ungelatinized and gelatinized starches. *Carbohydrate Polymers, 117*, 845-852. doi:10.1016/j.carbpol.2014.10.038

Kitamura, A., & Kinjo, M. (2018). Determination of diffusion coefficients in live cells using fluorescence recovery after photobleaching with wide-field fluorescence microscopy. *Biophysics and Physicobiology, 15*(0), 1-7. doi:10.2142/biophysico.15.0_1

Kugimiya, M. (1990). Separation of cotyledon cells of legumes by successive treatments with acid and alkali. *Nippon Shokuhin Kogyo Gakkaishi, 37*(11), 867-871. doi:10.3136/nskkk1962.37.11_867

Kumar, S., Sadiq, M., & Anal, A. (2021). Comparative study of physicochemical and functional properties of soaked, germinated and pressure cooked Faba bean. *Journal of Food Science and Technology, 59*(1), 257-267. doi:10.1007/s13197-021-05010-x

Leon, E., Piston, F., Aouni, R., Shewry, P., Rosell, C., Martin, A., & Barro, F. (2010). Pasting properties of transgenic lines of a commercial bread wheat expressing combinations of HMW glutenin subunit genes. *Journal of Cereal Science, 51*(3), 344-349. doi:10.1016/j.jcs.2010.02.002

Lemke, R., Zhong, Z., Campbell, C., and Zentner, R. (2007). Can Pulse Crops Play a Role in Mitigating Greenhouse Gases from North American Agriculture?. *Agronomy Journal*, *99*(6), 1719-1725. doi: 10.2134/agronj2006.0327s

Leterme, P. (2002). Recommendations by health organizations for pulse consumption. *British Journal Of Nutrition*, *88*(S3), 239-242. doi: 10.1079/bjn2002712

Li, H., Gidley, M. J., & Dhital, S. (2019). Wall porosity in isolated cells from food plants: Implications for nutritional functionality. *Food Chemistry, 279*, 416-425. doi:10.1016/j.foodchem.2018.12.024

Li, P., Dhital, S., Fu, X., Huang, Q., Liu, R., Zhang, B., & He, X. (2020). Starch digestion in intact pulse cotyledon cells depends on the extent of thermal treatment. *Food Chemistry, 315*, 126268. doi:10.1016/j.foodchem.2020.126268

Li, P., Dhital, S., Zhang, B., He, X., Fu, X., & Huang, Q. (2018). Surface structural features control in vitro digestion kinetics of bean starches. *Food Hydrocolloids, 85*, 343-351. doi:10.1016/j.foodhyd.2018.07.007

Li, P., Zhang, B., & Dhital, S. (2019). Starch digestion in intact pulse cells depends on the processing induced permeability of cell walls. *Carbohydrate Polymers, 225*, 115204. doi:10.1016/j.carbpol.2019.115204

Li, P., Zhang, B., Liu, R., Ding, L., Fu, X., Li, H., . . . He, X. (2023). Insights into the relations between cell wall integrity and in vitro digestion properties of granular starches in pulse cotyledon cells after dry heat treatment. *Food Science and Human Wellness, 12*(2), 528-535. doi:10.1016/j.fshw.2022.07.055

Liu, S., Chen, D., & Xu, J. (2018). The effect of partially substituted lupin, soybean, and navy bean flours on Wheat Bread Quality. *Food and Nutrition Sciences, 09*(07), 840-854. doi:10.4236/fns.2018.97063

Maninder, K., Sandhu, K., & Singh, N. (2007). Comparative study of the functional, thermal and pasting properties of flours from different field pea (Pisum sativum L.) and pigeon pea (Cajanus cajan L.) cultivars. *Food Chemistry, 104*(1), 259-267. doi:10.1016/j.foodchem.2006.11.037

Marinangeli, C., and Jones, P. (2010). Whole and fractionated yellow pea flours reduce fasting insulin and insulin resistance in hypercholesterolaemic and overweight human subjects. *British Journal Of Nutrition*, *105*(1), 110-117. doi: 10.1017/s0007114510003156

Marsh, K., Barclay, A., Colagiuri, S., & Brand-Miller, J. (2011). Glycemic index and glycemic load of carbohydrates in the diabetes diet. *Current Diabetes Reports, 11*(2), 120-127. doi:10.1007/s11892-010-0173-8

Maskus, H., Bourr´e, L., Fraser, S., Sarkar, A., & Malcolmson, L. (2016). Effects of grinding method on the compositional, physical, and functional properties of whole and split yellow pea flours. *Cereal Foods World, 61*(2), 59–64. https://doi.org/10.1094/cfw-61-2-0059

Ma, Z., Boye, J., Simpson, B., Prasher, S., Monpetit, D., & Malcolmson, L. (2011). Thermal processing effects on the functional properties and microstructure of lentil, chickpea, and pea flours. Food Research International, 44(8), 2534–2544. https://doi.org/10.1016/J.Foodres.2010.12.017

Malcolmson, L., and Han, J. (2019). Pulse Processing and Utilization of Pulse Ingredients in Foods. *Health Benefits Of Pulses*, 129-149. doi: 10.1007/978-3-030-12763-3_9

Masood, T., Shah, H., and Zeb, (2014). Effect of sprouting time on proximate composition and ascorbic acid level of mung bean (Vigna radiate L.) and chickpea (Cicer Arietinum L.) seeds. *The Journal Of Animal and Plant Sciences,*, *3*(24), 850-859.

Mccrory, M., Hamaker, B., Lovejoy, J., & Eichelsdoerfer, P. (2010). Pulse consumption,satiety, and weight management. Advances in Nutrition, 1(1), 17–30. https://doi.org/ 10.3945/An.110.1006

Mikac, U., Sepe, A., & Serˇsa, I. (2015). MR microscopy for non-invasive detection of water distribution during soaking and cooking in the common bean. *Magnetic Resonance Imaging, 33*(3), 336–345. https://doi.org/10.1016/j.mri.2014.12.001

Millar, K. A., Barry-Ryan, C., Burke, R., Hussey, K., McCarthy, S., & Gallagher, E. (2017). Effect of pulse flours on the physiochemical characteristics and sensory acceptance of baked crackers. *International Journal of Food Science & Technology, 52*(5), 1155-1163. doi:10.1111/ijfs.13388

Millar, K., Barry-Ryan, C., Burke, R., McCarthy, S., & Gallagher, E. (2019). Dough properties and baking characteristics of white bread, as affected by addition of raw, germinated and Toasted Pea Flour. *Innovative Food Science & Emerging Technologies, 56*, 102189. doi:10.1016/j.ifset.2019.102189

Miñarro, B., Albanell, E., Aguilar, N., Guamis, B., & Capellas, M. (2012). Effect of legume flours on baking characteristics of gluten-free bread. *Journal of Cereal Science, 56*(2), 476-481. doi:10.1016/j.jcs.2012.04.012

Mohsenin, N. (1970). Physical properties of plant and animal materials. New York, USA:Gordon and Breach Science Publishers.

Moraghan, J., and Grafton, K. (2001). Genetic diversity and mineral composition of common bean seed. *Journal Of The Science Of Food And Agriculture*, *81*(4), 404-408. doi: 10.1002/1097-0010(200103)81:4<404::aid-jsfa822>3.0.co;2-h

Mordor intelligence. (2020). Peas Market | Growth | Trends | Forecast. Retrieved 17 June 2020, from https://www.mordorintelligence.com/industry-reports/peas-market

Moud, A. A. (2022). Fluorescence recovery after photobleaching in colloidal science: Introduction and application. *ACS Biomaterials Science & Engineering, 8*(3), 1028-1048. doi:10.1021/acsbiomaterials.1c01422

Norton, I., Moore, S., & Fryer, P. (2007). Understanding food structuring and breakdown: Engineering approaches to obesity. *Obesity Reviews, 8*(s1), 83–88. https://doi.org/10.1111/j.1467-789x.2007.00324.x

Oliveira, B., de Moura, A., and Cunha, L. (2019). Increasing Pulse Consumption to Improve Human Health and Food Security and to Mitigate Climate Change. *Climate Change Management*, 21-35. doi: 10.1007/978-3-319-75004-0_2

Oomah, B., Blanchard, C., and Balasubramanian, P. (2008). Phytic Acid, Phytase, Minerals, and Antioxidant Activity in Canadian Dry Bean (Phaseolus vulgaris L.) Cultivars. *Journal Of Agricultural And Food Chemistry*, *56*(23), 11312-11319. doi: 10.1021/jf801661j

Oomah, B., Patras, A., Rawson, A., Singh, N., and Compos-Vega, R. (2011). Chemistry of pulses. In B. Tiwari, A. Gowen and B. McKenna, *Pulse Foods Processing, Quality and Nutraceutical Applications* (1st ed., pp. 16-25). London: Academic Press.

Paksoy, M., & Aydin, C. (2005). Determination of some physical and mechanical properties of pea (Pisum Sativum L.) seeds. *Pakistan Journal of Biological Sciences*, 9 (1), 26–29. https://doi.org/10.3923/Pjbs.2006.26.29

Paladugula, M. P., Smith, B., Morris, C. F., & Kiszonas, A. (2021). Incorporation of yellow pea flour into white pan bread. *Cereal Chemistry, 98*(5), 1020-1026. doi:10.1002/cche.10441

Pallares Pallares, A., Gwala, S., Pälchen, K., Duijsens, D., Hendrickx, M., & Grauwet, T. (2021). Pulse seeds as promising and sustainable source of ingredients with naturally bioencapsulated nutrients: Literature review and outlook. *Comprehensive Reviews in Food Science and Food Safety, 20*(2), 1524-1553. doi:10.1111/1541-4337.12692

Pallares Pallares, A., Loosveldt, B., Karimi, S. N., Hendrickx, M., & Grauwet, T. (2019). Effect of process-induced common bean hardness on structural properties of in vivo generated boluses and consequences for in vitro starch digestion kinetics. *British Journal of Nutrition, 122*(04), 388-399. doi:10.1017/s0007114519001624

Pälchen, K., Michels, D., Duijsens, D., Gwala, S., Pallares Pallares, A., Hendrickx, M., . . . Grauwet, T. (2021). *In vitro* protein and starch digestion kinetics of individual chickpea cells: From static to more complex *in vitro* digestion approaches. *Food & Function, 12*(17), 7787-7804. doi:10.1039/d1fo01123e

Parada, J., & Aguilera, J. (2007). Food microstructure affects the bioavailability of several nutrients. *Journal of Food Science, 72*(2), R21–R32. https://doi.org/10.1111/j.1750-3841.2007.00274.x

Parmar, N., Singh, N., Kaur, A., Virdi, A., & Thakur, S. (2016). Effect of canning on colour, protein and phenolic profile of grains from kidney bean, field pea and chickpea. *Food Research International,* 89, 526–532. https://doi.org/10.1016/J.Foodres.2016.07.022

Peleg, M. (1988). An empirical model for the description of moisture sorption curves. *Journal of Food Science*, 53(4), 1216–1217. https://doi.org/10.1111/J.1365-2621.1988.Tb13565.X

Pharmacopeia, U. S. (1995). Simulated gastric fluid. United States Pharmacopeial Convention, 23 pp. 2053–pp). Rockville, Maryland, USA: The National Formulary 9(U.S. Pharmacopeia Board of Trustees.

Pharmacopeia, U. S. (2000). Simulated gastric fluid. United States Pharmacopeial Convention, 24 p. 2235). Rockville, Maryland, USA: The National Formulary 9 (U.S. Pharmacopeia Board of Trustees.

Pelgrom, P., Vissers, A., Boom, R., & Schutyser, M. (2013). Dry fractionation for production of functional pea protein concentrates. *Food Research International, 53*(1),232–239. https://doi.org/10.1016/j.foodres.2013.05.004

Pietrasik, Z., and Janz, J. (2010). Utilization of pea flour, starch-rich and fiber-rich fractions in low fat bologna. *Food Research International*, *43*(2), 602-608. doi: 10.1016/j.foodres.2009.07.017

Piteira, M., Maia, J., Raymundo, A., and Sousa, I. (2006). Extensional flow behaviour of natural fibre-filled dough and its relationship with structure and properties. *Journal Of Non-Newtonian Fluid Mechanics*, *137*(1-3), 72-80. doi: 10.1016/j.jnnfm.2006.03.008

Price, C., Kiszonas, A., Smith, B., & Morris, C. (2021). Roller milling performance of dry yellow split peas: Millstream composition and functional characteristics. *Cereal Chemistry, 98*(3), 462–473. https://doi.org/10.1002/cche.10385

Pulsecanada. (2020). Environmental Sustainability | Pulse Canada. Retrieved 23 June 2020, from http://www.pulsecanada.com/food-industry/pulse-benefits/sustainability/

Ramdath, D., Liu, Q., Donner, E., Hawke, A., Kalinga, D., Winberg, J., & Wolever, T. (2017). Investigating the relationship between lentil carbohydrate fractions and in vivo postprandial blood glucose response by use of the natural variation in starch fractions among 20 lentil varieties. *Food & Function, 8*(10), 3783–3791. https://doi.org/10.1039/c7fo00972k

Raza, H., Ameer, K., Zaaboul, F., Sharif, H., Ali, B., Shoaib, M., . . . Zhang, L. (2019). Effects of ball-milling on physicochemical, thermal and functional properties of extruded chickpea (Cicer arietinum L.) powder. *CyTA - Journal of Food, 17*(1), 563-573. doi:10.1080/19476337.2019.1617352

Ray, H., Bett, K., Tar'an, B., Vandenberg, A., Thavarajah, D., and Warkentin, T. (2014). Mineral Micronutrient Content of Cultivars of Field Pea, Chickpea, Common Bean, and Lentil Grown in Saskatchewan, Canada. *Crop Science*, *54*(4), 1698-1708. doi: 10.2135/cropsci2013.08.0568

Raigar, R., Prabhakar, P., & Srivastav, P. (2016). Effect of different thermal treatments on grinding characteristics, granular morphology, and yield of ready-to-eat wheat grits. *Journal of Food Process Engineering*, 40(2), E12363. https://doi.org/10.1111/Jfpe.12363

Rawal, V., & Navarro, D. (2019). The global economy of pulses (1st ed., p. 190). Rome,Italy: FAO. https://doi.org/10.4060/I7108EN

Rehman, Z., & Shah, W. (2005). Thermal heat processing effects on antinutrients, protein and starch digestibility of food legumes. *Food Chemistry*, 91(2), 327–331. https://doi.org/10.1016/J.Foodchem.2004.06.019

Resio, A., Aguerre, R., & Suarez, C. (2006). Hydration kinetics of amaranth grain. *Journal of Food Engineering*, 72(3), 247–253. https://doi.org/10.1016/JJfoodeng.2004.12.003

Robinson, G. H., Balk, J., & Domoney, C. (2019). Improving pulse crops as a source of protein, starch and micronutrients. *Nutrition Bulletin, 44*(3), 202-215. doi:10.1111/nbu.12399

Roe, M., Pinchen, H., Church, S., & Finglas, P. (2015). Mccance and Widdowson's the composition of foods seventh summary edition and updated composition of foods integrated dataset. Nutrition Bulletin, 40(1), 36–39. https://doi.org/10.1111/ Nbu.12124

Romano, A., Giosafatto, C., Al-Asmar, A., Masi, P., Aponte, M., & Mariniello, L. (2018). Grass pea (Lathyrus sativus) flour: Microstructure, physico-chemical properties and in vitro digestion. *European Food Research and Technology, 245*(1), 191-198. doi:10.1007/s00217-018-3152-y

Rondeau-Mouro, C., Defer, D., Leboeuf, E., & Lahaye, M. (2008). Assessment of cell wall porosity in Arabidopsis thaliana by NMR spectroscopy. *International Journal of Biological Macromolecules, 42*(2), 83-92. doi:10.1016/j.ijbiomac.2007.09.020

Rosell, C. (2011). The science of doughs and bread quality. In 2362589298 1608564890 V. R. Preedy, 2362589299 1608564890 R. R. Watson, & 2362589300 1608564890 V. B. Patel (Authors), *Flour and breads and their fortification in health and disease prevention* (pp. 3-14). London, UK: Elsevier/Academic Press.

Rosell, C. M., Bajerska, J., & F., E. S. (2016). *Bread and its fortification: Nutrition and Health Benefits*. Boca Raton, FL, Florida: CRC Press/Taylor & Francis Group.

Rosell, C., Santos, E., and Collar, C. (2005). Mixing properties of fibre-enriched wheat bread doughs: A response surface methodology study. *European Food Research And Technology*, *223*(3), 333-340. doi: 10.1007/s00217-005-0208-6

Rovalino-Córdova, A. M., Fogliano, V., & Capuano, E. (2018). A closer look to cell structural barriers affecting starch digestibility in beans. *Carbohydrate Polymers, 181*, 994-1002. doi:10.1016/j.carbpol.2017.11.050

Rovalino-Córdova, A. M., Fogliano, V., & Capuano, E. (2019). The effect of cell wall encapsulation on macronutrients digestion: A case study in kidney beans. *Food Chemistry, 286*, 557-566. doi:10.1016/j.foodchem.2019.02.057

Sadowska, J., Błaszczak, W., Fornal, J., Vidal-Valverde, C., & Frias, J. (2003). Changes of wheat dough and bread quality and structure as a result of germinated pea flour addition. *European Food Research and Technology, 216*(1), 46-50. doi:10.1007/s00217-002-0617-8

Saha, S., Singh, G., Mahajan, V., & Gupta, H. (2009). Variability of nutritional and cooking quality in bean (*Phaseolus vulgaris L*) as a function of genotype. *Plant Foods for Human Nutrition*, 64(2), 174–180. https://doi.org/10.1007/S11130-009-0121-4

Sahin, S., & Sumnu, S. (2011). Physical properties of foods (pp. 1–2). New York: Springer.

Scafaro, A., Von Caemmerer, S., Evans, J., & Atwell, B. (2011). Temperature response of mesophyll conductance in cultivated and wild Oryza species with contrasting mesophyll cell wall thickness. *Plant, Cell and Environment*, 34(11), 1999–2008. https://doi.org/10.1111/J.1365-3040.2011.02398.X

Sen Gupta, D., Thavarajah, D., Knutson, P., Thavarajah, P., McGee, R., Coyne, C., and Kumar, S. (2013). Lentils (Lens culinaris L.), a Rich Source of Folates. *Journal Of Agricultural And Food Chemistry*, *61*(32), 7794-7799. doi: 10.1021/jf401891p

Schwanz Goebel, J. T., Kaur, L., Colussi, R., Elias, M. C., & Singh, J. (2019). Microstructure of indica and japonica rice influences their starch digestibility: A study using a human digestion simulator. *Food Hydrocolloids, 94*, 191-198. doi:10.1016/j.foodhyd.2019.02.038

Shakerardekani, A., Karim, R., Vaseli, N., Vaseli, N., Karim, R., & Shakerardekani, A. (2012). The effect of processing variables on the quality and acceptability of pistachio milk. *Journal*

of Food Processing and Preservation, 37(5), 541-545. doi:10.1111/j.1745-4549.2012.00676.x

Shapter, F., Henry, R., & Lee, L. (2008). Endosperm and starch granule morphology in wild cereal relatives. *Plant Genetic Resources: Characterization and Utilization*, 6(2),85–97. https://doi.org/10.1017/S1479262108986512

Sharma, P., Chakkaravarthi, A., Singh, V., & Subramanian, R. (2008). Grinding characteristics and batter quality of rice in different wet grinding systems. *Journal of Food Engineering, 88*(4), 499-506. doi:10.1016/j.jfoodeng.2008.03.009

Shevkani, K., Kaur, M., & Singh, N. (2021). Composition, pasting, functional, and microstructural properties of flours from different split dehulled pulses (Dhals). *Journal of Food Processing and Preservation,* 45(6). https://doi.org/10.1111/Jfpp.15485

Shi, L., Fu, X., Tan, C., Huang, Q., & Zhang, B. (2017). Encapsulation of Ethylene Gas into Granular Cold-Water-Soluble Starch: Structure and Release Kinetics. *Journal of Agricultural and Food Chemistry, 65*(10), 2189-2197. doi:10.1021/acs.jafc.6b05749

Simonato, B., Curioni, A., and Pasini, G. (2015). Digestibility of pasta made with three wheat types: A preliminary study. *Food Chemistry*, *174*, 219-225. doi: 10.1016/j.foodchem.2014.11.023

Singhal, P., Kaushik, G., & Mathur, P. (2013). Antidiabetic potential of commonly consumed legumes: A review. *Critical Reviews in Food Science and Nutrition*, 54(5), 655–672. https://doi.org/10.1080/10408398.2011.604141

Singh, J., Dartois, A., & Kaur, L. (2010). Starch digestibility in food matrix: A review. *Trends in Food Science & Technology*, 21(4), 168–180. https://doi.org/10.1016/J.Tifs.2009.12.001

Singh, B., Singh, J., Kaur, A., & Singh, N. (2017). Phenolic composition and antioxidant potential of grain legume seeds: A review. *Food Research International*, 101, 1–16. https://doi.org/10.1016/J.Foodres.2017.09.026

Singh, N. (2017). Pulses: An overview. *Journal of Food Science & Technology, 54*(4), 853–857. https://doi.org/10.1007/s13197-017-2537-4

Smith, B., Bean, S., Herald, T., & Aramouni, F. (2012). Effect of HPMC on the quality of wheat-free bread made from carob germ flour-starch mixtures. *Journal of Food Science, 77*(6). doi:10.1111/j.1750-3841.2012.02739.x

Sotome, I., Oshita, S., Kawagoe, Y., Torii, T., & Seo, Y. (2004). Measurement of membrane hydraulic conductivity by a newly developed method. *Transactions of the ASAE, 47*(4), 1207-1213. doi:10.13031/2013.16553

Souza, F., & Marcos-Filho, J. (2001). The seed coat as a modulator of seed-environment relationships in Fabaceae. *Revista Brasileira De Botanica, ˆ 24*(4), 365–375. https://doi.org/10.1590/s0100-84042001000400002

Sreerama, Y., Sashikala, V., Pratape, V., and Singh, V. (2012). Nutrients and antinutrients in cowpea and horse gram flours in comparison to chickpea flour: Evaluation of their flour functionality. *Food Chemistry*, *131*(2), 462-468. doi: 10.1016/j.foodchem.2011.09.008

Sun, L., & Miao, M. (2019). Dietary polyphenols modulate starch digestion and glycaemic level: A review. *Critical Reviews in Food Science and Nutrition, 60*(4), 541–555. https://doi.org/10.1080/10408398.2018.1544883

Sutivisedsak, N., Moser, B., Sharma, B., Evangelista, R., Cheng, H., and Lesch, W. et al. (2010). Physical Properties and Fatty Acid Profiles of Oils from Black, Kidney, Great Northern, and Pinto Beans. *Journal Of The American Oil Chemists' Society*, *88*(2), 193-200. doi: 10.1007/s11746-010-1669-8

Stejskal, E. O., & Tanner, J. E. (1965). Spin diffusion measurements: Spin echoes in the presence of a time-dependent field gradient. *The Journal of Chemical Physics, 42*(1), 288-292. doi:10.1063/1.1695690

Snyder, C., Bruulsema, T., Jensen, T., and Fixen, P. (2009). Review of greenhouse gas emissions from crop production systems and fertilizer management effects. *Agriculture, Ecosystems and Environment*, *133*(3-4), 247-266. doi: 10.1016/j.agee.2009.04.021

Szczebyło, A., Halicka, E., Jackowska, M., & Rejman, K. (2019). Analysis of the global pulses market and programs encouraging consumption of this food. *Zeszyty Naukowe Sggw W Warszawie - Problemy Rolnictwa Swiatowego*, ´ 19(3), 85–96. https://doi.org/10.22630/Prs.2019.19.3.49, 34.

Thakur, S., Scanlon, M., Tyler, R., Milani, A., & Paliwal, J. (2019). Pulse Flour Characteristics from a Wheat Flour Miller's Perspective: A Comprehensive Review. *Comprehensive Reviews in Food Science and Food Safety, 18*(3), 775-797. doi:10.1111/1541-4337.12413

Thavarajah, D., Mcswain, M., Johnson, C., Kumar, S., & Thavarajah, P. (2019). Pulses, global health, and sustainability: *Future trends. Health Benefits of Pulses*, 1–17. https://doi.org/10.1007/978-3-030-12763-3_1

Thorne, M., Thompson, L., and Jenkins, D. (1983). Factors affecting starch digestibility and the glycemic response with special reference to legumes. *The American Journal Of Clinical Nutrition*, *38*(3), 481-488. doi: 10.1093/ajcn/38.3.481

Tiwari, B., & Singh, N. (2012). *Pulse chemistry and technology*. Cambridge, United Kingdom: Royal Society of Chemistry

Tiwari, B., Tiwari, U., Jagan Mohan, R., & Alagusundaram, K. (2008). Effect of various pre-treatments on functional, physiochemical, and cooking properties of pigeon pea (Cajanus cajan L). *Food Science and Technology International*, 14(6), 487–495. https://doi.org/10.1177/1082013208101023

Tongwane, M., Mdlambuzi, T., Moeletsi, M., Tsubo, M., Mliswa, V., and Grootboom, L. (2016). Greenhouse gas emissions from different crop production and management practices in South Africa. *Environmental Development*, *19*, 23-35. doi: 10.1016/j.envdev.2016.06.004

Tosh, S., and Yada, S. (2010). Dietary fibres in pulse seeds and fractions: Characterization, functional attributes, and applications. *Food Research International*, *43*(2), 450-460. doi: 10.1016/j.foodres.2009.09.005

Tudorică, C., Kuri, V., and Brennan, C. (2002). Nutritional and Physico-chemical Characteristics of Dietary Fiber Enriched Pasta. *Journal Of Agricultural And Food Chemistry*, *50*(2), 347-356. doi: 10.1021/jf0106953

Tulbek, M., Lam, R., Wang, Y., Asavajaruand, P., and Lam, A. (2017). *Pea: A Sustainable Vegetable Protein Crop* (pp. 145-164). London: Academic press.

Turhan, M., Sayar, S., & Gunasekaran, S. (2002). Application of the Peleg model to study water absorption in chickpea during soaking. *Journal of Food Engineering*, 53(2), 153–159. https://doi.org/10.1016/S0260-8774(01)00152-2

Tzitzikas, E., Vincken, J., de Groot, J., Gruppen, H., & Visser, R. (2006). Genetic Variation in Pea Seed Globulin Composition. *Journal Of Agricultural And Food Chemistry,* 54(2), 425–433. https://doi.org/10.1021/jf0519008

Tóth, M., Kaszab, T., & Meretei, A. (2022). Texture profile analysis and sensory evaluation of commercially available gluten-free bread samples. *European Food Research and Technology, 248*(6), 1447-1455. doi:10.1007/s00217-021-03944-2

Vishwanathan, K., Singh, V., & Subramanian, R. (2011). Wet grinding characteristics of soybean for soymilk extraction. *Journal of Food Engineering, 106*(1), 28-34. doi:10.1016/j.jfoodeng.2011.04.002

Voda, A., Homan, N., Witek, M., Duijster, A., Van Dalen, G., Van der Sman, R., . . . Van Duynhoven, J. (2012). The impact of freeze-drying on microstructure and rehydration properties of carrot. *Food Research International, 49*(2), 687-693. doi:10.1016/j.foodres.2012.08.019

Voragen, A. G., Coenen, G., Verhoef, R. P., & Schols, H. A. (2009). Pectin, a versatile polysaccharide present in plant cell walls. *Structural Chemistry, 20*(2), 263-275. doi:10.1007/s11224-009-9442-z

Wang, N., and Daun, J. (2004). Effect of variety and crude protein content on nutrients and certain antinutrients in field peas(Pisum sativum). *Journal Of The Science Of Food And Agriculture*, *84*(9), 1021-1029. doi: 10.1002/jsfa.1742

Wang, N., and Daun, J. (2006). Effects of variety and crude protein content on nutrients and anti-nutrients in lentils (). *Food Chemistry*, *95*(3), 493-502. doi: 10.1016/j.foodchem.2005.02.001

Wang, N., Hatcher, D., Tyler, R., Toews, R., and Gawalko, E. (2010). Effect of cooking on the composition of beans (Phaseolus vulgaris L.) and chickpeas (Cicer arietinum L.). *Food Research International*, *43*(2), 589-594. doi: 10.1016/j.foodres.2009.07.012

Wang, M., Wichienchot, S., He, X., Fu, X., Huang, Q., & Zhang, B. (2019). In vitro colonic fermentation of dietary fibers: Fermentation rate, short-chain fatty acid production and changes in microbiota. *Trends in Food Science & Technology, 88*, 1-9. doi:10.1016/j.tifs.2019.03.005

Wani, I., Sogi, D., Hamdani, A., Gani, A., Bhat, N., & Shah, A. (2016). Isolation,composition, and physicochemical properties of starch from legumes: A review. Starch - Starke, ¨ 68(9–10), 834–845. https://doi.org/10.1002/Star.201600007

Wani, I., Sogi, D., Wani, A., Gill, B., & Shivhare, U. (2010). Physico-chemical properties of starches from Indian kidney bean (Phaseolus Vulgaris) cultivars. International Journal of Food Science and Technology, 45(10), 2176–2185. https://doi.org/10.1111/J.1365-2621.2010.02379.X

Watanabe, H., & Fukuoka, M. (1992). Measurement of moisture diffusion in foods using pulsed field gradient NMR. *Trends in Food Science & Technology, 3*, 211-215. doi:10.1016/0924-2244(92)90193-z

Watanabe, H., Fukuoka, M., & Shimada, S. (1994). Measurement of moisture diffusion in a soybean seed by pulsed-field-gradient NMR method. *Developments in Food Engineering,* 236-238. doi:10.1007/978-1-4615-2674-2_71

Wolever, T., Jenkins, D., Jenkins, A., and Josse, R. (1991). The glycemic index: methodology and clinical implications. *The American Journal Of Clinical Nutrition*, *54*(5), 846-854. doi: 10.1093/ajcn/54.5.846

Wood, J., Knights, E., & Choct, M. (2011). Morphology of chickpea seeds (cicer arietinumL.): Comparison of desi and kabuli types. *International Journal of Plant Sciences, 172*(5), 632–643. https://doi.org/10.1086/659456

Wood, J., & Malcolmson, L. (2011). Pulse milling technologies. In B. Tiwari, A. Gowen, & B. Mckenna (Eds.), *Pulse Foods: Processing, quality and nutraceutical applications* (1st ed., pp. 193–222). London, UK: Academic Press.

Xu, Y., Thomas, M., and Bhardwaj, H. (2013). Chemical composition, functional properties and microstructural characteristics of three kabuli chickpea (Cicer arietinumL.)as affected by different cooking methods. *International Journal Of Food Science and Technology*, *49*(4), 1215-1223. doi: 10.1111/ijfs.12419

Xiong, W., Zhang, B., Dhital, S., Huang, Q., & Fu, X. (2019). Structural features and starch digestion properties of intact pulse cotyledon cells modified by heat-moisture treatment. *Journal of Functional Foods, 61*, 103500. doi:10.1016/j.jff.2019.103500

Xiong, W., Zhang, B., Huang, Q., Li, C., Pletsch, E., & Fu, X. (2018). Variation in the rate and extent of starch digestion is not determined by the starch structural features of cooked whole pulses. *Food Hydrocolloids, 83*, 340–347. https://doi.org/10.1016/j.foodhyd.2018.05.022

Xu, M., Jin, Z., Simsek, S., Hall, C., Rao, J., & Chen, B. (2019). Effect of germination on the chemical composition, thermal, pasting, and moisture sorption properties of flours from chickpea, lentil, and yellow pea. *Food Chemistry, 295*, 579-587. doi:10.1016/j.foodchem.2019.05.167

Yalçin, I., Ozarslan, ¨ C., & Akbas¸, T. (2007). Physical properties of pea (Pisum sativum) seed. *Journal of Food Engineering,* 79(2), 731–735. https://doi.org/10.1016/J.Jfoodeng.2006.02.039

Yousif, A., Kato, J., & Deeth, H. (2007). Effect of storage on the biochemical structure and processing quality of adzuki bean (vigna angularis). *Food Reviews International, 23*(1), 1–33. https://doi.org/10.1080/87559120600865172

Yu, Y., Wang, L., Qian, H., Zhang, H., & Qi, X. (2018). Contribution of spontaneously-fermented sourdoughs with pear and navel orange for the bread-making. *LWT, 89*, 336-343. doi:10.1016/j.lwt.2017.11.001

Zare, F., Orsat, V., and Boye, J. (2015). Functional, Physical and Sensory Properties of Pulse Ingredients Incorporated into Orange and Apple Juice Beverages. *Journal Of Food Research*, *4*(5), 143. doi: 10.5539/jfr.v4n5p143

Zentner, R., Lafond, G., Derksen, D., Nagy, C., Wall, D., and May, W. (2004). Effects of tillage method and crop rotation on non-renewable energy use efficiency for a thin Black Chernozem in the Canadian Prairies. *Soil And Tillage Research*, *77*(2), 125-136. doi: 10.1016/j.still.2003.11.002

Zhang, B., Wang, K., Hasjim, J., Li, E., Flanagan, B., Gidley, M., & Dhital, S. (2014). Freeze-Drying Changes the Structure and Digestibility of B-Polymorphic Starches. *Journal of Agricultural and Food Chemistry, 62*(7), 1482-1491. doi:10.1021/jf405196m

Zhang, L., & Mccarthy, M. (2013). Nmr study of hydration of navy bean during cooking. LWT - Food Science and Technology, 53(2), 402–408. https://doi.org/10.1016/J.Lwt.2013.03.011

Zhao, X., Du, F., Zhu, Q., Qiu, D., Yin, W., & Ao, Q. (2010). Effect of superfine pulverization on properties of Astragalus membranaceus powder. *Powder Technology, 203*(3), 620-625. doi:10.1016/j.powtec.2010.06.029

Zhao, X., Yang, Z., Gai, G., & Yang, Y. (2009). Effect of superfine grinding on properties of ginger powder. *Journal of Food Engineering, 91*(2), 217-222. doi:10.1016/j.jfoodeng.2008.08.024

Zucco, F., Borsuk, Y., and Arntfield, S. (2011). Physical and nutritional evaluation of wheat cookies supplemented with pulse flours of different particle sizes. *LWT - Food Science And Technology*, *44*(10), 2070-2076. doi: 10.1016/j.lwt.2011.06.007

Appendix

Diffusion data fits for the cotyledon cells sample supporting chapter 5.

Diffusion data fits for Abayomi's samples. Data was recorded over the period 5 – 8 July on the 500 MHz spectrometer at 298 K. Little delta was constant at 1.5 ms and Big delta was varied between 30 ms and 1250 ms. Data was fitted to a single component. Some of the longer big delta datasets show a systematic error in the fits – possibly indicating another component. However, overall, the fits don't look too bad.

Sample 1RPT (Sample 1 was originally recorded at 293 K, not 298 K, since the VT was switched off: 1RPT is at 298 K). Recorded 5/7/22

1: D 30 ms

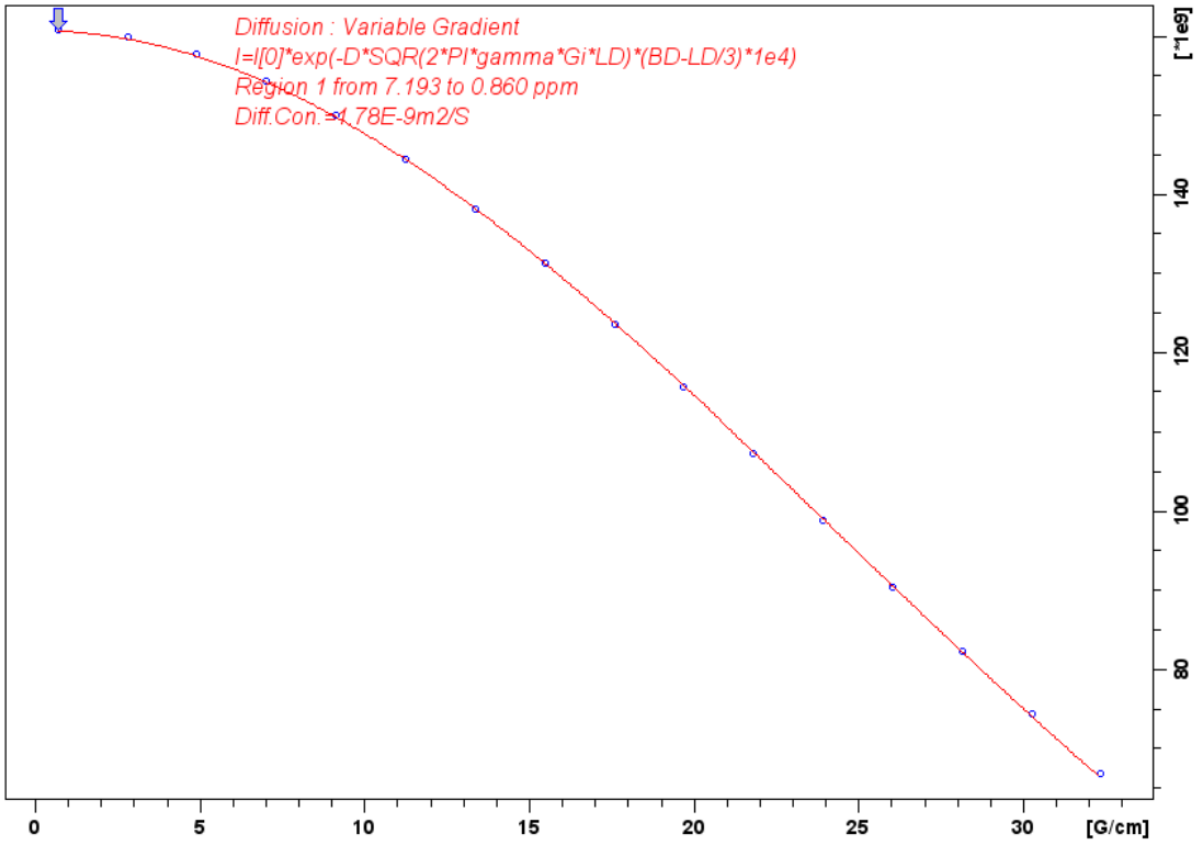

1RPT: D 40 ms

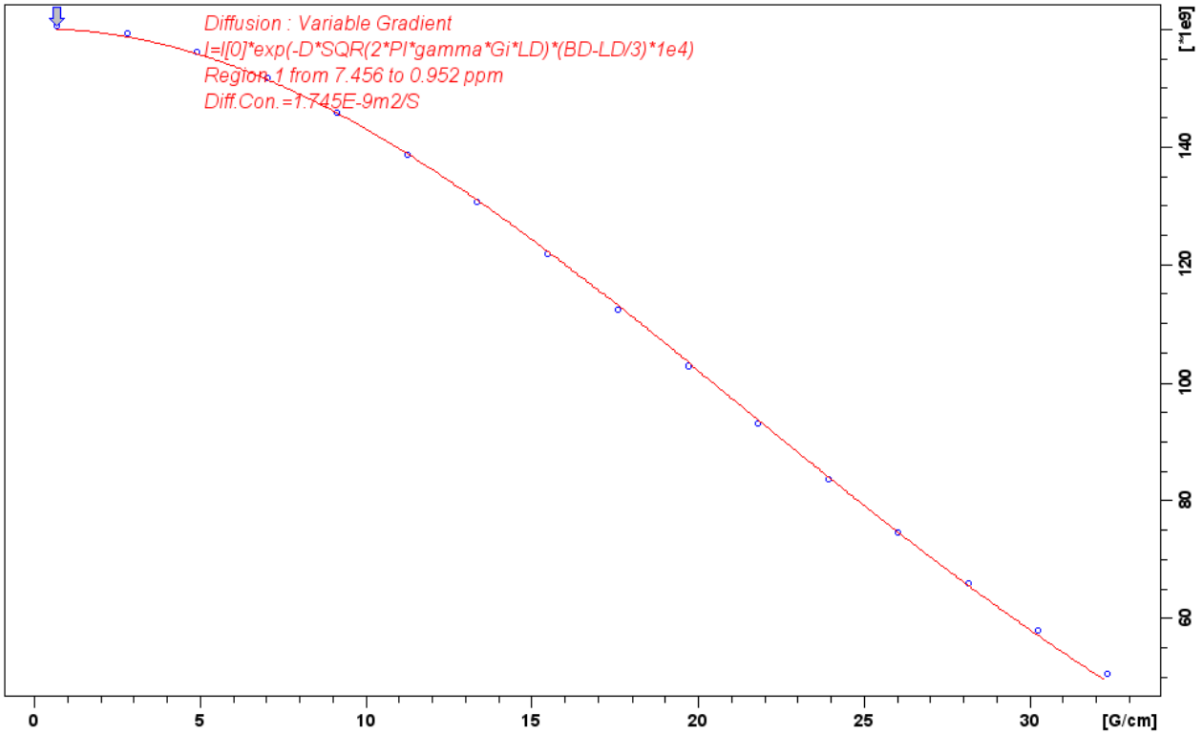

1RPT: D 50 ms

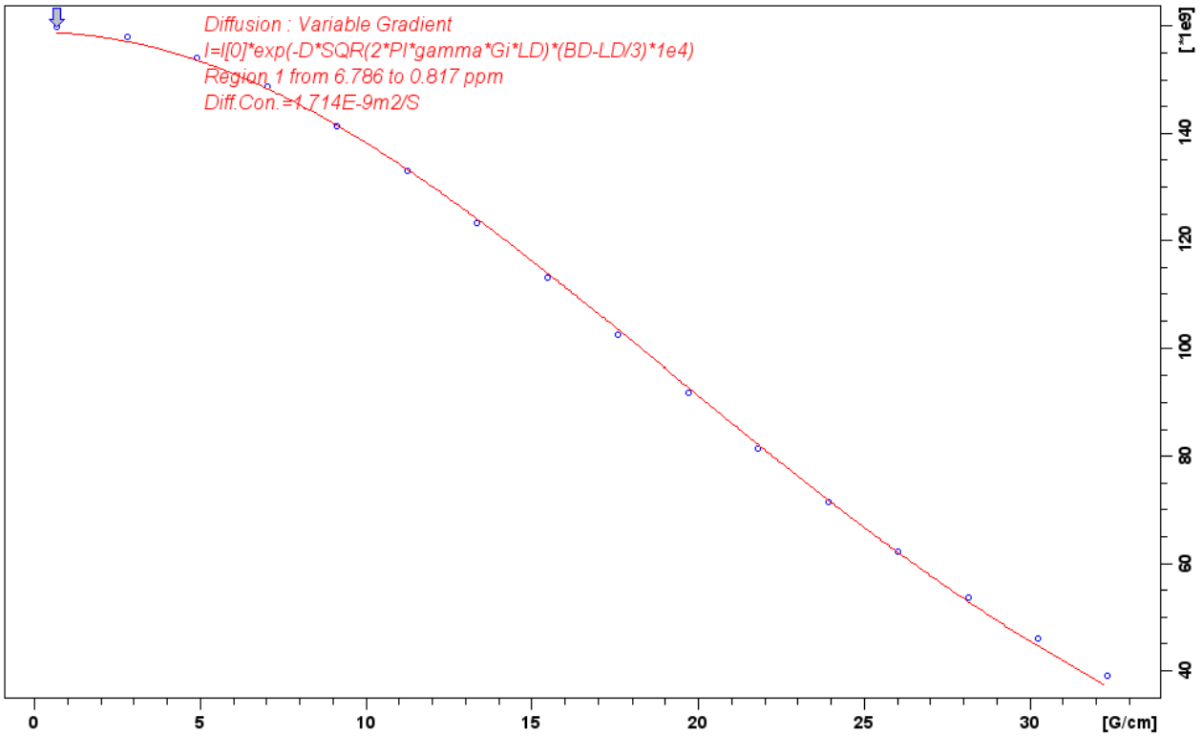

1RPT: D 60 ms

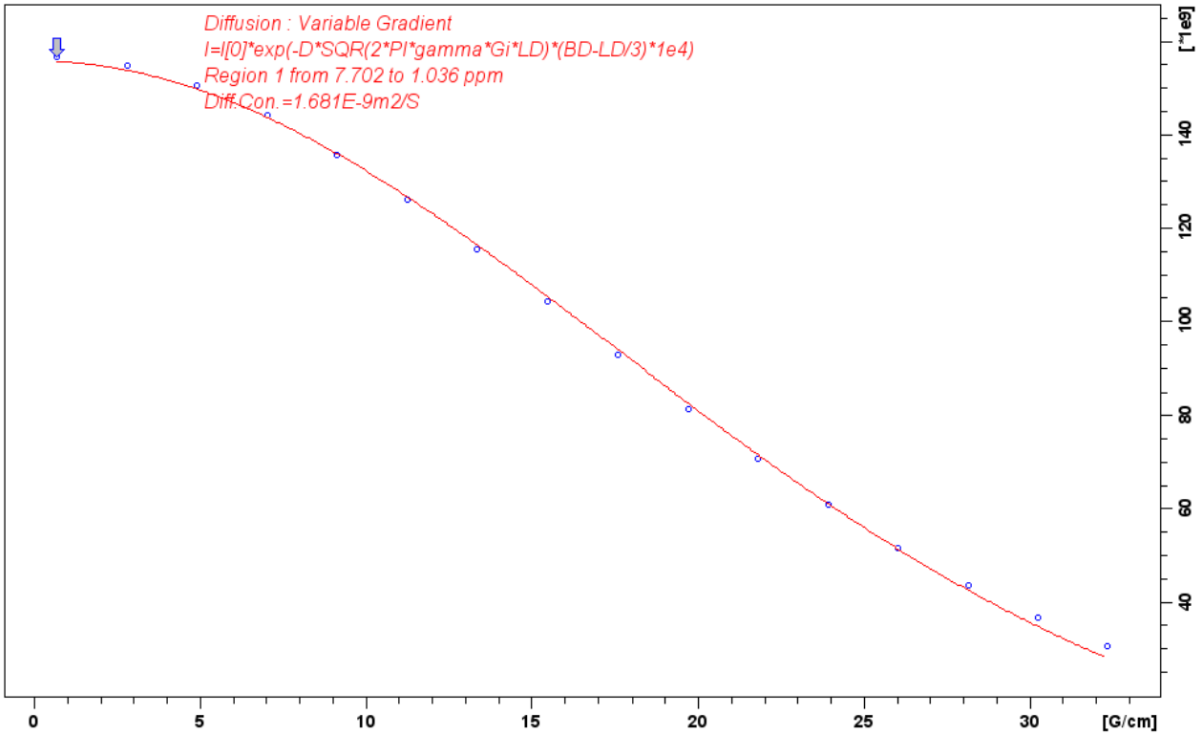

1RPT: D 80 ms

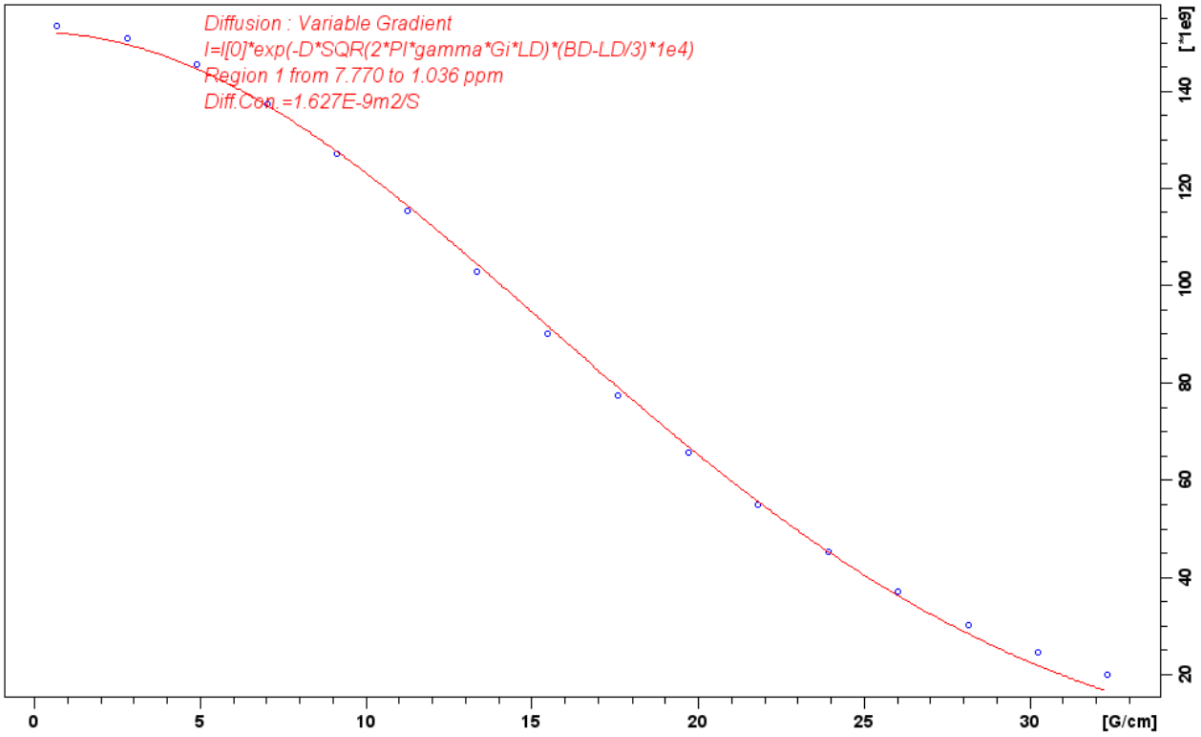

1RPT D 100 ms

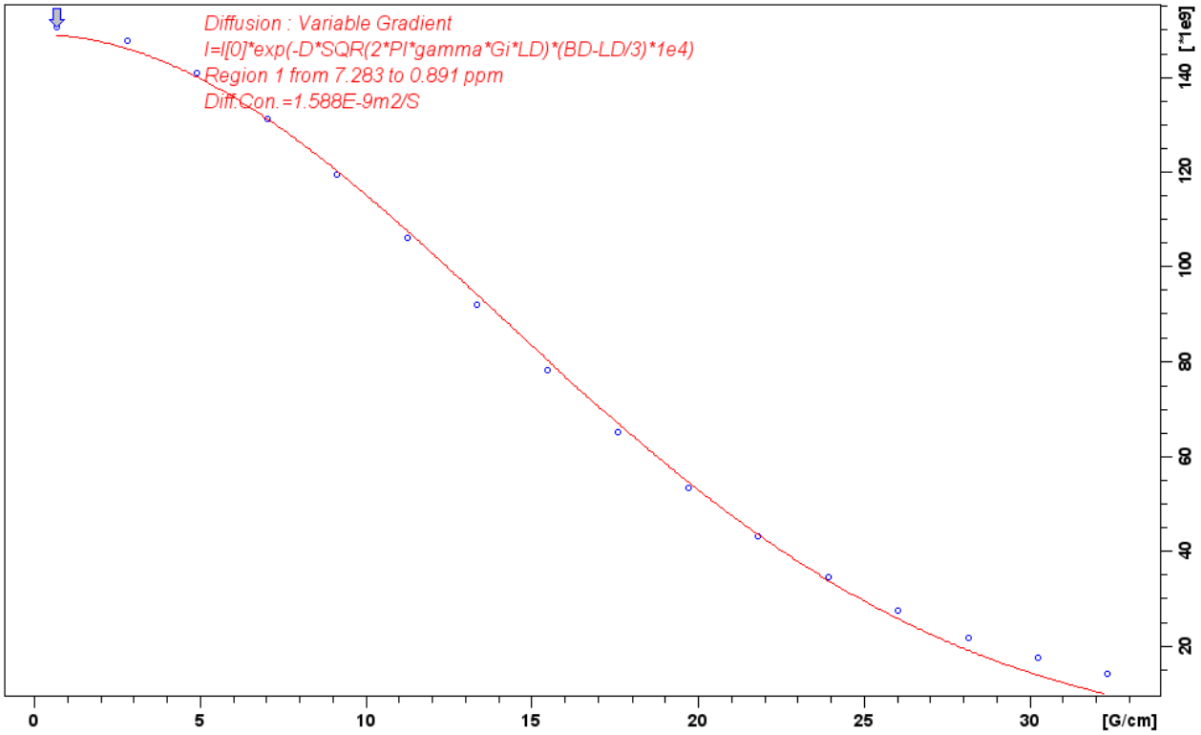

1RPT: D 250 ms

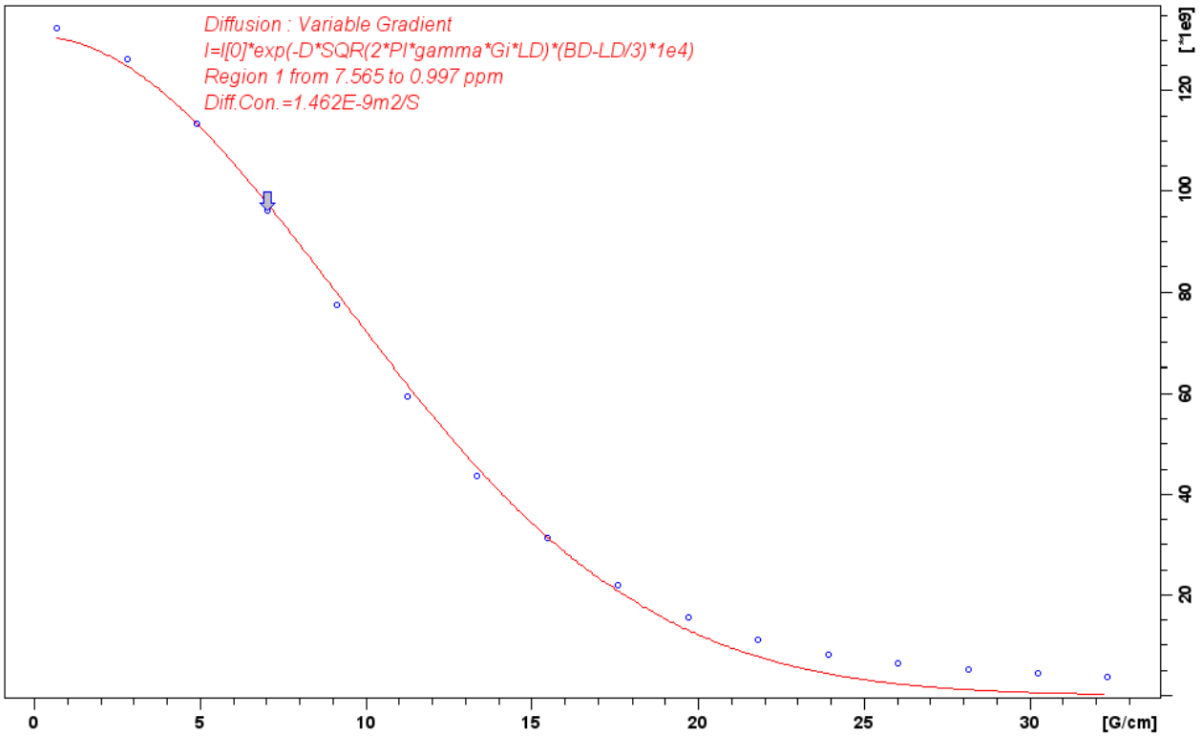

1RPT: D 500 ms

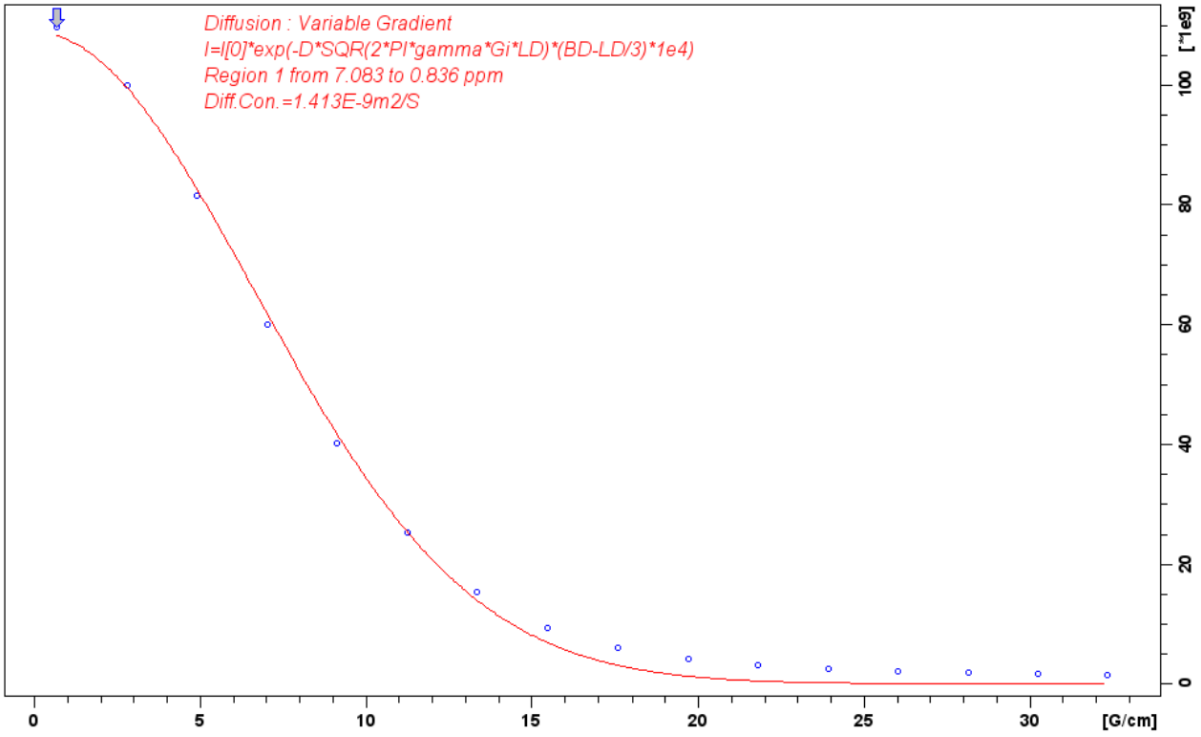

1RPT: D 750 ms

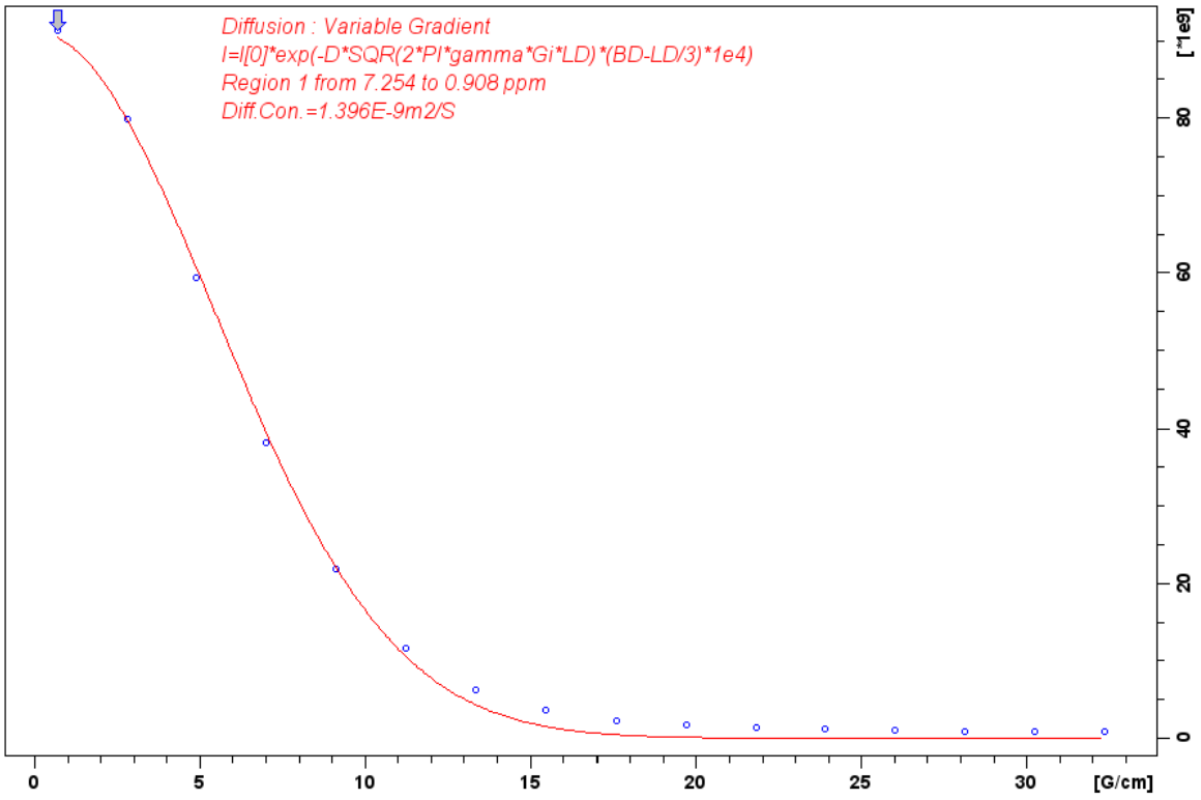

1RPT: D 1000 ms

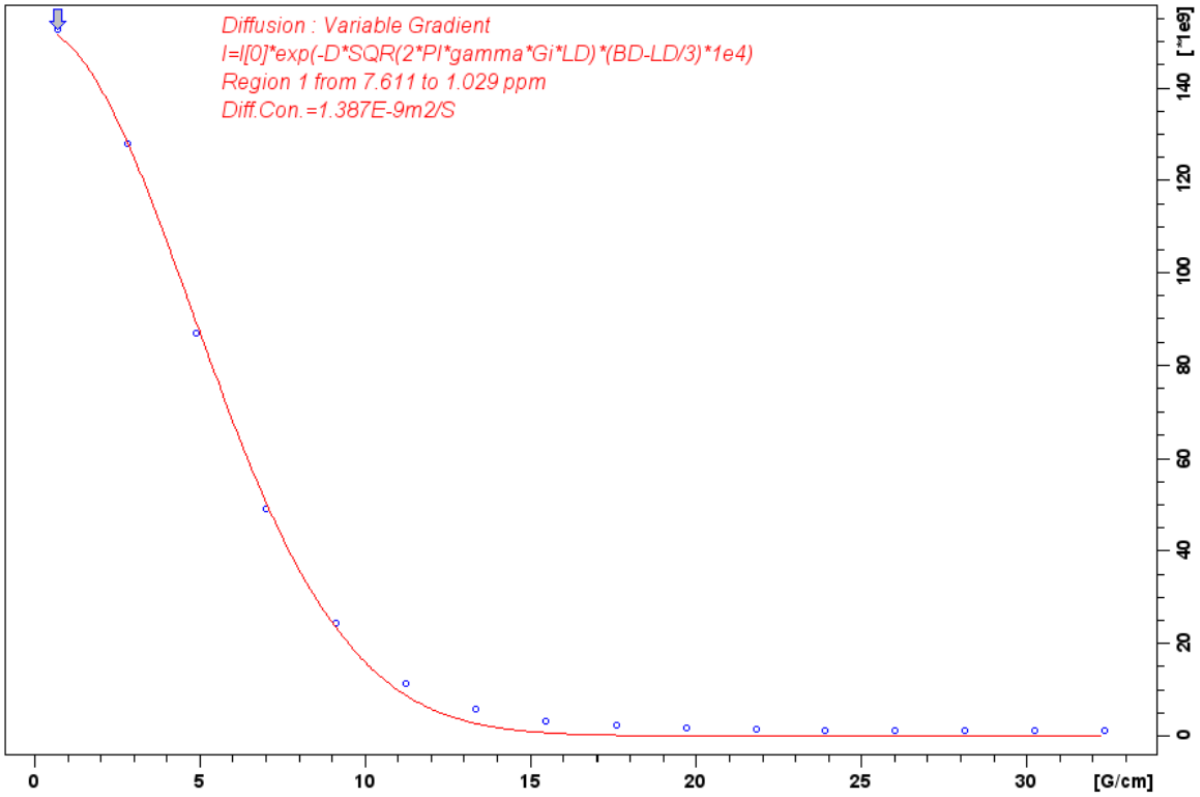

1RPT; D 1250 ms

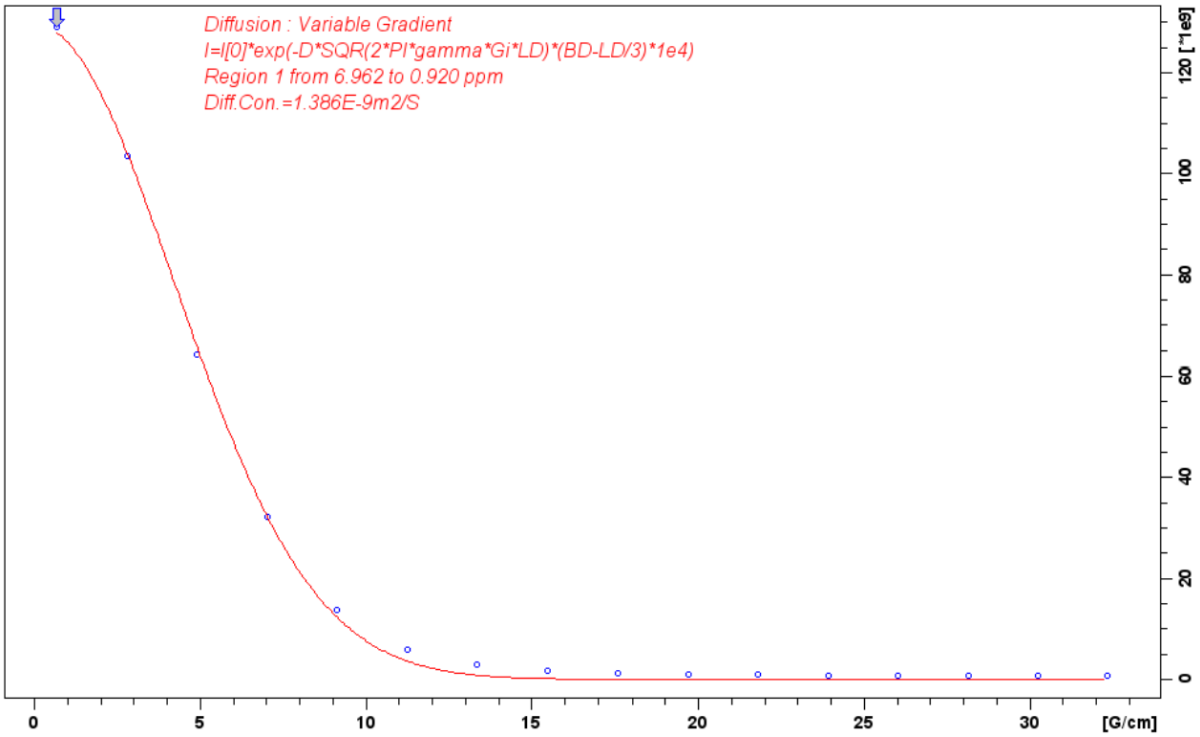

Sample 2 Recorded 6/7/22

2: D 30 ms

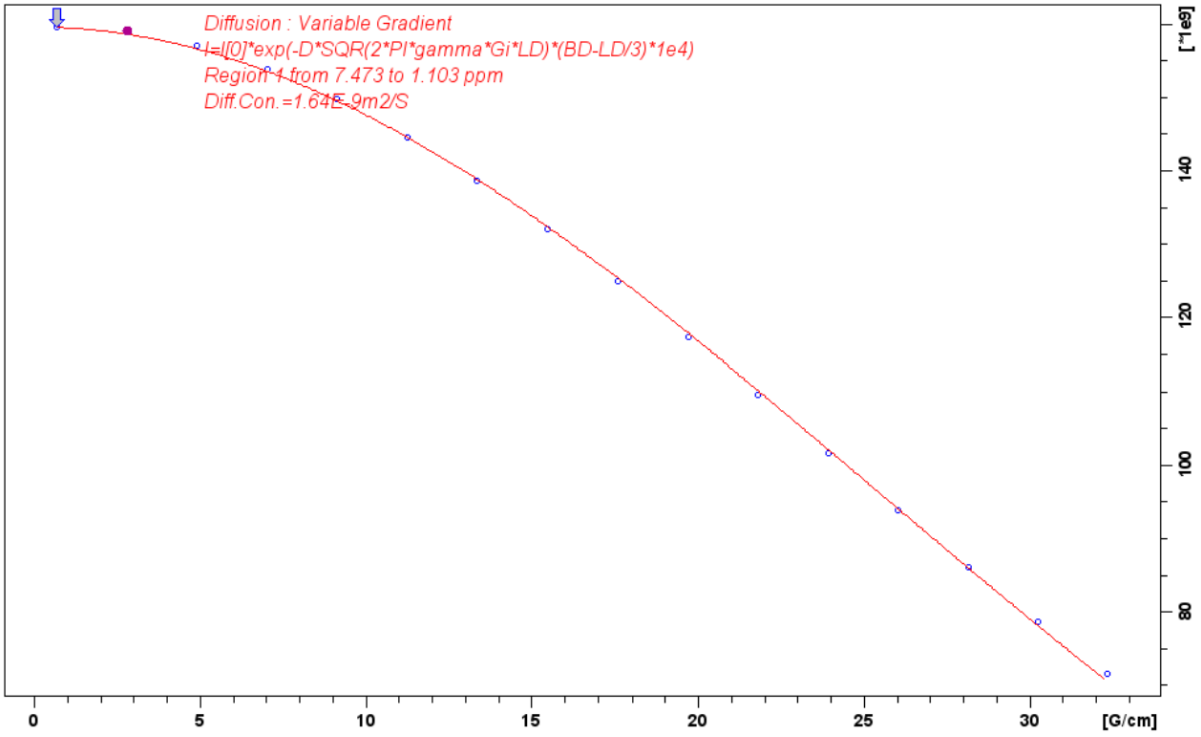

2: D 40 ms

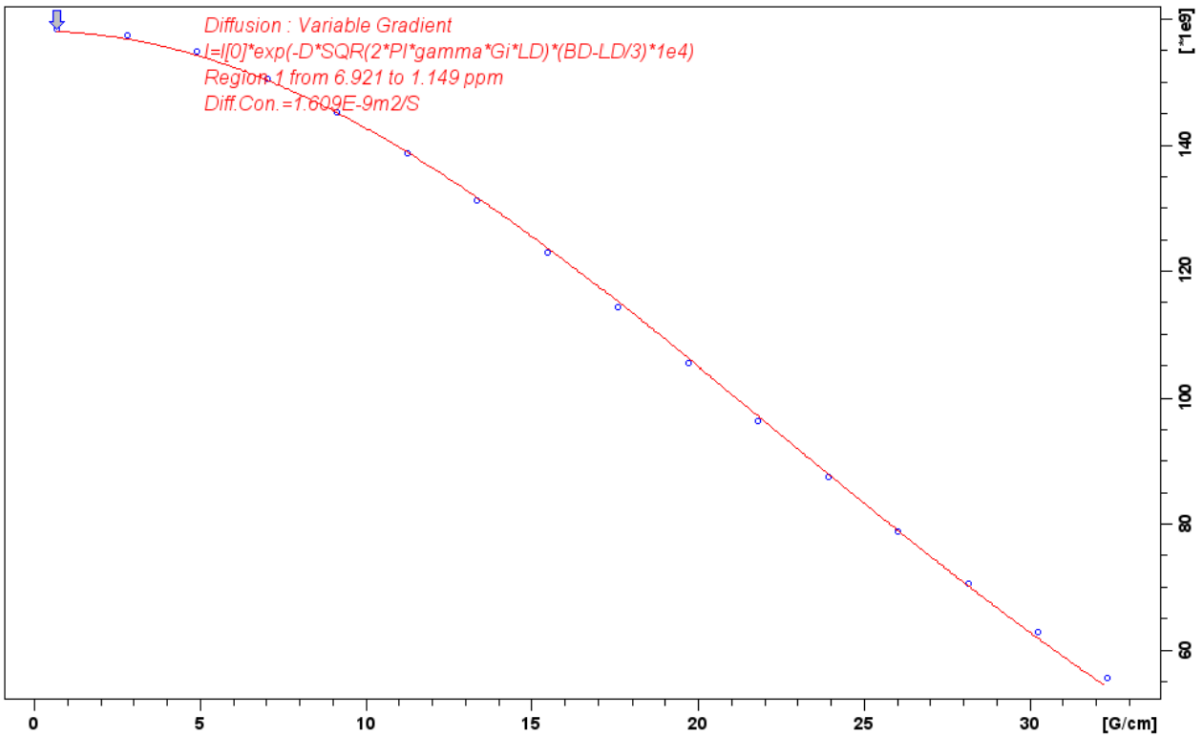

2: 50 ms

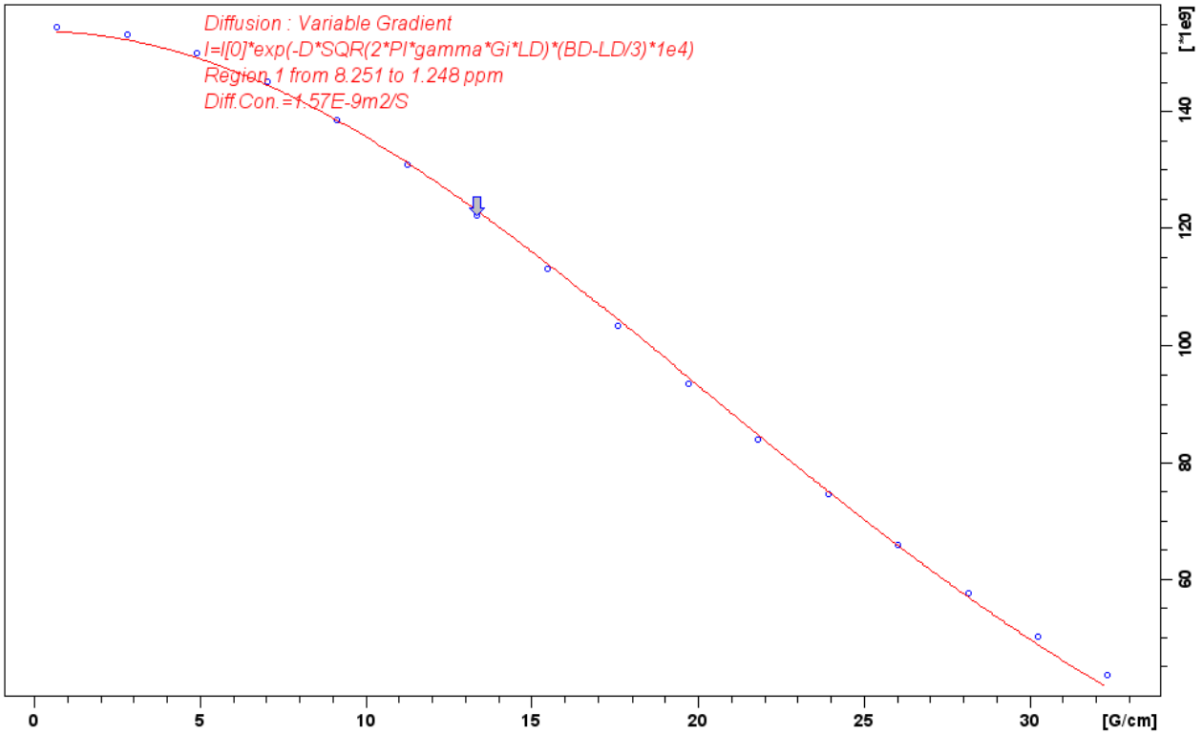
Diffusion : Variable Gradient
I=I[0]*exp(-D*SQR(2*PI*gamma*Gi*LD)*(BD-LD/3)*1e4)
Region 1 from 8.251 to 1.248 ppm
Diff.Con.=1.57E-9m2/S
[*1e9]
140
120
100
80
60
0
5
10
15
20
25
30
[G/cm]

2: 60 m

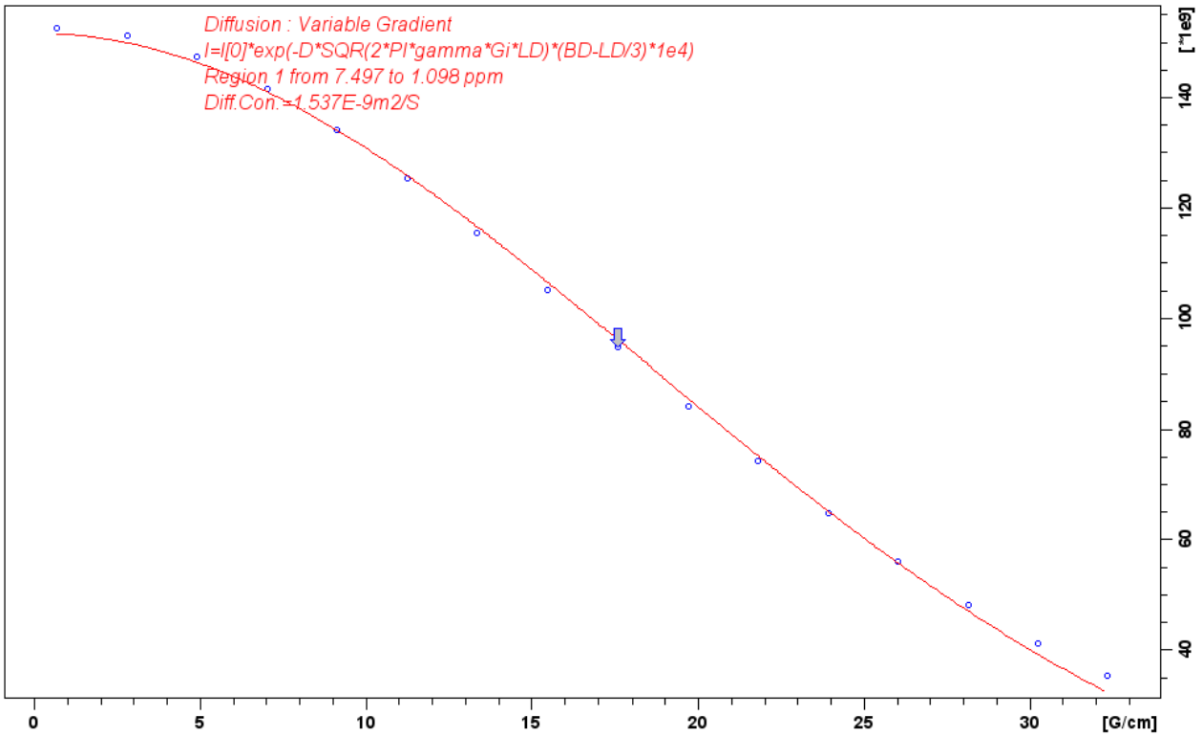
Diffusion : Variable Gradient
I=I[0]*exp(-D*SQR(2*PI*gamma*Gi*LD)*(BD-LD/3)*1e4)
Region 1 from 7.497 to 1.098 ppm
Diff.Con.=1.537E-9m2/S
[*1e9]
140
120
100
80
60
40
0
5
10
15
20
25
30
[G/cm]

2: 80 m

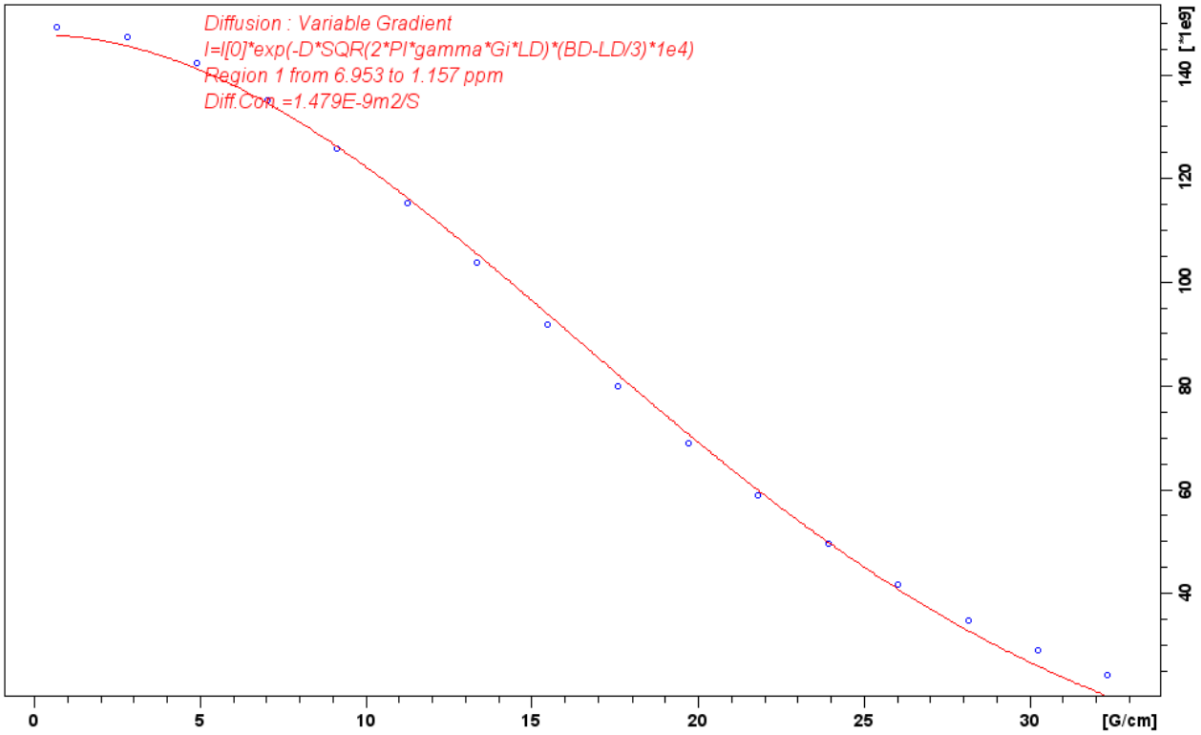
Diffusion : Variable Gradient
I=I[0]*exp(-D*SQR(2*PI*gamma*Gi*LD)*(BD-LD/3)*1e4)
Region 1 from 6.953 to 1.157 ppm
Diff.Con.=1.479E-9m2/S
[*1e6]
140
120
100
80
60
40
0
5
10
15
20
25
30
[G/cm]

2: 100 m

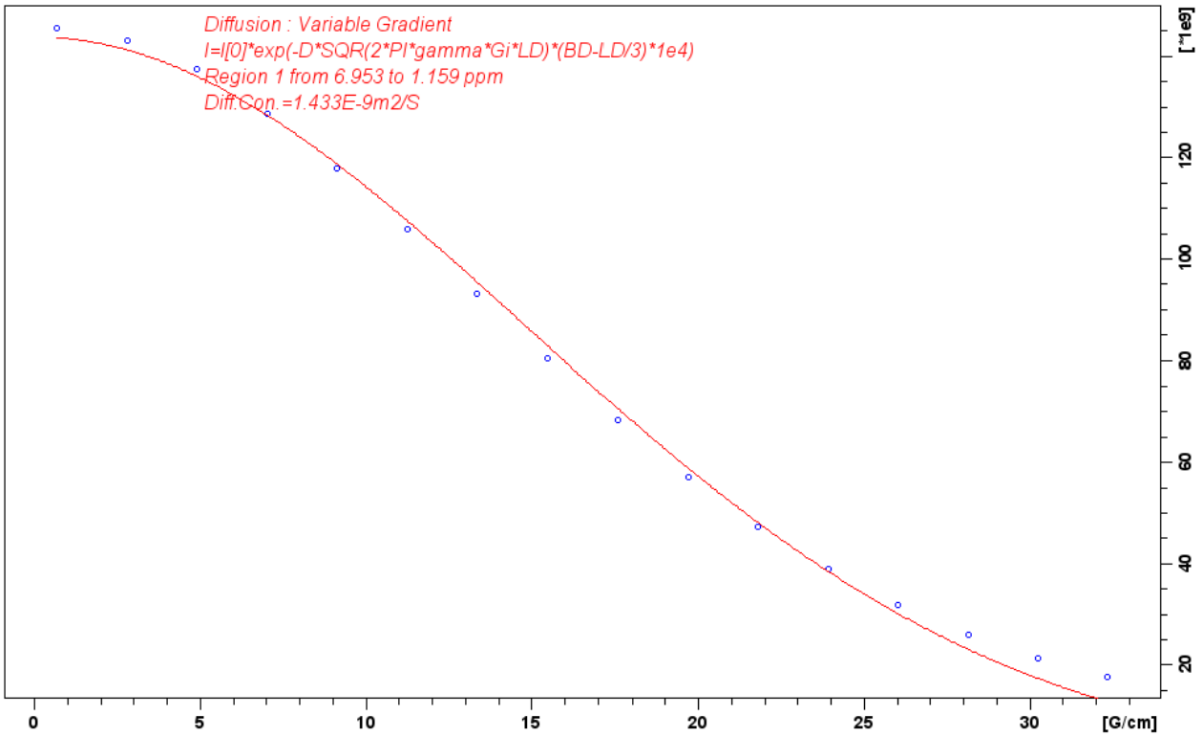
Diffusion : Variable Gradient
I=I[0]*exp(-D*SQR(2*PI*gamma*Gi*LD)*(BD-LD/3)*1e4)
Region 1 from 6.953 to 1.159 ppm
Diff.Con.=1.433E-9m2/S
[*1e6]
120
100
80
60
40
20
0
5
10
15
20
25
30
[G/cm]

2: 250 m

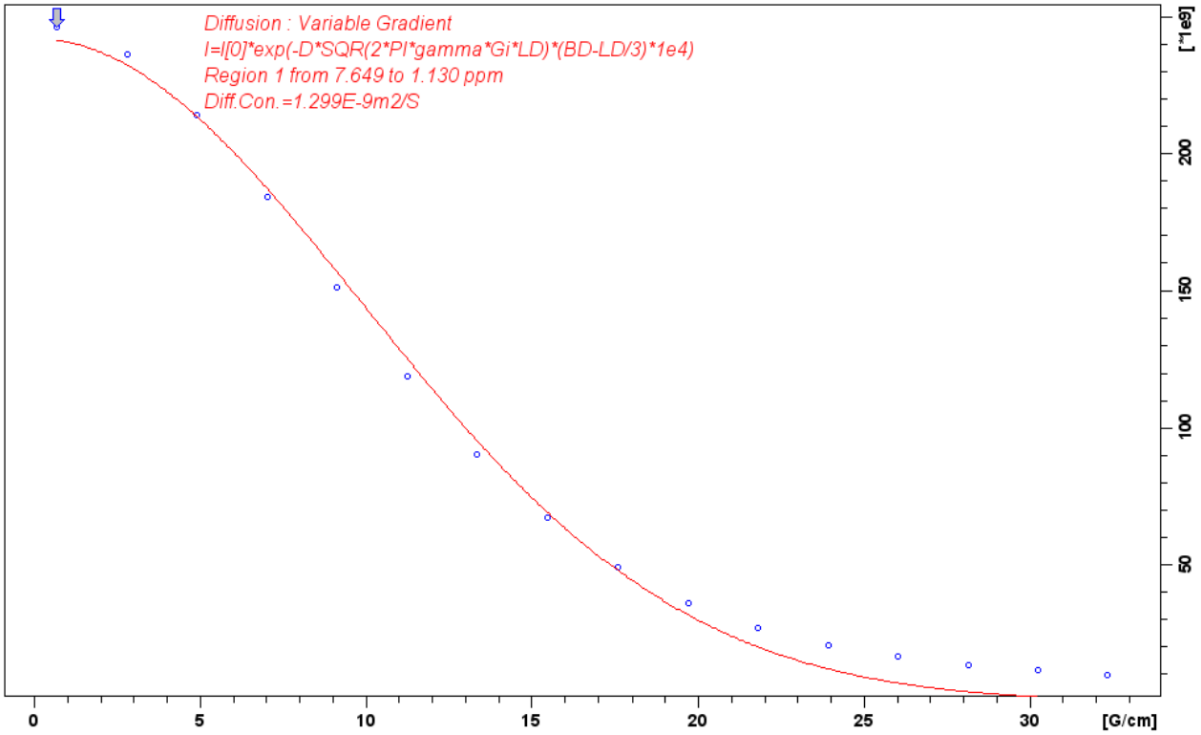
Diffusion : Variable Gradient
I=I[0]*exp(-D*SQR(2*PI*gamma*Gi*LD)*(BD-LD/3)*1e4)
Region 1 from 7.649 to 1.130 ppm
Diff.Con.=1.299E-9m2/S
[*1e9]
200
150
100
50
0
5
10
15
20
25
30
[G/cm]

2: 500 m

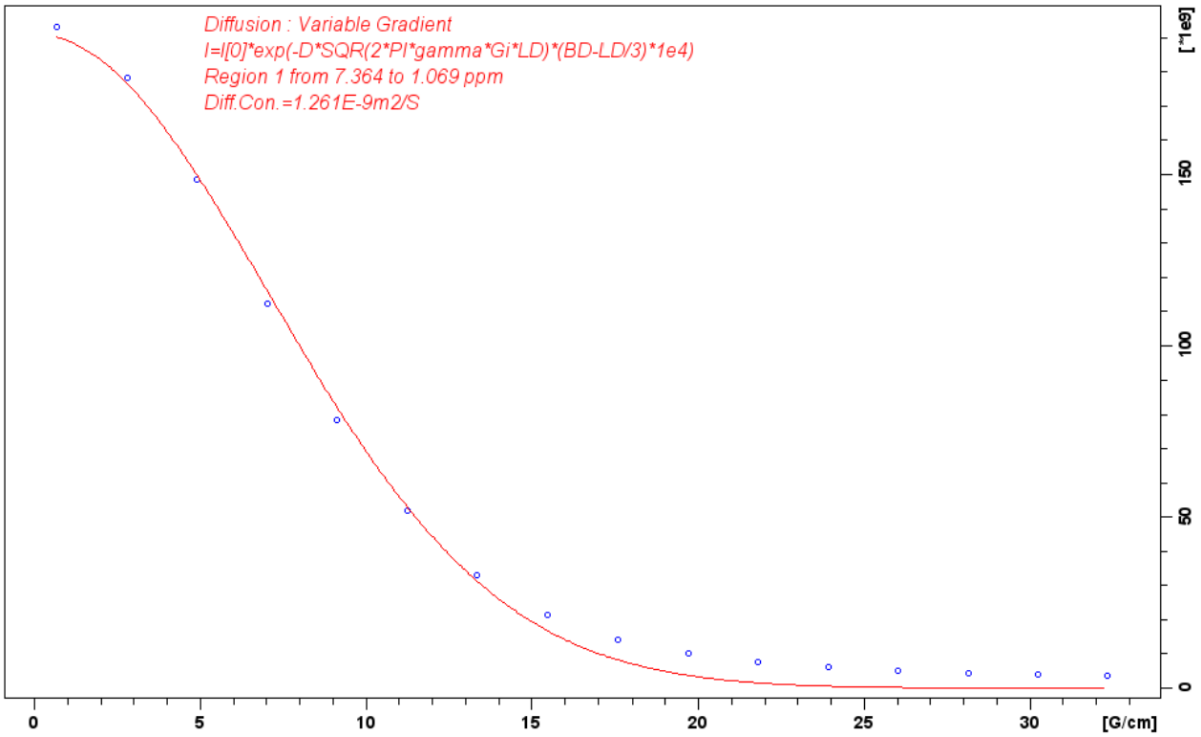
Diffusion : Variable Gradient
I=I[0]*exp(-D*SQR(2*PI*gamma*Gi*LD)*(BD-LD/3)*1e4)
Region 1 from 7.364 to 1.069 ppm
Diff.Con.=1.261E-9m2/S
[*1e9]
150
100
50
0
5
10
15
20
25
30
[G/cm]

2: 750 m

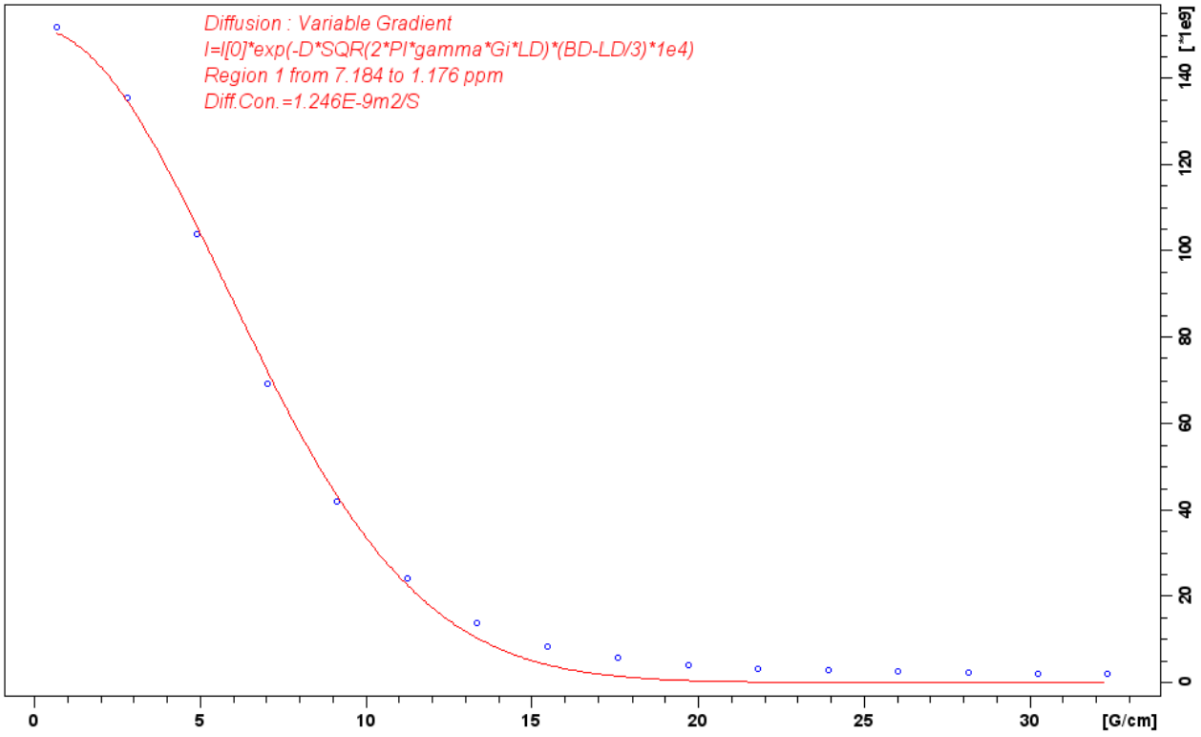

2: 1000 m

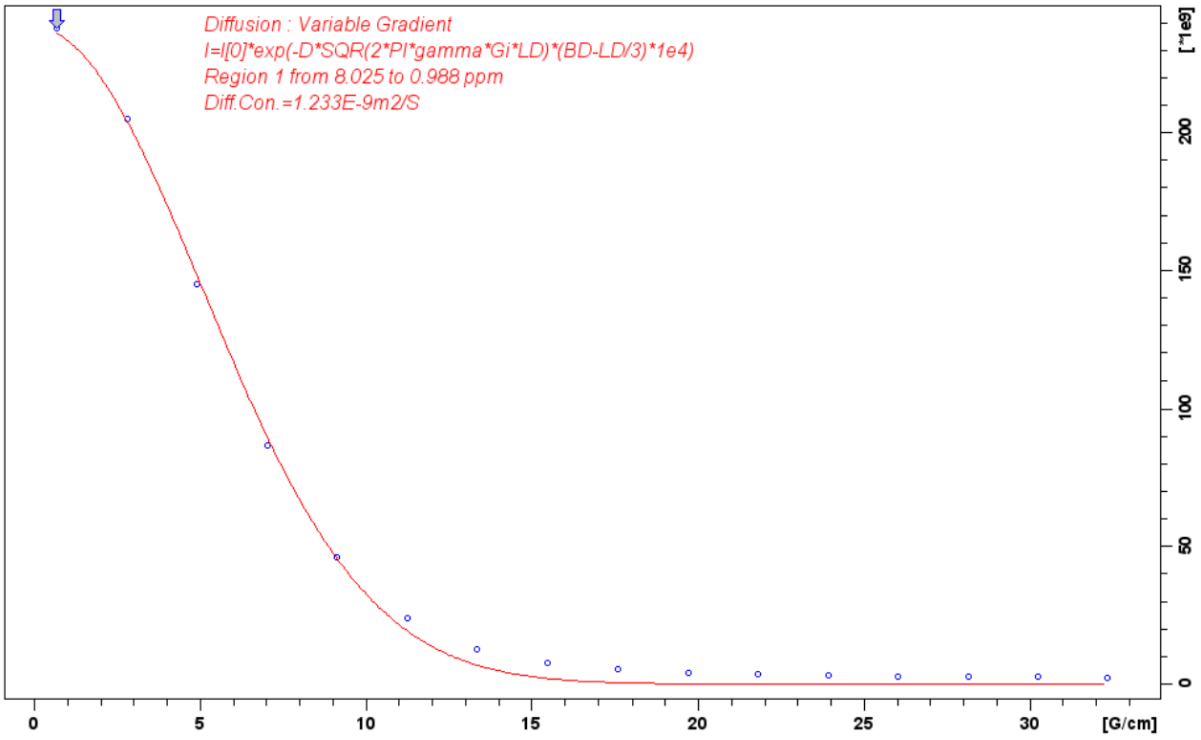

2: 1250 m

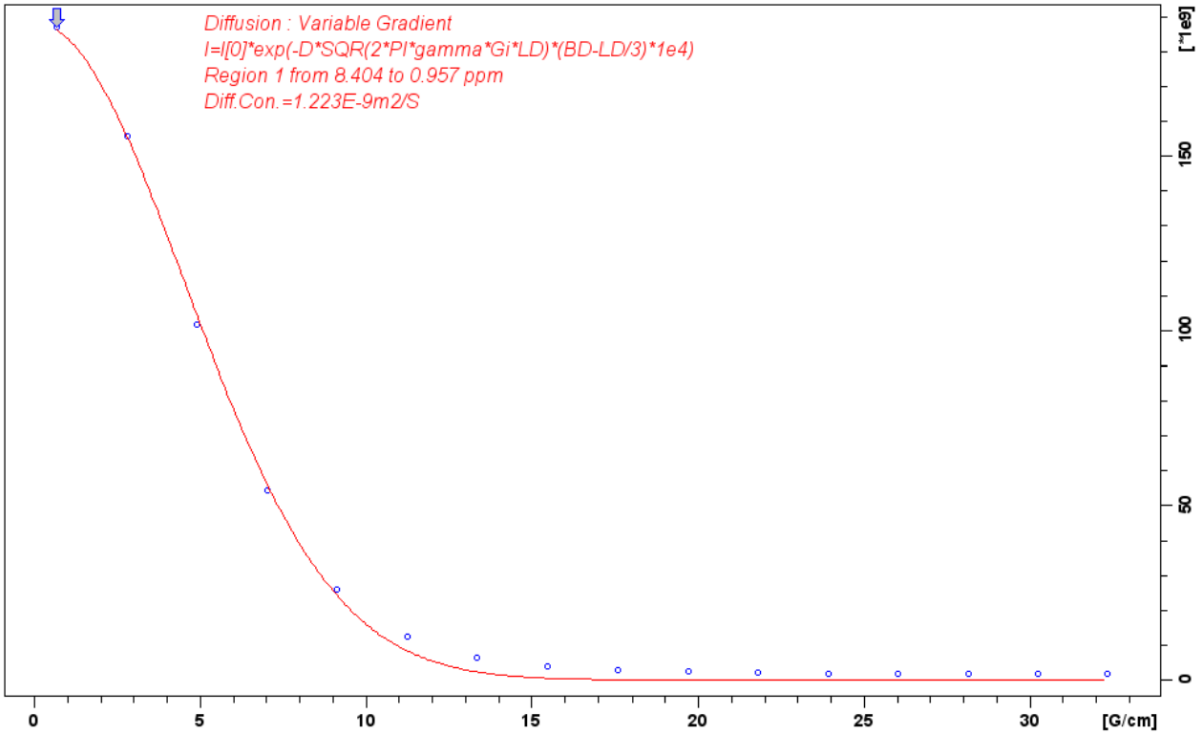

SAMPLE 3 Recorded 6/7/22

3: D 30 m

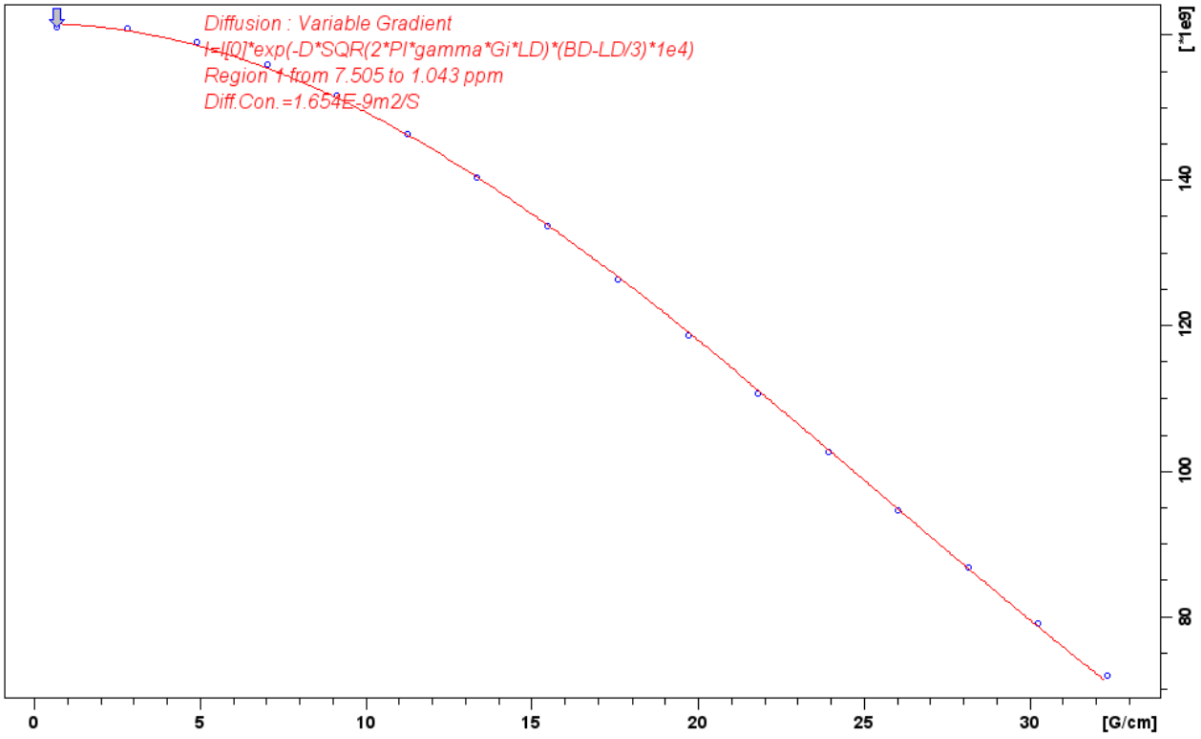

3: 40 m

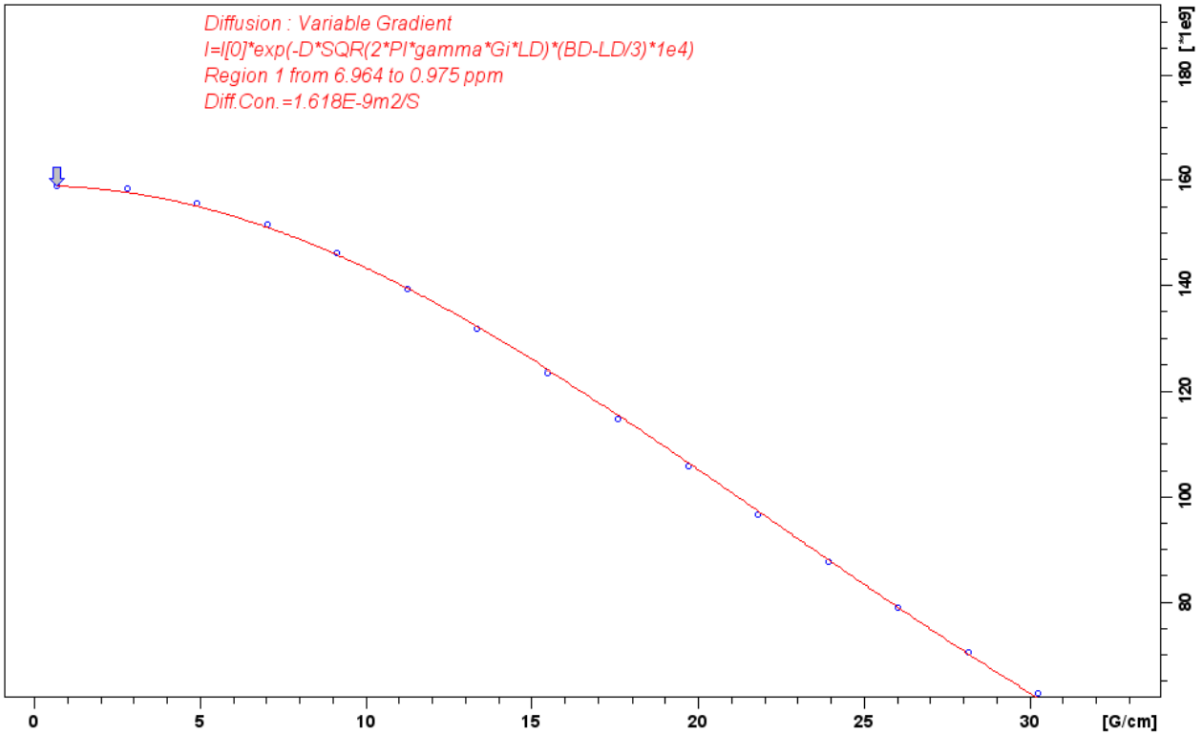
Diffusion : Variable Gradient
I=I[0]*exp(-D*SQR(2*PI*gamma*Gi*LD)*(BD-LD/3)*1e4)
Region 1 from 6.964 to 0.975 ppm
Diff.Con.=1.618E-9m2/S
[*1e9]
180
160
140
120
100
80
0
5
10
15
20
25
30
[G/cm]

3: 50 ms

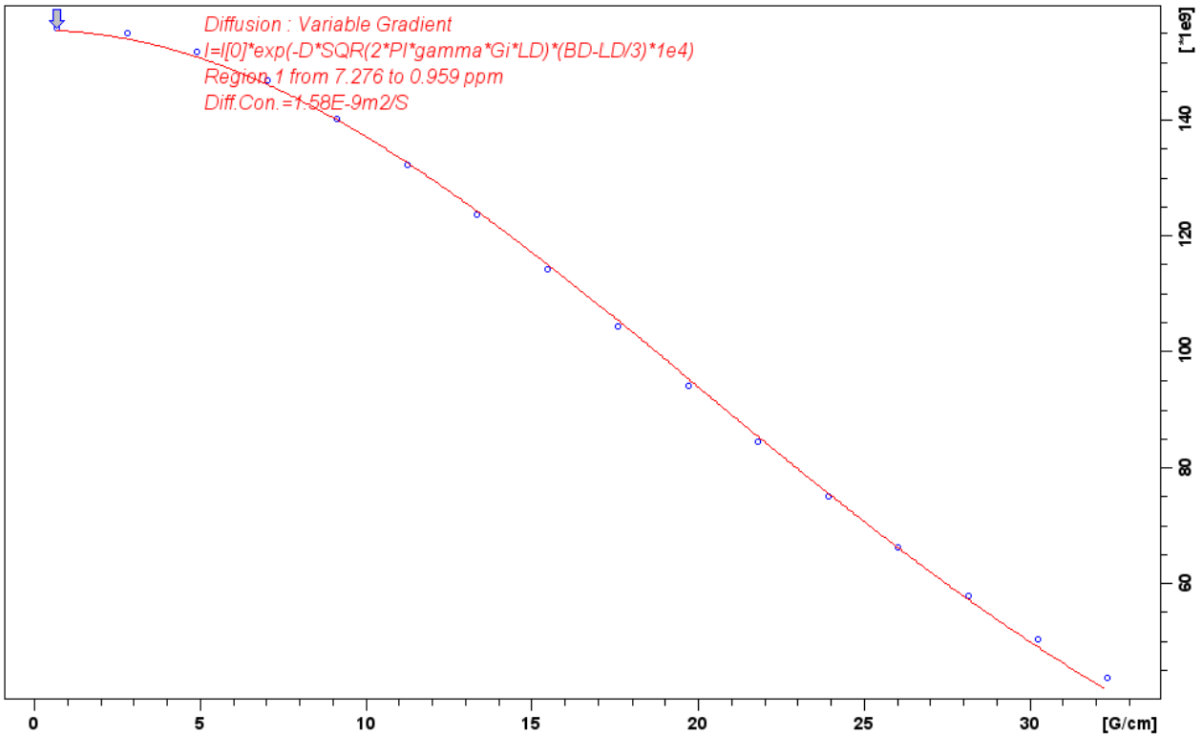
Diffusion : Variable Gradient
I=I[0]*exp(-D*SQR(2*PI*gamma*Gi*LD)*(BD-LD/3)*1e4)
Region 1 from 7.276 to 0.959 ppm
Diff.Con.=1.58E-9m2/S
[*1e9]
140
120
100
80
60
0
5
10
15
20
25
30
[G/cm]

3: 60 ms

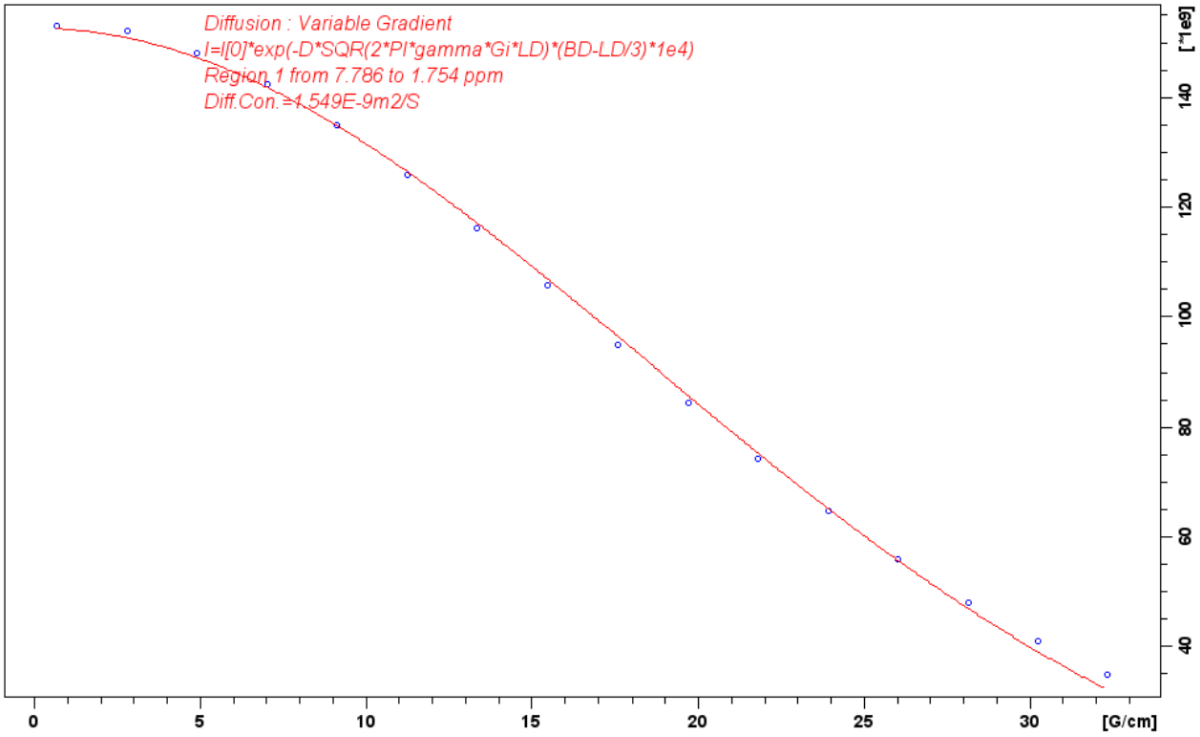

3: 100 m

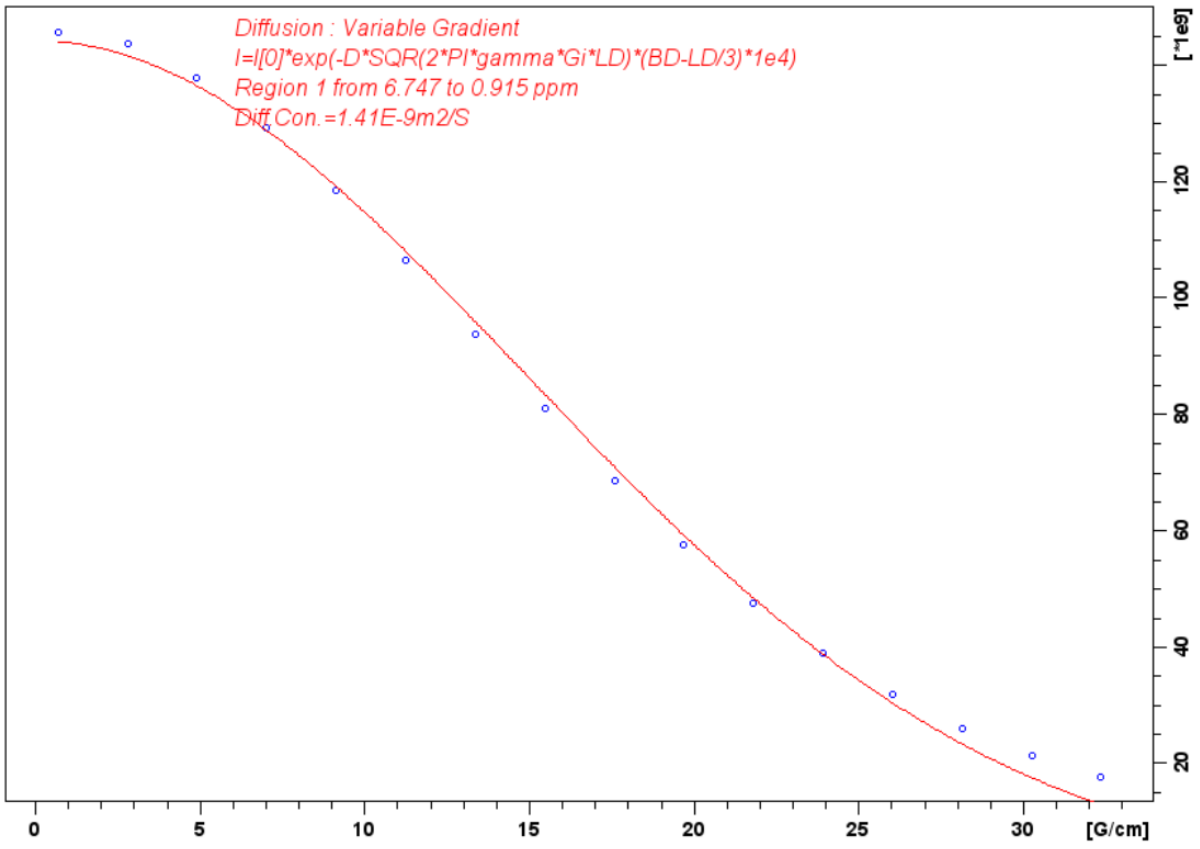

3: 250 ms

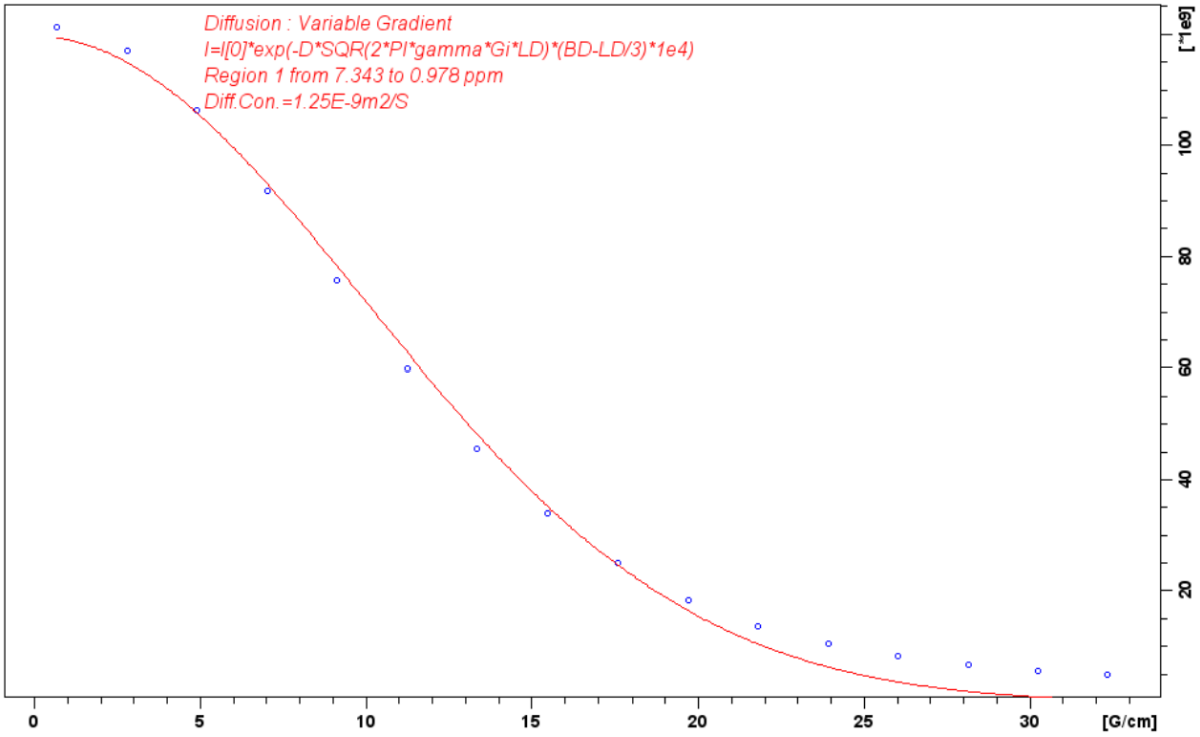

3: 500 ms

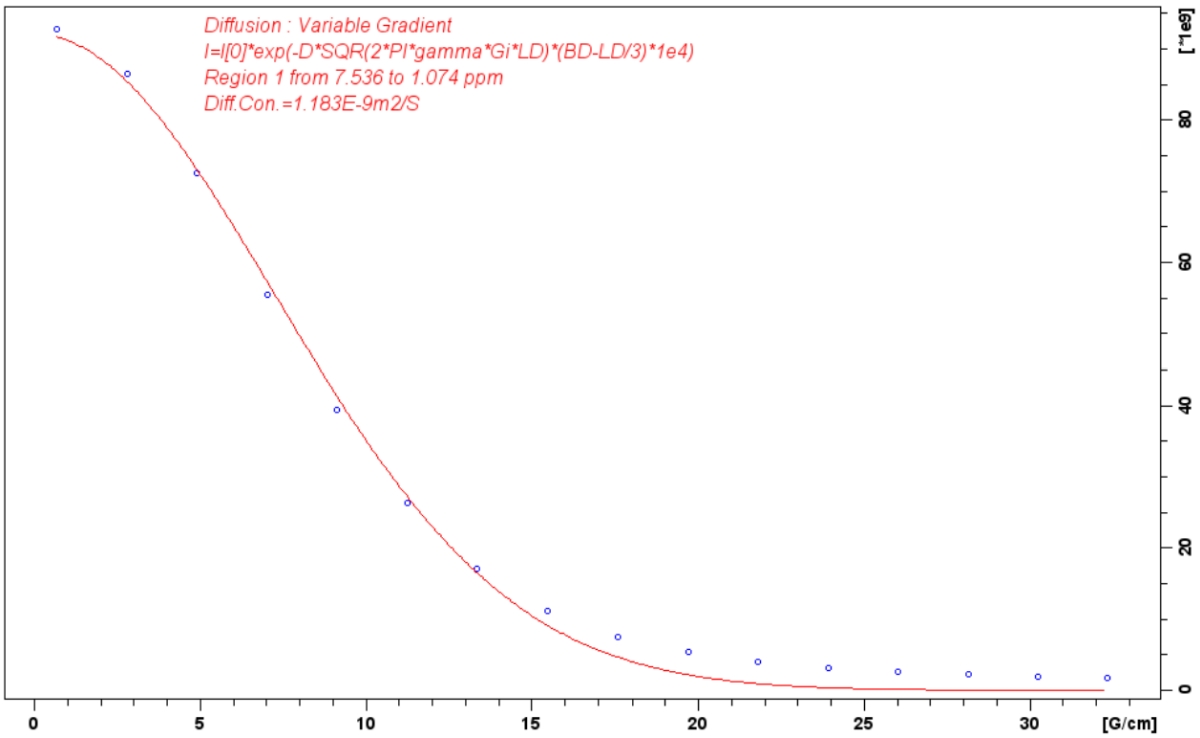

3: 750 m

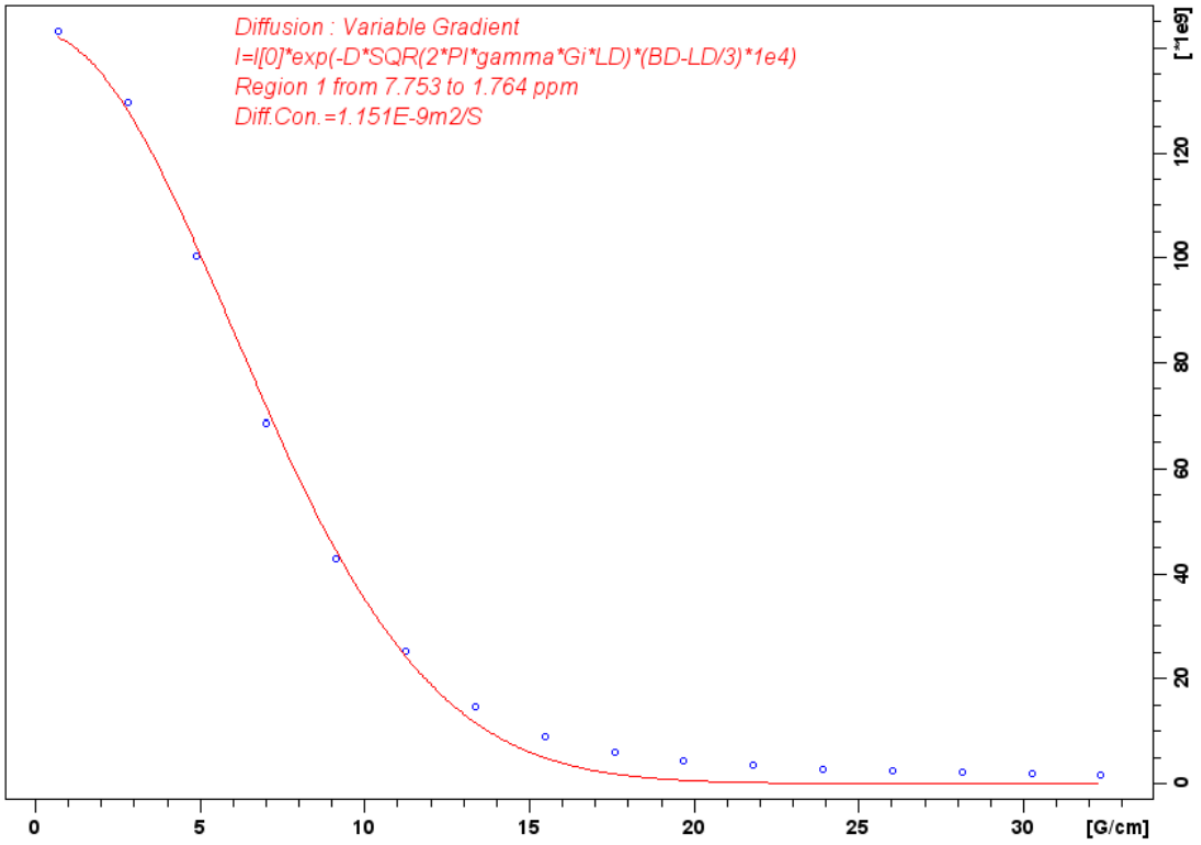

3: 1000m

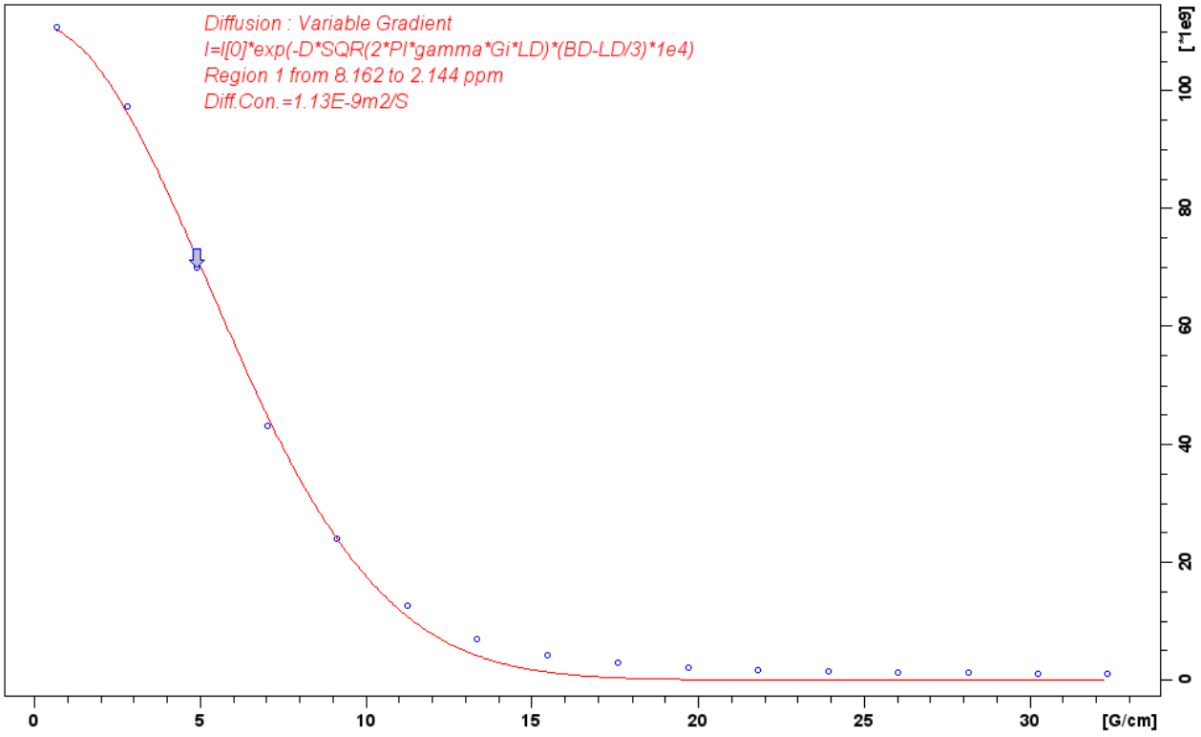

3: 1250 ms

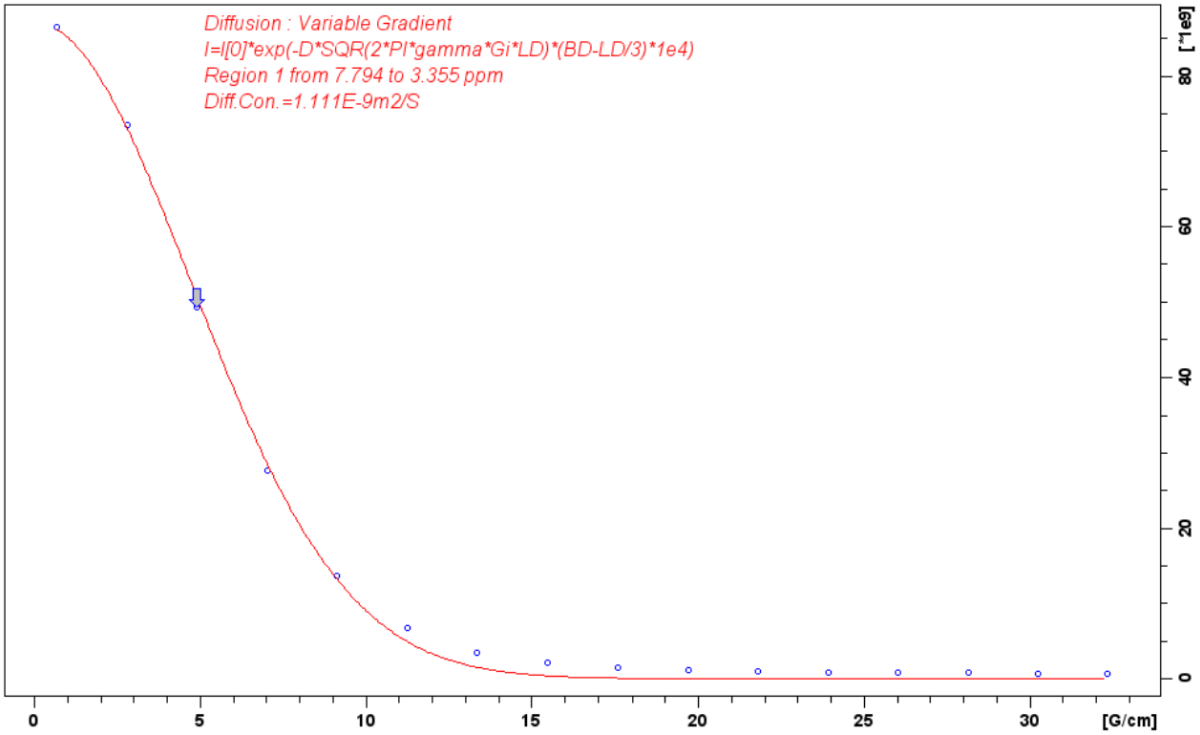

SAMPLE 4 Recorded 6/7/22

4: D 30 ms

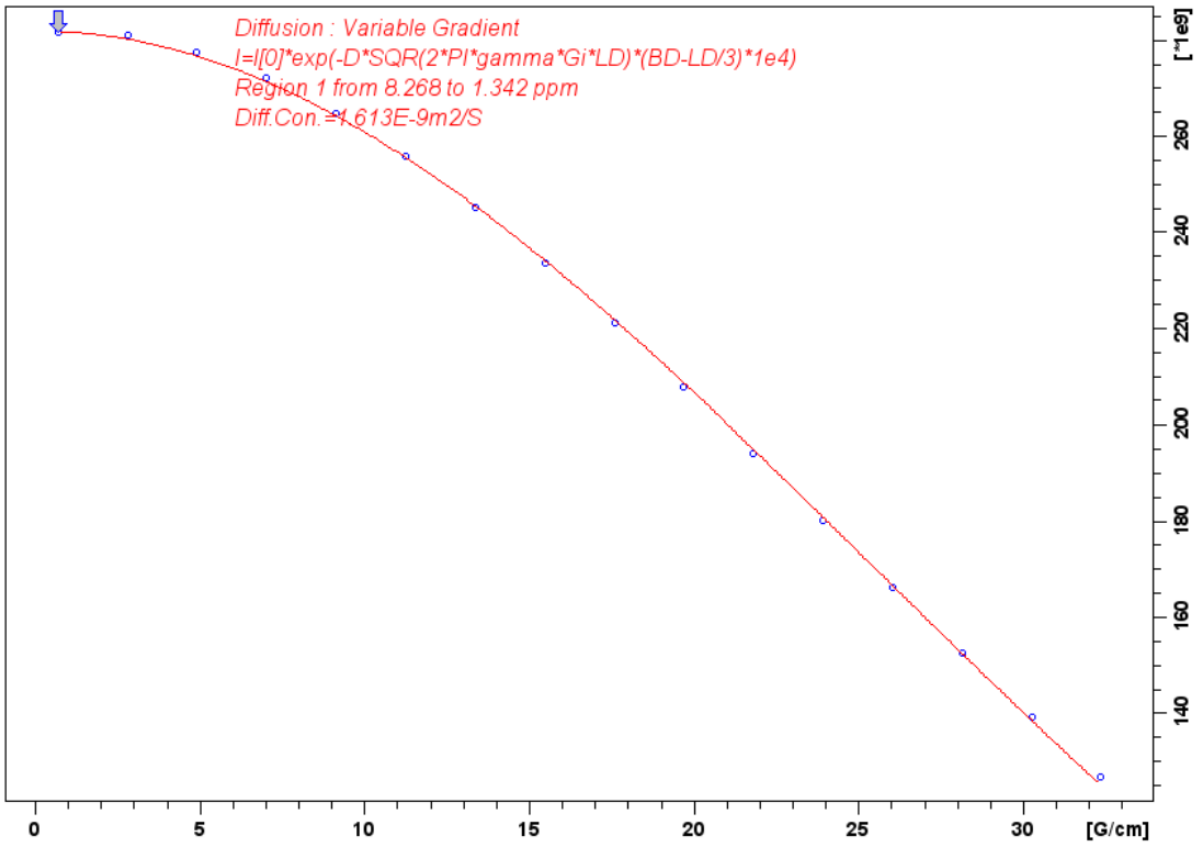

4: 40 ms

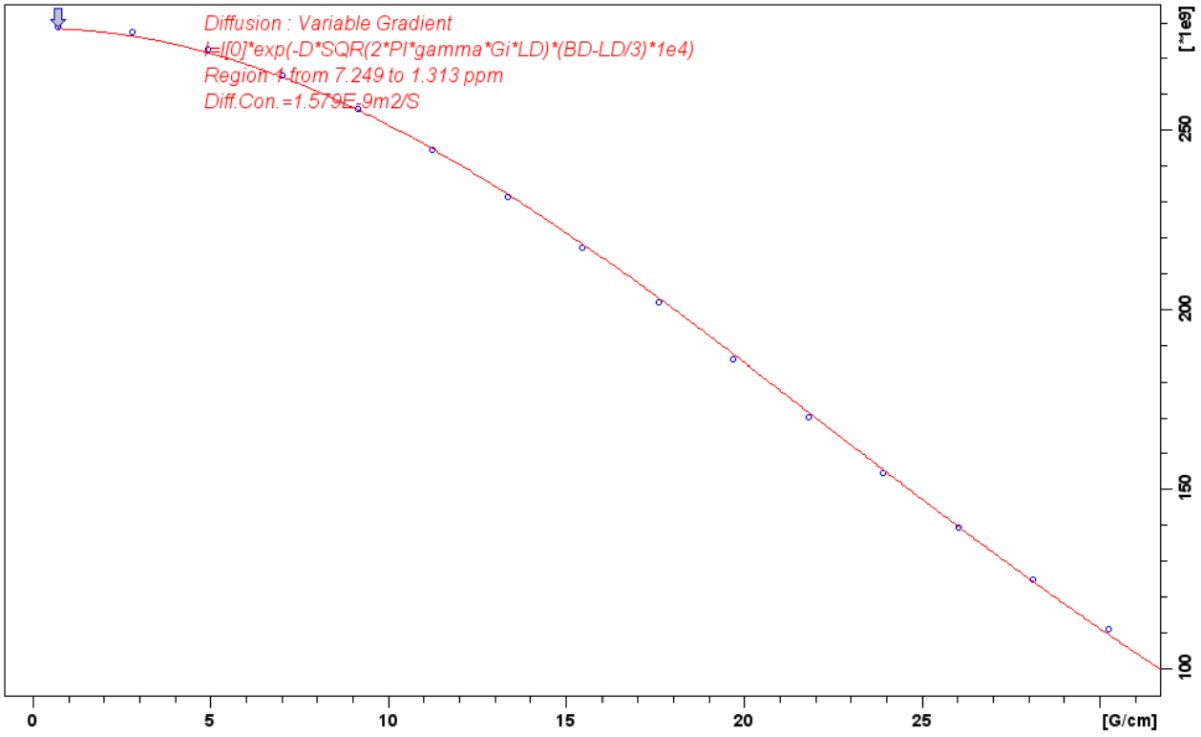
Diffusion : Variable Gradient
I=I[0]*exp(-D*SQR(2*PI*gamma*Gi*LD)*(BD-LD/3)*1e4)
Region 1 from 7.249 to 1.313 ppm
Diff.Con.=1.579E-9m2/S
[*1e9]
250
200
150
100
0
5
10
15
20
25
[G/cm]

4: 50 ms

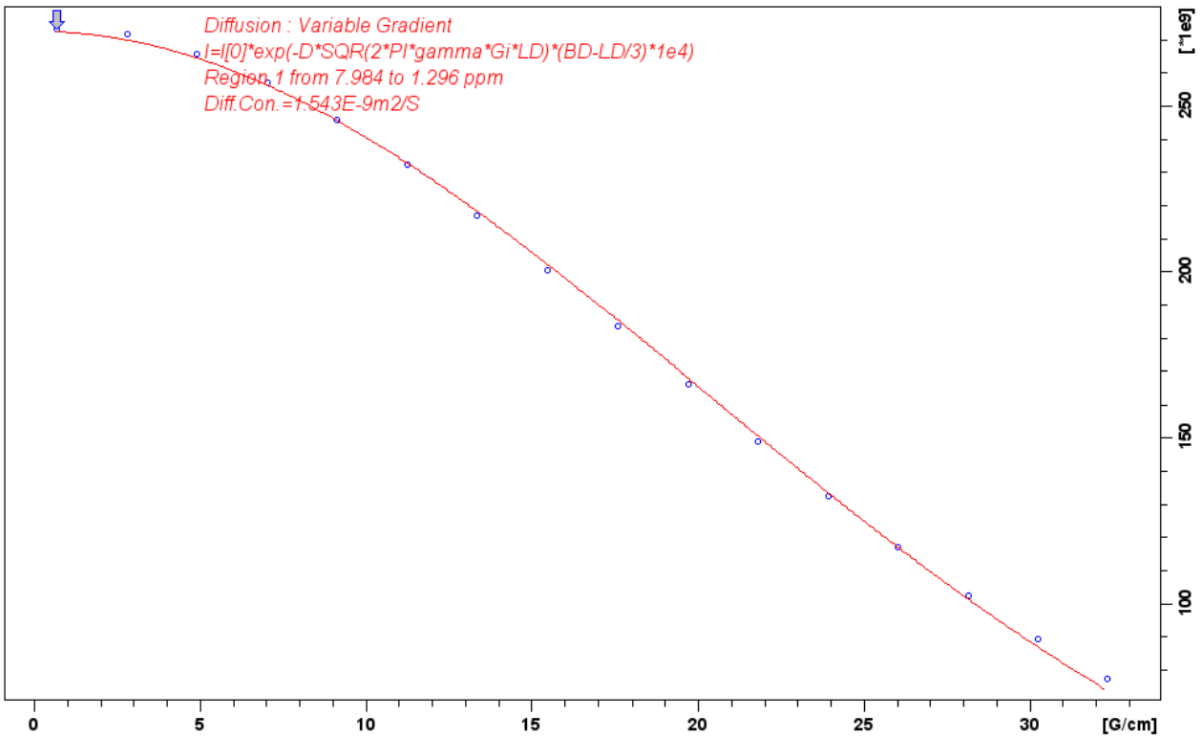
Diffusion : Variable Gradient
I=I[0]*exp(-D*SQR(2*PI*gamma*Gi*LD)*(BD-LD/3)*1e4)
Region 1 from 7.984 to 1.296 ppm
Diff.Con.=1.543E-9m2/S
[*1e9]
250
200
150
100
0
5
10
15
20
25
30
[G/cm]

4: 60 ms

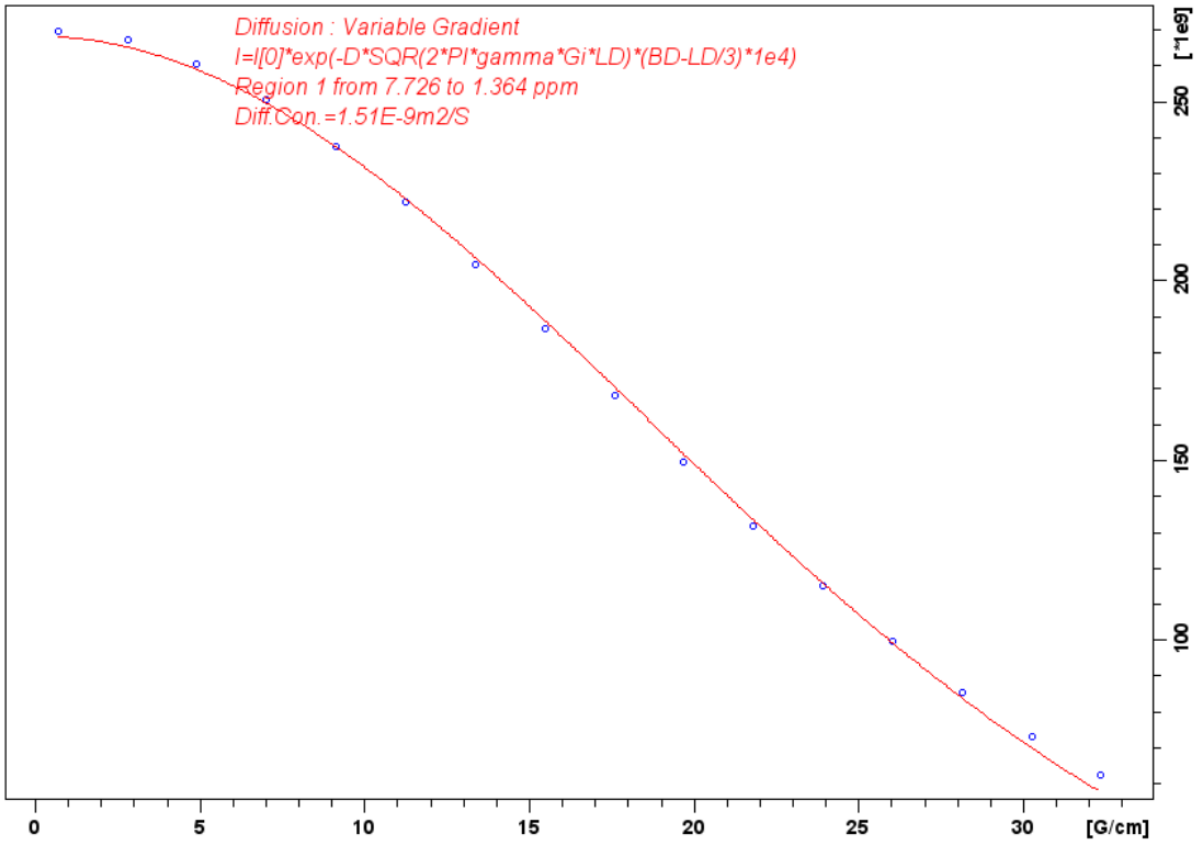
Diffusion : Variable Gradient
I=I[0]*exp(-D*SQR(2*PI*gamma*Gi*LD)*(BD-LD/3)*1e4)
Region 1 from 7.726 to 1.364 ppm
Diff.Con.=1.51E-9m2/S
[*1e9]
250
200
150
100
0
5
10
15
20
25
30
[G/cm]

4: 100 ms

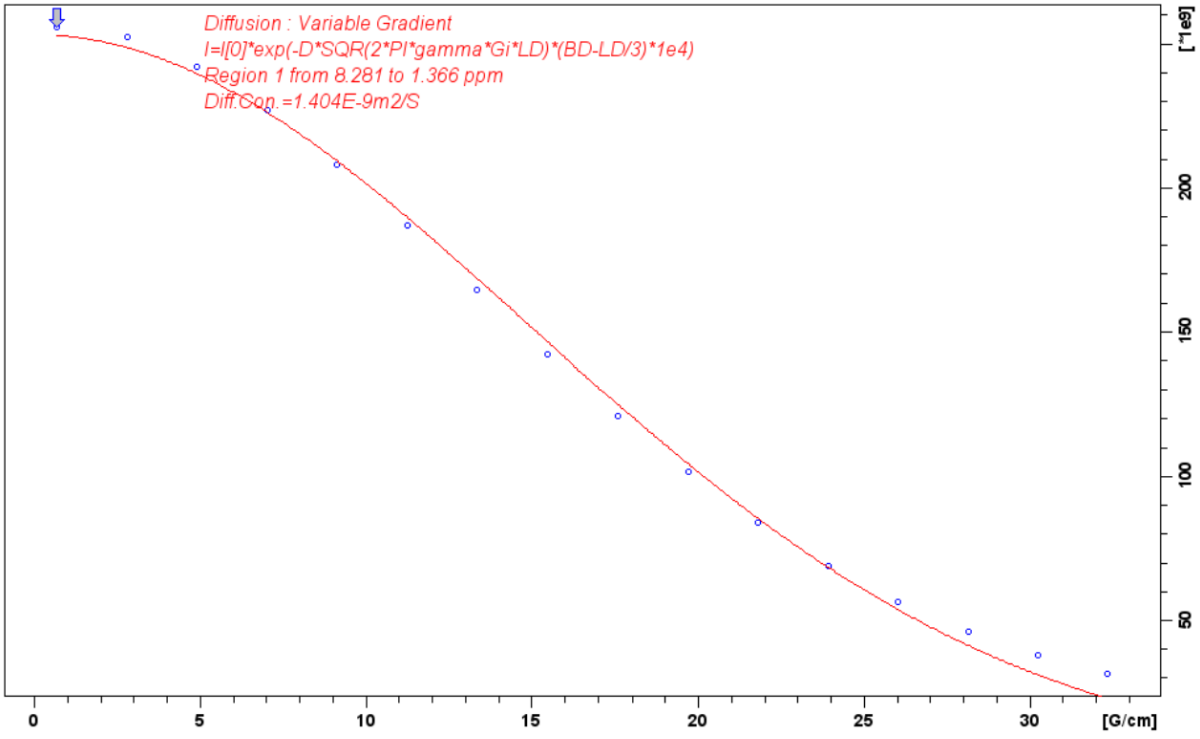
Diffusion : Variable Gradient
I=I[0]*exp(-D*SQR(2*PI*gamma*Gi*LD)*(BD-LD/3)*1e4)
Region 1 from 8.281 to 1.366 ppm
Diff.Con.=1.404E-9m2/S
[*1e9]
200
150
100
50
0
5
10
15
20
25
30
[G/cm]

4: 250

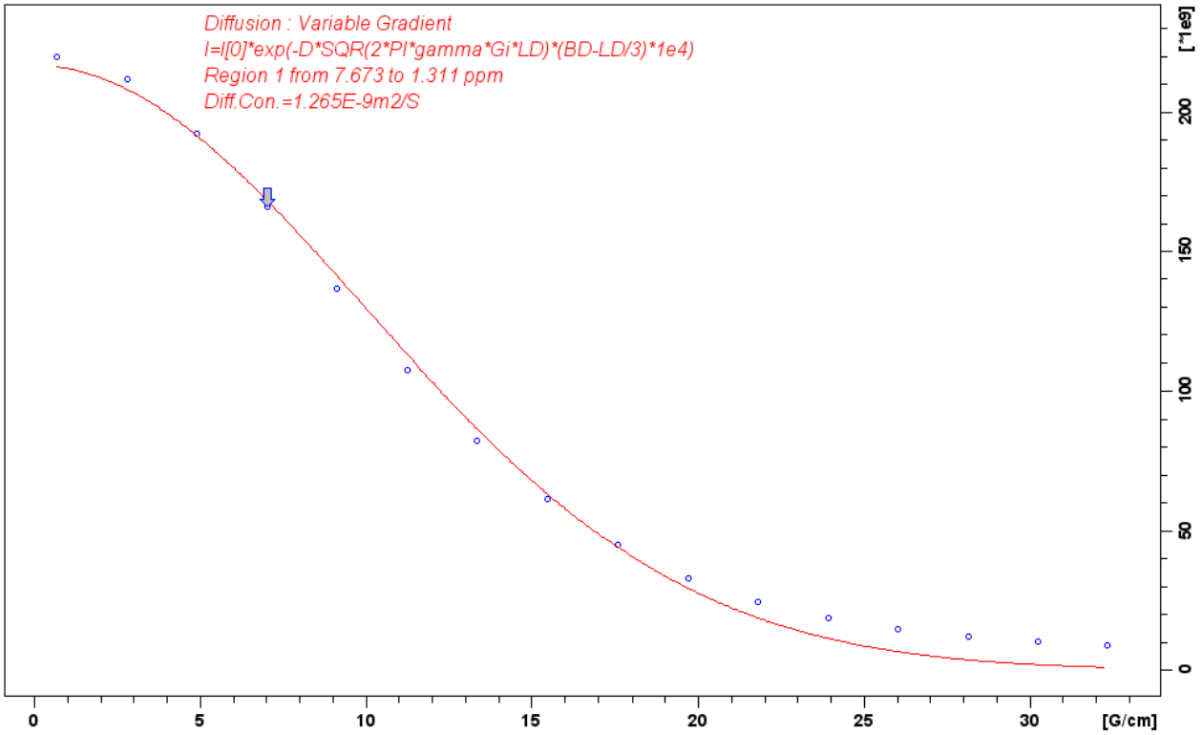

4: 500 ms

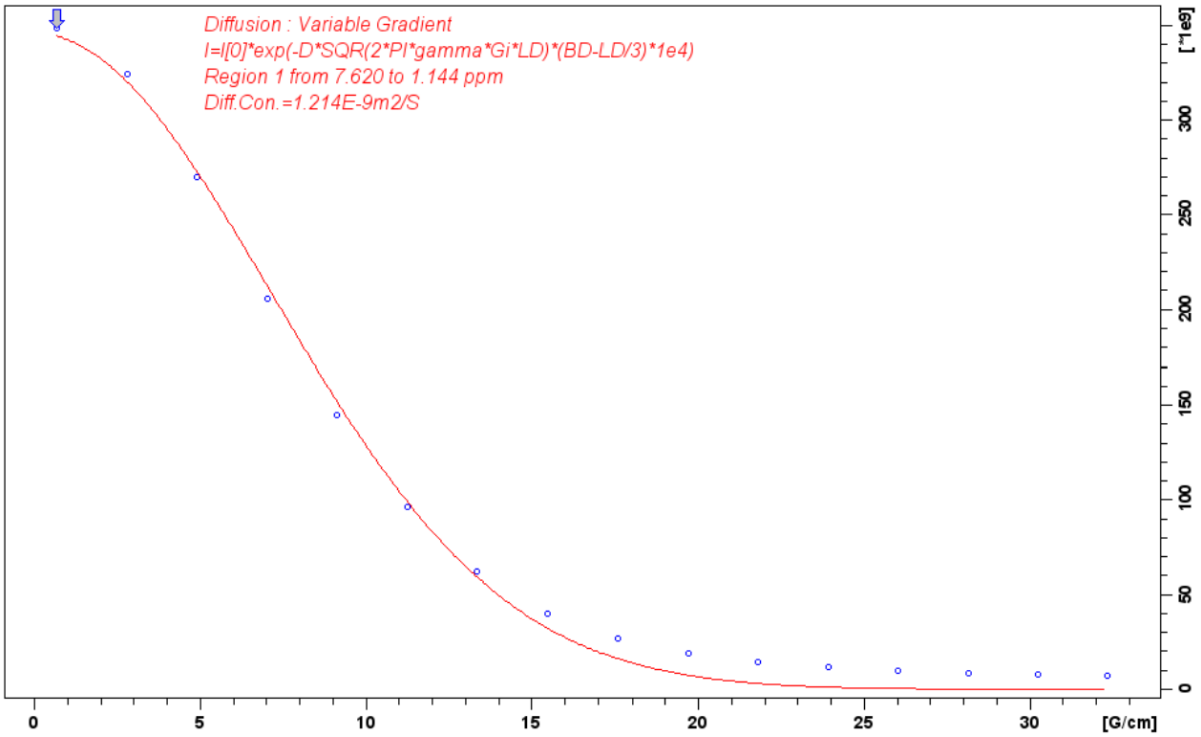

4: 750 ms

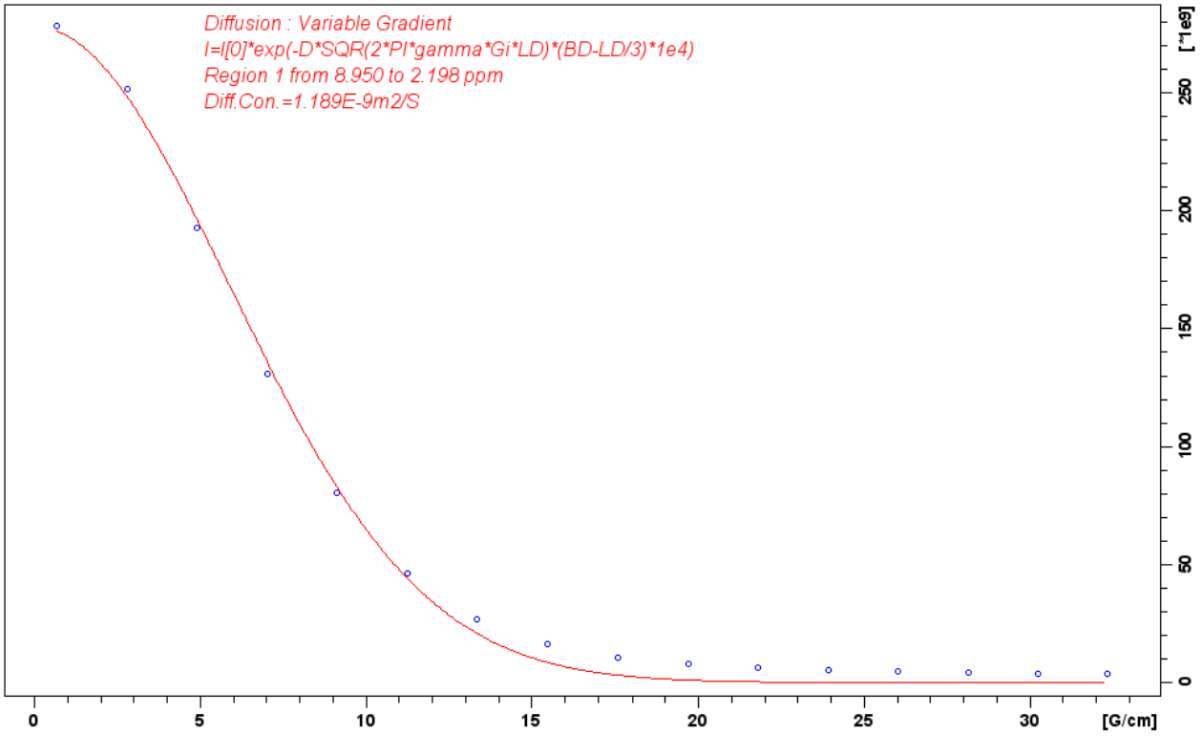

4: 1000 ms

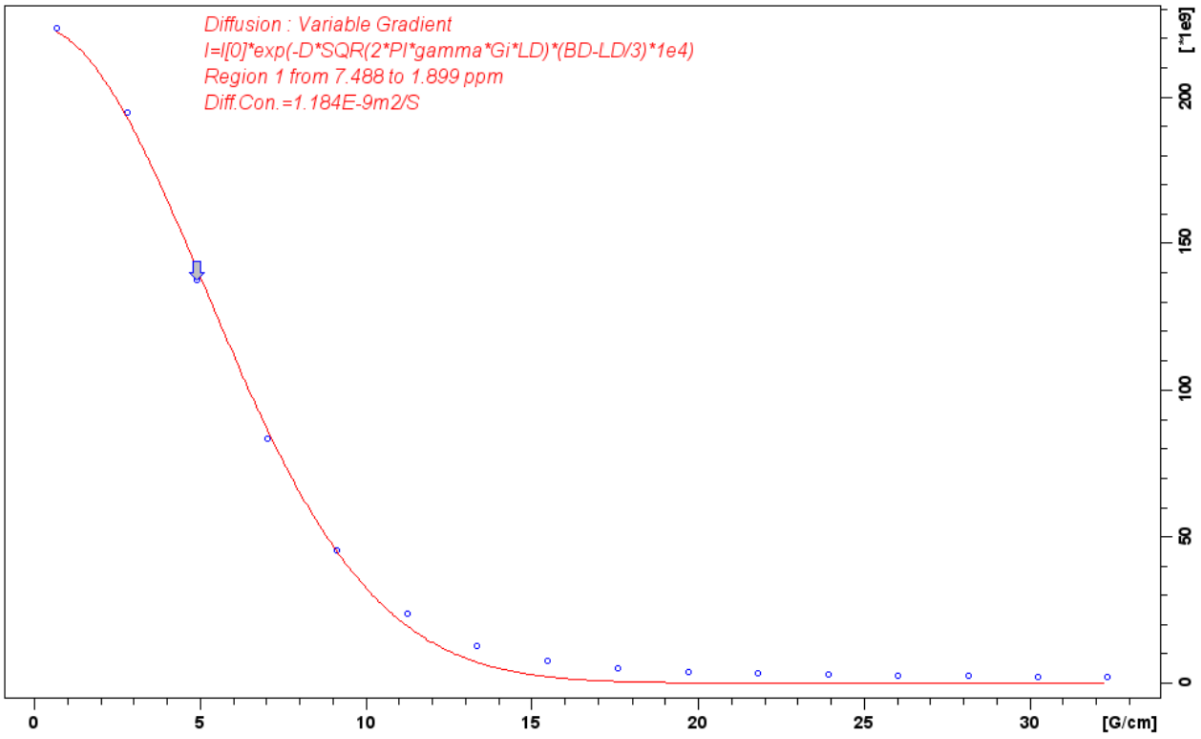

4: 1250

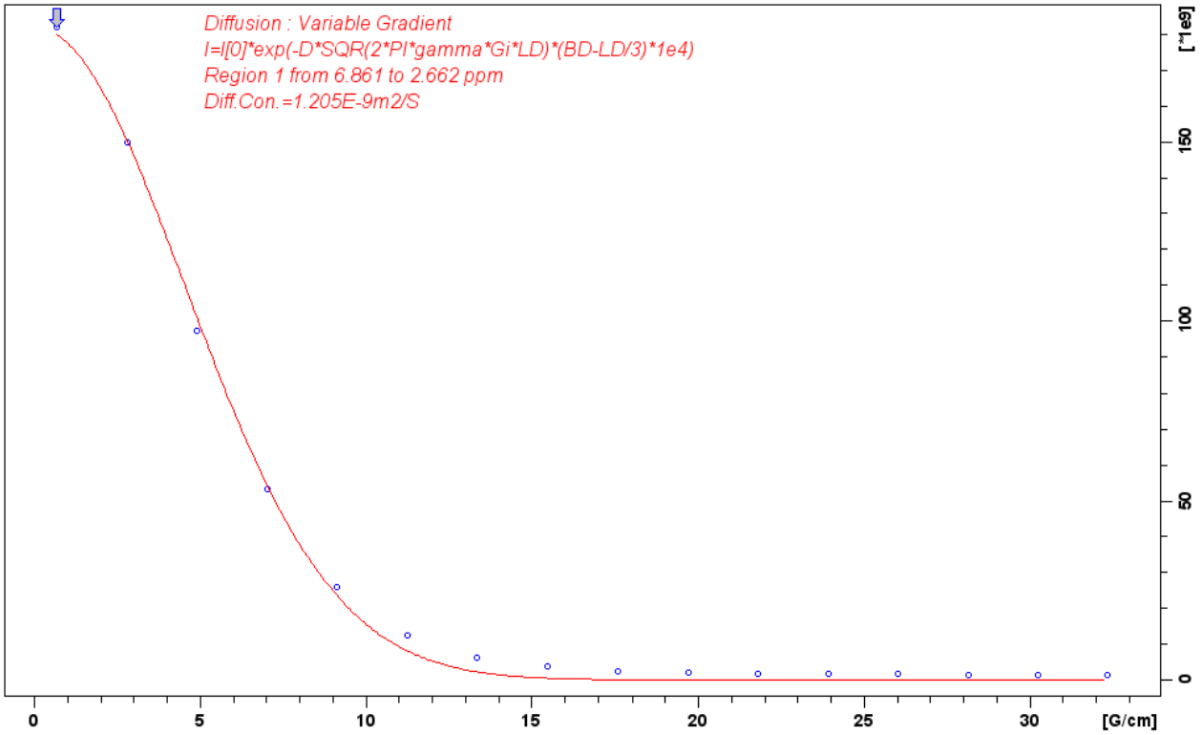

Sample 5: Recorded 7/7/22

5: D 30 ms

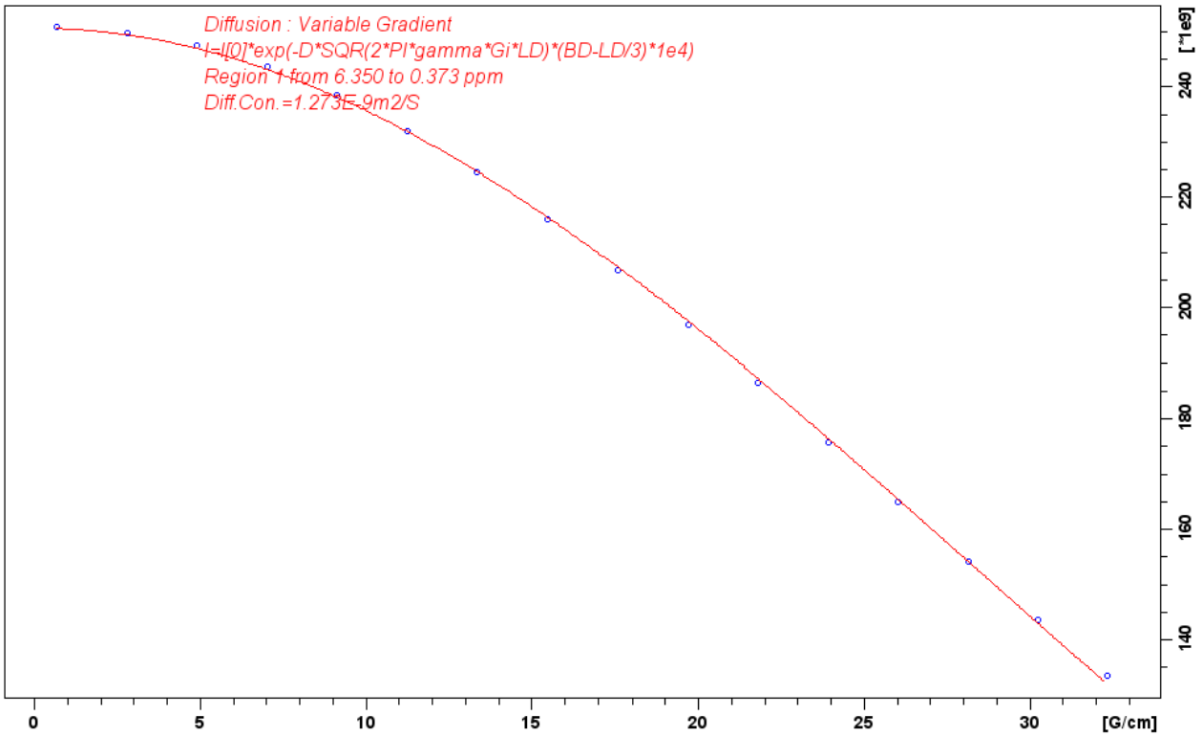

Unfortunately, no more data was recorded for sample 5.

SAMPLE 6 Recorded 8/7/22

6: D 30 ms

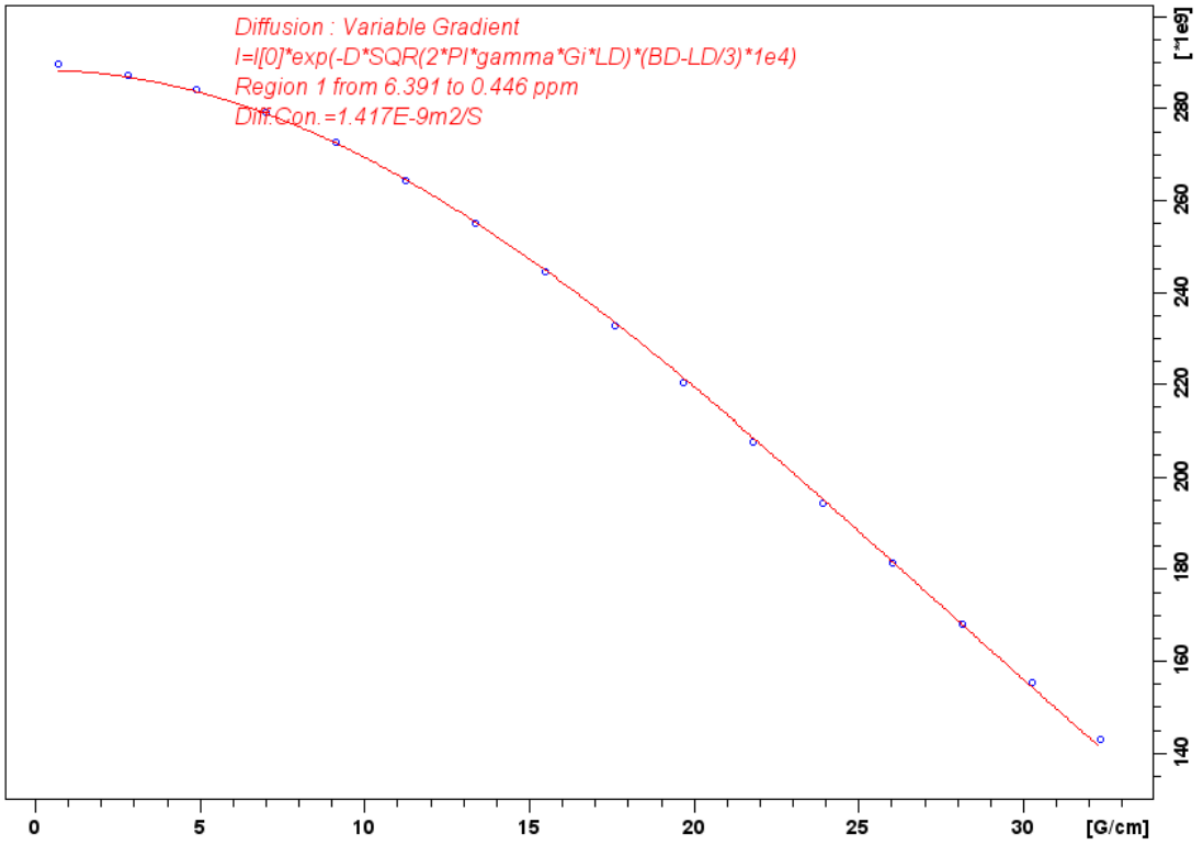

6: 40 ms

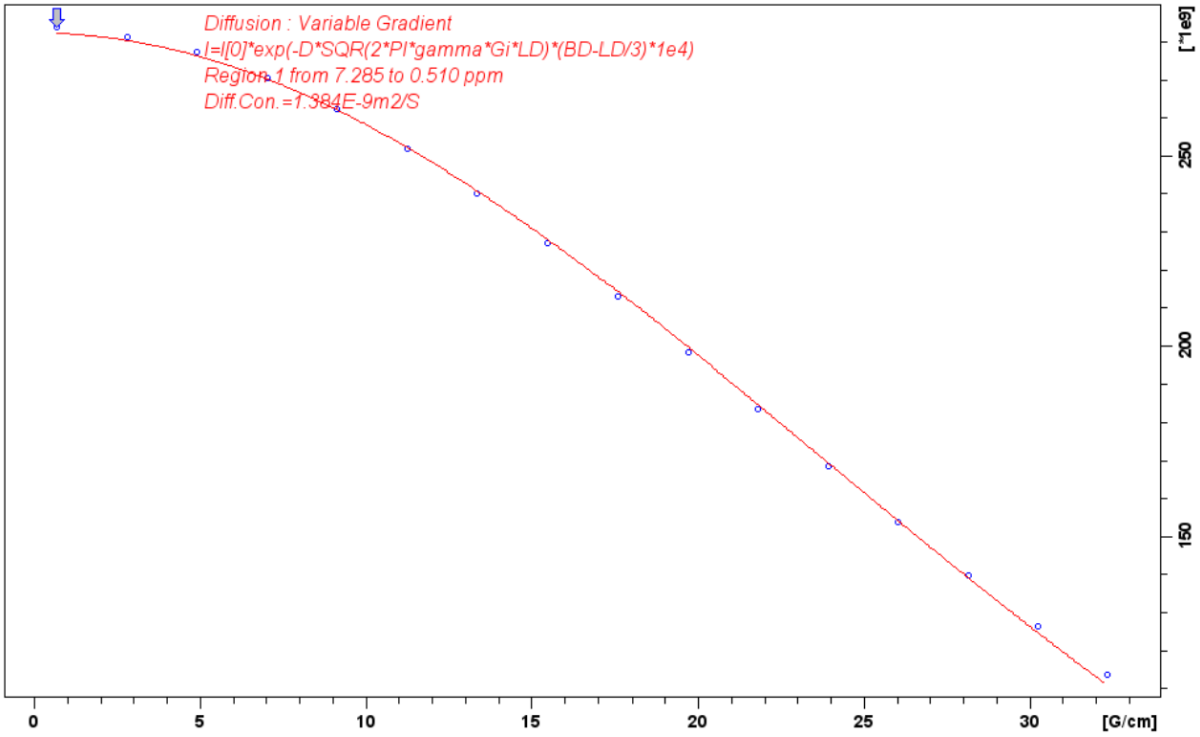

6: 50 ms

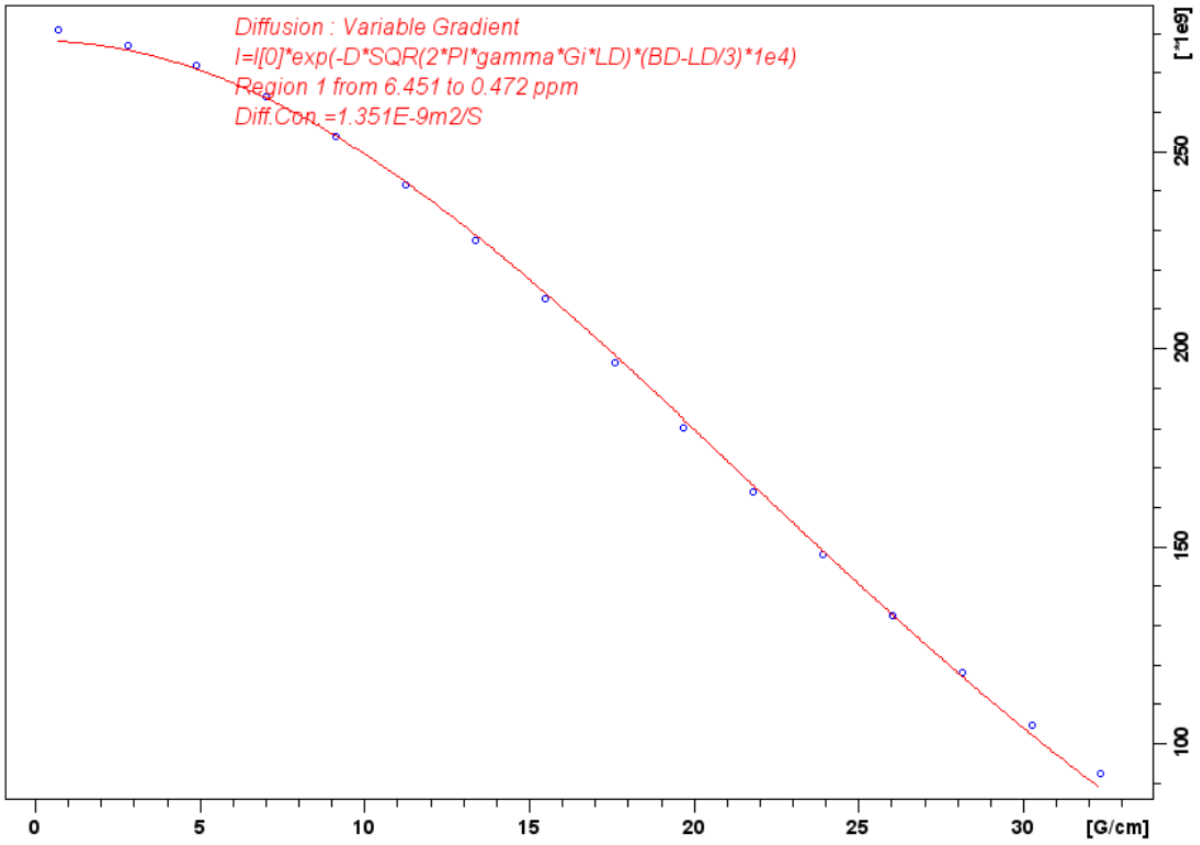
Diffusion : Variable Gradient
I=I[0]*exp(-D*SQR(2*PI*gamma*Gi*LD)*(BD-LD/3)*1e4)
Region 1 from 6.451 to 0.472 ppm
Diff.Con.=1.351E-9m2/S
[*1e9]
250
200
150
100
0
5
10
15
20
25
30
[G/cm]

6: 60 ms

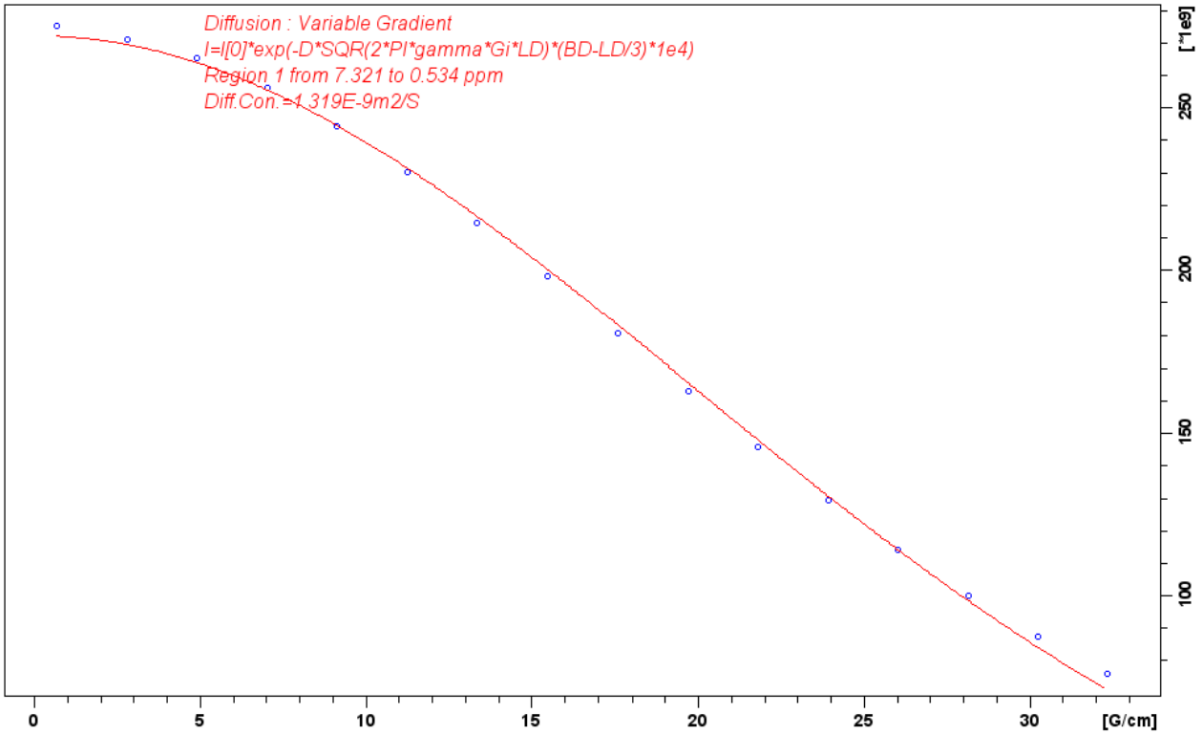
Diffusion : Variable Gradient
I=I[0]*exp(-D*SQR(2*PI*gamma*Gi*LD)*(BD-LD/3)*1e4)
Region 1 from 7.321 to 0.534 ppm
Diff.Con.=1.319E-9m2/S
[*1e9]
250
200
150
100
0
5
10
15
20
25
30
[G/cm]

6: 80 ms

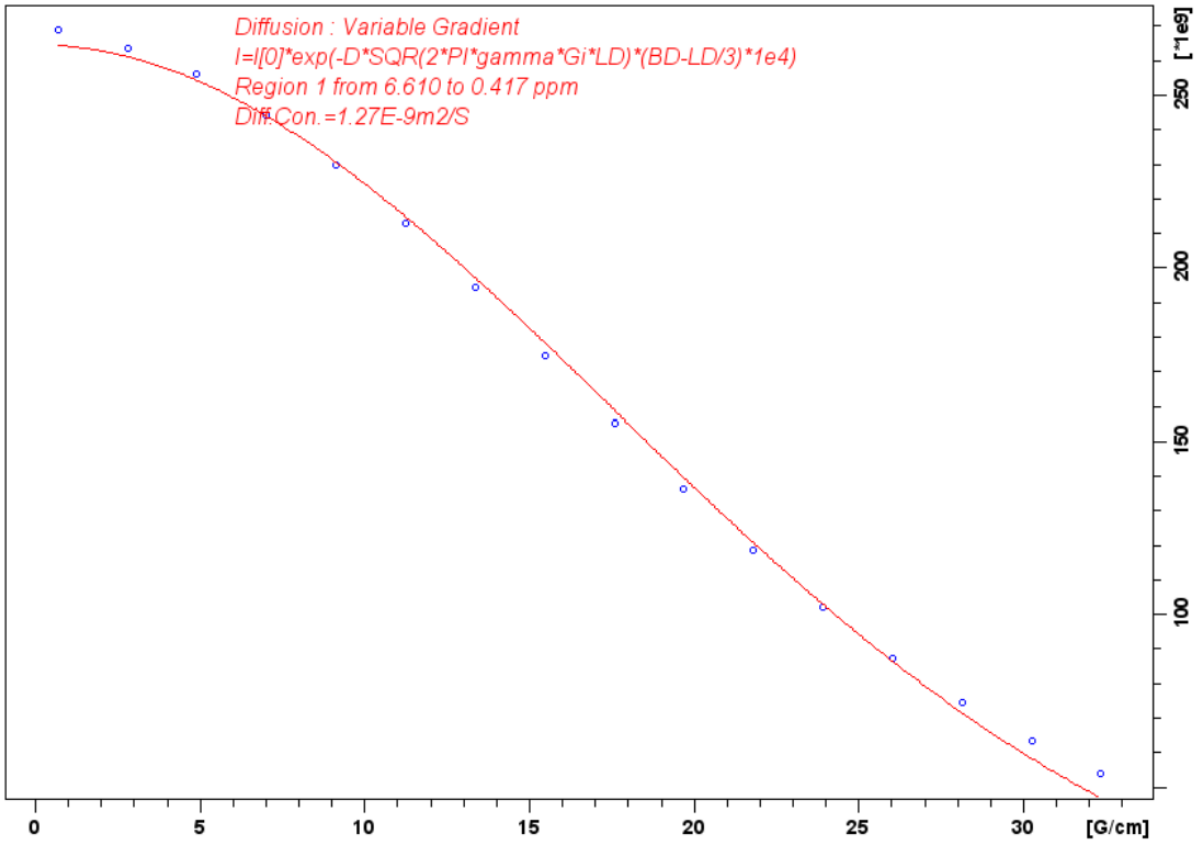

6: 100 ms

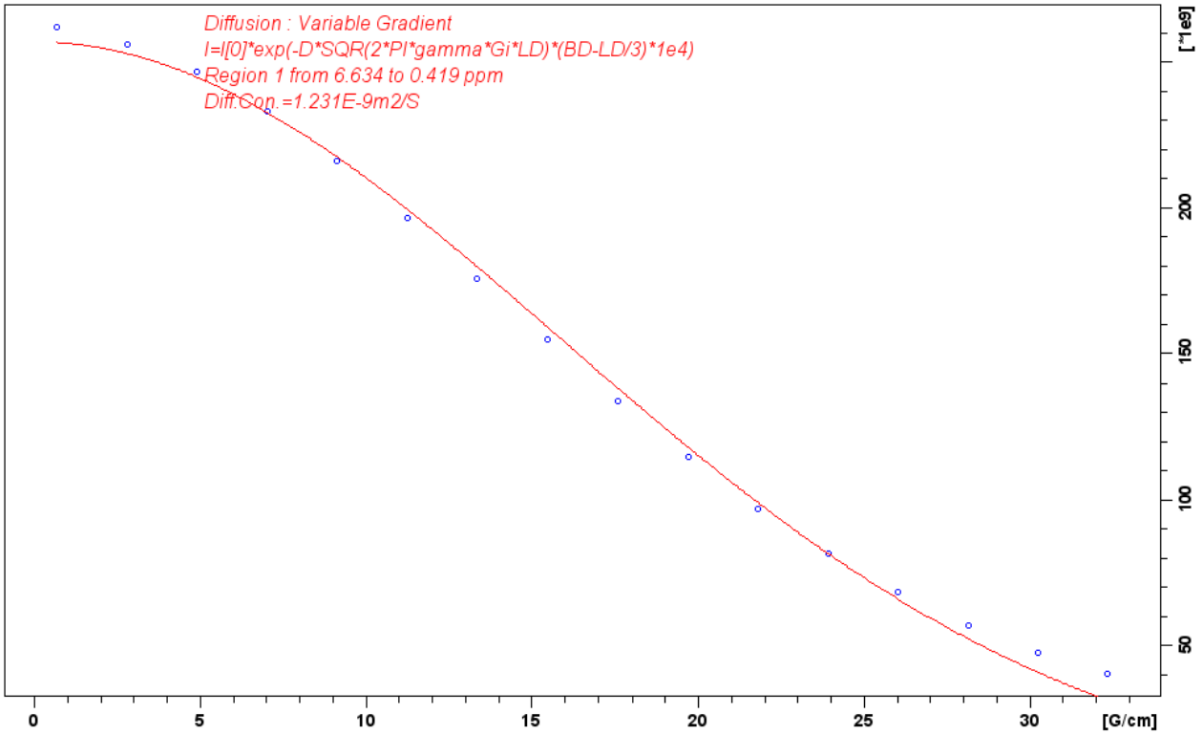

6: 250 ms

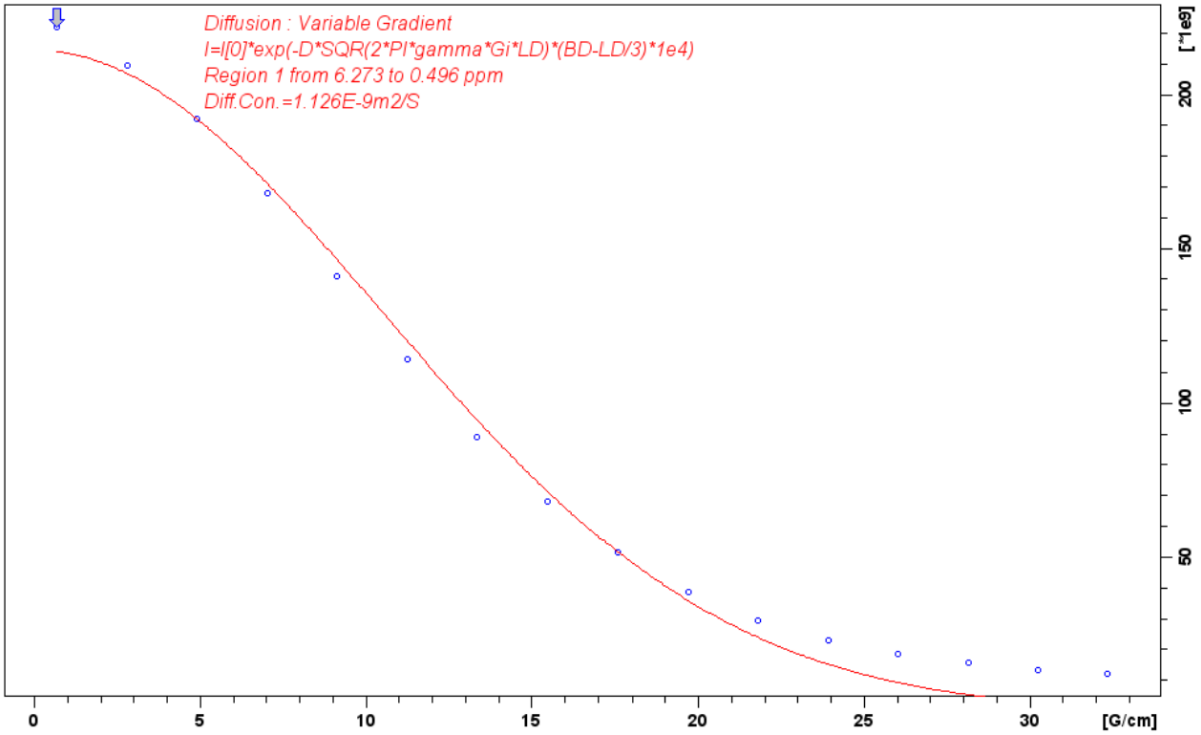

6: 500 ms

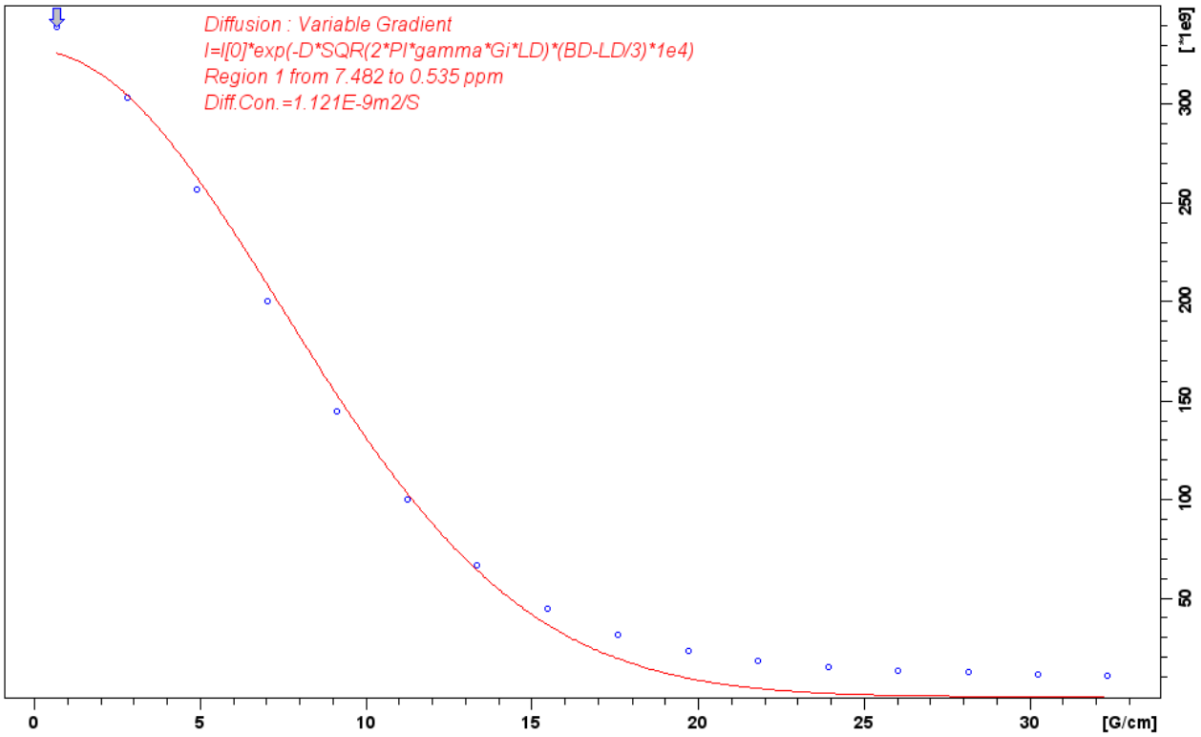

6: 750 ms

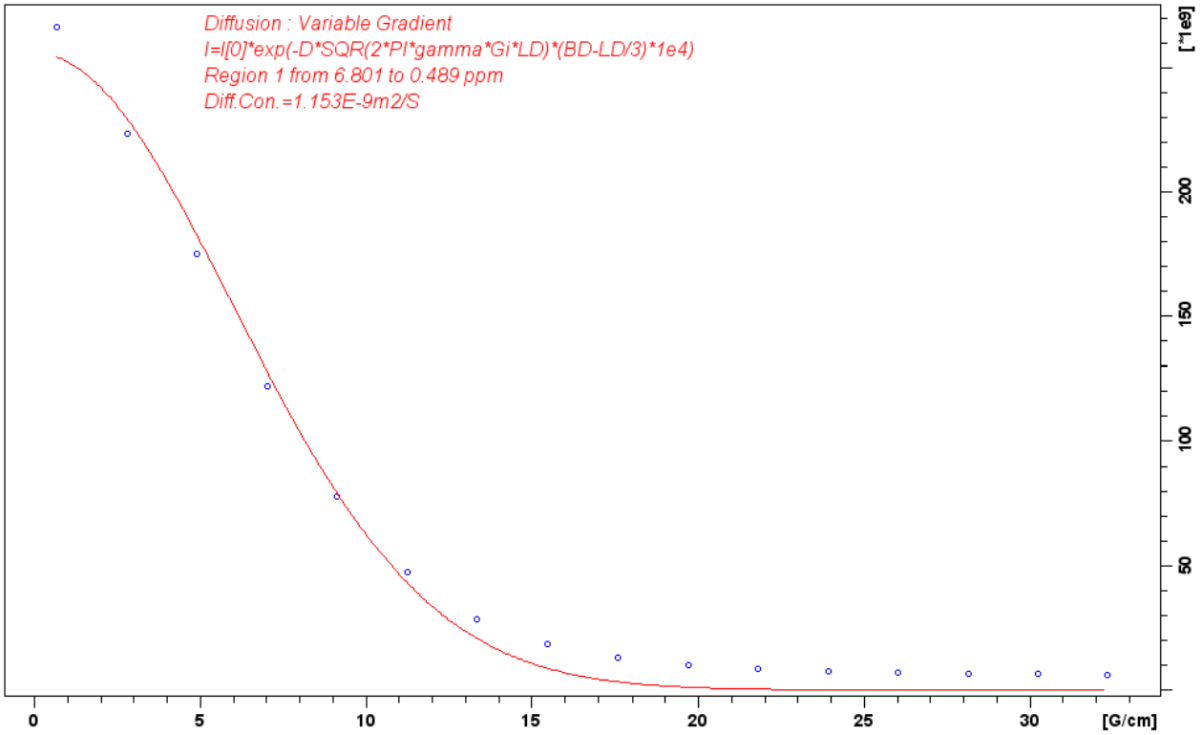

6: 1250 ms

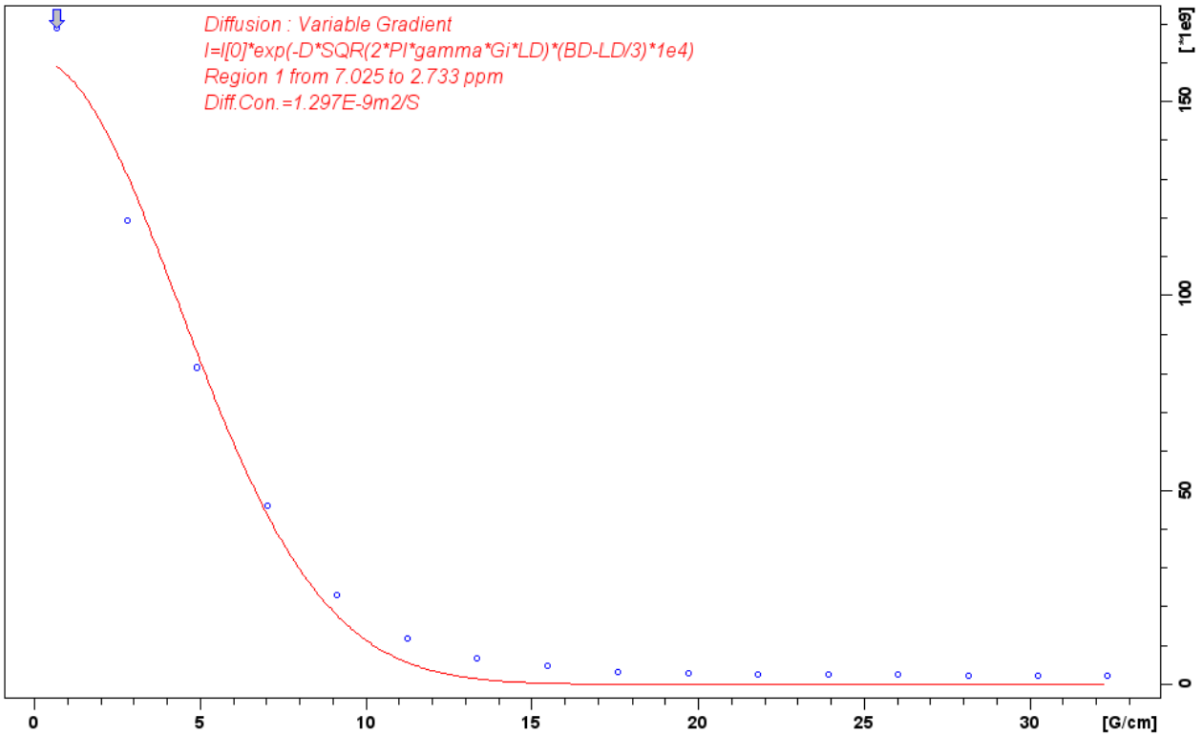

Fig 1 Diffusion data fits for the cotyledon cells sample supporting chapter 5.

A schematic overview of the rationale behind Chapter 6 experimental design.

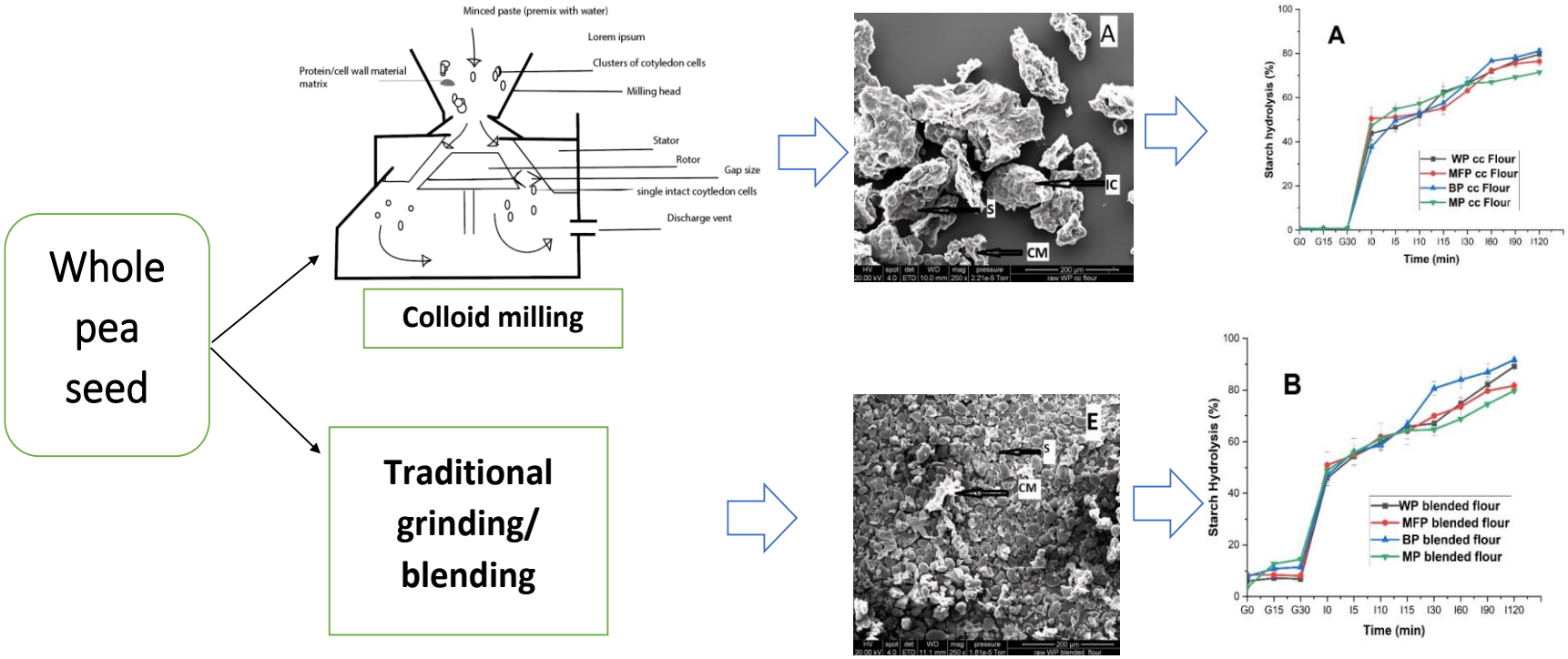

Fig 2 A schematic overview of the rationale behind Chapter 6 experimental design.

Table 1. Colloid milling trials for designing the “cotyledon flour “in chapter

	Starting material (premix)	Speed (HZ)	The gap between the stator and rotor	Comments (observed under light and scanning electron microscope)
Ist Trial	Large clusters of cotyledon cells	10	Kept constant at 300µm Premix was run the mill several times	No effect on the clusters of cotyledon cell
2nd Trial	Large clusters of cotyledon cells	20	Kept constant at 300µm Premix was run through the mill several times	No effect on the clusters of cotyledon cell
3rd Trial	Large clusters of cotyledon cells	50	Kept constant at 300µm Premix was run through the mill several times	all cotyledon cells were released from the cluster, however, the integrity of the cell wall was compromised (all cotyledon cells were broken down)
4th Trial	Large clusters of cotyledon cells	45	Kept constant at 300µm Premix was run through the mill several times	all cotyledon cells were released from the cluster, however, the integrity of the cell wall was compromised (all cotyledon cells were broken down)
5th Trial	Large clusters of cotyledon cells	40	Kept constant at 300µm Premix was run through the mill several times	Same result as 3rd and 4th Trail
6th Trial	Large clusters of cotyledon cells	30	The starting gap was at 300µm, the premix was run through the mill, then the gap was reduced from 300 – 50 µm and the premix was run through the mill after each reduction in the gap	The clusters of cotyledon cells were released with a large number of single intact cotyledon cells and some broken cells.

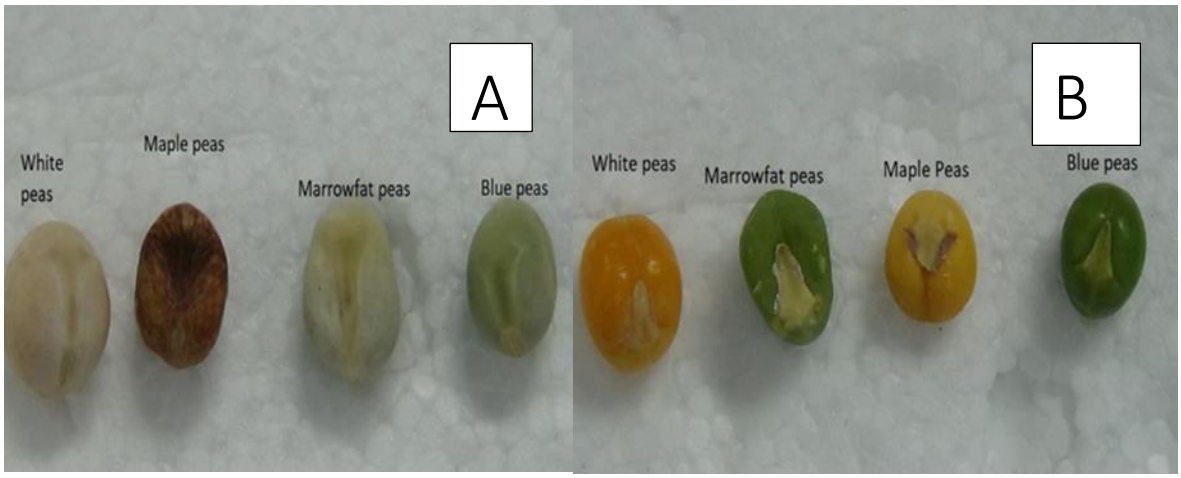

The New Zealand pea varieties used for this study: (A) with a seed coat and (B) without a seed coat.

MASSEY UNIVERSITY
TE KUNENGA KI PŪREHUROA
UNIVERSITY OF NEW ZEALAND

GRADUATE RESEARCH SCHOOL

STATEMENT OF CONTRIBUTION
DOCTORATE WITH PUBLICATIONS/MANUSCRIPTS

We, the candidate and the candidate's Primary Supervisor, certify that all co-authors have consented to their work being included in the thesis and they have accepted the candidate's contribution as indicated below in the *Statement of Originality*.

Name of candidate:	Ajala Abayomi Wasiu
Name/title of Primary Supervisor:	Professor Jaspreet Singh
In which chapter is the manuscript /published work:	Chapter 2

Please select one of the following three options:

(●) The manuscript/published work is published or in press

- Please provide the full reference of the Research Output:

Ajala, A., Kaur, L., Lee, S. J., & Singh, J. (2023). Native and processed legume seed microstructure and its influence on starch digestion and glycaemic features: A Review. Trends in Food Science & Technology, 133, 65-74. doi:10.1016/j.tifs.2023.01.011

( ) The manuscript is currently under review for publication – please indicate:

- The name of the journal:

Trends in Food Science & Technology

- The percentage of the manuscript/published work that was contributed by the candidate: 90.00

- Describe the contribution that the candidate has made to the manuscript/published work:

The candidate carried out 90% of the preparation of the published work

( ) It is intended that the manuscript will be published, but it has not yet been submitted to a journal

Candidate's Signature:	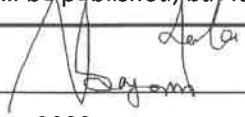
Date:	06-May-2023
Primary Supervisor's Signature:	
Date:	22nd May,

This form should appear at the end of each thesis chapter/section/appendix submitted as a manuscript/ publication or collected as an appendix at the end of the thesis.

MASSEY UNIVERSITY
TE KUNENGA KI PŪREHUROA
UNIVERSITY OF NEW ZEALAND

GRADUATE RESEARCH SCHOOL

STATEMENT OF CONTRIBUTION
DOCTORATE WITH PUBLICATIONS/MANUSCRIPTS

We, the candidate and the candidate's Primary Supervisor, certify that all co-authors have consented to their work being included in the thesis and they have accepted the candidate's contribution as indicated below in the *Statement of Originality*.

Name of candidate:	Ajala Abayomi Wasiu
Name/title of Primary Supervisor:	Professor Jaspreet Singh
In which chapter is the manuscript /published work:	Chapter 4

Please select one of the following three options:

(●) The manuscript/published work is published or in press

- Please provide the full reference of the Research Output:

Ajala, A., Kaur, L., Lee, S., & Singh, J. (2022). Influence of seed microstructure on the hydration kinetics and oral-gastro-small intestinal starch digestion in vitro of New Zealand pea varieties. Food Hydrocolloids, 129, 107631. https://doi.org/10.1016/j.foodhyd.2022.107631

( ) The manuscript is currently under review for publication – please indicate:

- The name of the journal:

Food Hydrocolloids

- The percentage of the manuscript/published work that was contributed by the candidate: 90.00

- Describe the contribution that the candidate has made to the manuscript/published work:

The candidate carried out 90% of the preparation of the published work

( ) It is intended that the manuscript will be published, but it has not yet been submitted to a journal

Candidate's Signature:	
Date:	06-May-2023
Primary Supervisor's Signature:	
Date: 22nd May.	

This form should appear at the end of each thesis chapter/section/appendix submitted as a manuscript/ publication or collected as an appendix at the end of the thesis.

MASSEY UNIVERSITY
TE KUNENGA KI PŪREHUROA
UNIVERSITY OF NEW ZEALAND

GRADUATE RESEARCH SCHOOL

STATEMENT OF CONTRIBUTION
DOCTORATE WITH PUBLICATIONS/MANUSCRIPTS

We, the candidate and the candidate's Primary Supervisor, certify that all co-authors have consented to their work being included in the thesis and they have accepted the candidate's contribution as indicated below in the *Statement of Originality*.

Name of candidate:	Ajala Abayomi Wasiu
Name/title of Primary Supervisor:	Professor Jaspreet Singh
In which chapter is the manuscript /published work:	Chapter 5

Please select one of the following three options:

○ The manuscript/published work is published or in press

- Please provide the full reference of the Research Output:

Ajala, A., Kaur, L., Lee, S. J., & Singh, J. (2023) Cell wall permeability in relation to in vitro starch digestion of pulse cotyledon cells.manuscript in preparation

○ The manuscript is currently under review for publication – please indicate:

- The name of the journal:

Food Research international

- The percentage of the manuscript/published work that was contributed by the candidate: 85.00

- Describe the contribution that the candidate has made to the manuscript/published work:

The candidate carried out 85% of the preparation of the published work

◉ It is intended that the manuscript will be published, but it has not yet been submitted to a journal

Candidate's Signature:	
Date:	06-May-2023
Primary Supervisor's Signature:	
Date: 22nd May	

This form should appear at the end of each thesis chapter/section/appendix submitted as a manuscript/ publication or collected as an appendix at the end of the thesis.

MASSEY UNIVERSITY
TE KUNENGA KI PŪREHUROA
UNIVERSITY OF NEW ZEALAND

GRADUATE RESEARCH SCHOOL

STATEMENT OF CONTRIBUTION
DOCTORATE WITH PUBLICATIONS/MANUSCRIPTS

We, the candidate and the candidate's Primary Supervisor, certify that all co-authors have consented to their work being included in the thesis and they have accepted the candidate's contribution as indicated below in the *Statement of Originality*.

Name of candidate:	Ajala Abayomi Wasiu
Name/title of Primary Supervisor:	Professor Jaspreet Singh
In which chapter is the manuscript /published work:	Chapter 6

Please select one of the following three options:

○ The manuscript/published work is published or in press

- Please provide the full reference of the Research Output:

Ajala, A., Kaur, L., Lee, S., & Singh, J. (2022). Microstructural, nutritional, and in vitro starch digestion properties of a novel cotyledon flour designed via Micronization Techniques. Food Hydrocolloids (under review)

◉ The manuscript is currently under review for publication – please indicate:

- The name of the journal:

Food Hydrocolloids

- The percentage of the manuscript/published work that was contributed by the candidate: 90.00

- Describe the contribution that the candidate has made to the manuscript/published work:

The candidate carried out 90% of the preparation of the published work

○ It is intended that the manuscript will be published, but it has not yet been submitted to a journal

Candidate's Signature:	
Date:	06-May-2023
Primary Supervisor's Signature:	
Date: 22nd May.	

This form should appear at the end of each thesis chapter/section/appendix submitted as a manuscript/ publication or collected as an appendix at the end of the thesis.